A functional study of

ADAMTS7 gene variants

Xiangyuan Pu

A thesis submitted to the University of London

for the degree of Doctor of Philosophy

Centre for Clinical Pharmacology

William Harvey Research Institute

Barts and the London School of Medicine and Dentistry

Queen Mary, University of London

March, 2014

Barts and The London
School of Medicine and Dentistry

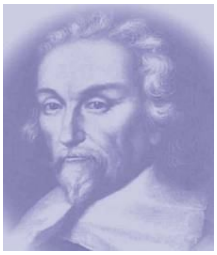

I dedicate this thesis to my parents and my fiancée.

Without their endless love, support and encouragement,

none of my achievements would be possible.

Abstract

Background: Recent studies have revealed an association between genetic variants at the *ADAMTS7* (a disintegrin-like and metalloprotease with thrombospondin type 1 motif, 7) locus and susceptibility to coronary artery disease (CAD). ADAMTS-7 has been reported to facilitate vascular smooth muscle cell (VSMC) migration and promote neointima formation. We sought to study the functional mechanisms underlying this relationship and to further investigate the role of ADAMTS-7 in atherosclerosis.

Methods and Results: *In vitro* assays showed that the CAD-associated non-synonymous single nucleotide polymorphism rs3825807, which results in a serine to proline (Ser-to-Pro) substitution at residue 214 in the ADAMTS-7 pro-domain, affected ADAMTS-7 pro-domain cleavage. Immunohistochemical analyses showed that ADAMTS-7 localised to vascular smooth muscle cells (VSMCs) and endothelial cells (ECs) in human coronary and carotid atherosclerotic plaques. Cell migration assays demonstrated that VSMCs and ECs from individuals who were homozygous for the adenine (A) allele (encoding the Ser214 isoform) had increased migratory ability compared with cells from individuals who were homozygous for the G allele (encoding the Pro214 isoform). Western blot analyses revealed that media conditioned by VSMCs of the A/A genotype contained more cleaved ADAMTS-7 pro-domain and more of the cleaved form of thrombospondin-5 (TSP-5, an ADAMTS-7 substrate that had been shown to be produced by VSMCs and inhibit VSMC migration). In *in vitro* angiogenesis assays, ECs of the A/A genotype exhibited increased capillary-like network formation. ADAMTS-7 over-expression in ECs by transfection of an *ADAMTS7*-214Ser expressing plasmid significantly accelerated

EC migration and *in vitro* angiogenesis, whereas ADAMTS-7 knockdown by shRNA had opposite effects. Preliminary proteomics analyses of conditioned media of ECs over-expressing ADAMTS-7 and ECs with ADAMTS-7 knockdown indicated that ADAMTS-7 can cleave thrombospondin-1 (TSP-1), a well-recognised angiogenesis inhibitor.

Conclusion: The results of this study indicate that rs3825807 has a functional effect on ADAMTS-7 maturation, TSP-5 cleavage, VSMC and EC migration, and angiogenesis. As VSMC migration and angiogenesis play important roles in atherosclerosis, these results provide a mechanistic explanation for the association between rs3825807 and CAD.

Table of Contents

Abstract 3
Table of Contents 5
Acknowledgements 10
Index of figures 12
Index of tables 15
List of abbreviations 16

Chapter 1 Introduction 21
1.1 Cardiovascular diseases (CVDs) – the number one global killer 21
1.2 Atherosclerosis – common cause of CVDs 23
1.2.1 LDL retention and EC dysfunction 24
1.2.2 Leukocyte activation and foam cell formation 27
1.2.3 SMC migration and fibrous cap formation 29
1.2.4 Extracellular Matrix proteins and atherosclerosis 30
1.2.5 Intraplaque angiogenesis and plaque progression 34
1.2.6 Plaque rupture 35
1.3 Genetic basis of CVDs 37
1.3.1 Familial clustering and heritable basis of CVDs 37
1.3.2 Genetic risk factors 38
1.3.3 Monogenic and polygenic CVD 38
1.4 Genetic approaches to study CVDs 39
1.4.1 Linkage study 39
1.4.2 Candidate gene association study 41
1.4.3 Genome-Wide Association Study (GWAS) 42
1.4.4 GWAS and the *ADAMTS7* gene locus 45
1.5 Extracellular matrix proteases and atherosclerosis 49
1.5.1 Matrix metalloproteinase family (MMPs) 50
1.5.2 The “A disintegrin and metalloproteinase” (ADAM) family 51
1.5.3 The “ADAM with thrombospondin motifs” (ADAMTS) family 51
1.6 ADAMTS-7 56
1.6.1 Identification and protein domain organization 56

1.6.2 Expression, localization and regulation 57
1.6.3 Activation 60
1.6.4 Potential substrates of ADAMTS-7 61
1.6.4.3 Alpha2-macroglobulin (A2M) 66
1.6.5 ADAMTS-7 and bone and joint disease 67
1.6.6 ADAMTS-7 and cardiovascular disease 68
1.7 Hypothesis and Aims 70
1.7.1 Hypothesis 70
1.7.2 Aims: 71

Chapter 2 Materials and Methods 72
2.1 Cell culture 72
2.1.1 Human vascular smooth muscle cells (VSMCs) isolation and culturing 72
2.1.2 Human umbilical vein endothelial cells (HUVECs) isolation and culturing 73
2.1.3 Human Embryonic Kidney 293 (HEK293) cell line culturing 74
2.1.4 Preservation and recovery of cells 75
2.2 Immunocytochemistry of VSMC marker and ADAMTS-7 76
2.2.1 Verification of VSMCs by the specific marker alpha-actin 76
2.2.2 ADAMTS-7 staining in VSMCs 77
2.3 Immunohistochemical staining of human atherosclerotic plaque 78
2.3.1 ADAMTS-7 and SMA double immunofluorescent staining in carotid atherosclerotic plaques 78
2.3.2 ADAMTS-7, TSP-5 and vWF single staining in carotid atherosclerotic plaques 79
2.3.3 ADAMTS-7 and SMA double staining in coronary atherosclerotic plaques 80
2.4 Genotyping 81
2.4.1 Genotyping by the KASPar method 81
2.4.2 VSMC Genotyping for rs3825807 by restriction enzymes 84
2.4.3 Genotyping by sequencing 86
2.5 Cell proliferation, senescence and apoptosis assays 87
2.5.1. Proliferation assay 87
2.5.2 VSMC senescence assay 89
2.5.3 VSMC apoptosis assay 89
2.6 Migration assay 91

2.6.1 Migration assay (Scratch assay) 91
2.6.2 VSMC trans-well migration assay 94
2.7 Real-time reverse transcription PCR (qRT-PCR) 95
2.7.1 RNA isolation 95
2.7.2 cDNA synthesis 96
2.7.3 Real-time RT-PCR 96
2.8 Allelic imbalance analysis 98
2.9 *ADAMTS7* plasmids cloning 100
2.9.1 *ADAMTS7*$_{Pro\text{-}Cat}$ pCMV5 plasmid cloning 100
2.9.2 Utilisation previously constructed *ADAMTS7*$_{Pro\text{-}Cat}$ short form and *ADAMTS7* full length plasmids 103
2.10 Transfection 108
2.10.1 *ADAMTS7*$_{Pro\text{-}Cat}$ plasmids HEK293 cell transfection 109
2.10.2 *ADAMTS7* full length plasmids EC transfection 109
2.11 *In vitro* TSP-5 cleavage assay 110
2.11.1 *In vitro* TSP-5 cleavage by VSMC conditioned media 110
2.11.2 *In vitro* TSP-5 cleavage by transfected HEK293 conditioned media 111
2.12 *ADAMTS7* shRNA lentiviral particles packing 111
2.12.1 *ADAMTS7* shRNA lentiviral plasmid 111
2.12.2 *ADAMTS7* shRNA lentiviral particle packaging 112
2.13 Infection of EC with *ADAMTS7* shRNA lentiviral particles 113
2.13.1 *ADAMTS7* shRNA lentiviral particles transduction 113
2.13.2 *ADAMTS7* knock-down EC cell line selection 114
2.14 Western blotting assays 115
2.14.1 Sample preparation 115
2.14.2 Protein concentration quantitation 118
2.14.3 Gel electrophoresis and protein transfer 119
2.14.4 Immunoblotting 120
2.15 EC Capillary-like network formation assay 121
2.16 Proteomics 123
2.17 Bruneck Study cohort 125
2.18 Southampton Atherosclerosis Study (SAS) 126
2.19 Bioinformatics 127
2.20 Statistical analyses 128

Chapter 3 Functional study of *ADAMTS7* variants in VSMC 129
3.1 Results 130
3.1.1 Verification of SMCs isolated from human umbilical arteries 130
3.1.2 Isolated VSMCs express ADAMTS-7 132
3.1.3 ADAMTS-7 is expressed in human atherosclerotic plaques 133
3.1.4 TSP-5 is expressed in human carotid atherosclerotic plaques 137
3.1.5 Genotyping of VSMCs for CAD-related SNPs at the *ADAMTS7* locus 138
3.1.6 The CAD-related SNPs at the *ADAMTS7* locus have no effects on VSMC proliferation, senescence and apoptosis 139
3.1.7 Influence of CAD-related *ADAMTS7* SNPs on VSMC migration 143
3.1.8 CAD-related *ADAMTS7* SNPs have no effect on *ADAMTS7* mRNA level in VSMCs 149
3.1.9 Effect of SNP rs3825807 on ADAMTS-7 pro-domain cleavage 152
3.1.10 Influence of SNP rs3825807 genotype on TSP-5 cleavage 155
3.1.11 SNP rs3825807 affects ADAMTS-7 activation 157
3.1.12 Further experiments confirming an effect of SNP rs3825807 on TSP-5 cleavage 164
3.1.13 Further experiments confirming an effect of SNP rs3825807 on VSMC migration 166
3.1.14 protein modelling – SNP rs3825807 effect on ADAMTS-7 structure 168
3.2 Discussion 171
3.2.1 Effect of SNP rs3825807 on ADAMTS-7 pro-domain cleavage, TSP-5 cleavage, and VSMC migration 173
3.2.2 Effect of SNP rs3825807 on ADAMTS-7 pro-domain cleavage, TSP-5 cleavage and cell migration 179

Chapter 4 Functional study of *ADAMTS7* and SNP rs3825807 in endothelial cell migration and *in vitro* angiogenesis 182
4.1 Results 183
4.1.1 ADAMTS-7 colocalises with ECs in human atherosclerotic plaques 183
4.1.2 ECs express ADAMTS-7 184
4.1.3 SNP rs3825807 genotyping results 185
4.1.4 SNP rs3825807 has no effect on EC proliferation 185
4.1.5 SNP rs3825807 has an effect on EC migration 186
4.1.6 SNP rs3825807 has no effect on *ADAMTS7* mRNA expression in ECs 188
4.1.7 Augmented *ADAMTS7* expression in ECs increases their migration 189

4.1.8 *ADAMTS7* knockdown impairs EC migration 191
4.1.9 Augmented *ADAMTS7* expression in ECs increases capillary-like network formation 192
4.1.10 *ADAMTS7* knockdown in ECs retards capillary-like network formation 194
4.1.11 SNP rs3825807 affects EC tube formation 196
4.1.12 Preliminary data of proteomics analysis 197
4.1.13 TSP-1 Western blotting preliminary results support the proteomics data 199
4.2 Discussion 201
4.2.1 Effects of *ADAMTS7* and SNP rs3825807 on EC migration and angiogenesis 201
4.2.2 TSP-1 - a possible substrate of ADAMTS-7? 203

Chapter 5 Population study 206
5.1 Bruneck study 207
5.2 Southampton Atherosclerosis Study 208
5.3 ADAMTS-7 proportion in the plaque intima correlates with intima thickness 209

Chapter 6 General Discussion 211
6.1 *ADAMTS7* – a potential therapeutic target to CVDs 211
6.2 Future work 214

Reference 216
Appendix I Reagents details 236
Appendix II: Publications 248

Acknowledgements

First of all, I would like to thank my family, my father Tianyin Pu, my mother Huicun Li and my older sister XiuJuan Pu, for their endless love, support and encouragement, without whom none of my achievements would be possible. And special thanks to my fiancée, Dr. Lujing Tang, for her deep love and patience while waiting for me during the past 8 long years, including the four years of my PhD study, she gives me hope and encourages me to stay strong.

I am incredibly grateful for the help of my supervisors. My principal supervisor Professor Shu Ye has always been patient, kind and provided daily supervision and guidance during this PhD project. He has also been a great friend to me giving me support when I was depressed and desperate, not only in relation to my academic life. My secondary Supervisor Professor Mark Caulfield has been always kind and provided a lot of support for this PhD project. Also, a lot of thanks to my co-supervisor Dr. Qingzhong Xiao, as he taught me the experimental skills I needed throughout this project.

Moreover, I would like to thank Professor Jianhua Zhu and Dr. Li Zhang in Zhejiang University for giving me an opportunity to apply for a PhD scholarship to study at Queen Mary University of London. Also, they have been supportively providing me with a lot of helpful suggestions during this study.

I also acknowledge, with sincere thanks and appreciation, my colleagues within the Clinical Pharmacology department who have been kind, supportive and made me feel very comfortable in the department and in the laboratory.

Many thanks to our collaborators: Professor Chuanju Liu in New York University who provided ADAMTS7 plasmids; Proteomics core facility in Oxford University provided proteomic analysis and data analysis. Also great appreciation to the sample donors without whom this project would be impossible.

Finally, I would like thank our funding bodies. This PhD project was supported by the British Heart Foundation and National Institute for Health Research. The Chinese Scholarship Council has provided me with the scholarship to study here.

Index of figures

Figure 1.1 World Health Organization data of cardiovascular diseases 23
Figure 1.2 Atherosclerotic plaque formation 24
Figure 1.3 GWAS flowchart 43
Figure 1.4 C4D Manhattan plot 46
Figure 1.5 CARDIoGRAM Manhattan plot 47
Figure 1.6 Lancet GWAS *ADAMTS7* locus 48
Figure 1.7 Schematic representations of MMP, ADAM and ADAMTS structure 52
Figure 1.8 Structure of ADAMTS7 57
Figure 1.9 Hypothesis of this project 70

Figure 2.1. Schematic representation of the KASPar genotyping 82
Figure 2.2. A representative KASPar genotyping cluster 83
Figure 2.3. A representative genotyping results by restricted enzyme digestion 84
Figure 2.4. The structure of pCMV5 vector and restricted enzymes in its' multiple cloning site 101

Figure 3.1. Verification of the homogenicity of the isolated VSMC cultures 131
Figure 3.2. Representative images showing presence of ADAMTS7 in cultured VSMCs 132
Figure 3.3. ADAMTS7 is present in human coronary artery atherosclerotic plaque samples 133
Figure 3.4. ADAMTS7 is present in human carotid artery atherosclerotic plaque samples 134
Figure 3.5. ADAMTS7 is detected by fluorescent immunostaining in human carotid artery atherosclerotic plaque samples 136
Figure 3.6. TSP-5 is present in human carotid artery atherosclerotic plaque samples .. 137
Figure 3.7. CAD-related SNPs in the *ADAMTS7* gene locus have no effect on VSMC proliferation 140
Figure 3.8. CAD-related SNPs in the *ADAMTS7* gene locus have no effect on VSMC senescence 141

Figure 3.9. CAD-related SNPs in the *ADAMTS7* gene locus have no effect on VSMC apoptosis 142
Figure 3.10 SNP rs3825807 affects VSMC migration 144
Figure 3.11 Effect of SNP rs3825807 on VSMC migration in SFM and inflammatory condition 145
Figure 3.12 SNPs rs1994016 and rs4380028 affect VSMC migration in CM conditions 146
Figure 3.13 SNPs rs1994016 and rs4380028 affect VSMC migration in SFM conditions 146
Figure 3.14 SNPs rs1994016 and rs4380028 affect VSMC migration in inflammatory conditions 147
Figure 3.15 Effect of SNP rs3825807 on VSMC migration 148
Figure 3.16. CAD-associated SNPs do not affect *ADAMTS7* mRNA expression level in VSMCs 150
Figure 3.17. CAD-associated SNPs have no effect on *ADAMTS7* mRNA expression levels in isolated VSMCs by allelic expression imbalance assay 151
Figure 3.18. Location of SNP rs3825807 and the resulting Ser-to-Pro substitution 152
Figure 3.19. Effect of CAD-related SNP rs3825807 on ADAMTS7 pro-domain cleavage in whole cell protein extracts 153
Figure 3.20. Effect of CAD-related SNP rs3825807 on ADAMTS7 pro-domain cleavage in conditioned media 154
Figure 3.21. Influence of CAD-related SNP rs3825807 on TSP-5 cleavage 155
Figure 3.22. *In vitro* TSP-5 digestion assay 156
Figures 3.23. SNP rs3825807 has an effect on ADAMTS7 activation 158
Figures 3.24. SNP rs3825807 has an effect on ADAMTS7 pro-domain processing 159
Figures 3.25. SNP rs3825807 affects amount of cleaved ADAMTS7 pro-domain in the cell surface washes 161
Figure 3.26. Cell surface washes Western blotting with anti-cMyc 162
Figure 3.27. SNP rs3825807 has no effect on ADAMTS7 total protein in cell lysates 163
Figure 3.28. Influence of CAD-related SNP rs3825807 on TSP-5 cleavage 165
Figure 3.29. Effect of SNP rs3825807 on VSMC migration by trans-well invasion assay 167
Figure 3.30. Functional effect of SNP rs3825807 Prediction 168
Figure 3.31. SNP rs3825807 is predicted to affect the secondary structure of ADAMTS-7 169
Figure 3.32. ADAMTS-7 secondary structure prediction 170

Figure 4.1. ADAMTS7 colocalises with ECs and associated with neo-vessels in human atherosclerotic plaque 183
Figure 4.2 ADAMTS7 is expressed in ECs 184
Figure 4.3. SNP rs3825807 has no effect on EC proliferation 186
Figure 4.4. SNP rs3825807 has an effect on EC migration 187
Figure 4.5. SNP rs3825807 has no effect on *ADAMTS7* mRNA expression level in ECs 188
Figure 4.6. ADAMTS7 over-expression accelerates EC migration 190
Figure 4.7. ADAMTS7 knock-down severely impairs EC migration 191
Figure 4.8. ADAMTS7 over-expression increases *in vitro* angiogenesis 193
Figure 4.9. ADAMTS7 knock-down retards *in vitro* angiogenesis 195
Figure 4.10. SNP rs3825807 has an effect on EC tube formation 197
Figure 4.11. Western blot detection of TSP-1 in EC conditioned medium 200

Figure 5.1. SNP rs3825807 associated with angiographic score in CAD patients 208
Figure 5.2. ADAMTS7 proportion in intima correlates with plaque intima thickness in the human coronary atherosclerotic plaques 209

Index of tables

Table 1.1 Risk factors for atherosclerosis..... 22
Table 1.2 Subgroups of ADAMTS family..... 54

Table 3.1 CAD-related SNPs' genotyping results for VSMCs 138
Table 3.2. Linkage disequilibrium of CAD-related SNPs in isolated VSMCs 139
Table 3.3. CAD-related SNPs' genotyping results for coronary artery plaque samples 139

Table 4.1. Isolated ECs SNP rs3825807 genotyping results 185
Table 4.2. Proteomics preliminary data 198

Table 5.1. Association between rs3825807 and carotid atherosclerosis in the Bruneck Study 207

List of abbreviations

2D-GE	2-dimensional gel electrophoresis
2-ME	β-Mercaptoethanol
A2M	Alpha2-macroglobulin
ADAM	A disintegrin and metalloproteinase
ADAMTS	ADAM with thrombospondin motifs
ALOX5AP	Arachidonate 5-lipoxygenase-activating protein
ApoE	Apolipoprotein E
APS	Ammonium persulfate
Beta-ECGF	Beta-Endothelial Cell Growth Factor human
BHF	British Heart Foundation
BMP	Bone morphogenetic protein
BrdU	5-bromo-2'-deoxy-uridine
BSA	Bovine serum albumin
CAD	Coronary artery disease
CHD	Coronary heart disease
ChIP	Chromatin immunoprecipitation
Co-IP	Coimmunoprecipitation
COMP	Cartilage oligomeric matrix protein
CRF	Conventional risk factor
CSPG	Chondroitin sulphate proteoglycan
CVD	Cardiovascular disease

DMEM	Dulbecco's Modified Eagle's Media
DSPG	Dermatan sulphate proteoglycan
EC	Endothelial cell
ECGS	Endothelial cell growth supplement
ECL	Enhanced chemiluminescence
ECM	Extracellular matrix
FBS	Fetal Bovine Serum
GAG	Glycosaminoglycans
GEP	Granulin-epithelin precursor
GM	Genetic modification
GWAS	Genome-Wide Association Study
HBSS	Hank's Buffered Salt Solution
HEK293	Human Embryonic Kidney 293
HPLC	High-Performance Liquid Chromatography
HRP	Horseradish peroxidase
HSPG	Heparan sulphate proteoglycan
HUVEC	Human vein endothelial cells
ICAM-1	Intercellular adhesion molecule-1
ICC	Immunocytochemistry
IFN-γ	Interferon-γ
IHC	Immunohistochemistry
IL-1 β	Interleukin-1β
KASP	KBiosciences Competitive Allele Specific PCR genotyping system

KSPG	Keratan sulphate proteoglycan
LC	Liquid chromatography
LD	Linkage disequilibrium
LDL	Low-density lipoprotein
LDLR	LDL receptor
LOD	Logarithmic odds of linkage
MCF	Macrophage colony-stimulating factor
MCP	Monocytes chemoattractant protein
MI	Myocardial infarction
miRNA	MicroRNA
MMP	Matrix metalloproteinase
MS	Mass spectrometry
NBT/BCIP	Nitro-blue tetrazolium/5-bromo-4-chloro-3'-indolyphosphate
NHGRI	National Human Genome Research Institute
NHLBI	National Heart, Long, and Blood Institute
NPHSII	Northwick Park Heart Study II
PBS	Phosphate buffered saline
PC	Pro-protein convertase
PDGF	Platelet-derived growth factor
PGRN	Progranulin
PI	Propidium iodide
PLAC	Protease and lacunin
POD	Peroxidase

PSS	Physiological saline solution
qRT-PCR	Quantitative (real-time) reverse transcription PCR
RISC	RNA-induced silencing complex
RNAi	RNA interference
ROS	Reactive oxygen species
RT	Room temperature
RT-PCR	Reverse Transcription PCR
SAS	Southampton Atherosclerosis Study
SA-ß-Gal	Senescence Associated ß-galactosidase
SDS	Sodium-dodecyl-sulfate
SDS-PAGE	SDS-polyacrylamide gel electrophoresis
SEM	Standard error of the mean
SFM	Serum-free media
ShRNA	Small hairpin RNA
SINQ	Spectral Index Normalised Quantitation
siRNA	Small interfering RNA
SMA	Smooth muscle α-actin
SMC	Smooth muscle cell
SNP	Single nucleotide polymorphism
SR	Scavenger receptor
TBST	Tris-Buffered Saline with 0.5% Tween 20
TGF-β	Transforming growth factor beta
TGN	Trans-Golgi network

TNF-α	Tumour necrosis factor alpha
TSP	Thrombospondin
TTP	Thrombotic thrombocytopenic purpura
UTR	Untranslated region
VCAM-1	Vascular cell adhesion molecule-1
VEGF	Vascular endothelial growth factor
VSMC	Vascular smooth muscle cell
vWFCP	Von Willebrand factor-cleaving protease
WHO	World Health Organization

Chapter 1

Introduction

1.1 Cardiovascular diseases (CVDs) – the number one global killer

Epidemiological studies of cardiovascular diseases (CVDs), specifically atherosclerotic coronary heart disease, started in the early 20th century, but for several decades, little progress was made to explain the disease mainly because of the lack of systematic approach (Luepker 2009). The first systematic study of CVDs was carried out in 1947 by Keys and colleagues who observed the occurrence of coronary heart disease (CHD) among Minnesota businessmen with 30 years follow up. The study revealed a significant relationship between CHD incidence and systolic blood pressure and serum cholesterol level (Keys et al. 1963). A year later, the National Heart, Lung and Blood Institute (NHLBI) established the Framingham Heart Study with the goal to understand the development of heart diseases by studying lifestyles of the residents of Framingham and Massachusetts. This study also found that elevations of blood pressure and cholesterol levels were associated with an increased incidence of (Kannel et al. 1961). The Framingham study first proposed the risk factor concept in which physiological and behavioral characteristics such as blood pressure, blood lipids, and cigarette smoke acted as predictors of subsequent disease events (Nabel and Braunwald 2012). Numerous studies around the world in the following decades adopted this method, confirming that the risk factors described by the early surveys predicted disease outcomes in different populations (Luepker 2009). These risk factors have been categorised into two major

groups: the group of risk factors with a dominant genetic component and the one with main underlying cause contributed by the environment (Table 1.1).

Table 1.1 Risk factors for atherosclerosis

Risk factors with significant genetic component	**Environmental factors**
Myocardial infarction	Smoking
Stroke	Diet
Total cholesterol	Exercise
HDL cholesterol	infection
Total triglycerides	Fetal environment
BMI	Air pollution
Blood pressure	Alcohol consumption
Lp(a) level	
Homocysteine level	
Type 2 diabetes	
Age	
Gender	

Cited from (Lusis et al. 2004)

With the identification of these risk factors, the concept that vascular disease and its complications, such as myocardial infarction and stroke, could be prevented was introduced. By controlling the risk factors for CVDs, such as lowering blood pressure, reducing plasma lipid concentration, and eradicating smoking, considerable progress has been made in reducing CVDs incidence and mortality in populations worldwide. But according to the latest World Health Organization (WHO) data in 2011, ischaemic heart disease and stroke are still the top two leading causes of death worldwide (Figure 1.1). Thus, further understanding of the pathogenesis of CVDs and development of new treatments for the disease are required.

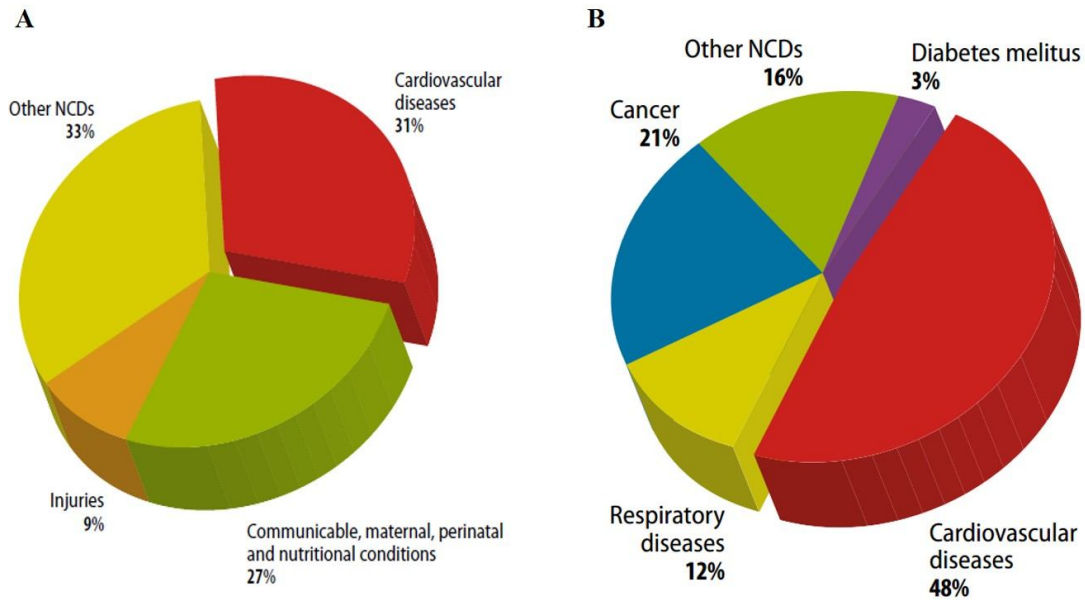

Figure 1.1 World Health Organization data of cardiovascular diseases. **A:** Distribution of major causes of death globally, with cardiovascular diseases the leading causes of death in the world, which are responsible for over 17 million deaths per year. **B:** Distribution of global non-communicable diseases (NCD, including CVDs, cancer, diabetes et al) by cause of death. Cited from <Global atlas on cardiovascular disease prevention and control. Geneva, World Health Organization, 2011>.

1.2 Atherosclerosis – common cause of CVDs

Atherosclerosis, a chronically progressing disease, is the primary cause of CHD and stroke. It is characterised by accumulation of lipids in large and medium sized arteries and subsequent formation of the atherosclerotic plaque composed of inflammatory cells, smooth muscle cells, lipids and extracellular matrix proteins (Figure 1.2) (Libby et al. 2011).

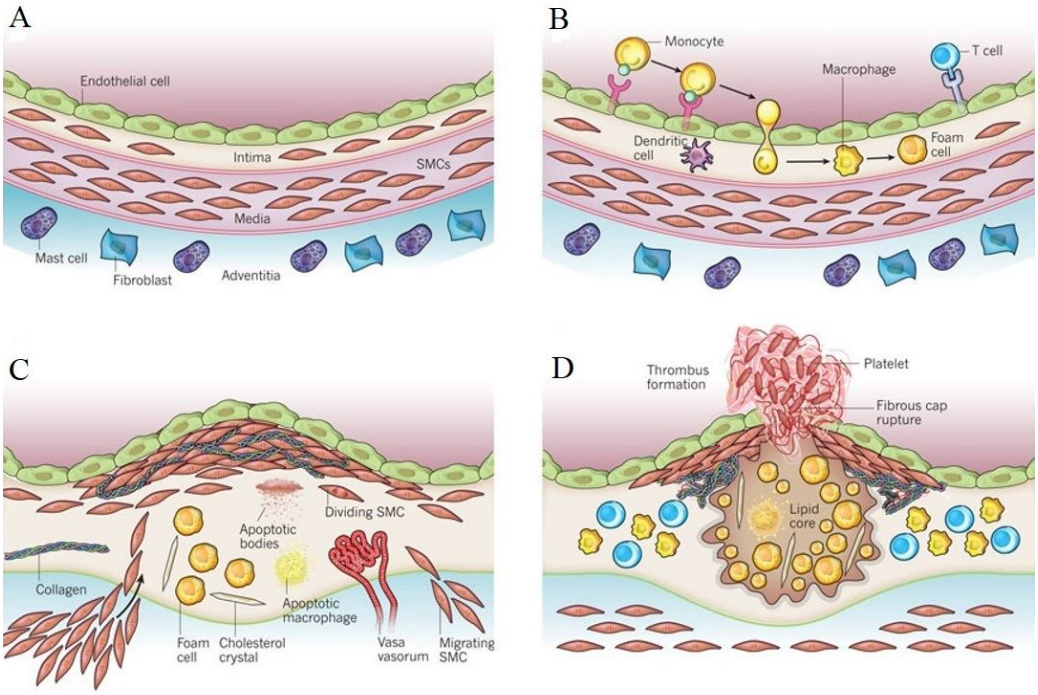

Figure 1.2 Atherosclerotic plaque formation. **A**: Normal structure of muscular arteries. **B**: The early steps of atherosclerosis: leukocytes attach and migrate into intima and monocyte-derived macrophages internalize lipids and transform to form-cells; **C**: SMC migration and their production of ECM contribute to the fibrous cap formation, as the plaque enlarges, endothelial cells migrate, proliferate and form neo-vessels to supple the growth of the plaque. **D**: Vulnerable plaque rupture and thrombosis formation. Figure cited and modified from (Libby et al. 2011).

1.2.1 LDL retention and EC dysfunction

Although considerable progress has been made in atherosclerosis research in the past 50 years, surprisingly, little is known about the early development of human atherosclerosis. The slow development of this disease makes it difficult to distinguish between lesion initiation and progression (Nakashima et al. 2008). There are two main hypotheses explaining initiation of atherosclerosis.

1.2.1.1 Response-to-injury hypothesis

The response-to-injury hypothesis was postulated by Ross, Glomset, and co-workers. This hypothesis originally presupposed endothelial desquamation as the key event in atherosclerosis initiation (Ross and Glomset 1976, Ross and Glomset 1976). However, it is now clear that the developing atheroma is covered by an intact endothelial layer throughout most stages of lesion progression (Williams and Tabas 1995). Thus, a refined response-to-injury hypothesis states that endothelial injuries that are insufficient to cause gross denudation but severe enough to cause endothelial cell dysfunction are key to atherosclerosis initiation (Ross 1993, Williams and Tabas 1995). Normally, the endothelial cells resist adhesion by leukocytes. However, risk factors of atherosclerosis such as high level of lipids, hypertension, hyperhomocysteinemia, blood flow turbulence, or smoking can injure the monolayer of endothelial cells and increase the permeability of endothelial layer. This increased permeability could facilitate lipid diffusion, mostly consisting of low-density lipoprotein (LDL) particles, into subendothelial space where they become trapped and modified by oxidation resulting in atherogenic ox-LDL particles.

1.2.1.2 Response-to-retention hypothesis

The response-to-retention hypothesis, proposed by Williams and Tabas in 1995, is another theory of atherosclerosis initiation (Williams and Tabas 1995). This hypothesis states that the retention of atherogenic lipoproteins associated with the extracellular matrix (ECM) in the arterial intima is an initial event in early atherogenesis, and the endothelial dysfunction is neither necessary nor sufficient for atherogenesis (Williams and Tabas

1995). This hypothesis further postulates that lipoprotein retention begins with predisposing stimuli (e.g. mechanical strain and/or cytokines) that enhance local synthesis of proteoglycans with high binding affinity for lipoproteins. These atherogenic lipoproteins enter the arterial intima and are bound and retained by proteoglycans (Williams and Tabas 1995, Little et al. 2002, Tabas et al. 2007). Positively charged residues of lipoproteins are bonding, via electrostatic interaction, with negatively charged side chains of proteoglycans called glycosaminoglycans (GAG) (Chait and Wight 2000, Kaplan and Aviram 2001, Williams 2001). The hypothesis further states that in their bound state the lipoprotein-proteoglycan complexes exhibit increased susceptibility to modification, via oxidation and/or aggregation, which in turn signal their uptake by macrophages to form foam cells (Kaplan and Aviram 2001, Nakashima et al. 2008) (see section 1.2.2 for further discussion). Furthermore, retained and modified lipoproteins enhance the production of proteoglycans with a high affinity for lipoproteins causing a cascade effect of the process (Chang et al. 2000). Thus, the response-to-retention hypothesis emphasizes the central role that ECM – lipoprotein play in atherosclerosis initiation (Nakashima et al. 2008).

In conclusion, these two hypotheses are not mutually exclusive. The response-to- retention hypothesis does not rule out the contribution of endothelial cell dysfunction to atherosclerosis initiation. Furthermore, these two theories are also consistent with the chronic inflammation hypothesis because retained and modified lipoproteins can stimulate the recruitment of inflammatory cells, such as monocytes and T-lymphocytes (Nakashima et al. 2008).

1.2.2 Leukocyte activation and foam cell formation

Modified LDL particles, mostly in the form of ox-LDL, can initiate expression of adhesion molecules by endothelial cells, including: intercellular adhesion molecule-1 (ICAM-1), vascular cell adhesion molecule-1 (VCAM-1), E-selectin and P-selectin (Kume et al. 1992, Khan et al. 1995, Shi et al. 2000, Eriksson et al. 2001). Moreover, increased permeability of endothelium and altered expression of adhesion molecules on the cell surface further promote recruitment of leukocytes by a process of rolling/adhesion to activated endothelial cells, subsequently allowing migration through the endothelial layer into the intima further aided by the action of chemokines (Ross 1999, Libby 2002, Libby et al. 2002). Monocyte chemoattractant protein-1 (MCP-1) is an important chemokine that recruits monocytes into intima (Gu et al. 1998). These monocytes migrate through the endothelial layer and mature into macrophages in response to cytokines/chemokines, such as the macrophage colony-stimulating factor (M-CSF) (Figure 1.2 B). These macrophages take up the trapped and modified LDL through scavenger receptors (SRs) e.g. SR-A and CD36 on their surface. The macrophages continually take up modified LDL and eventually become foam cells and contribute toward lesion progression (Ross 1999, Libby et al. 2002, Libby et al. 2011). At this stage, the accumulation of lipids in the subendothelial space can be observed as fatty streaks in the intima, which is the form of the earliest atherosclerotic lesion (Napoli et al. 1997).

Activated T lymphocytes are also involved in development of atherosclerotic lesions. (Hansson 2005). T lymphocytes can attach to adhesion molecules expressed on ECs, such as VCAM-1, and migrate through the EC layer into the intima, where they are activated

by macrophages that express class II major histocompatility complex (MHC-II) (Ross 1999). Although a significant decrease in the extent of atherosclerosis found in lymphocyte-deficient mice reflects an anti-atherosclerotic effect of T-lymphocytes (Uchida et al. 2010), cytokines secreted by different types of activated T-lymphocyte exert either pro-atherogenic or anti-atherogenic effects. The cytokines secreted by activated T-helper type 1 cells (Th1), such as interferon-γ (IFN-γ), exert pro-atherogenic effects. A significant reduction in atherosclerotic lesion was reported in IFN-γ deficient ApoE knock-out mice (Gupta et al. 1997, Whitman et al. 2002). This effect of IFN-γ is due to the dual activity of this cytokine. On the one hand it can activate macrophages to produce pro-inflammatory mediators including IL-1, IL-6 and TNF-α which are pro-atherogenic (Hansson 2001), while on another hand it can up-regulate the expression of SR-A and CD36 which increase ox-LDL uptake by macrophages (Lusis 2000). IFN-γ also inhibits production of ECM by SMC, increases production of metalloproteinases to degrade the ECM and induces apoptosis of foam cells. All these actions weaken the fibrous cap of an atherosclerotic lesion that protects the blood from the thrombogenic lipid core of the plaque, ultimately contributing the plaque rupture (Libby 2000, Lusis 2000, Libby 2006). Meanwhile, the major cytokines of Th2 cells counter the effect of Th1 cytokines and exert anti-atherogenic effect (Binder et al. 2004, Hansson 2005). IL-10 is a Th2-derived cytokine and IL-10 deficient mice showed increased cholesterol accumulation in macrophages and overall increase in size of atherosclerotic lesions, while over-expression of IL-10 in mice led to reduction in atherosclerotic lesion (Mallat et al. 1999, Pinderski et al. 2002, Caligiuri et al. 2003).

1.2.3 SMC migration and fibrous cap formation

Both SMC proliferation and migration are important processes in the formation of the fibrotic lesions and the progression of atherosclerosis (Figure 1.2 C) (Schwartz 1997, Libby et al. 2011). Vascular smooth muscle cell migration from the media to the intima is another dominant process that contributes to the progression of the plaque. Normally, VSMCs are restricted to the media of blood vessels, maintaining a contractile/differentiated phenotype and have low ability to migrate and proliferate. However, on various environmental cues, VSMCs can undergo transition from a quiescent, contractile/differentiated phenotype to a synthetic/dedifferentiated phenotype, with a high rate of migration/proliferation (Owens 1995, Hao et al. 2003, Wang et al. 2009). Activated macrophages and T lymphocytes in the plaque can secrete multiple cytokines and growth factors, such as platelet-derived growth factor-BB (PDGF-BB) and transforming growth factor-β (TGF-β), that can stimulate VSMCs to transit from a quiescent phenotype to a synthetic/migratory phenotype and to migrate into the intima from the media layer (Lusis 2000, Owens et al. 2004, Wang et al. 2009). The fibrous cap consists of a mixture of leukocytes, lipids, and debris, which may form a necrotic core. The lesion can grow larger due to continued leukocyte recruitment, SMC migration/proliferation and ECM production (Ross 1999). Apart from cytokines and growth factors secreted by the macrophages and the activated endothelial cells, thrombin can also induce SMC migration and proliferation. ECM proteins also have effect on SMC phenotype transition, for instance, fibronectin, collagen I and collagen III can induce shifts towards the synthetic phenotype, while laminin, collagen IV and thrombospondin induce the opposite effect (Owens et al. 2004, Rzucidlo et al. 2007, Orr et al. 2009, Wang et al. 2009).

With the presence of many atherogenic cytokines, such as activated platelet released TGF-β, migrated SMC in the intima then can proliferate and produce various ECM components, such as collagens, proteoglycans and fibronectin, resulting in the formation of a collagen-rich fibrous cap (Geng and Libby 2002, Libby et al. 2002) (Doran et al. 2008). Although endothelial cells, macrophages and SMCs all contribute to ECM production, SMCs are the principal connective tissue producer in atherosclerotic lesions (Falk 2006), thus forming an extension part of this study, CHD-associated SNPs in the *ADAMTS7* gene locus can affect ADAMTS-7 protein activation and cleavage of its substrate TSP-5 and further affect SMC migration.

1.2.4 Extracellular Matrix proteins and atherosclerosis

The ECM is composed of a mixture of vastly different macromolecules including collagen, elastin, glycoproteins and proteoglycans, conferring tensile strength and viscoelasticity to the arterial wall. Not only does the ECM provide the structural integrity of the artery wall, but it also participates in several key events such as cell proliferation, migration, apoptosis, lipoprotein retention and thrombosis. Thus, ECM turnover and remodelling have been proved to be involved in the pathogenesis of multiple diseases, such as atherosclerosis, arthritis and cancer (Katsuda and Kaji 2003). The following sections will look at the key components of ECM in greater detail in terms of their involvement in atherosclerosis.

1.2.4.1 Collagen

Among these macromolecules, collagen is the principal constituent of vascular ECM. To date, 25 types of collagen have been identified and thirteen types of them are present in the vascular wall. Their main function is to help maintain the structural integrity of the vascular wall, enhance its flexibility, and in addition, play a role in various cellular events including adhesion, proliferation, migration, and apoptosis. Five types of collagen (collagen I, III, IV,V and VIII) play pivotal roles in the pathogenesis of atherosclerosis because they accumulate in atherosclerotic lesions, as reviewed by (Plenz et al. 2003).

Collagen I, III and V are fibrillar collagens and comprise up to 60% of the total protein found in atherosclerotic plaque (Plenz et al. 2003). Collagen I and III are rigid and elastic respectively, while collagen V forms thin fibres. Collagen I forms the bases of the collagen fibre networks with alterations in Collagen III and V proportions giving rises to tissue structures in determining vessels tensile strength and elastic resilience (Ottani et al. 2001, Plenz et al. 2003). Collagen IV is the predominant constituent of basement membrane which underlies the endothelium and surrounds SMCs in the arterial wall. Collagen VIII, a network-forming collagen, interacts with other components of ECM, may contribute in the maintenance of vessel wall integrity and structure (Plenz et al. 2003).

Increasing evidence revealed that these collagens participate in cell processes, such as proliferation, migration and apoptosis. Fibrillar collagen I polymers inhibit VSMC proliferation and migration. In contrast, monomeric collagen I promote VSMC proliferation and migration (Chistiakov et al. 2013). Studies showed that Type IV collagen

expression increased in the atherosclerotic arteries, and that atherosclerotic lesions often contain thick deposition of Type IV collagen and multiple layers of basement membrane around SMCs (Stary et al. 1995, Rekhter 1999). Collagen IV can also induce apoptosis of vascular endothelial cells and SMCs, which may represent another pro-atherogenic effect of Type IV collagen (Panka and Mier 2003). Data also indicated that collagen VIII might promote VSMC migration and invasion in the atherosclerotic intima via interaction with integrin receptors and modulation of the synthesis of MMPs (Plenz et al. 2003). *In vitro* studies on cultured ECs demonstrated Collagen VIII involvement in processes of EC differentiation and organization and *in vitro* angiogenesis (Iruela-Arispe et al. 1991).

1.2.4.2 Glycoprotein

Various types of glycoprotein such as fibronectin and thrombospondin (TSP) are deposited in the atherosclerotic plaque. Like collagen, many of these glycoproteins have the ability to regulate cell proliferation and migration (Katsuda and Kaji 2003). Fibronectin is an adhesive glycoprotein, which possesses the ability to bind to various macromolecules as well as to cells, and influences the proliferation and migration of SMC (Katsuda and Kaji 2003). TSPs are a family of large multimeric ECM proteins that influence adhesion, migration, proliferation and survival of a variety of cell types (Armstrong and Bornstein 2003). The family consists of thrombospondins 1-5 and can be categorised into two subgroups: (A) TSP-1 and TSP-2, which are homotrimers; (B) TSP-3, 4 and 5 (also designated cartilage oligomeric matrix protein or COMP), which are homopentamers (Lawler 2000). The subgroup (A) attracted a lot of attention recently due to its ability to inhibit the migration and proliferation of cultured ECs and angiogenesis *in*

vivo (Armstrong and Bornstein 2003). However, TSP-1 has also been reported to have the ability to promote VSMC proliferation and migration (Patel et al. 1997) and to possess a latent TGF-β activation action (Crawford et al. 1998).

1.2.4.3 Proteoglycan

Proteoglycans are a group of macromolecules with a core protein to which glycosaminoglycans (GAG) are covalently attached (Ivey and Little 2008). Depending on the attached GAG chains, proteoglycans can be categorised into several families: chondroitin sulphate proteoglycans (CSPGs), dermatan sulphate proteoglycans (DSPGs), heparan sulphate proteoglycans (HSPGs), and keratan sulphate proteoglycans (KSPGs). Except for KSPGs, all other proteoglycans have been identified in blood vessels and synthesised by vascular cells. Endothelial cells produce mainly HSPGs (such as perlecan and syndecan), whereas VSMCs produce mainly CSPGs and DSPGs (like versican and biglycan). CSPGs and DSPGs that accumulate in the plaque show a marked affinity for native LDL particles and can accelerate oxidation of LDL, and further facilitate phagocytosis by macrophages. This in turn induces the deposition and retention of modified LDL particles, which can further cause endothelial injury and stimulate VSMC proliferation and migration, thereby leading to further progression of plaque (Hurtcamejo et al. 1992, Katsuda and Kaji 2003). HSPGs have been proposed to be antiatherogenic (Engelberg 2001), as decreased HSPGs are associated with increased atherosclerosis (Edwards et al. 2004, Tran et al. 2007, Tran-Lundmark et al. 2008). However, a proatherogenic effect of HSPG has also been reported (Tran-Lundmark et al. 2008).

1.2.5 Intraplaque angiogenesis and plaque progression

Angiogenesis also plays an important role in plaque progression and stability. As the plaque enlarges, the ensuing hypoxia and/or inflammatory cell infiltration is thought to promote intraplaque angiogenesis. Endothelial cells migrate, proliferate and form neo-vessels to support the growth of the plaque (Figure 1.2 C). In the early to mid-20th century, intraplaque angiogenesis and subsequent haemorrhage was hypothesized to be a major contributor to the progression of coronary atherosclerosis by several leading pathologists (Virmani et al. 2005). Much evidence now supports this hypothesis. Expression of the major angiogenic factors such as vascular endothelial growth factor (VEGF) is up-regulated during atherogenesis (Donners et al. 2010). It has been reported that DNA vaccination against VEGFR2, the major receptor for VEGF inhibited atherosclerotic plaque growth by reducing plaque neovascularisation in LDL receptor (LDLR) deficient mice (Petrovan et al. 2007). Moulton and colleagues demonstrated that the treatment of hypercholesterolemic Apolipoprotein E (ApoE) null mice with the angiogenesis inhibitors reduced plaque neovascularisation and plaque size by 70% to 85% (Moulton et al. 1999, Herrmann et al. 2006).

These studies clearly support the contribution of angiogenesis to plaque growth. However, the basic question remains about how angiogenesis contributes to plaque progression. One thought is that these immature blood vessels are inherently leaky, thereby increasing the infiltration of leukocytes, and thus amplifying the local inflammation. Data by Moulton et al. pointed out that a 60% reduction in $CD31^+$ capillaries in the intima and the adventitia was correlated with a 31% reduction of plaque area and a 51% reduction in plaque

macrophage content. This finding clearly supported the notion that plaque angiogenesis may contribute to atherosclerosis progression by providing a vascular network for inflammatory cell infiltration (Moulton et al. 2003, Herrmann et al. 2006). Moreover, the new blood vessels in the plaque are characterised not only by paucity of tight junctions and a discontinuous basement membrane but also by a relative lack of SMC. These neovessels are not only leaky but also unable to control intraluminal pressure and therefore fragile and prone to micro-haemorrhage and thrombosis (Herrmann et al. 2006).

Thrombin is a potent stimulator of SMC migration and proliferation. It triggers platelet release of growth factors such as platelet-derived growth factor (PDGF) from their alpha granules, stimulating SMC migration and proliferation which in turn contribute to plaque growth (Geng and Libby 2002, Libby et al. 2002, Libby et al. 2011). In addition, sequestration of red blood cells may contribute to the increase of free-cholesterol load of the plaque (Virmani et al. 2005). Plaque angiogenesis therefore contributes to the progression of atherosclerosis.

1.2.6 Plaque rupture

Atherosclerotic plaques that have a large lipid-rich necrotic core and/or a thin fibrous cap are prone to rupture. If this happens, the coagulation factors in the blood come in to contact with tissue factor, the main pro-thrombotic stimulus found in the lipid core of the atherosclerotic plaque which triggers thrombus formation (Figure 1.2 D) (Libby et al. 2011). The thrombus can block the artery and cause acute ischaemic events (Libby et al.

2002). Plaque rupture is the most common cause of acute ischaemic complications of atherosclerosis, such as myocardial infarction (MI) and ischaemic stroke (Libby 1995, Davies 1996, Virmani et al. 2000).

Several factors can contribute to formation of a thin fibrous cap. These include: SMC apoptosis, reduced ECM production, and increased ECM degradation. There is evidence suggesting that the cytokine IFN-γ produced by activated T lymphocytes in the plaque inhibits ECM production by SMCs whereas inflammatory cytokines such as interleukin-1β (IL-1 β) and tumour necrosis factor alpha (TNF-α) can stimulate macrophages and other leukocytes in the plaque to produce ECM-degrading enzymes such as matrix metalloproteinases (MMPs) (Libby et al. 2002). The rupture-prone plaques have fewer SMCs and are abundant in leukocytes. The repairing and protective capabilities of SMCs and their migration into the atherosclerotic lesion, proliferation, and ECM synthesis activity are considered beneficial for the stability of the plaque. Senescence and impaired function and/or death of SMCs are likely to be detrimental to the process. It is unknown why fewer SMCs are present at rupture sites, but apoptotic cell death could play an important role in plaque instability (Geng et al. 1997, Falk 2006).

1.3 Genetic basis of CVDs

1.3.1 Familial clustering and heritable basis of CVDs

Familial clustering of CHD had been noticed in the early last century and family history of CHD has long been considered a risk factor for the disease. Data of The Heath Family Tree Study and the NHLBI Family Heart Study indicate that high-risk families only represent about 11-14% of the general population but account for 72% of early CHD, 48% of CHD at all ages, 86% of early strokes, and 68% of all stroke, respectively (Williams et al. 2001). A number of twins or adoptee studies to estimate the extent of genetic influence have been reported. In a Swedish study of 21,000 twins born between 1886 and 1925, it was found that the relative hazard of both male twins dying of CHD before the age of 55 years, as compared to those with only one twin, was 8.1 for monozygotic and 3.8 for dizygotic twins (Marenberg et al. 1994). One explanation for these findings is the notion that the etiology of CHD has a genetic component although shared environmental influences can not be ruled out. Furthermore, the landmark Danish study of 1000 families with adopted children revealed that the death of a biological parent before the age of 50 years caused by vascular disease was associated with a 4.5-fold increase in mortality for the offspring from the same cause, whereas the death of an adoptive parent from similar causes did not significantly increase this risk (Sorensen et al. 1988), thereby strengthening the genetic-component argument. In addition, the anatomy of coronary disease, for instance, left main or proximal coronary disease, has also been revealed to be heritable (Fischer et al. 2005, Fischer et al. 2007), while coronary calcification and carotid intima-media thickness are also more prevalent in those with a family history of premature CHD

(Wang et al. 2003, Nasir et al. 2004, Nasir et al. 2007). Taken together, these studies provided convincing evidence that CVDs have a heritable component.

1.3.2 Genetic risk factors

Since the Framingham study first proposed the risk factor concept, epidemiological studies have revealed quite a few risk factors for CVDs which can be grouped into factors with an important genetic component and those that are largely environmental. However, these studies indicate that family history of CVDs is the most significant independent risk factor. A substantial proportion of an individual's susceptibility to CHD is attributable to genetic factors. The estimated heritability for CHD ranges from 40% to 60%. Multiple genes are implicated in risk factors such as blood pressure, total plasma cholesterol level, and type 2 diabetes (Lusis 2000). Identifying such genes can lead to a greater understanding of the pathogenesis of the disease and may contribute to better risk prediction, prevention, diagnosis and treatment of the disease.

1.3.3 Monogenic and polygenic CVD

In a small percentage of cases, CVD in a patient is caused by mutation of a single gene and can be inherited in a Mendelian fashion. An example of such case is familial hypercholesterolemia which is caused by mutations in one of the genes encoding the low-density lipoprotein receptor, Apolipoprotein B100, proprotein convertase subtilisin/kexin type 9 and low density lipoprotein receptor adapter protein 1. However, in the vast

majority of cases, CVD is a complex disorder and has no predictable pattern of inheritance. It is believed to be associated with many DNA variants in multiple genes each having a modest effect size. Since the genes of most Mendelian diseases associated with CVD have been identified, current research is focused on the identification of genetic variants associated with susceptibility to complex CVD (Nabel 2003, Soutar and Naoumova 2007, Patel and Ye 2011).

1.4 Genetic approaches to study CVDs

To find the genetic factors involved in the pathogenesis of CVDs, several technologies have been used. The principle underlying these approaches obtains genetic information from different individuals, some with CVD and some without, and then determines differences between the two sets of genomes. Given current high costs of whole genome sequencing, various DNA markers are used to identify the disease predisposed genome regions. The following sections will look at the most important technologies in greater detail.

1.4.1 Linkage study

Linkage study is performed by identifying DNA markers, such as microsatellite polymorphisms (short tandem repeat DNA sequences), that co-transmit with the disease in families. Since the genomic positions of the co-transmitted DNA markers are known, they can be used as a tool to identify regions of the genome that contain genes that

predispose to disease. Several linkage studies of CHD have been reported (Kullo and Ding 2007).

For instance, Helgadottir and colleagues performed a linkage study with 1,068 microsatellite markers in 713 individuals with a history of myocardial infarction from 296 families in Iceland, and found a locus on chromosome 13 with a linkage signal. Subsequently, they fine-mapped the interval by genotyping additional 120 microsatellite markers and 48 SNPs in this region in 802 cases of myocardial infarction and 837 controls, and found that a 4-SNP haplotype spanning the *ALOX5AP* gene (encoding arachidonate 5-lipoxygenase-activating protein) was associated with a two-fold higher risk of myocardial infarction (Helgadottir et al. 2004). A further study in a case-control set from England confirmed that the *ALOX5AP* gene was associated with CHD. It was also found to be associated with stroke in Icelandic and Scottish populations (Helgadottir et al. 2005).

The largest linkage study of CHD to date is the British Heart Foundation Family Heart Study which included 4,175 CHD cases from 1,933 families recruited throughout the UK and genotyped 416 microsatellites. The study identified a locus on chromosome 2, with suggested linkage for CHD, logarithmic odds of linkage (LOD) scores of 2.70 and 2.10 for coronary artery disease and myocardial infarction respectively (Samani et al. 2005), however, which are less than 3, the traditional significance threshold for a linkage (Dawn Teare and Barrett 2005).

Using this approach, more than 40 loci have been identified, but few of these have been replicated between studies (Stylianou et al. 2012). This may be due to a number of reasons including phenotypic heterogeneity and locus heterogeneity of complex disease and the low statistical power of this method to detect modest genetic effects (Patel and Ye 2011).

1.4.2 Candidate gene association study

Association studies directly compare allele frequencies of the genetic variants between those with a clinical condition (cases) and those without (controls) that are biologically unrelated. In contrast to linkage study, association study has greater statistical power for detecting genes with small effect sizes (Patel and Ye 2011).

Due to the limitation of technology and knowledge of the human genome, previously, the association study approach was used only to study variation in genes related to known pathological pathways or risk factors for the diseases under investigation. The hypothesis for this so-called 'candidate gene' approach is that, if a given protein is encoded by a gene being involved in the pathogenesis of disease, variation in that gene may alter either the expression or function, or both, of that protein, consequently leading to disease. Although many studies using this approach have been reported and from these studies a number of genes have been suggested to be associated with CHD, there have also been a lot of discrepancies among the studies and few findings have been confirmed (Winkelmann et al. 2000). This is also true for candidate gene studies of other complex disorders. One likely explanation is that the sample sizes of those studies were too small, and therefore,

the studies were prone to false-positive and false-negative findings. Although this is not a problem specific to the candidate gene study approach itself, the technique does have some limitations. Firstly, due to the nature of this approach, such studies can not identify novel disease genes and pathways. Secondly, such studies usually focus on gene exons, introns and immediate flanking regions, and therefore can not identify disease associated variations in the intergenic regions which contain DNA regulatory elements such as enhancers and silencers (Patel and Ye 2011).

1.4.3 Genome-Wide Association Study (GWAS)

In GWAS (Figure 1.3), study subjects are genotyped for up to over a million DNA markers directly. In contrast to the 'candidate gene' approach which specifically tests one or a few genetic regions, GWAS investigates the entire genome. This approach has only become feasible after the completion of the Human Genome Project, and subsequently the HapMap project. The former project has determined the sequence of the 3 billion base pairs of the human genome and the positions of its approximately 20,000 genes, while the later one identified genetic variations in the human genome. The majority of genetic variants are single nucleotide polymorphisms (SNPs), so far more than 10 million common SNPs (minor allele frequency >5%) have been identified by the HapMap project (Altshuler et al. 2010). It is estimated that SNPs account for over 80% of all human genetic variations that attribute to disease predisposition (Tregouet et al. 2009, Roberts et al. 2010). Because DNA variants that are near each other tend to be inherited together, they can be in linkage disequilibrium (LD). Taking advantage of the HapMap Project which has

provided comprehensive knowledge of LD among SNPs throughout the human genome, a smaller number of SNPs can be chosen as 'tag' SNPs to capture information on many more SNPs across the whole genome (Altshuler et al. 2010).

Another important development that has made GWAS feasible is high-throughput genotyping that enables hundreds of thousands of SNP (and more recently up to two million SNPs) to be genotyped simultaneously in a microarray.

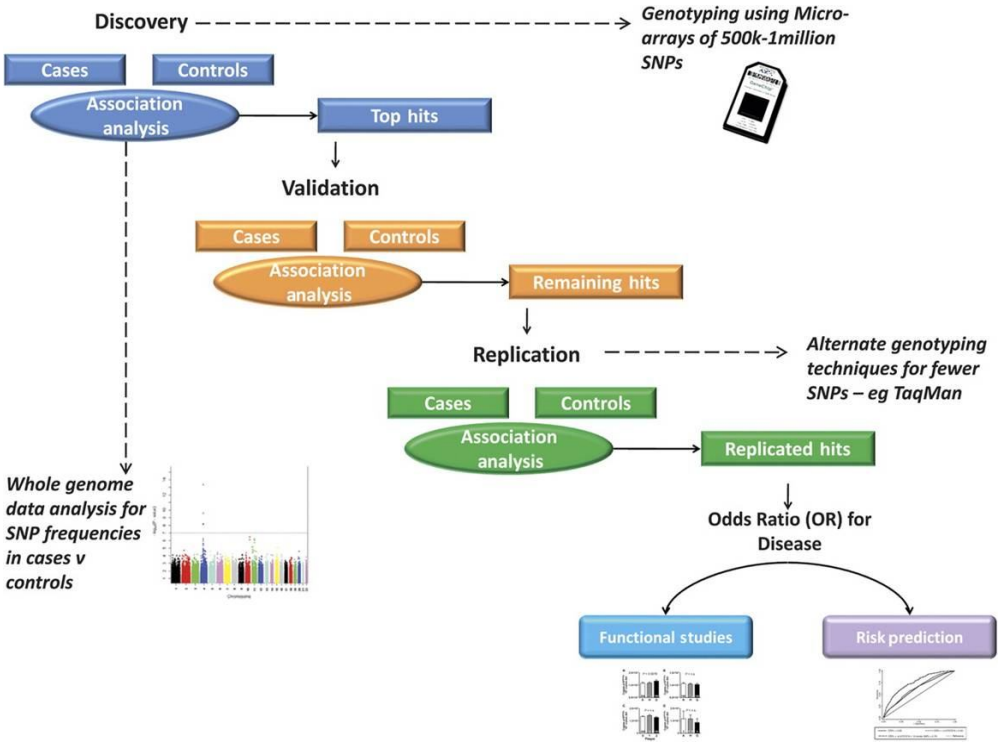

Figure 1.3 GWAS flowchart. GWAS are population-based, hypothesis-free, case-control studies. Thousands of individuals with a disease phenotype are recruited from the population, and need to be matched by disease-free individuals from the same population. DNA from "cases" and "controls" are genotyped using micro-array chips that can examine up to several millions of SNPs simultaneously. Stringent association analysis (divided into two stages of discovery and validation, each requiring an independent subset of individuals) are used to identify variants with statistically different frequencies between "cases" and "controls". P values of less than 5 x 10^-8 is used as stringent threshold to minimize the false positive association. Figure cited from (Patel and Ye 2011).

In the last few years, the GWAS approach has led to the identification of many susceptibility genes for many common diseases such as hypertension, diabetes, and of special interest to this thesis, CHD. To date, 46 genetic loci for CHD have been identified, of which the best known is the chromosome 9p21 locus, which was reported by three independent groups in 2007. As a marker for the disease's susceptibility, it has been replicated in many subsequent studies, strengthening its role in CHD pathogenesis. The functional study of 9p21 performed by our group revealed that the locus' variation has an impact on cyclin-dependent kinase inhibitor 2A and 2B (*CDKN2A* and *CDKN2B*) expression in VSMCs and thus influences VMSC proliferation, which likely represents an important mechanism for the association between this genetic locus and susceptibility to CAD (Motterle et al. 2012). An updated list of published GWAS can be found in the catalog of published genome-wide association studies (http://www.genome.gov/ gwastudies/) at the National Human Genome Research Institute (NHGRI).

The GWAS-identified loci define only the gene region nearest to the risk-associated SNPs. This means that in some cases the studies do not identify the causative gene itself and in almost all cases, never point to the causative SNP for the disease in question. Additional studies are required to identify the causal variants, because their inclusion in the risk algorithm will improve risk prediction and reduce uncertainty. Furthermore, results of GWAS often do not reveal the mechanisms behind the observed genetic association. Therefore, one of the current challenges in molecular genetics is to identify these functional variants reported in GWAS and reveal the underlying cellular processes by functional studies (Zeller et al. 2012). In addition, most of the GWAS findings are not

relevant to any known risk factor for CVDs, the following studies of these findings can uncover novel pathways and therapeutic targets for the disease.

1.4.4 GWAS and the *ADAMTS7* gene locus

In 2011, C4D consortium (The Coronary Disease Genetics Consortium) reported a large GWAS, with 575,000 genotyped SNPs in a discovery dataset comprising of 15,420 individuals with CAD (cases) (8,424 Europeans and 6,996 South Asian) and 15,062 controls. Replicated in an independent population sample of 21,408 cases and 19,185 controls identified 5 loci newly associated with CAD ($P<5 \times 10^{-8}$ in the discovery and replication analysis). Furthermore, the study also confirmed the association of 11 previously identified susceptibility loci, showing the great replicability of the study. The *ADAMTS7* locus is among these 5 newly identified loci, with the lead SNP rs4380028, residing at 7.6 kb upstream of the *ADAMTS7* gene, with risk allele C occurring at a frequency of 65% in the European population (Coronary Artery Disease Genetics 2011)(Figure 1.4).

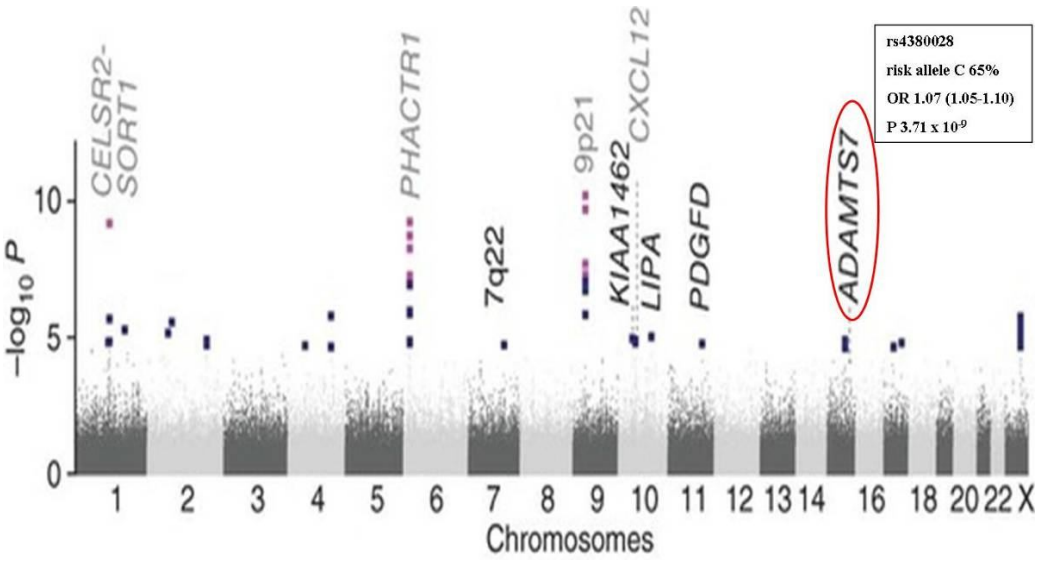

Figure 1.4 C4D Manhattan plot. The *ADAMTS7* locus was identified with the SNP rs4380028 as leading SNP to be associated with CHD. Figure cited from (Coronary Artery Disease Genetics 2011).

At the same time, CARDIoGRAM (Coronary ARtery DIsease Genome wide Replication And Meta-analysis) consortium performed a meta-analysis of 14 GWAS of CAD comprising 22,233 cases and 64,762 controls, all of European ancestry. They then genotyped the novel lead SNPs within the most promising loci, as well as a subset of previously reported CAD loci in up to 56,682 additional subjects (approximately half cases and half controls). Thirteen new loci were identified to be associated with CAD, and like the C4D study, this study showed very good replicability, with 10 of the 12 loci previously associated with CAD surpassing the genome-wide significance level. The CARDIoGRAM consortium also identified *ADAMTS7* locus associated with CAD, but with a different lead SNP rs3825807, a non-synonymous SNP with the risk allele A (frequency 0.57) (Figure 1.5). Adenine to guanine nucleotide allele substitution results in

a Serine (Ser) to Proline (Pro) amino acid substitution in the pro-domain region of ADAMTS-7 protein (Schunkert et al. 2011).

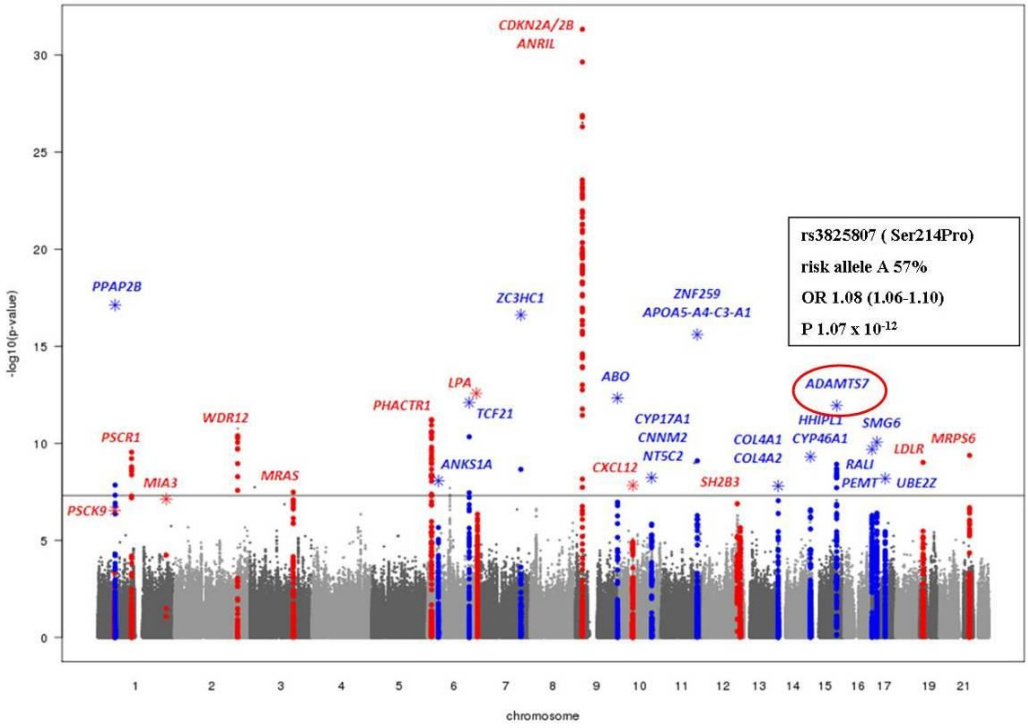

Figure 1.5 CARDIoGRAM Manhattan plot. Non-synonymous SNP rs3825807 in the *ADAMTS7* gene coding region was identified to be associated with CHD. Figure cited from (Schunkert et al. 2011).

Several months later, another GWAS also reported *ADAMTS7* as a novel locus for coronary atherosclerosis, with lead SNP rs1994016, residing in intron 8 of *ADAMTS7* gene, with risk allele C (frequency 0.6) (Figure 1.6). But more interestingly, this SNP was found not to be associated with myocardial infarction (Reilly et al. 2011), suggesting that ADAMTS-7 participates in the development and early progression of atherosclerosis but not plaque rupture and thrombosis leading to myocardial infarction.

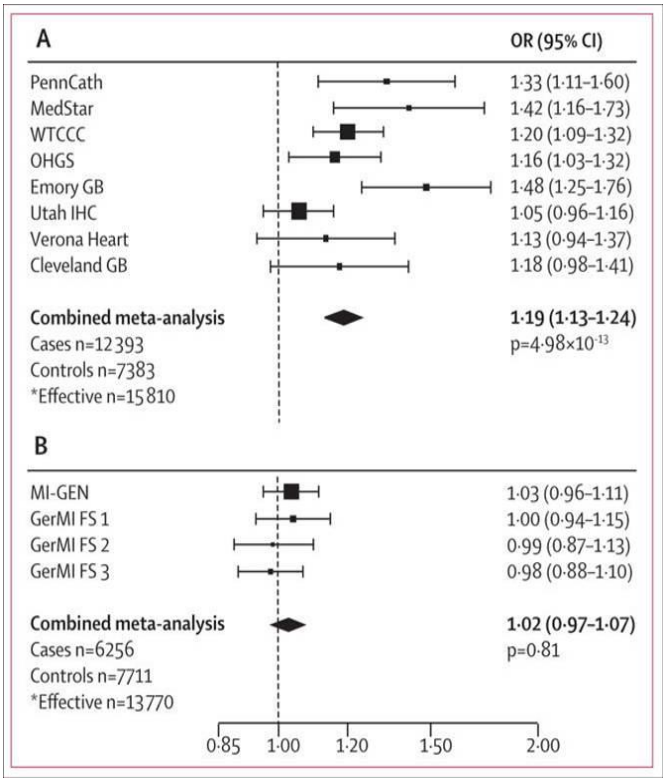

Figure 1.6 Lancet GWAS *ADAMTS7* locus. Association of rs1994016 (risk allele C 60%) at the *ADAMTS7* locus: (**A**) significant with angiographic CAD (AngCAD *vs* control); (**B**) not with early-onset myocardial infarction (MI *vs* control). Figure cited from (Reilly et al. 2011).

Finally, the latest attempt to increase the power to identify the polygenic component of CAD, CARDIoGRAM and C4D consortium combined forces to form the largest GWAS meta-analysis of CAD undertaken to date, CARDIoGRAMplusC4D consortium, which involved over 190,000 individuals (63,746 cases/130,681 controls). Fifteen new loci associated with the disease were identified and brought the susceptibility loci count up to 46. It is noteworthy that the *ADAMTS7* locus was replicated to be associated with CAD, with rs7173743 as lead SNP, with risk allele T frequency 0.58 (Deloukas et al. 2013).

All these GWAS indicate that *ADAMTS7* is a possible causal gene for CAD, but it remained unclear as to whether any of these SNPs, or other SNPs in LD have functional effects on *ADAMTS7* expression/activity and have an effect on the biological processes related to CAD. The key question of how ADAMTS-7 plays a role in the pathogenesis of CAD needs to be further addressed.

1.5 Extracellular matrix proteases and atherosclerosis

Physiologically, remodelling of the ECM is an integrated process of tissue development and maintenance. Overall, proteolytic activity is essential in aiding cell migration, removal of damaged tissue, and synthesis of new proteins which need to undergo all appropriate quality control checks (Skjot-Arkil et al. 2010). ECM remodelling also plays an important role in many pathological conditions, namely, in atherosclerosis, as discussed in section 1.2. VSMC migration from media to intima requires matrix proteases to catalyse the removal of the basement membrane around VSMC and to facilitate the cell's interaction with the interstitial matrix. This could promote the VSMC switch from a quiescent and contractile phenotype to a migrating and proliferating phenotype, to mediate tissue repair. Moreover, degradation of ECM could free sequestered growth factors surrounding VSMC and produce new matrix fragments to further promote VSMC migration and proliferation. In addition, plaque rupture which accounts for more than 80% of fatal MI in men results from net destruction of the ECM primarily driven by matrix proteases (Newby 2005). Almost all types of cells in atherosclerotic plaques including macrophages, SMCs, endothelial cells and T lymphocytes can produce a variety of proteinases which have been implicated in ECM degradation and in the pathogenesis of atherosclerosis (Murphy and

Nagase 2008). For example, the ECM molecule thrombospondin-5 (TSP-5), the best studied substrate of proteinase ADAMTS-7 which has been identified by GWAS as a susceptible gene for CHD, could maintain the contractile phenotype of SMC, thus the degradation of this ECM molecule by ADAMTS-7 leads to SMC migration from media to intima and contributes to the plaque growth (Wang et al. 2009).

1.5.1 Matrix metalloproteinase family (MMPs)

A major enzyme group involved in ECM remodelling is that of the matrix metalloproteinases (MMPs) (Murphy and Nagase 2008). MMPs are a family of zinc-containing proteolytic enzymes that share similar structure, especially from the arrangement of conserved domains, but differ in substrate specificity, their cellular source and inducibility. At present, 23 members of this family have been identified (Creemers et al. 2001). Numerous studies have demonstrated the presence of MMPs in atherosclerotic plaques and their involvement in the pathogenesis of atherosclerosis. Henney and colleagues were the first to demonstrate that stromelysins (a subgroup of the MMP family) are expressed in both macrophages and SMCs in atherosclerotic plaques (Henney et al. 1991). Subsequently, Galis and colleagues showed that MMP-1, -3, and -9 are present at the protein level in macrophages, SMCs, lymphocytes, and endothelial cells, with particular concentration in the vulnerable shoulder regions of plaque (Galis et al. 1994). Multiple members of the MMP family have now been reported to be involved in the pathogenesis of atherosclerosis, linking their expression with CVD, as reviewed by Galis and colleagues (Galis and Khatri 2002).

1.5.2 The "A disintegrin and metalloproteinase" (ADAM) family

The ADAMs are a family of both transmembrane and soluble proteolytic enzymes. Evidence suggests that members of this family are involved in the pathogenesis of CVD. For instance, Donners and colleagues showed that ADAM-10 was expressed in atherosclerotic plaques and associated with neovascularization through its interaction with VEGFR2 and mediation of VEGFR2 ectodomain shedding. In addition, they also reported that ADAM-10 could mediate VE-cadherin cleavage, increasing endothelial layer permeability and thus, leukocyte transmigration. Inhibition of ADAM-10 was shown to reduce endothelial cell and monocyte migration, which further confirmed that ADAM10 plays a critical role in the pathogenesis of atherosclerosis (Donners et al. 2010). Also, it has been shown that the expression of ADAM-15 and ADAM-9 in human atherosclerotic plaques is seven-fold and nine-fold higher than in normal arteries (Al-Fakhri et al. 2003). Another member of this family, ADAM-17, was also reported to be involved in atherosclerosis (Holdt et al. 2008). However, the function of this family has not been well characterised, and therefore further studies are still required to understand their mechanisms of action in health and disease.

1.5.3 The "ADAM with thrombospondin type-1 motifs" (ADAMTS) family

ADAMTSs are a family of proteinases which are structurally and evolutionarily related to the ADAMs and more distantly related to MMPs (Jones and Riley 2005) (Figure 1.7). In contrast to ADAMs and MMPs, all members of this family are secreted metalloproteinases with a conserved ancillary domain containing one or more thrombospondin type-1 like

repeats (TS) (Apte 2009). Following secretion, ADAMTS proteases may anchor to the cell-surface, such as in the case with ADAMTS-7 (Somerville, Longpre et al. 2004), ADAMTS-9 (Somerville et al. 2004a, Somerville et al. 2004b, Koo et al. 2006) and ADAMTS-10 (Somerville, Jungers et al. 2004). Other ADAMTSs, on the other hand, anchor to the extracellular matrix (i.e. ADAMTS-1 and ADAMTS-5) (Kuno and Matsushima 1998, Somerville et al. 2003).

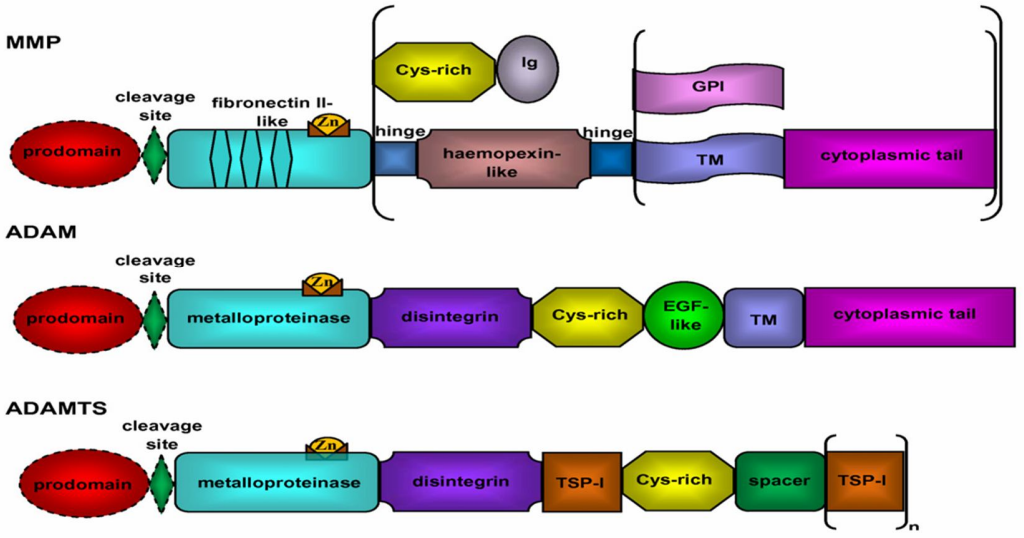

Figure 1.7 Schematic representations of MMP, ADAM and ADAMTS structure. These three families of proteinases are structurally and evolutionarily related, especially with respect to their domain regions, all belong to the metzincin superfamily (Porter et al. 2005, Paulissen et al. 2009). Figure cited from (Paulissen et al. 2009).

Like most zinc metalloproteases, ADAMTS proteases are synthesised as inactive zymogens. Proprotein convertases (PCs) will further process these zymogens by removing their pro-domain making these proteases active (Nakayama 1997, Zhou et al. 1999, Bergeron et al. 2000, Thomas 2002). Thus, these PCs have been demonstrated to have important roles in connective tissue organization, coagulation, inflammation, arthritis,

angiogenesis and cell migration (Apte 2004). Similar principles govern activation of some MMPs (Pei and Weiss 1995, Yana and Weiss 2000) and ADAMs (Cao et al. 2002, Leonard et al. 2005).

Furin is the best studied of the PCs implicated in proprotein processing within the constitutive secretory pathway and is the major PC to activate the ADAMTS proteases (Thomas 2002). Furin mostly resides in the trans-Golgi network (TGN), and thus the pro-domain processing that it mediates typically occurs intracellularly. But furin has also been detected at the plasma membrane (Mayer et al. 2003, Mayer et al. 2004) and as well as a shed, soluble form (Vidricaire et al. 1993). Previous studies on ADAMTS-1 (Kuno et al. 1999, Longpre and Leduc 2004), ADAMTS-4 (Wang et al. 2004), and ADAMTS-7 (Somerville et al. 2004) suggested that their zymogens were processed in the TGN by PCs, although some cell-surface processing of ADAMTS-7 was also observed (Somerville et al. 2004). ADAMTS-9 processing by furin was reported to occur at the cell-surface (Koo et al. 2006). Interestingly, the pro-domain processing of ADAMTS-9 was found to diminish its proteolytic activity against versican (Koo et al. 2007). Previously, analysis of ADAMTS-13 had shown no role for its propeptide in enzyme latency (Majerus et al. 2003). Thus, it appears that different mechanisms are used to process the pro-domain of the different members of the ADAMTS family, and that pro-domain cleavage can lead to activation in some ADAMTS family members but result in reduced activity in the case of ADAMTS-9 (Longpre et al. 2009).

To date, 19 members of this family have been identified in humans. Based on their sequence similarities and known substrates, the family members can be categorised into seven subgroups (Table 1.2). Among these subgroups, subgroup (a) is known as aggrecanases for their ability to process aggrecan; subgroup (b) can cleave the N-peptide of procollagen and thus are called procollagen N-proteinases; while subgroup (g) only has ADAMTS-13, vWFCP (von Willebrand factor-cleaving protease), which is least like any other ADAMTS (Porter et al. 2005). The functions of the rest ADAMTS family members have not been clearly revealed yet. In contrast to the MMP family, whose substrates are of much more broad-spectrum, ADAMTS family members have high substrate specificity, because the C-terminal ancillary regions of the enzymes, which influence protein recognition and matrix localization, reduce the risk of off-target effects.

Table 1.2 Subgroups of ADAMTS family

Subgroup	**Function**	**Member of ADAMTS family**
(a)	aggrecanases	ADAMTS-1,-4,-5,-8 and -15
(b)	procollagen N-proteinases	ADAMTS-2,-3 and -14
(c)	Unknown	ADAMTS-9 and -20
(d)	Unknown	ADAMTS-7, -12 and ADAMTS-6, -10
(e)	Unknown	ADAMTS-16 and -18
(f)	Unknown	ADAMTS-17 and -19
(g)	vWFCP	ADAMTS-13

Several studies have demonstrated the involvement of ADAMTS family members in CVD. ADAMTS-1 has been shown to be localised to SMCs and macrophage foam cells in vascular lesions, and has been important in cleavage of versican (Jonsson-Rylander et al. 2005, Wight 2005). In human fatty streak lesions, Jonsson-Rylander and colleagues

observed ADAMTS-1 staining with stronger intensity in the VSMCs and foam cells in the lesion compared with the media layer, and in their *in vitro* cell experiments, they found significantly more ADAMTS-1 expression in migrating and proliferating VSMCs. Furthermore, in their *in vivo* model, they observed increased intimal hyperplasia when comparing ADAMTS-1 transgenic/ApoE-deficient mice with ApoE deficiency (Jonsson-Rylander et al. 2005).

ADAMTS-4 and ADAMTS-8 have also received attention due to their expression in macrophage-rich areas of human carotid atherosclerotic plaques and coronary unstable plaques. (Wagsater et al. 2008). It has been shown that there is an association of ADAMTS-4 serum levels with the presence and severity of CHD (Zha et al. 2010, Chen et al. 2011). ADAMTS-1 and ADAMTS-8 have also been revealed to have anti-angiogenic activity (Vazquez et al. 1999).

ADAMTS-13, also known as von Willebrand factor-cleaving protease (vWFCP), is required for proteolytic modification of the von Willebrand Factor to an optimal size for proper coagulation (Zheng et al. 2002). vWF is a carrier protein for clotting factor VIII, supports platelet aggregation, and also mediates platelet adhesion to areas of vascular damage by binding to both the surface glycoproteins of platelets and to the exposed ECM components (Soejima et al. 2001, Porter et al. 2005). Mutations in ADAMTS-13 cause thrombotic thrombocytopenic purpura (TTP) (Levy et al. 2001, Apte 2004). However, knowledge of the ADAMTS family protease is still very limited, and functions of the majority members in this family remains to be further investigated.

1.6 ADAMTS-7

1.6.1 Identification and protein domain organization

ADAMTS7 is a protein coding gene, which has 24 exons and maps to chromosome 15q24 and spans 52.3 kb of genomic sequence in human. The protein encoded by the gene *ADAMTS7* is a member of ADAMTS family. It was first identified and cloned in 1999 by Hurskainen et al. They identified ADAMTS-7 with two thrombospondin type-1 like repeats, having a similar domain structure to ADAMTS-5, -6 and -8 (Hurskainen et al. 1999). However, in 2004, the same group reported a longer form of ADAMTS-7, or ADAMTS-7B. This was later characterised as the full-length version of the enzyme. They postulated that the previously cloned ADAMTS-7 may have an incomplete C terminus. The full length ADAMTS-7 has a domain organization similar to that of ADAMTS-12, with a total of eight TS repeats in its ancillary domain. The ADAMTS-7 protein is composed of 1686 amino acids with predicted molecular weight of 181 kDa (excluding the signal peptide) (Somerville et al. 2004).

Similar to other members of the ADAMTS family, ADAMTS-7 is initially synthesised as a zymogen which contains a signal peptide, a pro-domain, a catalytic metalloproteinase domain, a disintegrin-like domain, a central TS repeat, a cysteine-rich domain (CRD), and 7 additional TS repeats interspaced with two cysteine-free spacer domains. The secondary spacer domain is also a mucin-like domain, and like many ADAMTS proteases (e.g. ADAMTS-2, -3, -6, -10, -12, -16 and -19), ADAMTS-7 has a C-terminal PLAC (protease

and lacunin) domain containing six cysteines in the expected arrangement (Figure 1.8) (Somerville et al. 2004, Hanby and Zheng 2013, Patel and Ye 2013).

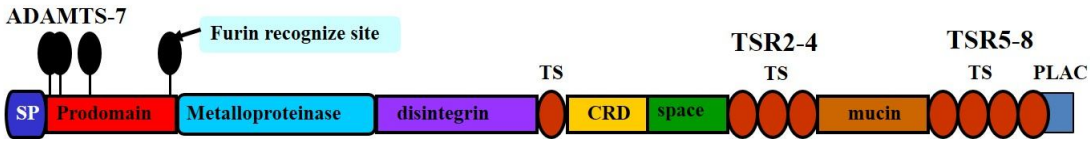

Figure 1.8 Structure of ADAMTS-7. ADAMTS-7 shares similar structure with other members of the family, with a totally of eight TSP-1 like repeats in its C-terminal ancillary domain.

1.6.2 Expression, localization and regulation

1.6.2.1 Expression

ADAMTS-7 is widely distributed in adult human tissues. *ADAMTS7* expression was detected as a 5.5 kb transcript with heart, pancreas, kidneys, skeletal muscle, and liver having the highest level of expression. Two additional transcripts of 8 kb and 4.5kb were also found in skeletal muscle (Liu et al. 2006). *ADAMTS7* mRNA has been found in normal human bone, cartilage, synovia, tendon, and ligament as well as in meniscus, skeletal muscle, and fat at lower levels (Liu et al. 2006, Hanby and Zheng 2013). The *ADAMTS7* gene expression was also found in mouse embryos (Somerville et al. 2004). In a more recent study, RT-PCR in various rat tissues detected *ADAMTS7* mRNA in the liver, embryo, ovaries, kidneys, testicle, lung, and thymus, and at lower levels in the spleen, heart, and brain. Low levels of *ADAMTS7* mRNA and protein in normal rat vascular walls was also reported by Wang and colleagues (Wang et al. 2009).

1.6.2.2 Localization

Like all other members of ADAMTS family enzyme, ADAMTS-7 is a secreted protein, however, evidence supports the notion that ADAMTS-7 could attach to the cell membrane after secretion. Conditioned media of HEK293 cells stably expressing Myc-tagged murine ADAMTS-7 exhibited a band with molecular weight of 250 kDa by SDS-polyacrylamide gel electrophoresis (SDS-PAGE) and western blotting. The discrepancy in the observed ADAMTS-7 size compared to the predicted molecular weight maybe due to glycosylation as there are several potential glycosylation sites within the ADAMTS-7 sequence. Treatment of stable cells expressing ADAMTS-7 with 0.5M NaCl for 30 min, which released more ADAMTS-7 in the conditioned media, supports the cell surface localization theory of secreted ADAMTS-7. Moreover, ADAMTS-7 was detectable by surface biotinylation experiments, and in some cells, recombinant ADAMTS-7 appears to be transiently associated with the outer leaflet of the plasma membrane. All these findings indicate that ADAMTS-7 could be in close proximity to the cell membrane (Somerville et al. 2004, Hanby and Zheng 2013).

1.6.2.3 Regulation

ADAMTS-7 production can be regulated by cytokines, growth factors and free radicals. Wang et al. (2009) showed that both the mRNA and protein of ADAMTS-7 in VSMCs were induced by the proinflammatory cytokines TNF-α and IL-1β, and by the growth factor PDGF-BB. Elevation of ADAMTS-7 level in VSMC by TNF- α was time-and dose-dependent as detected by RT-qPCR and Western blotting (Wang et al. 2009). Similarly,

Wagsater et al (2008) showed that the *ADAMTS7* mRNA level was up-regulated by TNF-α in the human monocyte/macrophage cell line THP-1 (Wagsater et al. 2008). Reactive oxygen species (ROS), such as hydrogen peroxide (H_2O_2), also increased *ADAMTS7* expression in VSMCs (Wang et al. 2009). In contrast, anti-inflammatory factor TGF-β downregulated *ADAMTS7* expression (Chait and Wight 2000). Interestingly, proatherosclerotic factors, including ox-LDL and homocysteine, did not alter *ADAMTS7* expression in VSMCs (Wang et al. 2009, Hanby and Zheng 2013).

Further studies revealed that *ADAMTS7* expression could be transcriptionally regulated. Analysis of the *ADAMTS7* promoter by using of the programs TESS and TFSEARCH revealed the presence of proinflammatory element binding sites, including transcription factor NF-κB and AP-1 sites. Chromatin immunoprecipitation (ChIP) assay confirmed the binding of NF-κB and AP-1 to the predicted binding sites within the *ADAMTS7* promoter. Inhibition of NF-κB and AP-1 pathway by application of an ectopic IκB adenovirus or c-Jun dominant-negative adenovirus ameliorated TNF-α induced *ADAMTS7* elevation in VSMCs by 61% and 44%, respectively, whereas application of the two viruses together completely abolished TNF-α induced *ADAMTS7* upregulation (Wang et al. 2009, Hanby and Zheng 2013). These data suggest that *ADAMTS7* expression can be regulated at transcriptional level, and NF-κB and AP-1 are essential for TNF-α mediated *ADAMTS7* induction.

A recent study provided evidence that *ADAMTS7* expression could also be regulated by microRNA (miRNA). A miRNA is a small, non-coding RNA molecule, classically 22-

nucleotides long, which functions via base-pairing with complementary sequences within mRNA molecules of a target gene, usually resulting in gene silencing via translational repression or target mRNA degradation. A Bioinformatics database search predicted a target site for miR-29a/b in the 3' untranslated region (UTR) of *ADAMTS7*, and experiments showed that a miR-29a/b mimic reduced *ADAMTS7* mRNA and protein expression in VSMC, whereas anti-miR-29a/b increased *ADAMTS7* expression levels (Du et al. 2012). These data suggest that miR-29a/b negatively regulates *ADAMTS7* expression (Wang et al. 2010, Hanby and Zheng 2013).

1.6.3 Activation

The active or mature form of ADAMTS-7 is derived by cleavage of the pro-domain by proprotein convertases, such as furin. There are three conserved pro-domain processing sites (RVLR^{58}, RVLRKR^{60} and RQQR^{220}, mouse ADAMTS-7 sequence annotation) in both human and mouse ADAMTS-7 pro-domain. However, human ADAMTS-7 has four additional furin processing sites which are not present in mouse. The pro-domain seems to be processed sequentially, as shown by experiments using a short form of Myc/His-tagged ADAMTS-7 consisting of the pro-domain and metalloprotease domain, designated ADAMTS-7$_{Pro\text{-}Cat\text{-}\mathrm{Myc/His}}$. SDS-PAGE of His-tagged proteins from mouse ADAMTS-7$_{Pro\text{-}Cat\text{-}\mathrm{Myc/His}}$–expressing HEK293 cells demonstrated two major protein bands of 50 kDa and 29 kDa on Coomassie Blue-stained gels, with several quantitatively minor intermediate bands. Western blotting using anti-c-Myc antibody demonstrated that these bands correspond to major forms of ADAMTS-7$_{Pro\text{-}Cat\text{-}\mathrm{Myc/His}}$. The amino acid sequence of the

50 kDa and 29 kDa major bands obtained by Edman degradation were ^{61}DVSTTQ and ^{221}SVSKEK, respectively, indicating processing following RVLRKR^{60} (50 kDa band) and RQQR^{220} (29 kDa band). The amino acid sequence of the 29 kDa band from human was ^{237}SVSKEKW, similar processing site but in human ADAMTS-7 annotation (Somerville et al. 2004). It is not very clear where the pro-domain processing cellular site is located, whether it is intracellular (Golgi apparatus, by intracellular furin) or happens on the cell surface. It is possible that both of these mechanisms exist, depending on the tissue and/or cell type.

So far, furin has been proved to be the major proprotein convertase for ADAMTS-7. CHO RPE.40 cells, which are furin-deficient, were used to determine which proprotein convertases could process ADAMTS-7. Cotransfection of this cell line with mouse ADAMTS-7$_{\textit{Pro-Cat}\text{-Myc/His}}$ and furin, PACE4, PC6B or PC7 revealed that furin was able to process ADAMTS-7 completely to the mature form (29 kDa). But the other proprotein convertases (PACE4, PC6B and PC7) processed ADAMTS-7 inefficiently to its mature form (Somerville et al. 2004).

1.6.4 Potential substrates of ADAMTS-7

As with other ADAMTS family members, ADAMTS-7 is likely to have high substrate specificity, with three potential ADAMTS-7 substrates reported to date. These include TSP-5 (also known as cartilage oligomeric matrix protein, COMP); progranulin (PGRN, also designated granulin-epithelin precursor, GEP) and alpha2-macroglobulin (A2M).

ADAMTS-7 can cleave TSP-5, A2M inhibits ADAMTS-7 mediated TSP-5 cleavage while GEP also disturbs TSP-5 cleavage by ADAMTS-7 by forming complex protein-protein networks (Luan et al. 2008, Hanby and Zheng 2013).

1.6.4.1 TSP-5 – the best-studied substrate of ADAMTS-7

TSP-5, the fifth member of the TSP family, also known as Cartilage Oligomeric Matrix Protein (COMP), is a 520 kDa pentameric glycoprotein with five identical subunits. It is highly expressed in the cartilage of joints, tendons, ligaments and vascular ECM (Riessen et al. 2001). TSP-5 is the best-known substrate of ADAMTS-7. Human TSP-5 mutations have been linked to two different autosomal-dominant forms of short-limb dwarfism: pesudoachondroplasia and multiple epiphyseal dysplasia, characterised by short stature, epiphyseal abnormalities, and early-onset osteoarthritis (Liu et al. 2006).

To date, most research on TSP-5 has focused on its role in bone and joint diseases. Fragments of TSP-5 have been detected in diseased cartilage, synovial fluid, and serum of patients with knee injuries, posttraumatic, primary osteoarthritis and rheumatoid arthritis (Liu et al. 2006). Several MMPs have been reported to degrade TSP-5 *in vitro*, including MMP-1, -3, -9, -13, -19 and -20. ADAMTS-4 has also been reported to cleave TSP-5 *in vitro* (Liu et al. 2006). However, the role of these proteases in TSP-5 degradation remains to be elucidated in *in vivo* animal models. ADAMTS-7 was identified as TSP-5 binding partner by a yeast two-hybrid screen using TSP-5 EGF-like domains as a bait. The direct interaction between TSP-5 and ADAMTS-7 was further characterised by using *in vitro* GST pull-down assays, indicating that purified human TSP-5 directly binds to the

C-terminus of ADAMTS-7. This interaction was verified using a coimmunoprecipitation (Co-IP) assay (Liu et al. 2006). Using ADAMTS-7 deletion mutants, the four C-terminal TS repeats of ADAMTS-7 were verified to be responsible for binding with TSP-5 EGF-like domain. More importantly, the same research group demonstrated that recombinant ADAMTS-7 cleaved TSP-5 *in vitro*, and the cleavage of TSP-5 by ADAMTS-7 was zinc ion and pH-dependent (Liu et al. 2006).

Several studies have also suggested an important role of TSP-5 in vascular disease. *TSP5* mRNA and protein expression were detected in cultured human VSMCs by Northern blotting and immunoprecipitation, and were found to be increased by growth factors TGF-β1 and TGF-β3 stimulation (Riessen et al. 2001). *In vitro* attachment assays demonstrated strong adhesion of VSMC to TSP-5 coated surfaces (Riessen et al. 2001). TSP-5 coated membranes also supported the migration of VSMC indicating TSP-5 may play a critical role in the adhesion and migration of VSMC (Riessen et al. 2001). Furthermore, TSP-5 has not only been found in normal human vessels but also in atherosclerotic and restenotic human arteries (Riessen et al. 2001). Strong staining of TSP-5 was found on the vast majority of VSMCs in human atherosclerotic and restenotic lesions (Riessen et al. 2001). These data indicate that TSP-5 may play a role in the pathogenesis of vascular disease setting such as atherosclerosis through regulating VSMC adhesion and migration (Riessen et al. 2001). More recent studies have underscored the important role of TSP-5 in vascular disease (Wang et al. 2009, Du et al. 2011). First, these studies demonstrated that ADAMTS-7 facilitated VSMC migration through cleaving TSP-5 (Wang et al. 2009). TSP-5 was shown to maintain the contractile and quiescent phenotype of VSMCs by

interacting with α7β1 integrin, and it was shown that cleavage of TSP-5 by ADAMTS-7 could switch VSMC phenotype from a quiescent one to a migratory one, facilitating VSMC migration and neointima formation after artery injury (Wang et al. 2009). Another study revealed that TSP-5 bound directly to bone morphogenetic protein-2 (BMP-2) through its C terminus and that inhibited BMP-2 receptor binding blocked BMP-2 osteogenic signaling, indicating that TSP-5 inhibits osteochondrogenic transition of VSMC and that TSP-5 is a novel inhibitor of vascular calcification (Du et al. 2011).

1.6.4.2 Granulin-epithelin precursor (GEP)

GEP, also known as progranulin, proepithelin, or plasma cell-derived growth factor, is a 88 kDa (593-aa) growth factor that is secreted from cells. GEP contains seven and a half repeats of a cysteine-rich motif in the order of P-G-F-B-A-C-D-E, where A-G is full repeat, and P is the one-half motif (Jian et al. 2013). Cleavage of GEP by proteases liberates smaller, 6 kDa peptides, which are named granulin A, granulin B, granulin C, etc. Epithelin 1 and epithelin 2 are synonymous with granulin A and granulin B, respectively. These 6 kDa peptides possess biological activity of their own, such as the ability to inhibit thrombin (Hanby and Zheng 2013). The precursor GEP has distinctive biological functions as well, for instance, it blocks the TNF-α signaling pathway by binding and exerting its anti-inflammatory activities through TNF receptors (Tang et al. 2011, Kawase et al. 2013). Granulin B, on the other hand, stimulates IL-8 expression in epithelial cells and is considered a proinflammatory molecule (Jian et al. 2013). GEP has also been implicated in wound healing, tumor growth and atherosclerosis. GEP is abundantly expressed in several human cancers, such as ovarian cancer (Davidson et al. 2004) and

hepatocellular carcinoma (Ho et al. 2008). An anti-GEP monoclonal antibody reduced tumor cell proliferation and tumor angiogenesis with reduced microvessel density and tumor VEGF level. GEP knock-out mice exhibited severe atherosclerotic lesions compared with GEP wild type mice using an ApoE knock-out background mice model (Kawase et al. 2013). These findings suggest great complexity of its role in human diseases.

Several proteinases have been reported to cleave GEP, including MMP-9, -12, and -14, elastase, and proteinase 3 (Jian et al. 2013). The interaction between ADAMTS-7 and GEP was revealed by a yeast two-hybrid assay, and a Co-IP assay further verified this interaction *in vivo*. Subsequent experiments demonstrated that 4 C-terminal TS repeats of ADAMTS-7 are required and sufficient for its interaction with GEP; each granulin unit of GEP but not the partial repeat is sufficient for binding to ADAMTS-7 C-terminal TS repeats. In an *in vitro* digestion assay, a recombinant ADAMTS-7 catalytic domain was able to cleave GEP and liberate smaller fragments (Bai et al. 2009). More fragments were observed when using intact ADAMTS-7 rather than using the catalytic domain alone, indicating that the full length of ADAMTS-7 cleaves GEP more efficiently. These data indicate that ADAMTS-7 is a novel GEP convertase (Bai et al. 2009). However further evidence is needed. In addition, studies also demonstrated that GEP can interact with TSP-5 and disrupt the cleavage of TSP-5 by ADAMTS-7, indicating these proteins act in concert to form protein-protein networks (Xu et al. 2007, Guo et al. 2010).

1.6.4.3 Alpha2-macroglobulin (A2M)

A2M, a member of the macroglobulin family, is a high-molecular weight homotetrameric glycoprotein found in the blood circulation of different species (Luan et al. 2008). The A2M molecule is synthesised mainly in the liver, but also locally by macrophages, fibroblasts, and adrenocortical cells. Human A2M is found at relatively high levels (2-4 mg/ml) in plasma and is the largest major non-immunoglobulin protein in plasma (Luan et al. 2008). Native A2M is composed of four identical 185 kDa subunits bound together via disulfide bonds, each of which has a unique sequence of amino acids that is susceptible to be cleaved by various proteases. Cleavage of this region, termed the 'bait region', triggers a conformational change in the structure of A2M and consequent entrapment of the proteases. A2M does not inactivate the entrapped proteases, but instead, it hinders the access of substrates to the active site of the proteases. Thus the major function of A2M is inhibition of proteases (Hanby and Zheng 2013, Rehman et al. 2013). A2M may act as a carrier protein because it binds to numerous growth factors and cytokines such as PDGF, basic fibroblast growth factor (b-FGF or FGF-2), TGF-β, TNF-α, IL-1β and IL-6. The biological activity of some growth factors and cytokines is inhibited when bound to A2M, like that of b-FGF, TNF-α and IL-1β, while some remain active, such as PDGF and IL-6 (Rehman et al. 2013).

ADAMTS-7, both in the intact and the truncated recombinant catalytic form, was demonstrated to be able to cleave A2M, as shown by altered migration of the protease and proteolysis of A2M by SDS-PAGE (Somerville et al. 2004). ADAMTS-7 was able to cleave A2M *in vitro*, giving rise to a major cleavage product with molecular weight 180

kDa and a faint fragment with molecular weight 105 kDa. Thus A2M can be considered a substrate of ADAMTS-7, and more importantly, A2M is the first identified endogenous inhibitor of ADAMTS-7 as A2M inhibits ADAMTS-7 mediated TSP-5 cleavage (Luan et al. 2008).

1.6.5 ADAMTS-7 and bone and joint disease

For years, investigation of the physiological roles of ADAMTS-7 has largely focused on its association with the pathogenesis of arthritis and disc disease. It is because of the observation that TSP-5 is predominantly found in the cartilage ECM, accounting for 1% of the wet weight of cartilage, and most importantly, increased fragments of TSP-5 were detected in the serum and synovial fluid of patients suffering from rheumatoid arthritis and osteoarthritis (Liu et al. 2006, Hanby and Zheng 2013). *ADAMTS7* over-expression was also observed in the cartilage and synovium of patients with rheumatoid arthritis. *In vitro* cleavage of TSP-5 by recombinant ADAMTS-7 showed the same TSP-5 cleaved fragments as those found in the serum and synovial fluid of patients with rheumatoid arthritis and osteoarthritis (Liu et al. 2006). A series of studies suggested that under physiological conditions, the expression of normal levels of *ADAMTS7* maintains the basal levels of TSP-5 cleavage in chondrocytes for chondrogenesis. However, in pathological states where *ADAMTS7* expression is up-regulated, the excess TSP-5 cleavage results in degenerative and inflammatory diseases of the joints and intervertebral discs (Liu et al. 2006, Xu et al. 2007, Bai et al. 2009, Hanby and Zheng 2013).

1.6.6 ADAMTS-7 and cardiovascular disease

ADAMTS-7 was first demonstrated to play a role in the pathogenesis of vascular disease in 2008. A study using a rat balloon injury model demonstrated that ADAMTS-7 facilitated VSMC migration by cleaving TSP-5 and promoted neointima formation following vascular mechanical injury (Wang et al. 2009). Neointima formation is regarded as an aggressive response to vessel injury such as that seen following coronary stent implantation (Patel and Ye 2013). Wang et al. demonstrated an initial decrease of ADAMTS-7 protein levels in the vessel wall within the first 24h after vascular injury, followed by a subsequent increase up to 2 weeks with maximal expression after 1 week. Notably, ADAMTS-7 accumulated preferentially in the neointima and colocalised with VSMCs (Wang et al. 2009). Overexpression of *ADAMTS7* in VSMCs by an adenovirus infection method enhanced VSMC migration/invasion in *in vitro* experiments and increased neointima formation *in vivo*, while suppression of *ADAMTS7* by small interfering RNA (siRNA) retarded VSMC migration *in vitro* and ameliorated neointima formation in response to injury *in vivo* (Wang et al. 2009). ADAMTS-7 may exert its effect on VSMC migration by cleavage of its primary substrate TSP-5. TSP-5 fragments increased parallel to ADAMTS-7 levels following mechanical injury of rat carotid artery. Similarly, *ADAMTS7* overexpression greatly decreased the full-length TSP-5 and increased fragments of TSP-5, while suppression of *ADAMTS7* had the opposite effect. Furthermore, replenishment of TSP-5 by adenovirus infection method attenuated ADAMTS-7 mediated VSMC migration (Wang et al. 2009). Concordant results were shown recently in a mouse ADAMTS-7 knockout model where the loss of ADAMTS-7 led to reduced neointima formation following carotid artery injury induced by ligation

(Aherrahrou et al. 2011). Since VSMC migration is an important process in atherogenesis while neointima formation is very relevant to restenosis after angioplasty, the results of these studies implicate ADAMTS-7 as an important player in the pathogenesis of CVDs.

The importance of ADAMTS-7 in CVD has now been further confirmed by GWAS, with several SNPs in the *ADAMTS7* gene locus found to be significantly associated with coronary artery disease (Coronary Artery Disease Genetics 2011, Reilly et al. 2011, Schunkert et al. 2011). However, it has remained unclear as to whether any of these SNPs found by GWAS or other SNPs in LD with them has a functional effect on *ADAMTS7* expression/activity and has an effect on the biological processes related to CAD. Functional studies of these variants at the *ADAMTS7* gene locus will provide possible mechanisms underlying these associations.

Furthermore, how ADAMTS-7 is involved in the pathogenesis of CAD needs to be further investigated. Although TSP-5 is being considered the primary substrate of ADAMTS-7, more substrates of ADAMTS-7 may emerge and further studies will extend our understanding of the disease pathogenesis and indicate possible therapeutic targets for the disease.

1.7 Hypothesis and Aims

1.7.1 Hypothesis

SNPs at the *ADAMTS7* locus could affect *ADAMTS7* mRNA expression and/or protein activity. Through this mechanism, these SNPs regulate VSMC and/or EC cell behaviours (i.e. proliferation, migration, senescence and/or apoptosis) and the development of atherosclerosis (Figure 1.9).

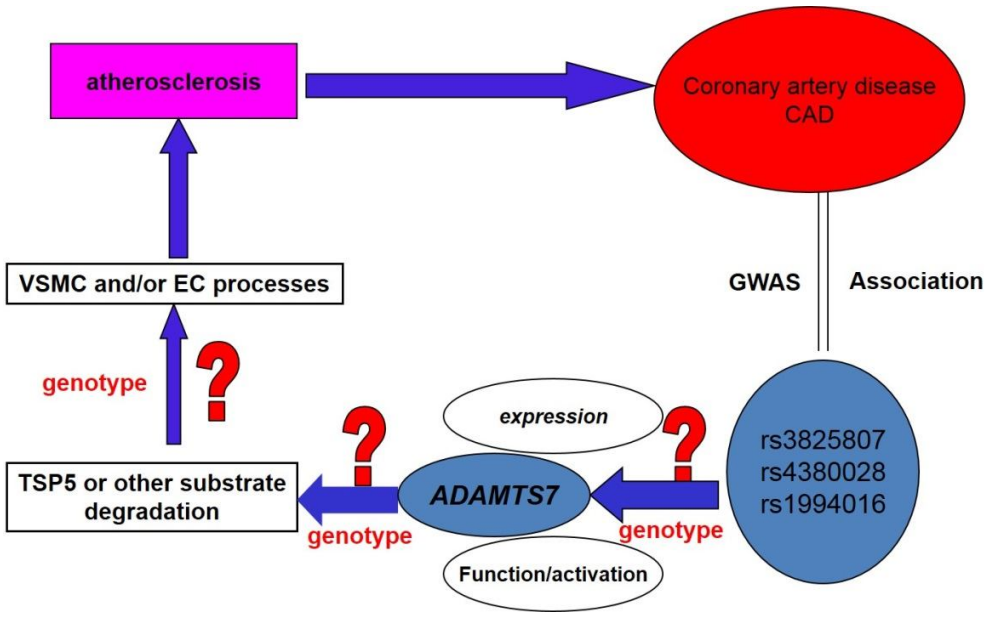

Figure 1.9 Hypothesis

1.7.2 Aims:

1. To investigate effects of CAD-associated variants of the *ADAMTS7* gene on proliferation, senescence, apoptosis and migration of VSMCs and ECs.

2. To study whether CAD-associated variants of the *ADAMTS7* gene influence *ADAMTS7* gene expression in VSMCs and/or ECs.

3. To investigate whether CAD-associated variants of the *ADAMTS7* gene affect ADAMTS-7 protein maturation/activation and TSP-5 cleavage.

4. To investigate effects of CAD-associated variants of the *ADAMTS7* gene on angiogenesis

5. To investigate effects of ADAMTS-7 on angiogenesis and related mechanisms.

Chapter 2 Materials and Methods

2.1 Cell culture

2.1.1 Human vascular smooth muscle cells (VSMCs) isolation and culturing

The protocol for isolating and utilising VSMCs from umbilical cords was approved by the appropriate ethics committee. We used a well-established method (Motterle et al. 2012) to isolate the VSMCs. Briefly, umbilical cords were collected from The Royal London Hospital and placed in physiological saline solution (PSS) buffer for short preservation. Umbilical cords were then put in the Dulbecco's Modified Eagle's Media (DMEM, Sigma) and arteries were dissected out. After carefully removing the adventitia, the vessel was divided into small segments and placed onto 0.2% gelatin (Sigma) coated T25 flasks. In order to facilitate attachment of the arterial segments to the flasks, the flasks were incubated in a humidified incubator 37˚C/5% CO_2 (all cell culture work in this project was carried out under this condition unless otherwise stated) for 2 hours upright to drain excess media. Then DMEM, supplemented with 20% FBS (Gibco), 2mM L-glutamine (Sigma), 1% penicillin and streptomycin (Sigma), was added into the flasks. The flasks were placed in an incubator for 7 days without any disturbance. After this period media were replaced every 2-3 days, until cells reached 70% confluence, the remaining tissue blocks were removed, and cells were harvested with 0.25% trypsin-EDTA (Sigma) and passaged into sterile T25 flasks coated with 0.04% gelatin.

VSMCs were maintained with Smooth Muscle Cell Growth Media 2 (PromoCell, detailed supplements of this media, please see Appendix Table 2.1.1). At about 90% confluence, cells were harvested and subcultured in the ratio of 1:3 to three new 0.04% gelatin coated T25 flasks with the Smooth Muscle Cell Growth Media 2. Passage 2 to passage 5 VSMCs were used in this project.

2.1.2 Human umbilical vein endothelial cells (HUVECs) isolation and culturing

HUVECs were generously donated by Centre for Biochemical Pharmacology of William Harvey Research Institute. They were isolated using a well-established method (Ulrich-Merzenich et al. 2002). Briefly, umbilical cords were collected from The Royal London Hospital and placed in physiological saline solution (PSS) buffer for short time preservation. During the isolation, Hank's Buffered Salt Solution (HBSS) was perfused to remove the blood remaining inside the umbilical vein. Afterwards, 3 ml of collagenase type I (1mg/mL in HBSS) was injected inside the vein and incubated for 15 minutes at 37℃ with agitation. Thereafter, 20 ml of M199 media supplemented with 10% human serum was used to neutralize the collagenase type I and to collect the free ECs. HBSS perfusion was followed aiming at collecting more cells. All cells were then centrifuged at 250 g for 5 minutes at RT. The cell pellet was then resuspended in M199 media supplemented with 10% human serum and transferred to a (0.2%) gelatin-coated T75 flask and incubated at 37°C, under a 5% CO_2 humidified atmosphere.

Primary EC culture was maintained with M199 (Sigma) media supplemented 15% FBS (Gibco) and EC culture growth factors (Final growth factor supplements concentration as described in Appendix Table2.1.2). Once the cells reached 90-100% confluence, cells were harvested with trypsin-EDTA and subcultured in the ratio of 1:3 into three sterile T75 flasks coated with 0.04% gelatin. Supplemented M199 media, prepared on described above, was used to further culture.

2.1.3 Human Embryonic Kidney 293 (HEK293) cell line culturing

Human Embryonic Kidney 293 (HEK293) cells were generously provided by Dr. Sadani Cooray from the Centre for Biochemical Pharmacology, William Harvey Research Institute. As the name implies, HEK293 cells, an adherent cell line, was originally derived from human embryonic kidney cells. Briefly, they were obtained from an aborted healthy fetus without known identity of the mother and the reason for the abortion. Then, these cells were cultured and transformed with an adenovirus. The number, 293, indicates 293rd experiment. HEK293 cells are very easy to grow and to be transfected and have been widely used in cell biology research for many years.

HEK293 cells were maintained in DMEM supplemented with 10% FBS, 2mM L-glutamine, 1% Penicillin-Streptomycin. Media was replaced every 2 days. At 90% confluence, cells were detached by Trypsin-EDTA and re-suspended at 1:3 dilutions in new flasks containing fresh pre-warmed media.

HEK293T cells were a generous gift from Dr. Qingzhong Xiao. HEK293T cell line, a variant of HEK293 cell line, contains the SV40 Large-T-antigen which allows for amplification of transfected plasmids and extended temporal expression of the desired gene products. This cell line is commonly used for the production of various viral vectors. HEK293T cells were maintained in DMEM supplemented with 10% FBS at 37˚C incubator with a humidified atmosphere and 5% CO_2. Media was replaced every 2 days. Once the cells reached 90% confluence, cells were harvested and re-suspended at 1:3 dilutions in new flasks containing fresh pre-warmed media.

2.1.4 Preservation and recovery of cells

Both isolated primary VSMCs, HUVECs and HEK293 cell line were preserved in liquid nitrogen for long term storage. Cells were cultivated to confluence, detached by Trypsin-EDTA and re-suspended in freezing media (10% dimethylsulfoxide, 40% DMEM and 50% FBS) in cryovials at a concentration of 1 x 10^7 cells/ml. To prevent cell death during freezing, cells were initially taken down gradually to -80℃ using a freezing container (Nalgene® Mr. Frosty), and then transferred to liquid nitrogen for long-term storage.

During recovery, cells were taken out from liquid nitrogen and transported on dry ice, quickly thawed by incubating at 37℃ in a water bath. After centrifuging at 250 g for 5 minutes, cells were re-suspended in fresh pre-warmed media and plated onto appropriate tissue culture plastics for further experiments.

2.2 Immunocytochemistry of VSMC marker and ADAMTS-7

Immunocytochemistry (ICC) is a commonly used technique, allowing visualisation of intracellular or extracellular proteins. This is achieved through the interaction between these proteins and their specific antibodies which are in turn labeled with enzymes or fluorophores. These tags develop color change or fluorescence which can be detected to show the localisation and/or interaction of proteins in any particular cell type. (For the titrations and the details for these antibodies used in ICC, see Appendix Table 2.2.1).

VSMCs were harvested and seeded 25,000 cells per chamber well in 0.04% gelatin coated BD Falcon^{TM} 8 chamber culture slides (BD Biosciences) with Smooth Muscle Cell Growth Media 2, after 24 hours further culturing, ICC assays were performed.

2.2.1 Verification of VSMCs by the specific marker alpha-actin

To check the homogeneity of the isolated VSMCs cultures, immunocytochemistry was used to detect markers for VSMC (α-smooth muscle actin, SMA), fibroblasts (DDR2) and ECs (CD144). 8 isolated primary VSMC cell lines from different individuals were chosen randomly for the immunocytochemical assays, 4 of which were subjected to double staining of alpha-actin and DDR2, the other 4 cells were stained with CD144. After 24 hours culturing in BD Falcon^{TM} 8 chamber culture slides, cells were fixed with 4% paraformaldehyde in PBS for 15 minutes at room temperature. Thereafter, the cells were treated with (for double staining) or without 0.1% triton X-100 before blocking with 1% bovine serum albumin (BSA) in PBS for 30mins, and then incubated with a goat anti-

human DDR2 polyclonal antibody (Santa Cruz Biotechnology) or a mouse anti-human CD144 monoclonal antibody (Santa Cruz Biotechnology), for 60mins at room temperature. The cells were then washed and incubated with a rabbit anti-goat IgG antibody conjugated with FITC fluorescence (Dako) and a mouse anti-human SMA monoclonal antibody conjugated with Cy3/red fluorescence (Sigma), or a rabbit anti-mouse IgG antibody conjugated with FITC fluorescence (Dako). Subsequently, the cell nuclei were stained with 4, 6-diamidino-2-phenylindole (DAPI). After mounting with fluorescent mounting media (Dako), the cells were visualised using a fluorescence microscope with a digital imaging system.

2.2.2 ADAMTS-7 staining in VSMCs

Eight isolated primary VSMC cell lines were randomly chosen and subjected to ADAMTS-7 ICC staining. The cells were fixed, permeablised and blocked as described before and then incubated with a rabbit anti-human ADAMTS-7 (spacer domain) polyclonal antibody (Abcam, this antibody was used for ADAMTS-7 staining in ICC and IHC assays). After washing, the cells were incubated with a goat anti-rabbit IgG antibody conjugated with FITC fluorescence (Santa Cruz Biotechnology) and a mouse anti-human SMA monoclonal antibody conjugated with Cy3/red fluorescence (Sigma). Nuclei were stained with propidium iodide (PI). The slides were observed using confocal fluorescent microscope (Leica Microsystems, TCS SP5 MP) after mounting with fluorescent mounting media (Dako, S3023).

2.3 Immunohistochemical staining of human atherosclerotic plaque

Similar to ICC staining, immunohistochemistry (IHC) staining can allow the visualization of a protein in the tissue sections by interaction between the protein and its specific antibody which is labeled with an enzyme or a fluorophore. In this study, formaldehyde-fixed paraffin-embedded human carotid and coronary atherosclerotic plaque sections were used to detect the presence of ADAMTS-7 (Details for antibodies used in this section, please see Appendix Table 2.3.1)

2.3.1 ADAMTS-7 and SMA double immunofluorescent staining in carotid atherosclerotic plaques

Human carotid atherosclerotic lesions were collected from several hospitals in UK, including St. Bartholomew's Hospital, Royal London Hospital, Cumberland Infirmary and Ayr Hospital. This work has been approved by Research Ethical Committee (REC, Project Number: 08/H0704/140). The plaque samples were collected from patients undergoing carotid artery endarterectomy procedure, fixed in formalin and transported to our lab. These samples were then embedded by paraffin and sectioned by Pathology Facility at the Barts Cancer Institute.

Before staining, these sections were deparaffinised, rehydrated and incubated with sodium citrate for antigen retrieval. Briefly, all the sections were incubated at 45℃ for 30 minutes to facilitate the attachment of the tissue sections to the slides before being deparaffinised

in xylene. Subsequently, these sections were incubated in 100% ethanol, 70% ethanol and distilled water to rehydrate. The sections were then incubated in a pre-warmed retrieval solution (10mM sodium citrate, 0.05% Tween-20, pH 6.0) in a water bath at 95˚C for 30min to retrieve antigens.

For fluorescence immunohistochemical staining, sections were blocked with 1% bovine serum albumin. A mouse anti-human SMA antibody conjugated with Cy3/red fluorescence (Sigma), and a rabbit anti-human ADAMTS-7 (spacer domain) antibody along with a goat anti-rabbit IgG antibody conjugated with FITC fluorescence (Santa Cruz Biotechnology) were used for double staining. Nuclei were stained with DAPI (4, 6-diamidino-2-phenylindole). After mounting, slides were examined using a laser scanning microscope (Zeiss LSM 510 Mark 4) and images taken using a digital camera.

2.3.2 ADAMTS-7, TSP-5 and vWF single staining in carotid atherosclerotic plaques

The same deparaffinisation and blocking procedures were carried out as described in section 2.3.1. Then sections were incubated with a rabbit anti-human ADAMTS-7 (spacer domain) antibody (Abcam) or a rat anti TSP-5 antibody (Millipore) or a rabbit anti-human vWF antibody (Abcam). Subsequently, the sections were incubated with a goat anti-rabbit IgG antibody conjugated with HRP or a Rabbit anti rat antibody conjugated with HRP (Dako), followed by DAB and counterstain with haematoxylin. After mounting, slides were examined and images were taken using a microscope with a digital camera.

A blocking peptide (Abcam) matching the epitope of the ADAMTS-7 (spacer domain) antibody (Abcam) was used to verify the specificity of ADAMTS-7 staining in carotid atherosclerotic plaque sections. Briefly, the rabbit anti-human ADAMTS-7 (spacer domain) antibody (Abcam) was incubated without or with a blocking peptide (Abcam) matching the epitope of this antibody (in the ratio of 5:1, 5 times amount of blocking peptide). After deparaffinization and retrieval of antigen, blocking with 3% H_2O_2 and 10% goat serum, the sections were then incubated with ADAMTS-7 (spacer domain) antibody solution or peptide blocked antibody solution, followed an anti-Rabbit secondary antibody conjugated with HRP (Dako), then DAB (3,3´-diaminodbenzidine) and subsequently and counterstain with haematoxylin. After mounting, slides were examined and images taken using a microscope with a digital camera.

2.3.3 ADAMTS-7 and SMA double staining in coronary atherosclerotic plaques

Formaldehyde-fixed, paraffin-embedded sections of coronary atherosclerotic plaque sections were generously provided by Dr. Poston from the Centre for Microvascular Research, William Harvey Research Institute. The same deparaffinisation and blocking procedures were carried out as described in section 2.3.1. The sections were then subjected to staining using a mouse anti-human SMA antibody (Dako) and a rabbit anti-human ADAMTS-7 (spacer domain) antibody (Abcam), then with a biotinylated swine anti-rabbit IgG secondary antibody (Dako) and subsequently an anti-mouse IgG alkaline phosphatase conjugated secondary antibody (Sigma), followed by avidin-conjugated

horseradish peroxidase (HRP), then DAB and subsequently NBT/BCIP (nitro-blue tetrazolium/5-bromo-4-chloro-3'-indolyphosphate). A methyl green counterstain was used before dehydrating and mounting the slides. The percentage of ADAMTS-7 stain area in coronary atherosclerotic plaque area and the percentage of SMA stain area in plaque area were quantified with the use of Image-Pro Software (Media Cybernetics).

2.4 Genotyping

Cell pellets of cultured VSMCs and ECs were collected for isolation of genomic DNA. Genomic DNA was isolated using the Wizard SV Genomic DNA Purification System (Promega). DNA concentrations of all samples were measured by Nanodrop2000 and diluted to 5 ng/μl for future use.

2.4.1 Genotyping by the KASPar method

Genotyping for rs3825807, rs1994016 and rs4380028 were performed by the KBiosciences Competitive Allele Specific PCR genotyping system (KASP) method. KASP is a homogeneous, fluorescent, endpoint-genotyping technology. Briefly, two allelic specific forward primers (one for each SNP allele) are designed; each of them contains a unique unlabelled tail sequence at the 5' end. One common reverse primer is designed as well. Two 5' fluor-labelled oligos, one labelled with FAM and one with HEX with sequences complementary to the 5' unlabelled tail of allelic specific primers. Quencher oligos bind with the fluor-labelled oligos quenching the fluorescent signal until required. In the initial stage of PCR, the appropriate allelic specific primer binds directly

to SNP upstream of the DNA template (with the 3' end of the primer positioned at the SNP site), the common primer also binds to template and the PCR proceeds. After the allelic specific primers incorporate into the new synthesised DNA sequence, the fluor-labelled oligos can bind to the 5' tail of the allelic specific primers, activating the fluorescence signal. If the DNA template only has one allele (homozygote), then only allelic specific primer can bind and one fluorescence signal can be detected (either FAM or HEX), and if the template has two alleles (heterozygote), then mixed signals will be detected (Figure 2.1). According the fluorescence signals, the genotype of DNA samples can be called. (Figure 2.2)

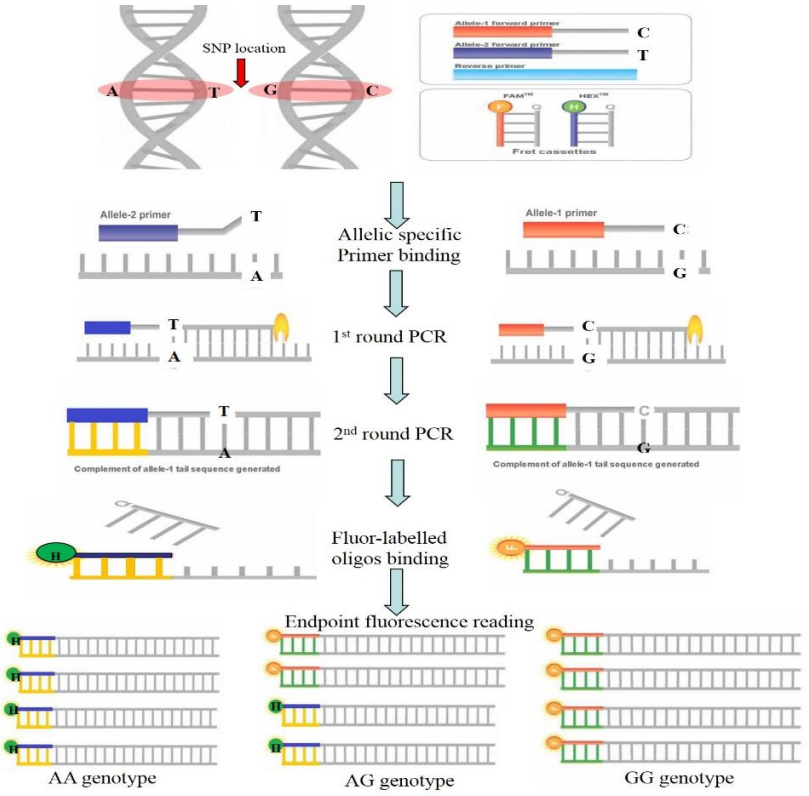

Figure 2.1 Schematic representation of the KASPar genotyping method (Cited and modified from http://www.lgcgenomics.com/genotyping/kasp-genotyping-reagents/how-does-kasp-work/).

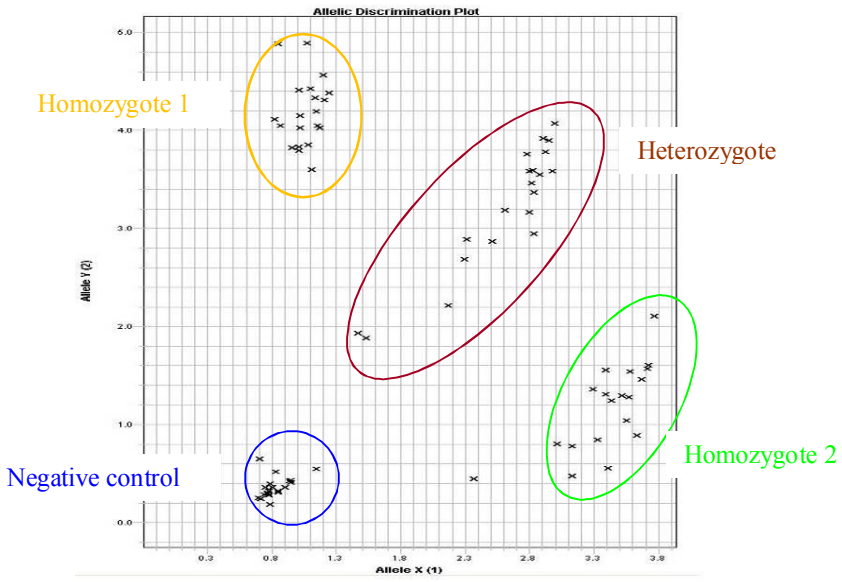

Figure 2.2. A representative KASPar genotyping clusters.

Briefly, 7.5ng of DNA template of each VSMC or EC was added into 384 well micro-plates and dried overnight, then the reaction mix was added into each of the wells and subjected to PCR (please see Appendix Table 2.4.1 for primers' sequence), subsequently, fluorescence signals were detected by ABI Prism 7900 HT Sequence Detection System (Applied Biosystems) and the results were analysed by ABI Prism software version 2.3. The genotyping data were exported from the SDS software in a text file and the fluorescent calls were converted into allele calls. The genotype frequencies were checked for agreement with Hardy-Weinberg equilibrium using the HWE program (http://www.oege.org/software/hwe-mr-calc.shtml).

2.4.2 VSMC Genotyping for rs3825807 by restriction enzymes

A restriction enzyme, also known as restriction endonuclease, is an enzyme that cuts DNA at specific recognition nucleotide sequences known as restriction sites. For one known SNP, the DNA sequence at the SNP location will vary between the alleles. If we can find one restriction enzyme can only recognise one allele but can not recognise the other one, and then this restriction enzyme can be used to distinguish the genotypes of DNA samples. To minimize the recognition site, the PCR technique is usually used to amplify a short fragment of DNA sequence that contains the SNP location. After amplification of DNA template, the PCR products are subjected to restriction enzyme digestion. Afterwards, PCR products are loaded on a 2% Agarose Gel and electrophoresis is performed. Different genotypes will display different band patterns. According to the number and the size of the bands, genotypes of the DNA samples can be called. This method is much more time consuming, so can only be used for small number of samples.

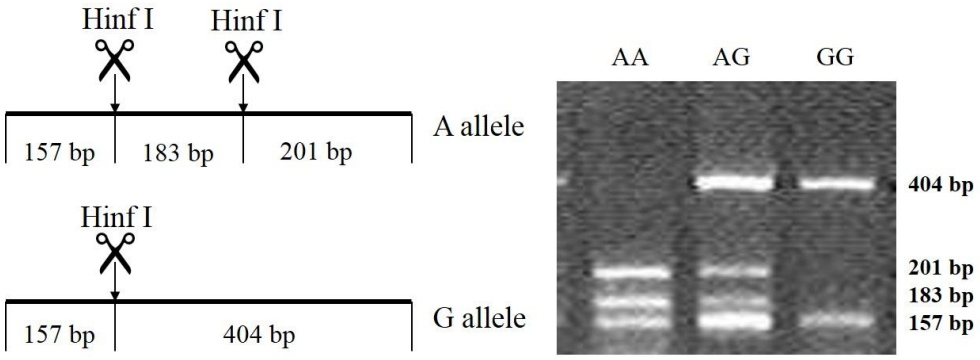

Figure 2.3. A Schematic representation of the restricted enzyme digestion and representative genotyping results.

The genotyping results of VSMC samples for rs3825807 were verified by the restriction enzyme digesting method described above. The relevant sequence containing rs3825807 was obtained from dbSNP website (http://www.ncbi.nlm.nih.gov/projects/SNP/). The NEBcutter V2.0 software (http://tools.neb.com/NEBcutter2/index.php) was used to search for differences in restriction sites between the different alleles. Hinf I was identified as a suitable restriction site for rs3825807 genotyping. PCR forward and reverse primers were designed using primer3 software (available at http://frodo.wi.mit.edu/, Appendix Table 2.4.2). The primers were designed in order to obtain a PCR product of about 561bp. However, there is another Hinf I recognition site in the PCR product sequence, which can cut both alleles of SNP rs3825807. This allowed the discrimination of the bands by agarose gel electrophoresis as cutting of the PCR products by the restriction enzyme will generate one fragment of 157bp and another of 404bp for G/G genotype, while for A/A genotype, three bands of 157bp, 201 bp and 183 bp will be detected. For A/G genotype, the Hinf I digestion will generate 4 bands of 157 bp, 183 bp, 201 bp and 404 bp (Figure 2.3). Briefly, DNA fragment containing rs3825807 site were amplified by PCR (PCR reagents and conditions are described in Appendix Table 2.4.3). The conditions for Hinf I (New England Biolabs Inc.) digestion of the PCR product was 37˚C for 24 hours. Afterwards, the samples were subjected to electrophoresis on a 2% agarose gel and the bands were visualised by a UV imaging system.

2.4.3 Genotyping by sequencing

DNA sequencing is the process of determining the nucleotide order of a given DNA fragment. The most commonly used DNA sequencing method is Sanger sequencing. In this method, a primer, a DNA polymerase, and four deoxynucleotides are used to generate new DNA strands that are copied from the DNA template. Four di-deoxynucleotides are also included to randomly terminate the DNA strand extension, thus resulting in a series of related DNA fragments that differ in length. The fragments are then size-separated by electrophoresis in a slab polyacrylamide gel, and the orders of the nucleotide of the DNA fragments can be determined. An alternative approach is to label each of the dideoxynucleotide chain-terminators with a separate fluorescent dye, which fluoresces at a different wavelength, these are detected and represented as 'peaks' of different colours, which can then be interpreted to determine the base sequence.

The genotype of rs3825807 for some of the samples was further verified by sequencing. Briefly, 13 VSMCs DNA samples were randomly chosen and amplified by PCR using the primers and conditions described in section 2.4.2. After electrophoresis on 2% agarose gel, the PCR products were purified by SV gel and PCR clean-up system (Promega), and subjected to fluorescent dideoxy sequencing (Sanger sequencing) carried out by The Barts and The London Genome Centre. According to the colors of peaks at rs3825807 location, the genotype of these DNA samples were determined.

2.5 Cell proliferation, senescence and apoptosis assays

These assays are designed to study whether the CHD-associated SNPs in *ADAMTS7* locus affect SMC and/or proliferation, senescence and apoptosis, which play vital roles during the pathogenesis of atherosclerosis. One day before the assays, VSMCs or ECs were trypsinized and seeded in duplicate in 96 well-plates (5,000 cells per well) and cultured in proper cell culture media (described before) overnight to let the cells settle down.

2.5.1. Proliferation assay

2.5.1.1 VSMC proliferation assay

5-Bromo-2'-deoxy-uridine (BrdU), a synthetic nucleoside that is an analog of thymidine, is not normally present in cellular DNA. However, during fast cell growth, if BrdU is present in high concentrations in the culture media, it can be incorporated into the cellular DNA, substituting for thymidine during DNA replication. The amount of BrdU incorporated is determined by a standard ELISA protocol, which involves "tagging" the incorporated nucleotide with an anti-BrdU antibody. And the amount of the BrdU is linear with proliferation of the cells. 5-bromo-2'-deoxy-uridine (BrdU) Labelling and Detection Kit III (Roche) was used to assess the proliferation of VSMCs. By this assay, proliferation of these isolated VSMCs can be measured to analyse whether SNPs in *ADAMTS7* locus affect SMC proliferation.

For the proliferation assay, VSMCs were cultured for a further 12 hours in fresh media in the presence of 10μM BrdU. The labeled cells were then fixed with ethanol. Prior to incubation with a monoclonal antibody to BrdU, DNA was partially digested with nucleases to allow the antibody to access BrdU. Next, the anti-BrdU antibody [labeled with peroxidase (POD)] was added. Finally, the POD substrate ABTS was added. POD catalyzes the cleavage of ABTS, producing a colored reaction product. The absorbance of the samples (at approx. 405 nm) is determined with a standard microplate (ELISA) reader.

2.5.1.2 EC proliferation assay

The following cells were used for EC proliferation assays:

ECs with different genotypes for rs3825807
ECs transfected with pcDNA3.1 vector control plasmid
ECs transfected with *ADAMTS7-214Ser* plasmid
ECs transfected with *ADAMTS7-214Pro* plasmid
ECs infected with non-target pLKO.1 control lentiviral particles
ECs infected with *ADAMTS7* shRNA lentiviral particles

Cell proliferation assay kit (Fluorometric-Blue) was used to detect cell proliferation following manufacturer's protocol. Briefly, 5000 cells / well were seeded into a 96-well plate. Twenty four hours later, fresh media with 10% proliferation assay reagent was added to the cells and they were further incubated for 6 hours. They were then harvested and subjected to fluorometer reading (Manual VICTOR2™, with Fluorescence and

Luminescence Technologies). The basic mechanism is that the proliferation assay reagent contains the redox dye resazurin which is not fluorescent, but upon reduction by viable metabolically active cells, the dye becomes highly fluorescent and the fluorescent signal is linear with viable metabolically active cell number. Therefore, viable metabolically active cells can be easily measured. BrdU assay was also performed to confirm the results of proliferation assay (please consult section 2.5.1.1 for full methodology description).

2.5.2 VSMC senescence assay

Senescence Associated ß-galactosidase (SA-ß-Gal) is an enzyme present in senescent cells, and it catalyzes the hydrolysis of X-gal, which produces a blue color in senescent cells. Thus the activity of this enzyme is used as a marker for senescence of cells.

After the overnight culture, cell senescence was assessed using a 96-Well Cellular Senescence Assay Kit (Cell Biolabs Inc) to quantify SA-ß-Gal as per manufacturer's instructions.

2.5.3 VSMC apoptosis assay

Apoptosis is a form of eukaryotic cell death (also known as programmed cell death), which is distinct from necrosis. Unlike necrosis which is characterised by cell swelling and rupturing of the plasma membrane due to its increased ion permeability, apoptosis is characterised by membrane blebbing, condensation of the cytoplasm, and the activation

of an endogenous endonuclease. This Ca^{2+}- and Mg^{2+}-dependent nuclease cleaves double-stranded DNA at the most accessible internucleosomal linker region, generating mono- and oligonucleosomes. In contrast, the DNA of the nucleosomes is tightly complexed with the core histones H2A, H2B, H3, and H4, and is thus protected from cleavage by the endonucleases. The yielded DNA fragments are discrete multiples of a 180-bp subunit, detected as a "DNA ladder" on agarose gels after extraction and separation of the fragmented DNA. The enrichment of mono- and oligonucleosomes in the cytoplasm of the apoptotic cell is due to the fact that DNA degradation occurs several hours before the plasma membrane breakdown, thus it can be used to detect apoptosis of cells.

For the apoptosis assay, after the overnight culture, cell apoptosis was measured using a Cell Death Detection ELISAPLUS kit (Roche) to quantify histone-complexed DNA fragments. After lysis of the cells, cell lysates were placed into a streptavidin-coated microplate and incubated with a mixture of anti-histone-biotin and anti-DNA-peroxidase. During the incubation interval, nucleosomes will be captured via their histone component by the anti-histone-biotin antibody, which will in turn be fixed to the streptavidin-coated microplate. Simultaneously, anti-DNA-peroxidase binds to the DNA part of the nucleosomes. After removal of the unbound antibodies, the amount of peroxidase retained in the immunocomplex is photometrically determined with ABTS as the substrate.

2.6 Migration assay

In order to investigate whether these CAD-associated SNPs affect the VSMC and/or EC migration, *in vitro* wound healing(scratch assays) and trans-well cell migration assays were performed.

2.6.1 Migration assay (Scratch assay)

The *in vitro* scratch assay is an easy straightforward method to study cell migration *in vitro*. This method is based on the observation that, upon creation of a new artificial gap, so called "scratch", on a confluent cell monolayer, the cells on the edge of the gap will move toward the opening to close the "scratch" until new cell-cell contacts are established again. The basic steps involve creation of a "scratch" on a monolayer of cells, capture of images at regular intervals during cell migration to close the scratch, and finally, the comparison of the images to determine the rate of cell migration (Liang et al. 2007).

2.6.1.1 VSMC scratch assay

VSMCs were cultured on 6-well plates. When cells reach 100% confluence, parallel lines were drawn with a maker pen on the back of each well and a linear wound was made vertical to these parallel lines by scraping cells with a sterile pipette tip. After washing the cells with PBS once and DMEM once, different media treatments were performed as below:

(1) Complete media: DMEM supplemented with 15% FBS

(2) Serum-free media

(3) Serum-free media with 10ng/ml PDGF-BB

(4) A/A genotype VSMC conditioned media

(5) G/G genotype VSMC conditioned media

Images of the wound at each crossing of the parallel lines and the gap were taken using an inverted microscope with a digital camera. The cells were then incubated at 37˚C with 5% CO_2, and images of the wound at each crossing of the parallel lines and the gap obtained again after 6, 9, and 12 hours, respectively. Image software was used to measure the distances between two edges of the wound of each picture taken at 0, 6, 9, 12 hours, respectively, and then the differences in distance between the two edges at the same crossing at 6, 9 and 12 hours comparing to the 0h point, respectively, were calculated. In media swapping assays, at the outset of the migration assay (i.e. at hour 0), the culture media of G/G genotype cells were replaced by A/A genotype cell conditioned media, and vice versa.

2.6.1.2 EC scratch assay

In order to investigate whether functional SNP rs3825807 affects EC migration, a migration assay was performed using ECs with different genotype of rs3825807. Effects of *ADAMTS7* over-expression and knock-down on EC migration were also investigated by scratch assay, using the following cells:

ECs with different genotypes of rs3825807

ECs transfected with pcDNA3.1 vector control plasmid

ECs transfected with *ADAMTS7-214Ser* plasmid

ECs transfected with *ADAMTS7-214Pro* plasmid

ECs infected with non-target pLKO.1 control lentiviral particles

ECs infected with *ADAMTS7* shRNA lentiviral particles

The assay was carried out as previously described (Liang et al. 2007). In brief, ECs were cultured on 12-well plates. When cells reached 100% confluence, parallel lines were drawn with a marker pen on the back of each well and a linear wound was made vertical to these parallel lines by scraping cells with a sterile pipette tip. After washing the cells with PBS and M199 media, fresh Human Endothelial-SFM (Life Technologies) was added. Thereafter, images of the wound at each crossing of the parallel lines were taken using an inverted microscope with a digital camera as time point 0 hour. The cells were incubated at 37˚C with 5% CO_2, and images of the wound at each crossing of the parallel lines obtained again after 3, 6, and 9 hours. Image software was used to measure the distances between two edges of the wound at each crossing of the parallel lines at 0, 3, 6, 9 hours. Then the difference in distance between the cell edges at fixed points compared at the different time point with 0h as reference was calculated.

2.6.2 VSMC trans-well migration assay

Trans-well migration assay employs a 24 well plate and an insert chamber which has a filter with 8-μm pore. The cells are seeded onto the insert chamber and high serum media or media containing specific chemoattractants is added into the chamber of 24-well plate. Then, cells migrate from the top chamber through the coated filter pores to the bottom chamber due to higher concentrations of nutrients or of chemoattractants. Calculation of the migrated cell number and comparison with different experimental groups will give quantitative results of cell invasive/migratory ability.

Trans-well migration assays were performed using polycarbonate membrane inserts (8-μm pore size; Greiner Bio-One Inc.) in 24-well cell culture plates. For each well, 50,000 VSMCs were seeded into the insert chamber covered with 200 μl of different media, as listed below:

(1) Serum-free media with 1% BSA
(2) HEK293 cell conditioned media containing ADAMTS-$7_{Pro\text{-}Cat}$-214Ser
(3) HEK293 cell conditioned media containing ADAMTS-$7_{Pro\text{-}Cat}$-214Pro

The inner chambers were pre-coated with 0.1% gelatin, and 500μl serum-free media with 1% BSA and PDGF-BB (100ng/ml, Sigma) were added in the chamber of 24-well plate. After incubating at 37°C for 6 and 9 hours, cells remaining inside the inner chamber were completely scraped off with cotton swabs, and cells that had migrated through to the lower surface of the insert were fixed in 4% paraformaldehyde, followed by haematoxylin

staining. Images of five random high power fields (200x) were taken from each inset, and cells were counted by using Image J. Migration activity was expressed as the mean number of cells that had migrated per well from the representative five random high power fields.

2.7 Real-time reverse transcription PCR (qRT-PCR)

SNP rs3825807 is located in the coding region and is a non-synonymous SNP resulting in a serine (Ser) to proline (Pro) substitution in the pro-domain of ADAMTS-7 (Schunkert et al. 2011). SNP rs1994016 resides in intron 8 of *ADAMTS7*, whilst SNP rs4380028 is located 7.6 kb upstream of the gene. Considering their physical locations in relation to the *ADAMTS7* gene, they might have an influence on *ADAMTS7* mRNA expression.

In order to investigate whether these SNPs affect expression of *ADAMTS7* mRNA and thus may be linked with coronary artery disease, qRT-PCR was used to determine whether genotype-specific differences in mRNA level exist.

2.7.1 RNA isolation

Total RNA of VSMCs and ECs were isolated from their pellets using SV total RNA isolation kit (Promega). Briefly, cells were cultivated in the condition described in section 2.1, at about 90% confluence, cells were washed with ice-cold PBS several times and harvested by scraping, and then cell pellets were collected by centrifuging at maximum speed for 2 minutes. Afterwards, 150 µl of lysis buffer provided with the kit was added to

lyse the pellets, and then the extraction was performed following the instructions of the kit. RNA concentration was measured by NanoDrop Spectrophotometer ND-2000.

2.7.2 cDNA synthesis

Total RNA samples of VSMCs and ECs were reverse transcribed into cDNA using ImProm-II™ Reverse Transcription System (Promega). Briefly, 1.25 μg of total RNA with 0.5ug of random primers were mixed (total volume 10 μl) and heated at 70℃ for 5minutes to melt secondary structure within the template, subsequently, samples were quickly chilled at 4℃ for 5 minutes. Then samples were subjected to RT-PCR to synthesise cDNA (PCR reagents and conditions are outlined in Appendix Table 2.7.1). After RT-PCR, all the cDNA samples were diluted to 5 ng/μl for real-time PCR.

2.7.3 Real-time RT-PCR

Real-time RT-PCR, also called quantitative RT-PCR (qRT-PCR) is a PCR based technology, which is used to simultaneously amplify and quantify a targeted DNA sequence. Complementary DNA samples are reverse transcribed from RNA samples. Instead of the end-point detection of PCR reaction product in standard PCR, this procedure is able to detect the reaction progress in real time, by labelling the new synthesised DNA during the reaction. The detected quantity of mRNA could be expressed as absolute copies of DNA templates in the samples or relative amount when normalised to additional normalising genes, such as 18s rRNA, beta-actin or GAPDH. These genes are required

for the maintenance of basic cellular function, and their expression level is relatively constant.

Two common labelling methods are used in this procedure; one is using non-specific fluorescent dyes that can intercalate with any double-stranded DNA; the other one is using sequence-specific DNA probes that are labelled with a fluorescent reporter, and this reporter only permits detection after hybridisation of the probe with its complementary DNA target. Comparing these two methods, the former one does not need a specific probe which is expensive, but can lead to greater variations in final results. The later method offers more accurate results at the expense of the assay. The most commonly used probe method is TaqMan Gene Expression Assay.

In this assay, two primers and one probe are provided, which can recognise specifically to target DNA sequence. The TaqMan probe has a fluorophore (reporter) labelled to the 5'-end of the oligonucleotide probe and a quencher at the 3'-end of probe. The emission of fluorescence signal by reporter is inhibited by the quencher as long as they are in proximity. During the extension of DNA strand, the annealed probe to the target sequence can be displaced and cleaved by the exonuclease activity of Taq polymerase, thus the reporter is separated from quencher and the fluorescence signals can be detected by an ABI Prism 7900HT instrument. During each cycle of the PCR process, fluorescence signal can be detected; hence, DNA templates can be quantified in real time during the process according to the fluorescence signals release from reporter.

After qRT-PCR, each sample will have an amplification curve, which contains a baseline phase, log-linear phase and plateau phase. A threshold line for detection of DNA-based fluorescence is set above the baseline phase and crossing the log-linear phase. This line was chosen automatically by the SDS software, but can be set up manually as well. The number of cycles at which the fluorescence exceeds the threshold is called the threshold cycle (C_t). Once the reaction done, Ct values for each gene were given by the SDS software, and then the ΔΔCt method was used to calculate the relative expression differences among different genotype groups.

The house-keeping gene beta-actin was used as internal reference to normalise gene expression in different genotype groups. The TaqMan Gene Expression Assay was used (Probes, qRT-PCR reagents and conditions are described in Appendix Table 2.7.2). The cDNA samples were loaded into a 384 well plate and running on Applied Biosystem 7900HT by the Barts and The London Genome Centre. And the results were analysed by the software SDS 2.3.

2.8 Allelic imbalance analysis

Allelic imbalance analysis is another method used in this study to investigate the effect of SNPs (Wang and Elbein 2007) on expression of *ADAMTS7* mRNA level. Both cDNA and gDNA samples were amplified by PCR and subjected to fluorescent dideoxy sequencing, the allelic ratio of cDNA was compared and normalised to the ratio of gDNA.

Unlike qRT-PCR, where the expression level of *ADAMTS7* mRNA is compared between different individuals with different genotypes, the method of allelic imbalance analysis compares the allelic expression level in mRNA of heterozygotes for SNP rs3825807. If the SNP affects the expression of mRNA levels of *ADAMTS7*, then one allele should have higher expression level of the mRNA than the other allele. This could be due to allelic-specific binding of transcriptional factors, microRNA or other elements that can regulate gene expression. For instance, individuals in heterozygous for rs3825807, as observed in the GWAS, allele A is associated with CAD. If rs3825807 affects the expression level of *ADAMTS7* mRNA, then the mRNA level of A allele should be higher than the level of G allele. If this were the case, after the sequencing, the allelic ratio of A/G should be >1 after normalisation by ratio of gDNA, otherwise, the SNP does not affect expression of mRNA level.

VSMC gDNA and cDNA samples were prepared as described in section 2.1.4 and 2.1.7. *ADAMTS7* cDNA sequence was obtained from Ensembl and PCR primers for amplification of a sequence containing the SNP rs3825807 were designed by the Primer3Plus programme (http://www.bioinformatics.nl/cgi-bin/primer3plus/primer3plus.cgi/). PCR reactions using cDNA/gDNA as template were performed as described in Appendix Table 2.8.1. Thereafter, purified PCR products were subjected to fluorescent dideoxy sequencing (Sanger sequencing) carried out by The Barts and The London Genome Centre. Sequencing chromatograms were analysed using the PeakPicker program (Ge et al. 2005) which calculates relative peak heights of the A and G nucleotides at the SNP site in the chromatograms derived from cDNA and gDNA respectively, standardised

against reference peaks in flanking sequences. Mann-Whitney test was performed to determine whether a difference between the ratios of standardised A nucleotide peak height over standardised G nucleotide peak height from cDNA and the corresponding ratio from gDNA exists.

2.9 *ADAMTS7* plasmids cloning

2.9.1 *ADAMTS7*$_{Pro\text{-}Cat}$ pCMV5 plasmid cloning

A short form of *ADAMTS7* plasmid, which was cloned by Somerville and colleagues and designated as *ADAMTS7*$_{Pro\text{-}Cat}$ Plasmid, expresses a protein consisting of the ADAMTS-7 signal peptide, pro-domain and metalloproteinase domain which sustains proteolytic activity (Somerville et al. 2004). We decided to clone a similar plasmid with these domain sequences into the vector pCMV5. The vector pCMV5 contains an HA-tag in its C-terminus and a multiple cloning site (MCS) for ease of insert manipulation (Figure 2.4).

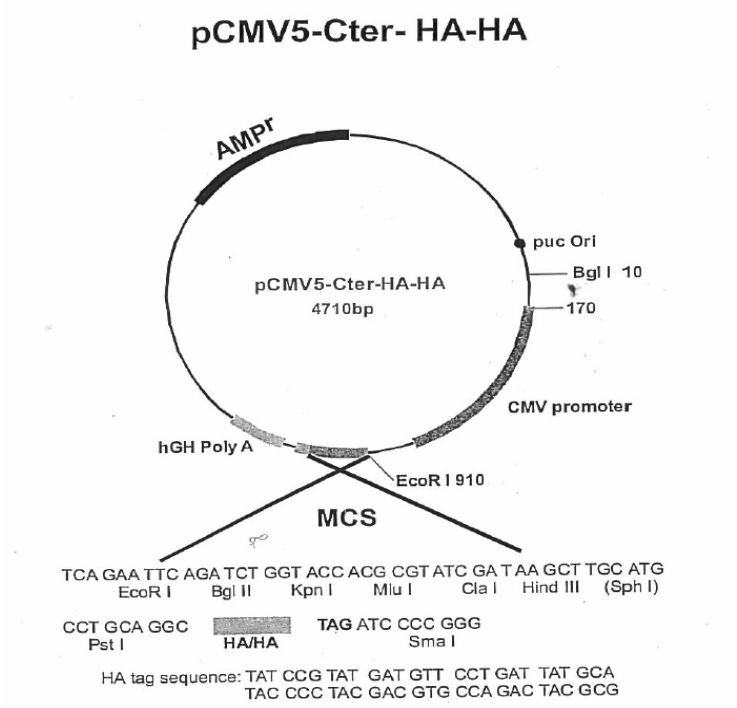

Figure 2.4. The structure of pCMV5 vector and restricted enzymes in its multiple cloning site.

2.9.1.1 Preparation *ADAMTS7*$_{Pro\text{-}Cat}$ plasmid insert cDNA and pCMV5 vector

Nested-PCR technology was used to amplify *ADAMTS7* cDNA sequence. Total RNA was extracted from VSMCs and reverse transcribed into cDNA (described in section 2.7). A pair of *ADAMTS7* cDNA primers flanking the whole insert sequence was designed by Prime3Plus. Additionally, an inside pair of primers, which contain restriction enzymes' recognising sites, were designed to amplify *ADAMTS7* cDNA sequence which encodes 552 amino acids of the ADAMTS-7 protein, including the ADAMTS-7 signal peptide, pro-domain and catalytic domain (Primers, reagents and reaction conditions of PCR were detailed in Appendix Table 2.9.1).

Amplified *ADAMTS7* cDNA insert was purified using PCR clean-up system (Promega). The insert and the vector were digested with Kpn I and Hind III. After dephosphorylation of vector pCMV5, both insert and vector were purified by PCR clean-up system and subsequently subjected to ligation at 4 ℃ overnight using T4 DNA ligase (Promega).

2.9.1.2 Transformation

Transformation is a molecular method that can be utilised to introduce exogenous genetic materials (exogenous DNA such as plasmid) into a cell through cell membrane direct uptake. Transformation occurs naturally in some species of bacteria, but with very low efficiency and stringent conditions. Artificial competence can be induced in laboratory procedures that involve making the cell passively permeable to DNA by incubation in a solution containing divalent cations (often calcium chloride) under cold conditions (on ice), and then briefly heat-shocked. This method works very well for circular plasmid DNA and usually has very high efficiency, thus being widely used for transformation, especially for plasmid. After uptake, the exogenous DNA can be expressed by the host cell. By this method, we can get large amounts of plasmid DNA or recombinant protein in a short time.

E. coli JM109 were used for the transformation. Briefly, 50 µl of competent cells were added to sterile Eppendorf tubes and incubated on ice for 30 minutes. The bacterial-DNA mixture was heat-shocked at 42℃ in a water bath for 60-70 seconds, followed by incubation on ice for 60-70 seconds. LB medium (500 µl) without antibiotics was added to each tube and incubated at 37℃ in a water bath for 1 hour. After centrifuging at 5000

rpm for 5 min, the resulting supernatant was discarded and the cells were resuspended in the remaining LB. The mixture was then plated to LB+Agar Petri dish plate with antibiotics and incubated overnight at 37℃ incubator (16-18 hours).

2.9.1.3 Purification and identification of *ADAMTS7*$_{Pro\text{-}Cat}$ pCMV5 plasmid

Colonies grown on the LB Agar plates were transferred into 5 ml LB medium with ampicillin (100 µg/ml) and placed into a shaking incubator (250 rpm) at 37℃ overnight. Plasmid DNA was then purified using Plasmid Miniprep Kits (Sigma) and subjected to sequencing at The Barts and The London Genome Centre. It unfortunately did not yield the correct *ADAMTS7* cDNA inserted pCMV5 plasmid by cloning of *ADAMTS7* cDNA into pCMV5 vector plasmid, as shown from DNA sequencing data. We have tried several times but were not successful in cloning this plasmid. *ADAMTS7* cDNA is G/C rich, which makes it difficult to manipulate by PCR-based cloning. The poor quality of *ADAMTS7* cDNA inserts stands as the most possible reason for failure of this cloning work.

2.9.2 Utilisation previously constructed *ADAMTS7*$_{Pro\text{-}Cat}$ short form and *ADAMTS7* full length plasmids

We used a previously constructed *ADAMTS7*$_{Pro\text{-}Cat}$ short form plasmid containing *ADAMTS7* cDNA sequence for expressing a protein consisting of the ADAMTS-7 signal peptide, pro-domain and metalloproteinase domain and a *ADAMTS7* full length plasmid containing *ADAMTS7* cDNA sequences for expressing a protein consisting of the full

length ADAMTS-7 protein followed by a c-Myc epitope ligated into pcDNA3.1 basic vector containing an Ampicillin resistance region (Bai et al. 2009). These plasmids were generously provided by Professor Chuanju Liu from Medical School of New York University. After sequencing of these two plasmid, we found that the *ADAMTS7* cDNA sequence contains the adenine (A) nucleotide at the rs3825807 site and therefore would be serine at position 214 of ADAMTS-7 pro-domain for both of these two plasmids. Thus, we named this plasmid *ADAMTS7*$_{Pro\text{-}Cat}$ *-214Ser* or *ADAMTS7 -214Ser* plasmid.

2.9.2.1 Site-directed mutagenesis

Site-directed mutagenesis is a molecular biology method that is used to make specific and intentional changes to the DNA sequence of a gene or any gene products, such as plasmid DNA (Edelheit et al. 2009). Using this technique, we can easily change (mutate) one nucleotide (a point mutation) or multiple nucleotides (multiple mutations) of template DNA to construct a new DNA sequence containing the mutation which can be used for studying the effect of this mutation on DNA, RNA and protein structure and biological activity. The basic procedure requires the synthesis of short DNA primers, which contain the desired mutation and is complementary to the template DNA sequence around the mutation site. The single-stranded primers are then extended using a DNA polymerase, which copies the rest of template DNA. The new copied DNA contains the mutated site.

For plasmid manipulations, special highly efficient commercial mutagenesis techniques have been developed. The technique can be described as whole plasmid mutagenesis, where two complementary mutagenic primers are used to amplify the entire plasmid in a

thermocycling reaction using a high-fidelity non-strand-displacing DNA polymerase such as *pfu* polymerase. The newly synthesised plasmid will contain the desired mutation. Because the template plasmid is usually of *E.coli* origin, and thus is methylated which can be eliminated by enzymatic digestion with a restriction enzyme such as *Dpn*I specific for methylated DNA. This leaves the reaction with only the *in vitro* mutated plasmid which can be introduced to *E. coli* for amplification.

Using *ADAMTS7*$_{Pro\text{-}Cat}$*-214Ser* or *ADAMTS7 -214Ser* plasmid as a template, we carried out site-directed mutagenesis using Quikchange Lightning kit (Agilent Technologies) to change adenine (A) to guanine (G) at the rs3825807 site. The new plasmids were verified by DNA sequencing, then we named these two new plasmids *ADAMTS7*$_{Pro\text{-}Cat}$*-214Pro* or *ADAMTS7-214Pro* plasmid, respectively, so the protein produced by these two new plasmids would be ADAMTS-7$_{Pro\text{-}Cat}$-214Pro or ADAMTS-7-214Pro, respectively. The site-directed mutagenesis reaction was carried out in accordance to manufacturer's recommendation (http://www.genomics.agilent.com/literature.jsp?crumbAction=push&tabId=AG-PR-1162&contentType=User+Manual) (see Appendix Table 2.9.2).

After the thermocycling reaction, the reaction mixture was incubated with restriction enzyme *Dpn*I at 37℃ in a water bath for 5 minutes to digest unmutated (methylated template) plasmid. Subsequently, the digested plasmids were transformed into XL-10 Gold ultracompetent cells provided by the kit.

2.9.2.2 Transformation of mutated *ADAMTS7$_{Pro-Cat}$-214Pro* or *ADAMTS7-214Pro* plasmid

For mutated *ADAMTS7$_{Pro-Cat}$-214Pro* or *ADAMTS7-214Pro* plasmid transformation, 45 µl of XL-10 Gold ultracompetent cells (Agilent Technologies) were taken out from -80 ℃ freezer and thawed on ice. Two microliters of β-Mercaptoethanol (2-ME, provided with site-direct mutagenesis kit) was added into the cells, mixed gently and incubated on ice for 10 minutes (2-ME has been shown to increase transformation efficiency). Subsequently, 2 µl of *Dpn*I digested plasmids were added to the cells and incubated on ice for 30 minutes. Then, the mixture was heat-shocked at 42 ℃ in a water bath for 30 seconds, following incubation on ice for 2 minutes. 450 µl of preheated (42 ℃) LB broth media without antibiotics was added to each tube and incubated at 37 ℃ for an hour with shaking at 225 rpm. After that, the mixture was plated on a LB Agar plate containing Ampicillin (100 µg/ml) and incubated with the plate upside down at 37 ℃ for 18 hours. On the next day, a lot of colonies were found on the plate and 10 colonies were randomly chosen for identification.

2.9.2.3 Plasmid identification

The purpose of plasmid identification is to answer two questions: whether the plasmid was successfully introduced into the bacteria and whether the plasmid was successfully mutated?

Ten colonies of each plasmid transformed bacteria were chosen randomly and a small part of each colony was picked with sterile tips, and then lysed in 50 µl rapid lysis buffer (2% SDS, 10% Triton X-100) by incubation at 95℃ for 5 min. Five microliter of supernatant was then used as DNA template to perform PCR (Using the conditions described in Appendix Table 2.9.3) following centrifugation at 16,100 rcf for 5 minutes. Samples were then loaded onto a 2% agarose gel for electrophoresis to check the product size. A PCR band of 307 bp appeared on the agarose gel to indicate the plasmid with *ADAMTS7* cDNA sequence was successfully introduced into the cells. To verify whether the mutation was successful, we performed DNA sequencing.

It was showed a right band size for all of the chosen colonies, suggesting *ADAMTS7* plasmids was successfully transformed into these colonies. And then we randomly chose 5 colonies among for each plasmid, and picked with sterile tips, put into 5 ml of LB Broth containing Ampicillin (100 µg/ml) and incubated at 37 ℃ overnight at 225 rpm in a rotation incubator. On the next day, 500 µl of cells suspension was mixed with sterile glycerol and kept at -80 ℃ as stock for future use, the rest was used to extract the plasmid DNA with QIAprep spin Miniprep kit (Qiagen) following manufacturer's protocol. Plasmid DNA concentration was quantified with a NanoDrop Spectrophotometer ND-2000 and subjected to fluorescent dideoxy sequencing (Sanger sequencing) carried out by The Barts and The London Genome Centre. By sequencing, it can be easily found out whether the mutation was successful. Successfully mutated plasmids and bacteria were used for subsequent applications. (Details for primers used for sequencing was described in Appendix Table 2.9.4 and 2.9.5).

2.10 Transfection

Similar to transformation technology, transfection is a molecular method that can deliberately introduce exogenous DNA into cells, but this term is often used for non-viral methods targeting eukaryotic cells. Transfection of animal cells typically involves introduction of transient pores in the cell membrane, to allow the uptake of exogenous genetic material (such as plasmid DNA or siRNA constructs). Three methods can be used for this purpose: calcium phosphate transfection, electroporation and lipofection. The first method uses positively charged calcium and negatively charged phosphate which forms a DNA-binding precipitate. Addition of this complex to cells allows its uptake and thus transient transfection with plasmid DNA of choice (Bacchetti and Graham 1977). Electroporation, on the other hand, utilises an intense electric field which can transiently increase the permeability of the cell membrane allowing DNA entry (Neumann et al. 1982). Finally, lipofection is a method that uses liposomes to transfect DNA into a cell. Liposomes are lipid vesicles which can easily fuse with the cell membrane, delivering the DNA into the cells (Felgner et al. 1987). This method has many advantages including high efficiency, ease of manipulation, reproducibility, low cell toxicity, and most importantly, its versatility for nucleic acid used and cell types targeted. It is suitable for all transfection applications. Thus this method is the most commonly used method for transfection in most laboratories.

2.10.1 *ADAMTS7$_{Pro-Cat}$* plasmids HEK293 cell transfection

ADAMTS7$_{Pro-Cat}$ short form plasmids were transfected into the HEK293 cell line to investigate whether rs3825807 is the functional SNP that can affect activation of ADAMTS-7 and SMC migration. HEK293 cells were cultured in 10% FBS supplemented DMEM, and when cells reached 40-60% confluence, transfection was performed. Briefly, 2 ml of 5% FBS supplemented DMEM without antibiotics was added into cells 1 hour before transfection. Fugene 6 (Roche) was used, the ratio of Fugene 6 and plasmid was 3:1 (3 µl Fugene 6 with 1 µg plasmid). After mixing Fugene 6 and plasmid with Optimal MEM (Promega), the mixture was incubated at RT for 30 minutes and added dropwise directly onto the cell layer. After 6 hour incubation, 2 ml of 10% FBS supplemented DMEM media with antibiotics was added into cells. After 16 hours, cells were replaced with serum-free media after washed in PBS several times. The serum-free culture media was harvested every day for 3 days. Harvested media were kept in -80 ℃ freezer for further experiments.

2.10.2 *ADAMTS7* full length plasmids EC transfection

Isolated primary EC cell lines were used for transfection of either *ADAMTS7-214Ser* or *ADAMTS7-214Pro* plasmid. In order to obtain optimal transfection efficiencies of primary cell lines, we purchased X-*tremeGENE* HP DNA Transfection reagent (Roche) for transfection. ECs were maintained in M199 media supplemented with 15% FBS and growth factors, and when the cells reached 50-70% confluence, transfection was performed. Briefly, the plasmid was mixed with Optimal MEM (Promega) in a sterile EP

tube, and then the X-tremeGENE HP DNA Transfection reagent was added into the mixture by gently pipetting up and down several times without touching the wall of the tube (the ratio of transfection reagent and plasmid was 3:1, 3 µl X-tremeGENE HP DNA Transfection reagent with 1 µg plasmid). Afterwards, the mixture was incubated at RT for 15 minutes, then added dropwise directly onto the cell layer. These cells were further cultivated for 18-72 hours before application for further experiments. The transfection efficiency was detected by Western blotting.

2.11 *In vitro* TSP-5 cleavage assay

TSP-5 is the best characterised substrate of ADAMTS-7. In order to investigate the effect of the SNP rs3825807 on ADAMTS-7 proteolytic activity, we incubated recombinant TSP-5 protein with conditioned media which contained activated ADAMTS-7. Genotype specific differences in ADAMTS-7 proteolytic activity were analysed by Western blotting for TSP-5 cleavage patterns (Liu et al. 2006).

2.11.1 *In vitro* TSP-5 cleavage by VSMC conditioned media

Recombinant TSP-5 (2µg) (Abcam) was incubated with 5µl concentrated media (1µg total proteins/µl) conditioned by VSMCs of the A/A or G/G genotype, in a digestion buffer (Appendix Table 2.11.1) at 37°C water bath for 8 hours. The digests, along with undigested TSP-5 and concentrated conditioned media were subjected to Western blot analysis with an anti-TSP-5 antibody (Millipore).

2.11.2 *In vitro* TSP-5 cleavage by transfected HEK293 conditioned media

Recombinant TSP-5 (2µg) (Abcam) was incubated with 1, 2 or 4 µl concentrated media (1µg total proteins/µl) from HEK293 cells transfected with either the *ADAMTS7*$_{Pro\text{-}Cat}$*-214Ser* or *ADAMTS7*$_{Pro\text{-}Cat}$*-214Pro* plasmid (described in section 2.1.10), in a digestion buffer at 37°C water bath for 8 hours. The digests, along with undigested TSP-5 and concentrated conditioned media were subjected to Western blot analysis with an anti-TSP-5 antibody (Millipore).

2.12 *ADAMTS7* shRNA lentiviral particles packing

In contrast to over-expression of *ADAMTS7* which upregulates the expression level of *ADAMTS7* and thus increases the function of ADAMTS-7 in the cells, knock-down of *ADAMTS7* will downregulate the *ADAMTS7* expression and decrease ADAMTS-7 function in the cells, thus both of these experiments give us valuable information of ADAMTS-7 biological function.

2.12.1 *ADAMTS7* shRNA lentiviral plasmid

In order to investigate the effects of *ADAMTS7* knock-down on EC migration, proliferation and in vitro angiogenesis (capillary-like network formation assay), 5 clones of MISSON® pLKO.1-puro *ADAMTS7* shRNA plasmid in Bacterial Glycerol Stock were purchased from Sigma (NM_014272, TRC Number: TRCN0000051233, TRCN0000051234, TRCN0000051235, TRCN0000051236, TRCN0000051237). This

work has been approved by College GM Safety Committee (GM Centre Registration Number: GM774). Personal training for genetic modification (GM) work has been obtained. Non-target pLKO.1 plasmid was generously donated by Dr. Xiao and used as vector control.

ADAMTS7 specific shRNA sequence was inserted into the lentiviral vector pLKO.1 with a puromycin resistance region which can be used for selection of creating a stable infection cell line. These plasmids were provided as bacterial glycerol stock, and thus need to be propagated. *ADAMTS7* shRNA pLKO.1 transfer plasmid for lentiviral particle packaging was then extracted. Briefly, each of the clones was propagated in 5ml LB broth with ampicillin (100 μg/ml), the plasmids have ampicillin resistance region and thus can propagate normally. Then *ADAMTS7* shRNA pLKO.1 transfer plasmids were extracted from bacteria and quantified by Nanodrop-2000.

2.12.2 *ADAMTS7* shRNA lentiviral particle packaging

In order to deliver *ADAMTS7* shRNA efficiently into ECs, a lentiviral particle packing system was used. This system required four components: transfer vector which has specific shRNA sequence inserted into a lentiviral vector such as pLKO.1, packaging vector and envelope vector, and HEK293T cells as host cell to package the lentiviral particles. The *ADAMTS7* shRNA pLKO.1 transfer plasmids were purchased from Sigma, packing plasmid psPAX2 and envelope plasmid pMD2.G were a kind gift from Dr. Qingzhong Xiao. HEK293T cells were used as host cells to package *ADAMTS7* shRNA lentiviral particles. *ADAMTS7* shRNA lentiviral particle packaging was performed

following protocol from Addgene (http://www.addgene.org/tools/protocols/plko/#E). Briefly, *ADAMTS7* shRNA pLKO.1 transfer plasmids, packing plasmid psPAX2 and envelope plasmid pMD2.G (ratio 5:4:1) were co-transfected into HEK293T cells using X-tremeGENE HP DNA Transfection reagent (Roche). Eighteen hours later, transfected cells were replaced with fresh DMEM with 15% FBS and further cultivated for 2 days before the first round of lentiviral particles' harvest was performed. Afterwards, fresh media was added and harvested after two days for second round of lentiviral particles' harvest. The harvested lentiviral particle solution was then filtered with 0.45 μm filter to remove cell debris, aliquoted and stored at -80℃ freezer for *ADAMTS7* shRNA lentiviral particles infection.

2.13 Infection of EC with *ADAMTS7* shRNA lentiviral particles

2.13.1 *ADAMTS7* shRNA lentiviral particles transduction

Delivery of foreign genetic material (DNA or RNA) into another cell using a viral vector is termed as transduction. Compared with traditional methods such as transfection to deliver genetic material, transduction can ensure that nearly 100% of cells are infected without severely affecting cell viability, especially for the cell lines that are difficult to transfect. Thus viral vectors provide a powerful method for molecular genetics experiments. Lentiviral vectors are created from lentivirus and modified by deletion of a part of the viral genome which is critical for viral replication. In such way, the modified viral vector can efficiently infect cells, and can also integrate its modified viral genome

into the host genome, thus using this viral vector and inserting shRNA or gene of interest into the viral vector can deliver shRNA or gene into the genome of target cells and stably express for long term.

Infection of ECs with *ADAMTS7* shRNA lentiviral particles was performed following protocol from Addgene (http://www.addgene.org/tools/protocols/plko/#E). Briefly, ECs were maintained normally and when the cells reached 70% confluence, fresh culture media containing 10 μg/ml Polybrene (Sigma) was added to cells. Polybrene is a cationic polymer used to increase the efficiency of viral infection. *ADAMTS7* shRNA lentiviral particles solution were defrosted from -80℃ freezer and added directly into ECs to infect the cells. After 24 hours post-infection, virus containing media were replaced with fresh EC media. The cells were further cultivated for 4 days before harvesting for protein extraction to examine the knock-down effect of 5 clones of *ADAMTS7* shRNA lentiviral vector by Western blotting.

2.13.2 *ADAMTS7* knock-down EC cell line selection

The *ADAMTS7* shRNA lentiviral particle solution that had the strongest knock-down effect on *ADAMTS7* was chosen to establish stable *ADAMTS7* knock-down EC cell lines. The lentiviral vector pLKO.1 has a puromycin resistance region which can be used to select infected cells. This puromycin resistance region would be integrated into EC genome along with *ADAMTS7* shRNA sequence if the lentiviral particles successfully infected the cells, and thus these infected cells could survive and grow in the media

containing puromycin, while the non-infected ECs are sensitive to puromycin and could not survive.

Because each cell line responds differently to puromycin selection, the optimal concentration of puromycin needs to be determined before selection of infected cell lines. Briefly, ECs were cultured in normal conditions until reached about 90% confluence, then media with puromycin was added into the cells with the final puromycin concentration from 1-4 μg/ml in 1 μg/ml increments. The optimal concentration of puromycin that results in complete cell death after 3-5 days in the media with puromycin should be used for selection. Finally, the concentration 2 μg/ml was chosen for cell line selection.

ECs were infected with the chosen *ADAMTS7* shRNA lentiviral particle solution as described earlier. After infection, media containing 2 μg/ml puromycin were added into cells to select stable infected cells for 10 days. During the selection, cells were handled normally with regular replacement of media containing puromycin and subculture.

2.14 Western blotting assays

2.14.1 Sample preparation

2.14.1.1 VSMC Sample preparation

VSMCs were cultured with primary smooth muscle cell culture media (as described in section 2.1). After the cells reached 90% confluence, they were starved with serum-free

media (Smooth Muscle Cell Basal Media 2, PromoCell). HEK293 cells were transfected with either *ADAMTS7*$_{Pro\text{-}Cat}$*-214Ser* or *ADAMTS7*$_{Pro\text{-}Cat}$*-214Pro* plasmid or vector control plasmid (as described in section 2.10) and starved with serum-free media. Following the same treatment, protein from conditioned media, cell surface washes or whole cell lysates were prepared as follows:

The culture media were harvested daily for 3 consecutive days. Culture media were then concentrated by centrifugal concentrators (Millipore) according to the manufacturer's protocol. Briefly, they were span down at 2000g for 5 minutes to remove cell debris. The supernatant was added into the filter column and centrifuged at 4000 g for 30 minutes. Afterwards, the concentrated sample was transferred into a sterile 0.5ml EP tube. In order to protect the proteolytic activity of ADAMTS-7 in the conditioned media for the *in vitro* digestion assay, protease inhibitor cocktail was not added into the concentrated samples. After each harvest of the serum-free media, cell surface washes samples were obtained by washing the cell layer with sterile 0.5M NaCl which can release ADAMTS-7 from the cell surface as previously described (Somerville et al. 2004). Afterwards, surface washes were concentrated by centrifugal concentrators as well (as described above). Protease inhibitor cocktail (Roche Applied Science, constituents are described in Appendix Table 2.14.1) was added into concentrated samples.

Starved cells were also scraped and lysed in protein lysis buffer (Appendix Table 2.14.2) to obtain total protein. To release the cell content, these were vortexed vigorously and sonicated for 2 minutes. Subsequently, they were incubated on ice for 45 min, then

supernatants were collected after centrifuging 16,100 rcf for 10 minutes at 4 ℃ and transferred into sterile tubes.

2.14.1.2 EC Sample preparation

Conditioned media and whole cell protein extracts of following cells were used for Western blotting:

ECs with different genotypes of rs3825807

ECs transfected with pcDNA3.1 vector control plasmid

ECs transfected with the *ADAMTS7-214Ser* plasmid

ECs transfected with the *ADAMTS7-214Pro* plasmid

ECs infected with non-target pLKO.1 control lentiviral particles

ECs infected with *ADAMTS7* shRNA lentiviral particles

ECs were cultured with M199 media supplemented with 15% FBS and growth factors. After cells reached 90% confluence, these cells were starved with Human Endothelial-SFM (Life Technologies). The culture media was harvested daily for 48 hours. Afterwards, culture media were collected and concentrated by centrifugal concentrators (Millipore) as described in the previous section.

Whole cell lysates of these cells were also prepared as described in section 2.14.1.1.

2.14.2 Protein concentration quantitation

Protein concentration was determined by Bradford assay. The Bradford assay, a colorimetric protein assay, is the most commonly used protein assay. This assay is based on an absorbance shift of the dye Coomassie Brilliant Blue G-250 where under acidic conditions the red form of the dye is converted into its blue form to bind to the protein being assayed. The binding of the protein stabilises the blue form of the Coomassie dye which has an absorption spectrum maximum of approximately at 595 nm. The change in the absorbance at 595 nm is directly proportional to the amount of blue form of Coomassie dye (linear from 0 -2000 μg/ml protein concentration), and thus to the amount of protein present in the sample. The colour change observed in this assay is monitored and quantitated using a spectrophotometer.

All the protein samples prepared above were quantitated using Bio-Rad Protein Assay Dye Reagent Concentrate (Bio-Rad). Briefly, 5x Assay Dye Reagent was diluted 4:1 with distilled water prior to use, then 2 μl of each protein sample was added into 1ml of diluted dye reagent (500x dilution), mixed well and incubated for 15 minutes at RT to stabilise the colour development. Subsequently, the samples were analysed by Bio-Rad's SmartSpec^{TM}Plus Spectrophotometer. The reading of the spectrophotometer then converted to the real protein sample concentration by multiplying 500 (dilution ratio).

2.14.3 Gel electrophoresis and protein transfer

Sodium-dodecyl-sulphate polyacrylamide gel electrophoresis (SDS-PAGE) is a technique widely used to separate proteins based on their molecular size when an electric field is applied to a gel. SDS is an anionic detergent, which denatures proteins and confers the polypeptide with a negative charge proportional to its size (molecular weight).

Equal amounts of protein (20-40 μg, depending on the assay) from each sample were mixed with 5x protein loading buffer (Recipe as described in Appendix Table 2.14.3), heated for 5 min at 95°C and loaded onto a SDS-PAGE gel. The gel consists of a separating gel and a stacking gel and the gel was made using Bio-Rad minigel system (Gel details are described in Appendix Table 2.14.4 and 2.14.5). A prestained protein marker was also loaded onto the gel, either ColorPlus™ Prestained Protein Ladder (10-230 kDa, NEB) or Prestained Protein Marker (7-175 kDa, NEB). The electrophoresis was performed according to the manufacturer's instructions. Briefly, 90 V for 30 minutes in the stacking gel and then 160 V until the samples reached the bottom in Bio-Rad Mini-Protean® tank with running buffer (Recipe described in Appendix Table 2.14.6).

Proteins separated by electrophoresis were then electro-blotted onto a nitrocellulose membrane (Hybond ECL, GE Healthcare) for 2.5 h at constant voltage of 60V with an ice bag in the transfer buffer (Recipe described in Appendix Table 2.14.7) to assure optimal temperature conditions during the transfer process.

2.14.4 Immunoblotting

The membranes were blocked in 5% non-fat milk/1x TBST (Recipe described in Appendix Table 2.14.8) for 1 hour at RT, followed by primary antibodies at 4℃ overnight, including anti-ADAMTS-7 pro-domain antibody (Abcam), anti-ADAMTS-7 spacer domain antibody (Abcam) which were used to detect ADAMTS-7 protein in conditioned media, cell surface washes and cell lysate of VSMC and EC; anti-TSP-5 antibody (Millipore) was used to detect the cleaved TSP-5 fragment in VSMC conditioned media and digests in *in vitro* TSP-5 digestion assay; anti-ADAMTS-7 pro-domain antibody (Abcam) and anti-cMyc antibody (Sigma-Aldrich) was used to detect ADAMTS-7 in conditioned media, cell surface washes and cell lysate of transfected HEK293 cells; anti-TSP-1 antibody (R&D system) was used to detect TSP-1 protein in EC conditioned media. Thereafter, appropriate secondary antibodies were incubated with membranes at RT for 1 hour after three times washing with 1x TBST, 10 minutes each time. Secondary antibodies including anti-rabbit IgG conjugated with HRP (for ADAMTS-7 antibodies, Cell signalling); anti-rat IgG conjugated with HRP (for TSP-5 antibody, Dako); anti-mouse IgG conjugated with HRP (for c-Myc and TSP-1 antibody, Cell signalling) (Antibodies details described in Appendix Table 2.14.9). Amersham ECL Plus Western blotting Detection Reagents (GE healthcare life science) and Amersham Hyperfilm ECL (GE healthcare life science) were used to develop the plot. Then the films were scanned using Epson Perfection V500 Photo Scanner and densitometry analysis was performed using Adobe Photoshop.

2.15 EC Capillary-like network formation assay

EC is the major cell type involved in angiogenesis, which is not only participating in pathological processes including tumour biology and atherosclerosis, but also vital in growth and development, as well as reproduction and tissue repair. In response to angiogenic signals, such as VEGF and FGF-2, ECs release proteases to degrade the surrounding ECM, migrate towards angiogenic signals, proliferate and form new blood vessels and eventually form three-dimensional vasculature. *In vivo* angiogenesis assays, such as sponge implantation, corneal, zebrafish, chick chorioallantoic membrane (CAM) and tumor angiogenesis models, are considered to be the most informative of these but are often expensive, time-consuming and require specialist training to perform (Staton et al. 2004). *In vitro* assays tend to be more rapid, less expensive and easier to interpret. *In vitro* angiogenesis assays operate on the principle that ECs form tubule-like structures when cultured on a supportive matrix. Assays involving a matrix derived from murine tumours, Matrigel, are now the most common in *in vitro* tubule formation assays (Donovan et al. 2001). This assay is widely used to identify stimulators or inhibitors of angiogenesis, as well as investigate genes and signalling pathway involved in angiogenesis. In this assay, substances that promote angiogenesis facilitate the formation of capillary-like structure, while the inhibitors of angiogenesis disturb its formation. This assay involves endothelial migration and proliferation, one protein or compound that affects either of these processes will affect the outcome of the assay.

In order to investigate the effect of SNP rs3825807 on angiogenesis, EC capillary-like network formation assay was performed. The assay was also used to assess the effect of *ADAMTS7* over-expression and knock-down on angiogenesis.

The following cells were used to for capillary-like network formation assay:

ECs with different genotypes of rs3825807
ECs transfected with pcDNA3.1 vector control plasmid
ECs transfected with *ADAMTS7-214Ser* plasmid
ECs transfected with *ADAMTS7-214Pro* plasmid
ECs infected with non-target pLKO.1 control lentiviral particles
ECs infected with *ADAMTS7* shRNA lentiviral particles

Matrigel™ Basement Membrane Matrix (BD) was defrosted at 4℃ in an ice bath one day before the assay. The next day, Matrigel was added into a 96-well plate (50µl/well) and incubated in 37℃ incubator for 1 hour. Afterwards, 15,000 cells per well in 100 µl Human Endothelial-SFM (Life Technologies) were added directly into the Matrigel coated well. The cells were then incubated at 37˚C with 5% CO_2, and images of the capillary-like structure at each well were obtained after 3, 6, and 9 hours, respectively using a light microscope with a digital camera. ImageJ's angiogenesis analyser was used to analyse the capillary-like structure of each well at 3, 6 and 9 hours after seeding.

2.16 Proteomics

TSP-5, the best studied ADAMTS-7 substrate known to regulate SMC migration, is not expressed in ECs (Riessen et al. 2001). Thus, it is likely that the effect of ADAMTS-7 on EC migration and angiogenesis is not through cellular TSP-5 mediated mechanism. Hence, a proteomic analysis was performed with the aim to identify the possible previously unknown substrates for ADAMTS-7, which might play a role in mediating the effect of ADAMTS-7 on angiogenesis.

Proteomics has become an increasingly common method for identifying proteins and characterise their amino acid sequences and posttranslational modifications. It requires proteolytic digestion of proteins prior to their analysis by mass spectrometry. The most common proteomic method is termed bottom-up proteomics. The proteins can be purified by 2-dimensional gel electrophoresis (2D-GE) resulting in one or a few proteins for proteolytic digestion prior to analysis by mass spectrometry. Alternatively, a protein mixture can be digested directly by protease, followed by separation of peptides by liquid chromatography (LC) coupled to tandem mass spectrometry, a technique known as shotgun proteomics.

In shotgun proteomics, the protein mixture from cells (either whole cell lysates or secreted proteins in conditioned media) is digested by a protease to produce a peptide mixture. The most commonly used enzyme is trypsin, because it cleaves specifically after the basic residues arginine (Arg) and lysine (Lys), if these are not followed by proline (Pro). The peptide mixture is then loaded directly onto a chromatography column (High-Performance

Liquid Chromatography, HPLC) to separate the peptides through hydrophobicity and charge. Subsequently, the peptides are ionised and separated by mass to charge ratio (m/z) in the first stage of tandem mass spectrometry (MS1). These peptides are further fragmented during collision-induced dissociation, producing fragmentation of peptides that are broken at different positions. The charged fragments are then separated in the second stage of tandem mass spectrometry. Afterwards, the fragmentation mass spectrometry data are analysed by commercially available software such as Mascot and the interpretation can reveal the peptides' sequence, or part of it, i.e., a sequence tag. This is then compared against a protein database to identify the best matched protein. Finally, the identified protein can also be quantified by various methods such as Spectral Index Normalised Quantitation (SINQ).

The following EC cell lines were used for the proteomics analysis in this project:

(1) HUVECs cultured in normal condition to serve as a control
(2) HUVECs transfected with the *ADAMTS7-214Ser* plasmid
(3) HUVECs infected with *ADAMTS7* shRNA lentiviral particles

These cells were starved with Human Endothelial-SFM (Life Technologies). The culture media were harvested daily for 48 hours. Afterwards, culture media were collected and concentrated by centrifugal concentrators (Millipore) according to the manufacturer's protocol. Briefly, after span down at 2000g for 5 minutes to remove cell debris, the supernatant was added into the filter column and centrifuged at 4000 g for 30 minutes.

The concentrated samples were transferred into a sterile tube and sent to Central Proteomics Facility, Oxford University for proteomic analysis.

2.17 Bruneck Study cohort

Subjects of this study were residents of the Bruneck area in Italy, who participated in the Bruneck Study, details of which have been described previously (Kiechl and Willeit, 1999a; Kiechl and Willeit, 1999b; Willeit et al, 2000). DNA samples for genotyping were available for 787 subjects. Ultrasound scanning of the right and left internal carotid and common carotid arteries was performed in 1990 and 1995 by the same experienced sonographer (Kiechl and Willeit, 1999a; Kiechl and Willeit, 1999b; Willeit et al, 2000). Atherosclerotic lesions were defined according to two ultrasound criteria: (1) wall surface (protrusion or roughness of the arterial boundary) and (2) wall texture (echogenicity). The atherosclerosis score, indicative of atherosclerosis severity, was calculated by summing all diameters at 8 well-defined segments of the common and internal carotid arteries. Incident atherosclerosis was defined by the occurrence of atherosclerotic lesions in segments previously free of atherosclerosis or enlargement of non-stenotic lesions by a relative increase in the plaque diameter exceeding twice the measurement error of the method. Intima-media thickness was assessed in plaque-free sections of the common carotid arteries.

2.18 Southampton Atherosclerosis Study (SAS)

A total of 1730 Caucasian patients underwent diagnostic or interventional coronary angiography at the Southampton General Hospital were recruited, of which 1342 had >50% diameter stenosis in at least one of the major epicardial coronary arteries, and the remaining 388 subjects showed normal angiogram. Demographic and clinical data were recorded including age, gender, height, weight, occupation, smoking status, presence or absence of hyperlipidaemia (defined as cholesterol >5.2mmol/l and/or triglyceride >3mmol/l), HDL level, LDL level, triglyceride level, hypertensive status (>160/95mmHg), diabetic status, the use of lipid-lowering drugs (mainly statins), presence or absence of previous myocardial infarction and family history of coronary artery disease (in a first degree relative below 65 years of age). Total cholesterol, HDL, LDL and triglyceride levels were measured using standard quality controlled enzymatic methods at the Southampton General Hospital. Data for total cholesterol, HDL, LDL, and triglyceride levels were available for 1591, 1060, 479, and 1465 subjects, respectively. One single consultant cardiologist assessed each angiogram. Demographical and clinical characteristics of the SAS subjects are described in (Ye et al, 2003). DNA was previously isolated from peripheral blood samples from these subjects and utilised for genotyping in this project. (This part of work was done by other group members, the information above was cited from PhD thesis of Dr. Anna Motterle)

2.19 Bioinformatics

F-SNP (available from Queen's University at http://compbio.cs.queensu.ca/F-SNP/) was used to identify possible functional effect of these GWAS-identified CAD-associated lead SNPs at the *ADAMTS7* gene locus, including functional assessment of protein coding, splicing regulation, transcriptional regulation, post translation by using various tools and databases (more information, please visit the 'Resource section' at http://compbio.cs.queensu.ca/F-SNP/).

PSIPRED (available from University College London Department of Computer Science Bioinformatics Group at http://bioinf.cs.ucl.ac.uk/psipred/) was used to predict possible functional effect of non-synonymous SNP rs3825807 on secondary structure of ADAMTS-7.

QUARK (available from University of Michigan at http://zhanglab.ccmb.med.umich.edu /QUARK/) was used to predict possible functional effect of non-synonymous SNP rs3825807 on 3D structure of ADAMTS-7.

2.20 Statistical analyses

Values for linkage disequilibrium (LD) between SNPs rs3825807, rs1994016 and rs4380028 in the HapMap and 1000 Genomes databases were obtained from Ensembl. Student's t-test (two groups) and One-way ANOVA (three groups) were used to analyse: real-time RT-PCR results by the ΔΔCt method; differences between genotypes in cell proliferation, senescence, apoptosis and migration distance in the scratch assay; band intensity in Western blot analyses. Paired Student's t-test was performed to analyse: allelic expression imbalance analysis results; VSMC migrated numbers in the trans-well migration assay; *in vitro* TSP-5 digestion assay results; differences between over-expression and controls or knock-down and control groups in EC migration and capillary-like network formation assay. In the Bruneck Study, associations of rs3825807 with carotid atherosclerosis were tested by logistic and linear regression analyses. Base models were adjusted for age and sex. Multivariable models were adjusted for variables correlated with atherosclerosis parameters in the Bruneck cohort, including presence or absence of hypertension, smoking status, diabetes mellitus, level of alcohol consumption, levels of high density lipoprotein and low density lipoprotein, ferritin, fibrinogen, anithrombin III, the factor V Leiden mutation, body mass index, waist-to-hip ratio and log-transformed concentrations of urinary albumin, high-sensitivity C-reactive protein and lipoprotein(a). Pearson linear Regression analysis was used to analyse the relationship of the proportion of ADAMTS-7 in the intima area and intima thickness of atherosclerotic plaque. Variables with a skewed distribution were normalised by logarithmic transformation. Mean and standard error of the mean (SEM) were calculated using SPSS10.0. All *p*-values were two-sided, and $p<0.05$ defined as significance.

Chapter 3

Functional study of *ADAMTS7* variants in VSMC

Three independent GWA studies revealed an association between genetic variants at the *ADAMTS7* locus and the susceptibility to coronary artery disease. However, the mechanisms underlying these associations have remained unclear. Thus, functional studies of these variants at the *ADAMTS7* gene locus were carried out in this part of study. Immunohistochemical analyses showed that ADAMTS-7 was expressed in human coronary and carotid atherosclerotic plaques, mostly localised to vascular smooth muscle cells (VSMCs) in the plaque. The colocalisation of ADAMTS-7 and VSMCs suggests they might be functionally related. Moreover, a previous study showed that ADAMTS-7 could facilitate VSMC migration through cleavage of its substrate TSP-5 and thus promote neointima formation after mechanical injury of rat carotid artery. Thus, we carried out the functional studies of the CAD-associated SNPs in VSMCs.

3.1 Results

3.1.1 Verification of SMCs isolated from human umbilical arteries

ECs form a monolayer facing the lumen of the blood vessel, so during the isolation of VSMCs, these cells may also migrate from the tissue and contaminate the VSMC primary cell culture. Fibroblasts are predominantly located in the adventitial layer of the artery. Although this layer was carefully removed during the isolation, a small number of fibroblasts may still be left and thus may form part of the contaminant. To verify that the cells isolated from human umbilical arteries were smooth muscle cells and not vascular ECs or fibroblasts, several isolated primary VSMC cell lines were subjected to ICC staining for markers of VSMCs, ECs, and fibroblasts, respectively.

VSMCs were isolated from approximately 160 human individuals' umbilical cords. Among them, around 30 samples failed to propagate the VSMC primary cell cultures leaving us with primary VSMCs from approximately 130 individuals. Isolated cells showed typical SMC morphology (Figure 3.1 A), and strong fluorescent signal was observed when the cells were stained for the VSMC marker, SM α-actin (SMA, Figure 3.1 B). Meanwhile, neither of the fibroblast cell marker DDR2 (Figure 3.1 C) nor the EC marker CD144 (Figure 3.1D) was detected, indicating that there was no detectable contamination of these two types of cells in the VSMC culture.

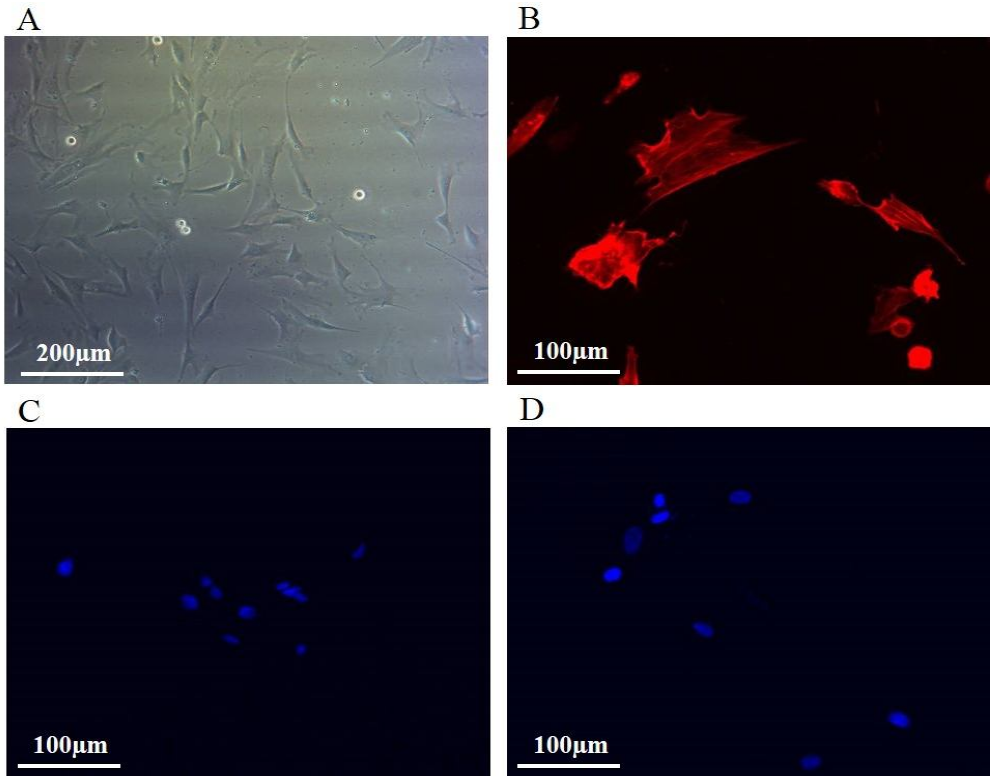

Figure 3.1 Verification of the homogeneity of VSMC cultures. Isolated VSMCs express high levels of the smooth muscle α-actin (SMA, red). Neither of the fibroblast cell marker discoidin domain-containing receptor 2 (DDR2, green) nor the EC marker cluster of differentiation 144 (CD144, green) is detected. **A**: Isolated VSMCs under bright field. **B**: staining with SM-actin-Cy3/red (red); **C**: staining with DDR2-FITC (green); **D**: staining with CD144-FITC. Cell nuclei were stained with DAPI (blue).

3.1.2 Isolated VSMCs express ADAMTS-7

Although ADAMTS-7 has been shown to be expressed in neointima of the blood vessel and colocalised with VSMCs in a rat injury model (Wang et al. 2009), the expression of ADAMTS-7 protein in human VSMCs had not been reported before. Thus, isolated VSMCs were subjected to ICC staining aiming to detect ADAMTS-7 protein expression in these cells. Eight primary cultures of VSMCs underwent double fluorescent immunostaining for SMA (red) and ADAMTS-7 (green). The nucleus was stained with propidium iodide (PI, blue). The staining showed that the ADAMTS-7 protein was expressed by human VSMCs (Figure 3.2).

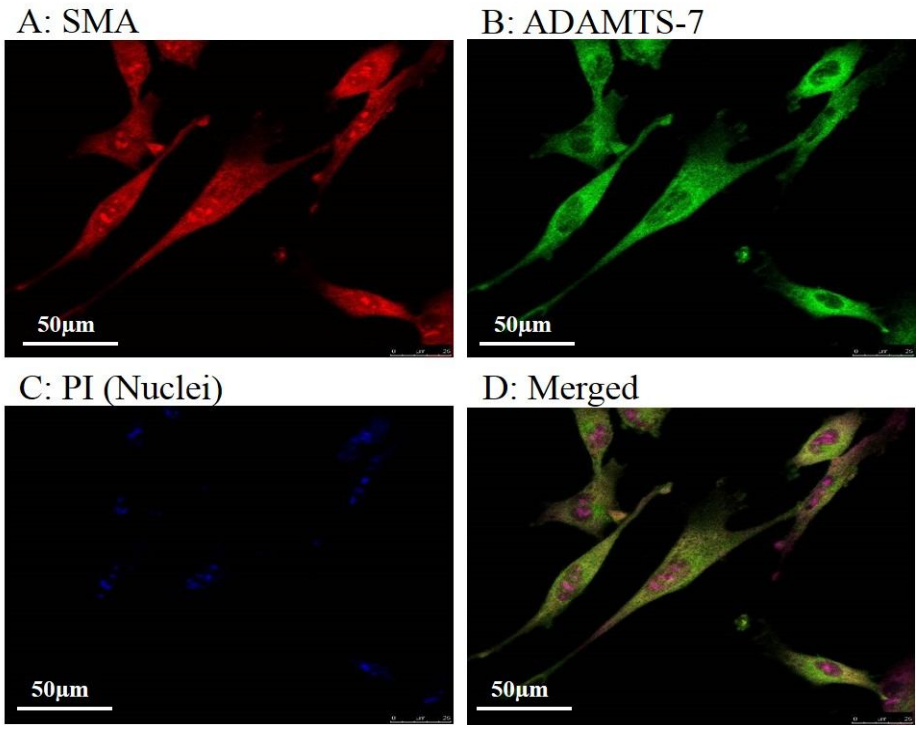

Figure 3.2 Representative images showing presence of ADAMTS-7 in cultured VSMCs. Isolated VSMCs express ADAMTS-7. **A**: staining with SM-actin-Cy3/red (red); **B**: staining with ADAMTS-7 - FITC (green); **C**: Cell nuclei staining with PI (blue); **D**: Merged.

3.1.3 ADAMTS-7 is expressed in human atherosclerotic plaques

3.1.3.1 ADAMTS-7 fluorescence staining in carotid atherosclerotic plaques

Sections of formalin-fixed paraffin-embedded tissue blocks of carotid atherosclerotic plaques were subjected to double fluorescent immunostaining for SMA (red) and ADAMTS-7 (green) and DAPI fluorescent staining for nuclei (blue). Confocal microscopy was used to examine the staining results. The experiment showed that ADAMTS-7 was expressed in the human atherosclerotic plaques, with strong staining in SMCs (Representative images are shown in Figure 3.3).

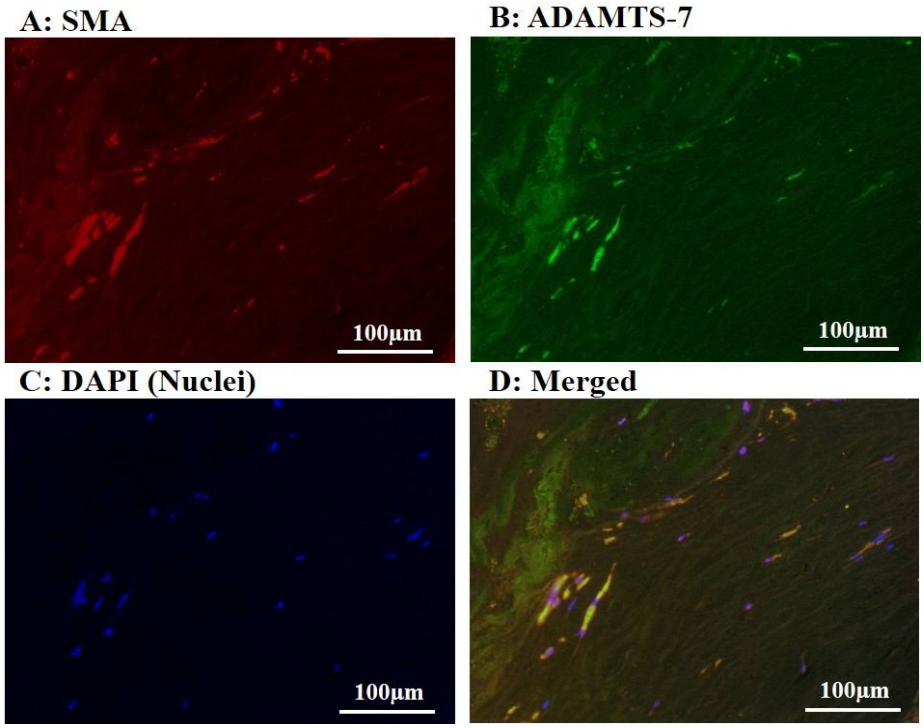

Figure 3.3 ADAMTS-7 is detected by fluorescent immunostaining in human carotid artery atherosclerotic plaques. Carotid atherosclerotic plaque sections underwent to double fluorescent immunostaining for SMA (red), ADAMTS-7 (green) and DAPI fluorescent staining for nuclei (blue), followed by confocal microscopy examination. **A**: SMA staining; **B**: ADAMTS-7 staining with an anti-ADAMTS-7 spacer domain antibody; **C**: nuclear staining; **D**: merged image from SMA, ADAMTS-7 and nuclear staining.

In order to verify the specificity of the ADAMTS-7 staining in carotid atherosclerotic plaque sections, a blocking peptide (Abcam) matching the epitope of the ADAMTS-7 (spacer domain) antibody (Abcam) was used (Figure 3.4). IHC staining of carotid artery atherosclerotic plaque sections with ADAMTS-7 spacer domain antibody showed that ADAMTS-7 was expressed in atherosclerotic plaques (Figure 3.4A). While the staining of ADAMTS-7 in carotid atherosclerotic plaque sections was totally blocked by using a blocking peptide matching the epitope of the ADAMTS-7 (spacer domain) antibody, indicating the ADAMTS-7 staining in the plaque by using this anti-spacer domain antibody is specific.

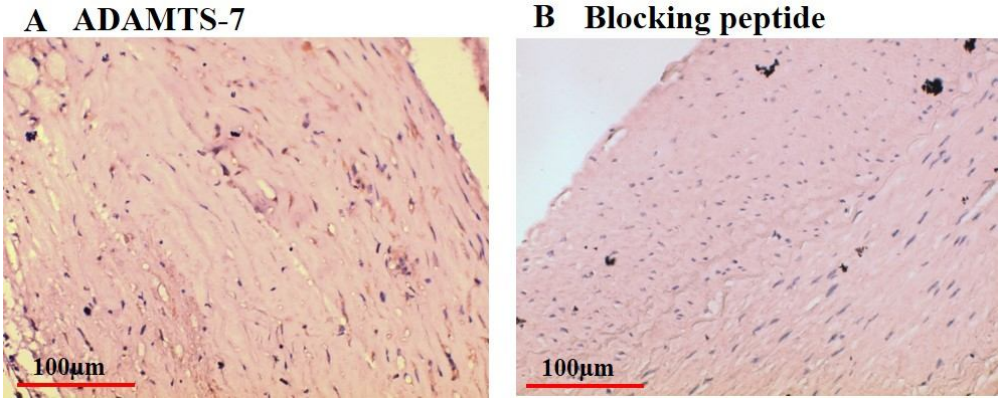

Figure 3.4 ADAMTS-7 is present in human carotid artery atherosclerotic plaques. **A**: A representative image of single immunostaining shows that ADAMTS-7 (brown) is expressed in carotid atherosclerotic plaques. **B**: Peptide blocking for ADAMTS-7 staining (a blocking peptide for ADAMTS-7 spacer domain antibody was used).

3.1.3.2 ADAMTS-7 staining in coronary atherosclerotic plaques

ADAMTS-7 has been shown to facilitate VSMC migration and neointima formation in a rat vascular injury model of post-angioplasty restenosis (Wang et al. 2009). However, the mechanisms underlying post-angioplasty restenosis are different from the pathogenesis of atherosclerosis, thus the role of ADAMTS-7 in atherosclerosis remains to be elucidated. More importantly, several GWAS studies have reported that SNPs in the *ADAMTS7* gene locus are strongly associated with CHD, making a strong case for *ADAMTS7* as a candidate gene for CHD (Coronary Artery Disease Genetics 2011, Reilly et al. 2011, Schunkert et al. 2011). In order to examine whether ADAMTS-7 protein was expressed in atherosclerotic plaques, and if so, in which cell type, IHC staining was performed using coronary artery atherosclerotic plaque sections.

Double immunostaining for ADAMTS-7 and the VSMC marker SMA showed that ADAMTS-7 was expressed and colocalised with a proportion of VSMCs in atherosclerotic plaques of coronary arteries (Figures 3.5). We observed that in the atherosclerotic plaques, VSMCs that accumulated ADAMTS-7 were mostly located near the intima-media border and the fibrous cap. ADAMTS-7 positive staining were detected both within cells (highlighted by black arrowheads) and in the extracellular spaces (highlighted by green arrowheads) (Figure 3.5B).

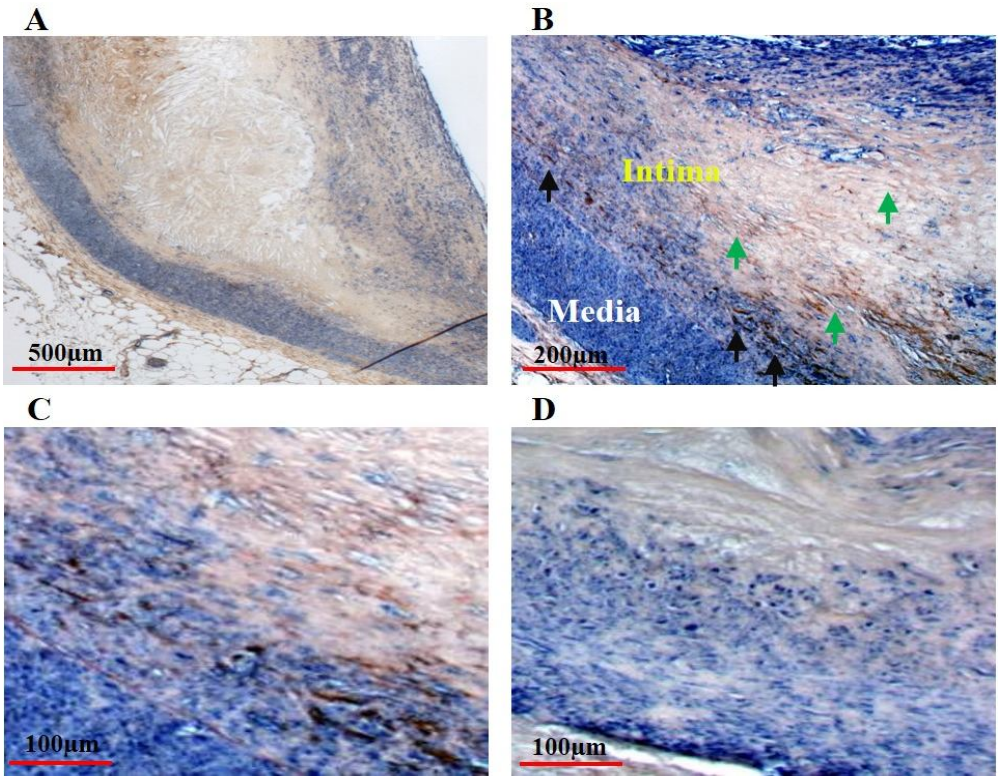

Figure 3.5 ADAMTS-7 is present in human coronary artery atherosclerotic plaques. Purple color (NBT/BCIP) indicates SMA staining, and dark brown color (DAB) indicates ADAMTS-7 staining. Panel **A**, **B** and **C** show the same location at 4x, 10x and 20x respectively. Black arrows in panel **B** indicate cell positive for both SMA and ADAMTS-7, while green arrows indicate extracellular ADAMTS-7 staining. **D:** Negative control. (ADAMTS-7 spacer domain antibody was used for ADAMTS-7 staining; negative control was performed with the secondary antibody only for all the staining, or otherwise stated)

3.1.4 TSP-5 is expressed in human carotid atherosclerotic plaques

TSP-5 is the best-studied substrate of ADAMTS-7 (Liu et al. 2006). A recent study in rats demonstrated that ADAMTS-7 facilitated VSMC migration by cleaving TSP-5, thereby promoting neointima formation following vascular mechanical injury (Wang et al. 2009). Studies have also shown that TSP-5 was expressed in human normal and atherosclerotic vessel wall and colocalised with VSMCs (Riessen et al. 2001). We verified TSP-5 expression in human carotid atherosclerotic plaque by immunostaining using a TSP-5 antibody as described in the Methods section of this chapter (Figure 3.6). As reported by Riessen and colleagues, TSP-5 was found to be present in human carotid atherosclerotic plaques and colocalised with a proportion of SMCs in the plaque (highlighted by black arrowheads in Figure 3.6A).

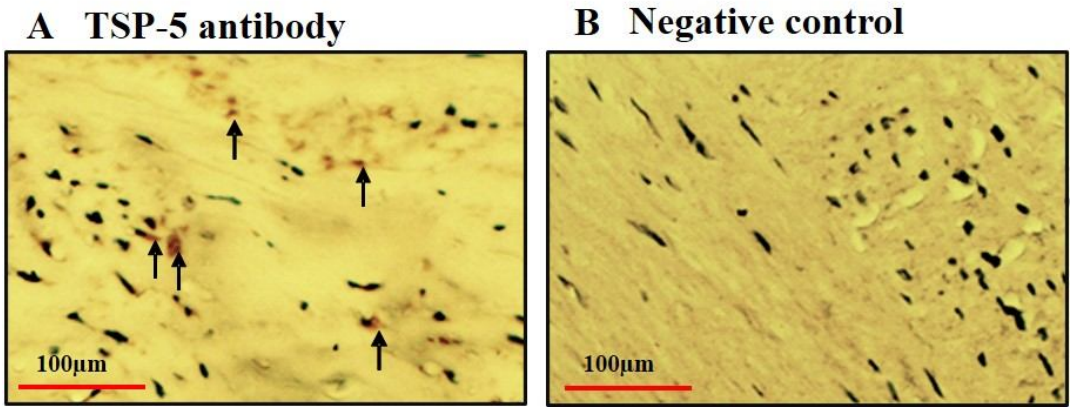

Figure 3.6 TSP-5 is present in human carotid artery atherosclerotic plaques. Dark brown color (DAB) indicates TSP-5 staining. **A**: A representative image of IHC staining shows that TSP-5 is present in human carotid atherosclerotic plaques and colocalises with a proportion of SMCs in the plaque (highlighted by black arrowheads). **B**: Negative control (with secondary antibody only).

3.1.5 Genotyping of VSMCs for CAD-related SNPs at the *ADAMTS7* locus

Genomic DNA from VSMCs was extracted and genotyped using the KASPar method for three CAD-associated SNPs at the *ADAMTS7* locus. The successful genotyping rate was 88.2% for rs3825807, 100% for rs1994016 and 97.6% for rs4380028. Out of these, thirteen samples were chosen for DNA sequencing to further confirm the genotype, among them 12 samples were correct, with one sample incorrectly genotyped. The restriction enzyme digestion method was also tested but showed less than 60% success rate. Finally, we combined the genotyping results of the three methods and obtained the following genotype information (Table 3.1, for detailed information of VSMC genotype, please see Appendix table 3.1.1) for the VSMC collection regarding the SNPs of interest. The genotype frequencies were in agreement with Hardy-Weinberg equilibrium.

Table 3.1 CAD-related SNPs' genotyping results for VSMCs

SNP	Genotype	Number	Frequency (%)
rs3825807	A/A	66	59 %
	A/G	35	31 %
	G/G	11	10 %
	Total	112	100 %
rs1994016	C/C	72	57 %
	T/C	52	41 %
	T/T	3	2 %
	Total	127	100 %
rs4380028	C/C	69	55 %
	T/C	42	34 %
	T/T	13	11 %
	Total	124	100 %

Linkage disequilibrium values (r^2) between these three SNPs in our VSMC sample collection were similar to those in the HapMap data set obtained using the SNAP Programme (Table 3.2).

Table 3.2 Linkage disequilibrium values (r^2) between the three *ADAMTS7* SNPs studied

SNP1	SNP2	HapMap	Our VSMC sample collection
rs3825807	rs1994016	0.87	0.76
rs3825807	rs4380028	0.52	0.67
rs1994016	rs4380028	0.57	0.63

Genomic DNA was also extracted from coronary atherosclerotic plaques (n=55) and genotyped for SNP rs3825807 using the KASPar method. The genotype frequency in this sample collection is shown in Table 3.3.

Table 3.3 Coronary artery plaque collection *ADAMTS7* SNP rs3825807 genotyping results

SNP	Genotype	Number	Frequency (%)
rs3825807	A/A	24	44 %
	A/G	20	36 %
	G/G	11	20 %
	Total	55	100 %

3.1.6 The CAD-related SNPs at the *ADAMTS7* locus have no effects on VSMC proliferation, senescence and apoptosis

The presence of ADAMTS-7 in atherosclerotic plaques and its colocalisation with VSMCs led us to investigate the role of the CAD-related *ADAMTS7* SNPs in VSMC biological processes involved in plaque progression, such as proliferation, senescence,

apoptosis and migration. Described in this section are results of assays of proliferation, senescence and apoptosis. Results of migration will be described in the next section.

3.1.6.1 VSMC proliferation

Proliferation of VSMCs isolated from different individuals was analysed using the BrdU labelling method (as described in section 2.5.1). No significant difference in proliferation was detected between the genotype groups of any of the three CAD-associated SNPs at the *ADAMTS7* gene locus studied (Figure 3.7), indicating that the association between these SNPs and CAD was not through regulation of VSMC proliferation.

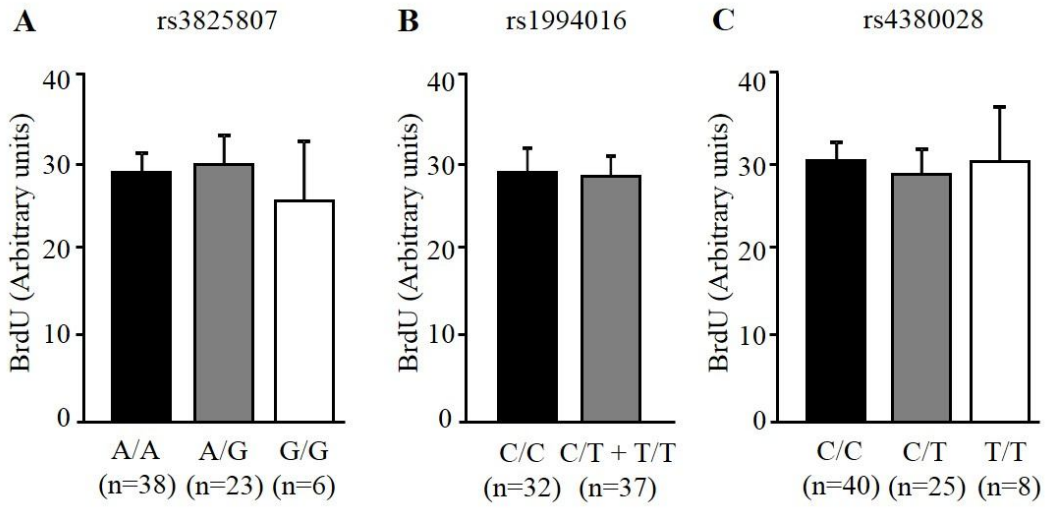

Figure 3.7 CAD-related SNPs at the *ADAMTS7* gene locus have no effect on VSMC proliferation. Data shown are values of cell proliferation as measured using BrdU assay (mean ± SEM). Statistically analysis performed using one-way ANOVA for SNP rs3825807 and rs4380028 and Student's t-test for rs1994016 (due to small sample size of rare allele homozygote T/T genotype, we combined the heterozygote group with rare allele homozygote group to increase the power of our analysis). No statistical significance was found.

3.1.6.2 VSMC senescence

The senescence assay method measuring the enzyme SA-ß-Gal produced by senescent cells was used. This assay showed no association between the SNPs studied and VSMC senescence (Figure 3.8).

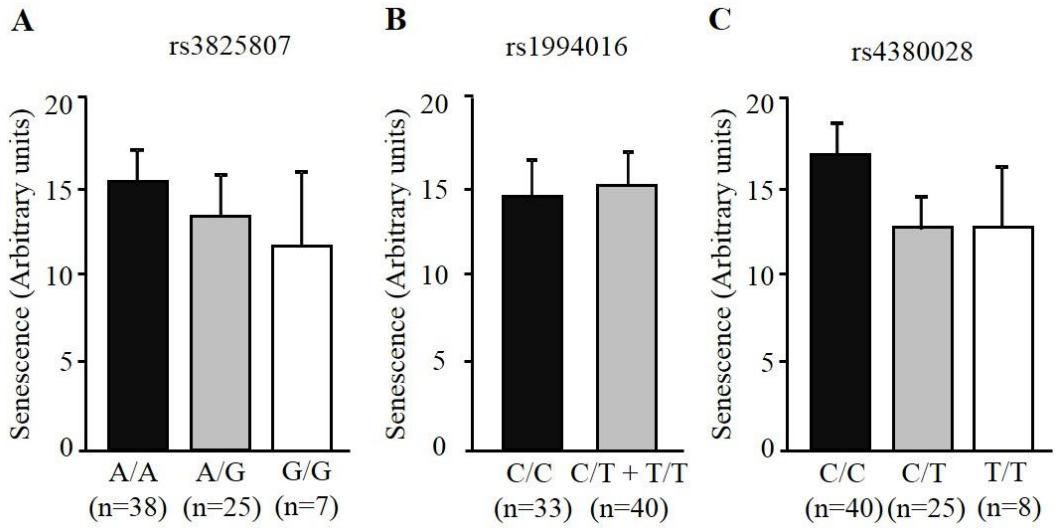

Figure 3.8 CAD-related SNPs at the *ADAMTS7* gene locus have no effect on VSMC senescence. Data shown are values of cell senescence (mean ± SEM). Statistically analysis performed using one-way ANOVA for SNP rs3825807 and rs4380028 and Student's t-test for rs1994016. No statistical significance was found.

3.1.6.3 VSMC apoptosis

Apoptosis is programmed cell death, where the genome of the cells is degraded into small DNA-histone complexes, which can be quantified. VSMC apoptosis is a critical process during the progression of atherosclerosis and also destabilises the atherosclerotic plaque, making it prone to rupture. Plaque rupture can cause myocardial infarction and stroke.

VSMC apoptosis assay was performed to investigate whether any of the three CAD-associated *ADAMTS7* SNPs studied affect VSMC apoptosis. The assay showed no association between these SNPs and VSMC apoptosis (Figure 3.9).

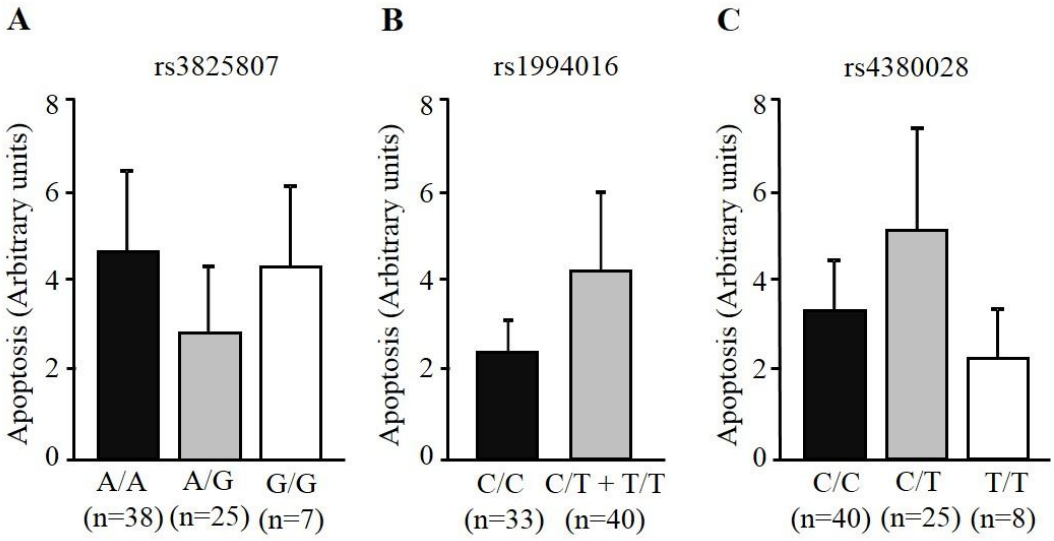

Figure 3.9 CAD-related SNPs at the *ADAMTS7* gene locus have no effect on VSMC apoptosis. Data shown are values of cell apoptosis (mean ± SEM). Statistically analysis performed using one-way ANOVA for SNP rs3825807 and rs4380028 and Student's t-test for rs1994016. No statistical significance was found.

3.1.7 Influence of CAD-related *ADAMTS7* SNPs on VSMC migration

It is generally recognised that SMC migration plays an important role in atherosclerosis. A recent study in rats showed that ADAMTS-7 facilitated VSMC migration and promoted neointima formation after balloon injury (Wang et al. 2009). Thus, we sought to investigate whether the CAD-associated SNPs at the *ADAMTS7* gene locus influence human VSMC migration. Scratch assays, as described in section 2.6.1, is a simple way to study cell migration. This method was used to study primary VSMCs from individuals of different genotypes for the CAD-associated *ADAMTS7* SNPs.

The scratch assay showed that VSMCs of the A/A genotype for rs3825807 had higher migratory ability, compared with G/G genotype of rs3825807 ($p<0.05$), and A/G genotype cells had migratory ability between that of A/A and G/G genotype cells; however, the difference between A/G and G/G genotypes was not significant (Figure 3.10).

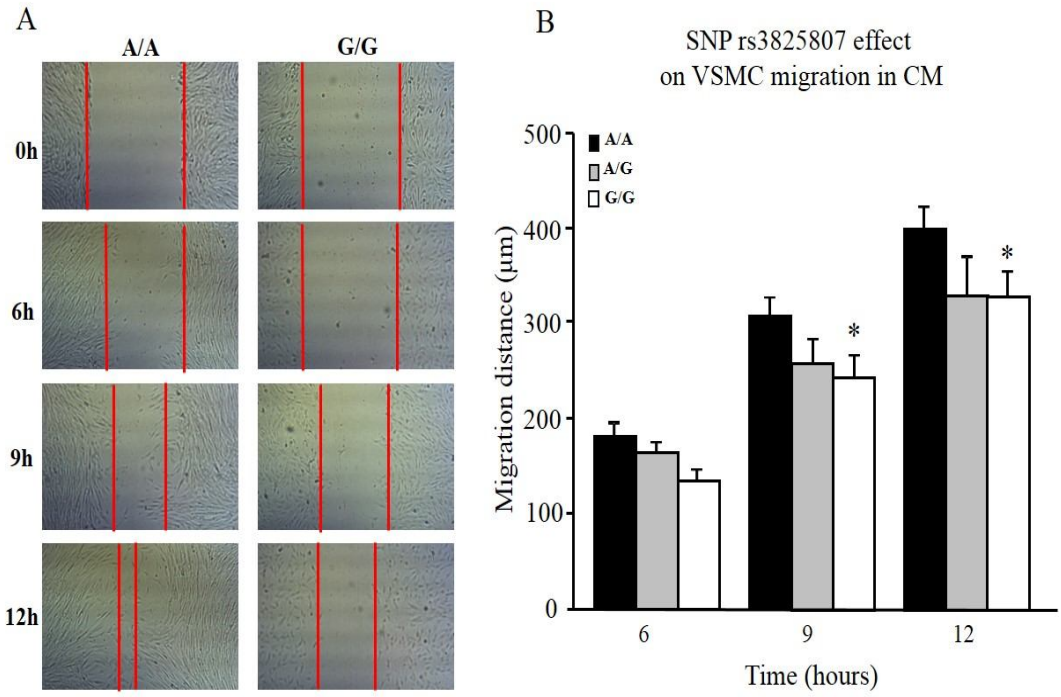

Figure 3.10 SNP rs3825807 affects VSMC migration. **A**: Representative pictures of rs3825807 homozygous genotypes at different time points of migration assay. **B**: Column chart represents migration distance (mean ± SEM) of VSMCs in DMEM supplemented with 15% FBS at different time points (n=5 for each genotype). One-way ANOVA (three genotype groups) and student's t-test (two genotype groups) was used to analyse the differences between genotype groups of the SNPs. * $p<0.05$ comparing A/A and G/G genotype group.

The effect of SNP rs3825807 on VSMC migration was observed in several cell culture conditions including culturing in media supplemented with 15% FBS (Figure 3.10), in serum-free media (Figure 3.11A), and in serum-free media with the addition of PDGF-BB (Figure 3.11B). In the presence of PDGF-BB, SNP rs3825807 still had an influence on VSMC migration, more interestingly, A/A genotype VSMCs showed much faster migration rates than both A/G and G/G genotype cells (Figure 3.11B). However, PDGF-BB treatment did not show strong stimulation on VSMC migration, possibly due to its low bioactivity after long period of storage.

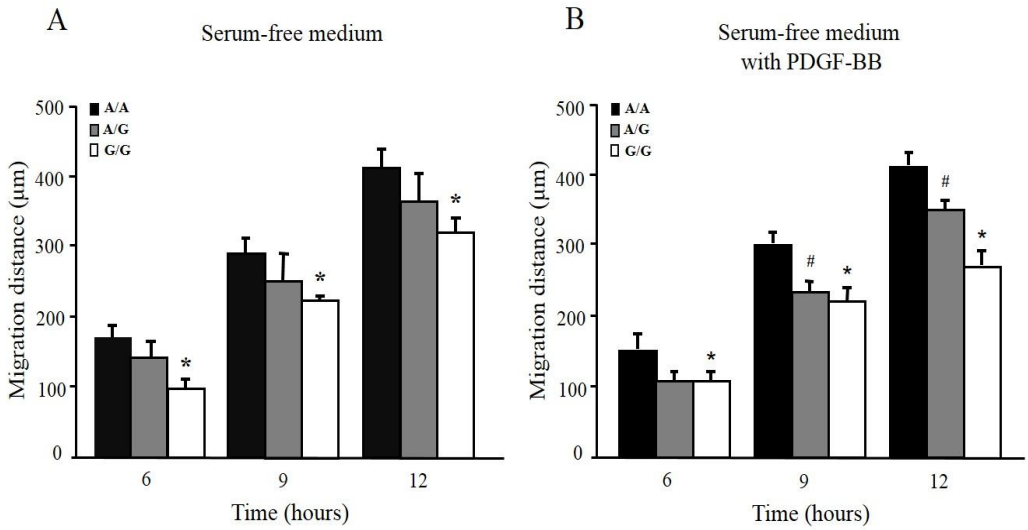

Figure 3.11 Effect of SNP rs3825807 on VSMC migration in serum-free media with or without PDGF-BB. Column charts represent migration distance (mean ± SEM) of VSMCs with serum-free media with or without PDGF-BB (10ng/ml) at different time points (n=5 for each genotype). One-way ANOVA (three genotype groups) and student's t-test (two genotype groups) was used to analyse the differences between genotype groups of the SNPs. * $p<0.05$ comparing A/A and G/G genotype group. # $p<0.05$ comparing A/A and A/G genotype group.

The other two CAD-associated SNPs at the *ADAMTS7* locus, rs1994016 and rs4380028, showed similar results to rs3825807, cells of the C/C genotype (risk allele homozygote) having greater migratory ability than cells of the C/T or T/T genotype (Figure 3.12-3.14). The similar effect of these three SNPs on VSMC migration is possibly due to the high LD between them.

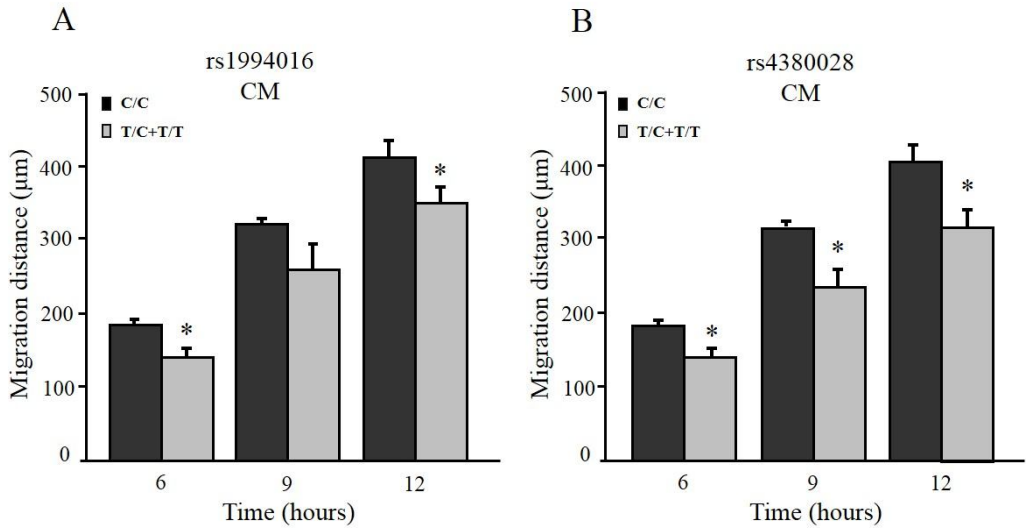

Figure 3.12 SNPs rs1994016 and rs4380028 affect VSMC migration in serum-containing media. Column charts represent migration distance (mean ± SEM) of VSMCs in DMEM supplemented with 15% FBS at different time points (n=3~5 for each genotype). Student's t-test was used to analyse the differences between genotype groups of the SNPs. * p<0.05 comparing C/C and T/C+T/T genotype group (we combined T/C and T/T due to availability of cells).

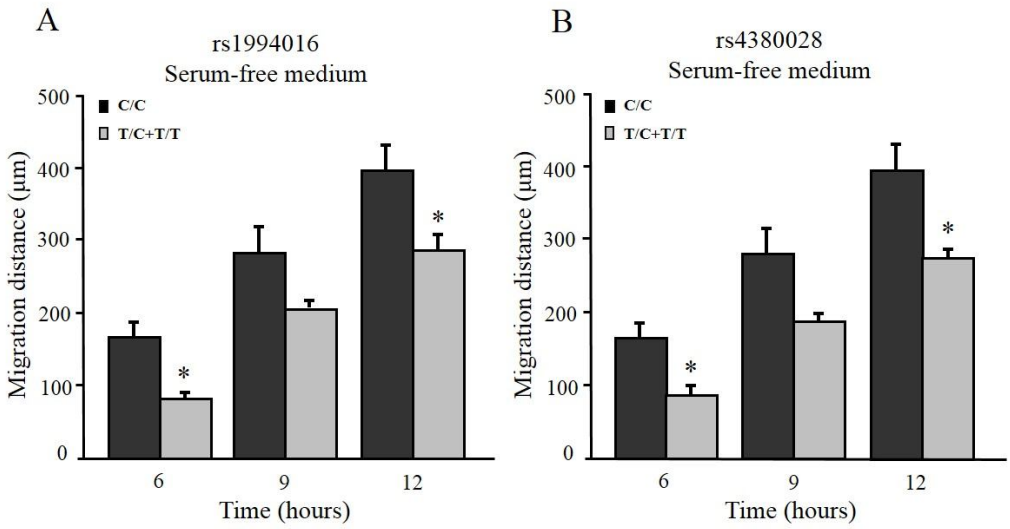

Figure 3.13 SNPs rs1994016 and rs4380028 affect VSMC migration in serum-free medium. Column charts represent migration distance (mean ± SEM) of VSMCs in serum-free media at different time points (n=3~5 for each genotype). Student's t-test was used to analyse the differences between genotype groups of the SNPs. * p<0.05 comparing C/C and T/C+T/T genotype group.

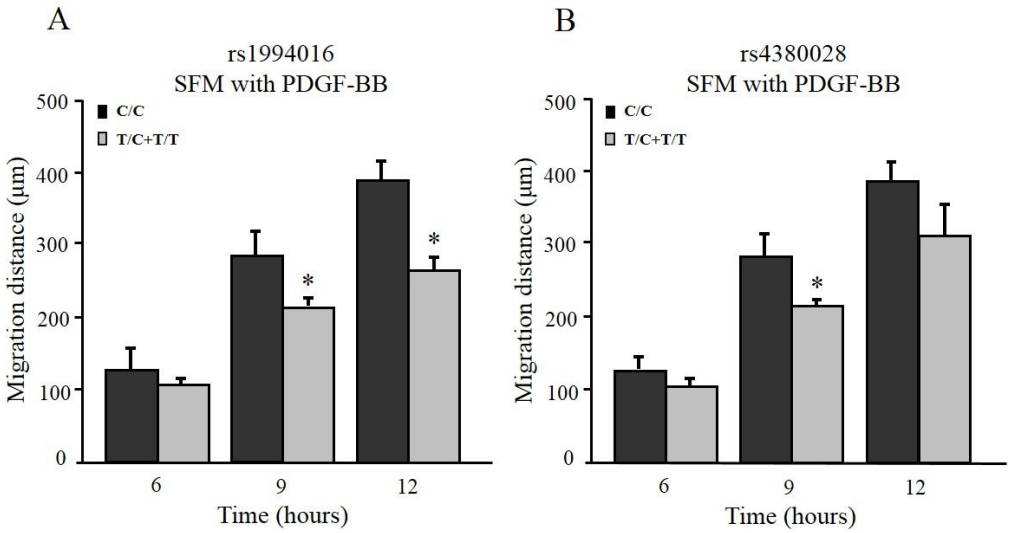

Figure 3.14 SNPs rs1994016 and rs4380028 affect VSMC migration in the presence of PDGF-BB. Column charts represent migration distance (mean ± SEM) of VSMCs in serum-free media with PDGF-BB (10ng/ml) at different time points (n=3~5 for each genotype). Student's t-test was used to analyse the differences between genotype groups of the SNPs. * $p<0.05$ comparing C/C and T/C+T/T genotype group.

The results from the scratch assay showed that the CAD-associated SNPs at the *ADAMTS7* locus could affect VSMC migration. Therefore we postulated that these three CAD-associated SNPs might affect *ADAMTS7* expression or ADAMTS-7 activation. Since ADAMTS-7 is a secreted protein, VSMCs with higher migratory ability could presumably have more ADAMTS-7 in the conditioned media and therefore have the ability to promote cell migration. To investigate whether this was the case, we collected conditioned media from VSMC cultures of different genotypes for rs3825807 and concentrated the media. Then, we added the concentrated conditioned media of A/A genotype cells into G/G genotype cells at the beginning of migration assay, and, conversely, A/A genotype cells with conditioned media of G/G genotype cells. The assay confirmed the previous finding that A/A genotype VSMCs had greater ability to migrate than VSMCs of the G/G genotype in serum-free media condition. More importantly, G/G cells with conditioned

media of A/A genotype cells showed increased migratory ability compared with G/G cells with serum-free media, indicating that A/A genotype cells likely secrete a migration-promoting factor into the media (Figure 3.15). This is consistent with our hypothesis in which the conditioned media from A/A genotype cells have more ADAMTS-7 and thus could promote VSMCs to migrate. Interestingly, A/A genotype cells with G/G genotype cell conditioned media did not show any effect on VSMC migration. One possible explanation is that A/A genotype cells can continuously secrete active ADAMTS-7 into the media, so the G/G genotype conditioned media could not affect the migratory ability of A/A genotype cells.

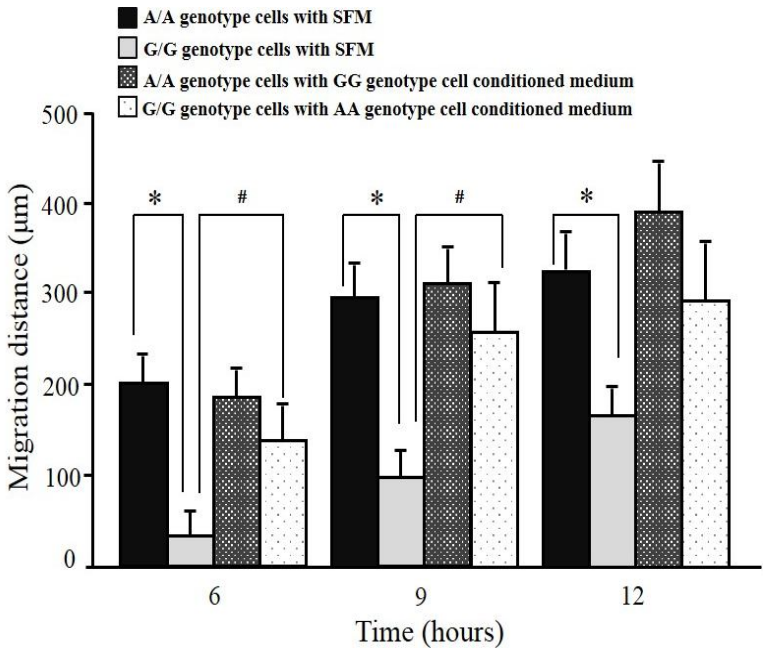

Figure 3.15 Effect of SNP rs3825807 on VSMC migration. Primary cultures of VSMCs of the A/A or G/G genotype for rs3825807 were subjected to scratch assays, with or without media swapping at the outset of the assay (i.e. at hour 0 of the assay, the culture media of G/G genotype cells was replaced by A/A genotype cell conditioned media, and vice versa). Column chart shows migration distances (mean ± SEM) (n=3 for each genotype). Student's t-test was used to analyse the differences between two groups. *p<0.05 comparing A/A genotype cells with SFM and G/G genotype cells with SFM; #p<0.05 comparing G/G genotype cells with A/A genotype cells' conditioned media versus G/G genotype cells with SFM.

3.1.8 CAD-related *ADAMTS7* SNPs have no effect on *ADAMTS7* mRNA level in VSMCs

The results from the migration assays support our hypothesis that the CAD-associated SNPs influence VSMC migration due to their effect on ADAMTS-7 production and/or activity in the culture media. This could be due to some or all of these SNPs having a genotypic effect on *ADAMTS7* mRNA expression level and consequently on ADAMTS-7 protein level.

In order to investigate whether these variants have an influence on *ADAMTS7* mRNA level in VSMCs, cells of different genotypes for SNPs rs3825807, rs1994016 and rs4380028 were subjected to *ADAMTS7* mRNA expression real-time RT-PCR analysis. No significant association between *ADAMTS7* mRNA level and genotype for any of these SNPs was detected in these assays, although in the case of rs1994016, lower *ADAMTS7* mRNA levels in T/T genotype cells were observed (Figure 3.16), suggesting a possible genotypic effect of this SNP on ADAMTS7 expression, however, need larger sample size to reach significant level.

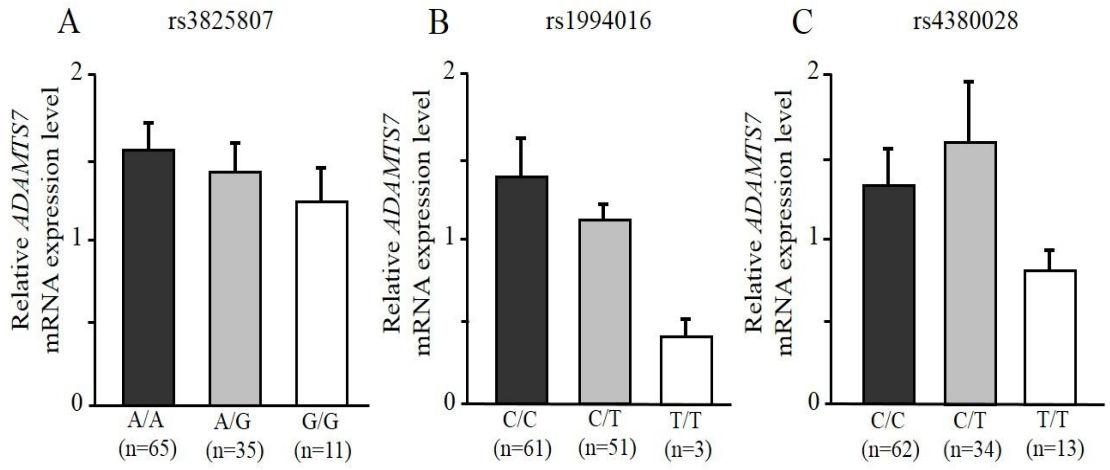

Figure 3.16 CAD-associated SNPs do not affect *ADAMTS7* mRNA expression level in VSMCs. The ΔΔCt method was used to analyse the data (beta-actin as internal control). Data shown are relative *ADAMTS7* mRNA expression to beta-actin (mean ± SEM). One-way ANOVA was used to analyse the difference between genotype groups of the SNP, $p>0.05$.

In addition to real-time RT-PCR, a second method was used to investigate whether the SNPs had an effect on *ADAMTS7* mRNA expression level, specifically, an allelic expression imbalance analysis of *ADAMTS7* was performed in VSMCs that were heterozygous for SNP rs3825807. If the SNP affects *ADAMTS7* mRNA expression, the ratio of the A allele versus the G allele should be different in cDNA from the ratio in gDNA. The analysis showed no difference in the A to G ratio between cDNA and gDNA samples (Figure 3.17), indicating that the SNP did not have an effect on *ADAMTS7* expression.

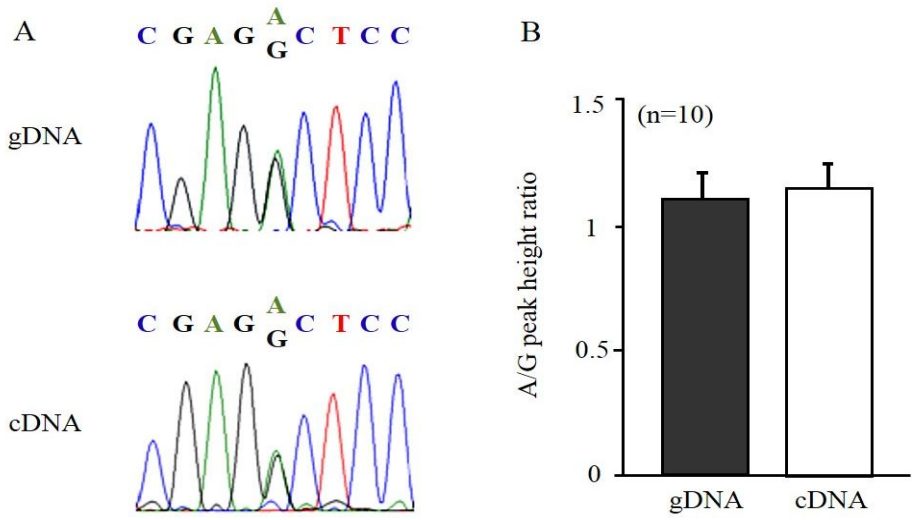

Figure 3.17 CAD-associated SNPs have no effect on *ADAMTS7* mRNA expression levels in VSMCs, determined by allelic expression imbalance assay. **A:** Chromagrams from gDNA and cDNA from isolated VSMCs, respectively. **B:** Schematic representation of the A/G ratios for gDNA and cDNA (mean ± SEM). Mann-Whitney test was performed to test a difference between the ratio of standardised A nucleotide peak height over standardised G nucleotide peak height from cDNA and the corresponding ratio from gDNA, n=10, P>0.05.

Since the results of qRT-PCR and allelic imbalance assays demonstrated that the CAD-associated SNPs at the *ADAMTS7* locus had no effect on *ADAMTS7* mRNA expression level, further experiments were conducted to investigate the possibility that they may have an impact on ADAMTS-7 protein activity. Of these SNPs, only rs3825807 causes an amino acid substitution, whereas rs1994016 is located in an intron and rs4380028 in the 3'-flanking region of the *ADAMTS7* gene. Thus the latter two SNPs are less likely to affect ADAMTS-7 protein activity than the non-synonymous SNP rs3825807. Therefore, the following experiments were focused on SNP rs3825807.

3.1.9 Effect of SNP rs3825807 on ADAMTS-7 pro-domain cleavage

SNP rs3825807 is located in exon 4 of the *ADAMTS7* gene and results in a serine (Ser) to proline (Pro) substitution in the pro-domain of ADAMTS-7 (Figure 3.18).

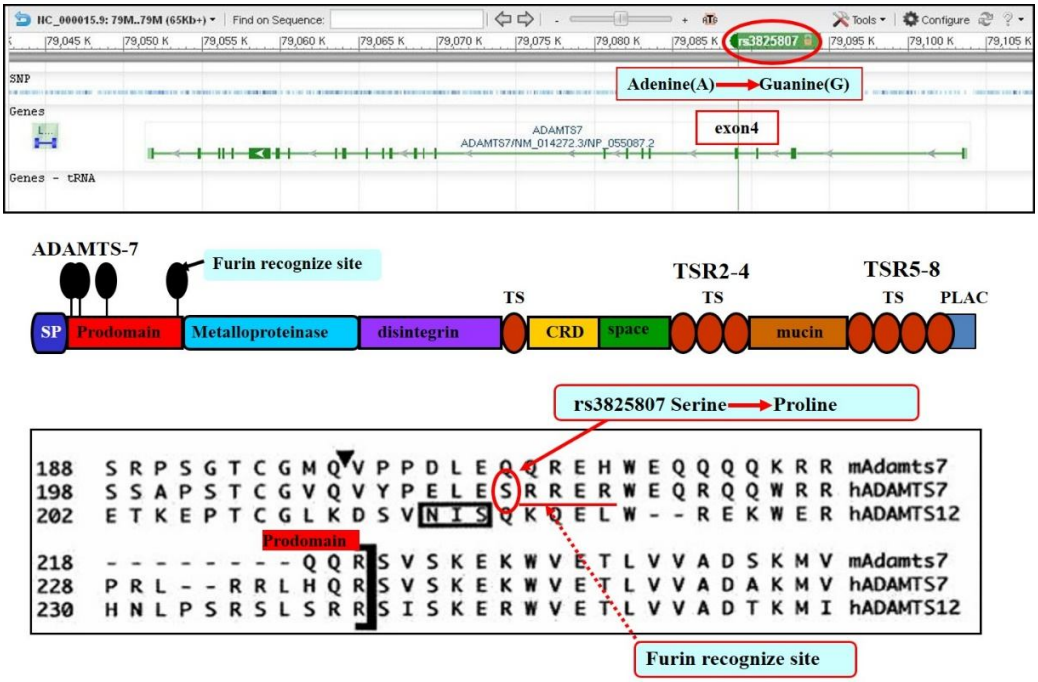

Figure 3.18 Location of SNP rs3825807 and the resulting Ser-to-Pro substitution. The upper panel indicates the location of SNP rs3825807 in the *ADAMTS7* gene. The middle panel is the schematic structure of ADAMTS-7 protein. The lower panel indicates the location of amino acid substitution resulted by SNP rs3825807 in ADAMTS-7 protein sequence. Figure cited and modified from (http://www.ncbi.nlm.nih.gov/projects/SNP/snp_ref.cgi?rs=3825807) (Somerville et al. 2004)

Although the qRT-PCR results showed that the rs3825807 genotype did not affect *ADAMTS7* mRNA expression level, Western blotting analysis was carried out to investigate if the SNP had an effect on ADAMTS-7 protein level in VSMCs. The analysis showed no difference in ADAMTS-7 protein level between different genotypes for

rs3825807, supporting the finding that the SNP did not affect *ADAMTS7* expression (Figure 3.19).

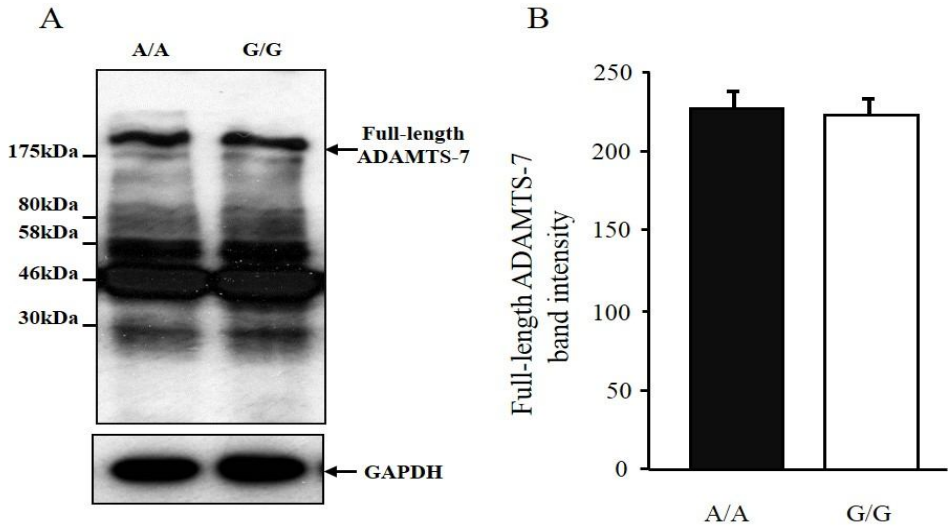

Figure 3.19 No effect of the CAD-related SNP rs3825807 on ADAMTS-7 protein level. **A**: A representative image of Western blot analysis of whole cell protein lysates of VSMCs of the A/A and G/G genotype for rs3825807. Equal amounts of protein (20μg) for each genotype was loaded and subjected to Western blotting using an ADAMTS-7 pro-domain antibody. **B**: Data shown in column chart are full-length ADAMTS-7 band intensity (mean ± SEM) in Western blot (n=3 for each genotype). Student's t-test was used to analyse the data, no statistical significance was found.

The Ser-to-Pro substitution resulting from SNP rs3825807 occurs at amino acid residue 214 of the ADAMTS-7 protein. This residue is located in the pro-domain and is immediately adjacent to a predicted core recognition site for furin, a proprotein convertase that has been demonstrated to cleave the ADAMTS-7 pro-domain, leading to its activation (Somerville et al. 2004). To investigate whether the SNP rs3825807 resulting in the Ser-to-Pro substitution had an effect on ADAMTS-7 pro-domain cleavage, Western blot analyses of conditioned media of VSMCs of different genotypes for this SNP were performed. Western blot analyses showed that VSMC conditioned media contained

cleaved ADAMTS-7 pro-domain (detected by a specific antibody to pro-domain of ADAMTS-7). The analyses showed that the amount of the cleaved ADAMTS-7 pro-domain in media conditioned by VSMCs of the A/A genotype was ~5 fold higher than in media conditioned by VSMCs of the G/G genotype (Figure 3.20).

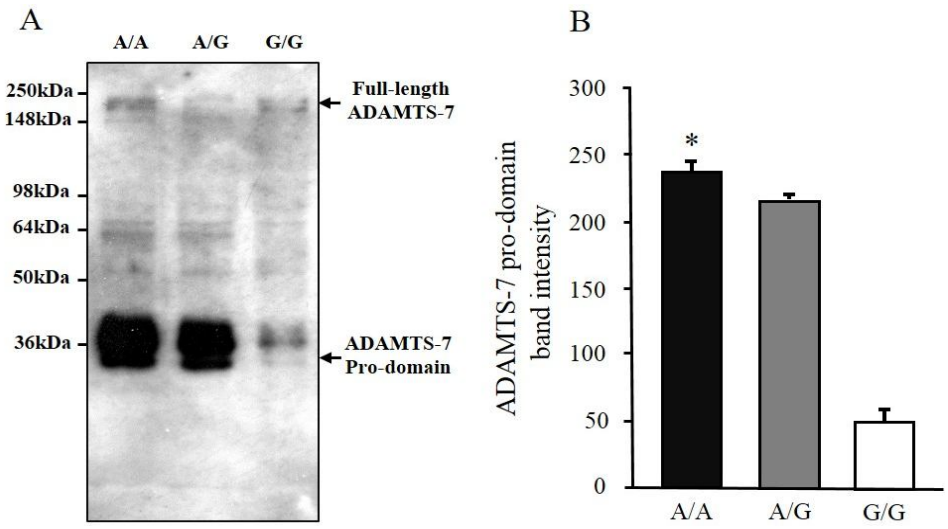

Figure 3.20 Effect of CAD-related SNP rs3825807 on ADAMTS-7 pro-domain cleavage in conditioned media. **A**: A representative image of Western blot analysis of cleaved ADAMTS-7 pro-domain in media conditioned by VSMCs of the A/A, A/G or G/G genotype for rs3825807. Equal amounts of proteins (20μg) for each genotype was loaded and subjected to Western blotting using an anti-ADAMTS-7 pro-domain antibody. **B**: Data shown in column chart are cleaved ADAMTS-7 pro-domain band intensity (mean ± SEM) (n=5 for each genotype). Student's t-test was used to analyse the data, *$p<0.05$ comparing A/A and G/G genotypes.

These data indicate that SNP rs3825807 has an effect on ADAMTS-7 pro-domain cleavage, supporting the hypothesis that SNP rs3825807 affects VSMC migration through its effect on ADAMTS-7 protein activation.

3.1.10 Influence of SNP rs3825807 genotype on TSP-5 cleavage

It is possible that the cleavage of the pro-domain could lead to the release of the active form of ADAMTS-7 with proteolytic activity to process its substrates. It has been shown that VSMCs produce the extracellular matrix protein TSP-5 which VSMCs adhere to (Riessen et al. 2001) and that ADAMTS-7 promotes VSMC migration via cleaving TSP-5 (Wang et al. 2009). Following the finding that *ADAMTS7* SNP influenced VSMC migration and ADAMTS-7 pro-domain cleavage, further experiments were carried out to investigate whether there was a difference in the concentration of cleaved TSP-5 in VSMC culture media between the three genotypes for rs3825807. The experiments showed that culture media of VSMCs of the A/A genotype for SNP rs3825807 contained more cleaved TSP-5, compared with the G/G genotype (Figure 3.21).

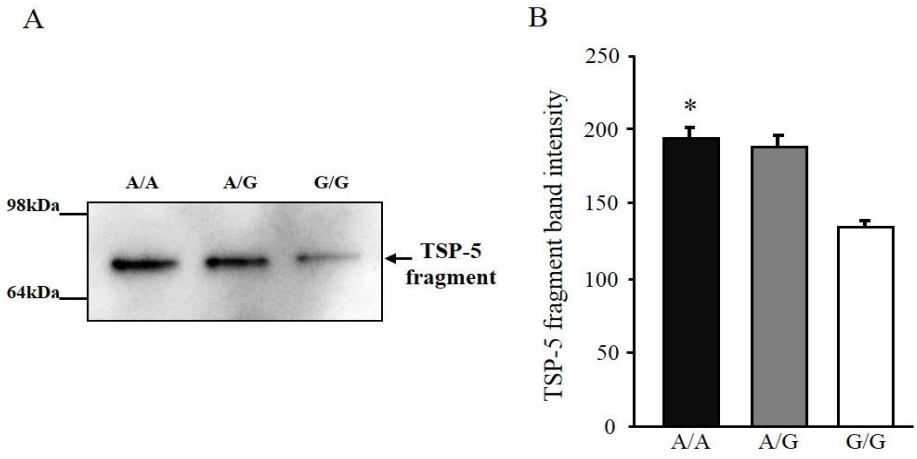

Figure 3.21 Influence of CAD-related SNP rs3825807 on TSP-5 cleavage. **A**: A representative image of Western blot analysis of cleaved TSP-5 in media conditioned by VSMCs of the A/A, A/G or G/G genotype for rs3825807. Equal amounts of protein (20µg) for each genotype was loaded and subjected to Western blot analysis using a specific TSP-5 antibody. **B**: Data shown in column chart are cleaved TSP-5 band intensity (mean ± SEM) (n=5 for each genotype). Student's t-test was used to analyse the data, *p<0.05 comparing A/A and G/G genotypes.

We showed that the conditioned media of the A/A genotype cells could promote VSMC migration, and subsequent Western blotting analyses showed that conditioned media of A/A genotype cells contained more cleaved ADAMTS-7 pro-domain and TSP-5 fragments. Thus, we further carried out *in vitro* assays of TSP-5 cleavage with media conditioned by VSMCs of either the A/A or G/G genotype to investigate whether conditioned media of A/A genotype cells have a higher ability to cleave TSP-5 than conditioned media of G/G genotype cells. The assays showed that the conditioned media were able to cleave TSP-5 and that the media conditioned by VSMCs of the A/A genotype had higher TSP-5 cleavage activity than media conditioned by VSMCs of the G/G genotype (Figure 3.22).

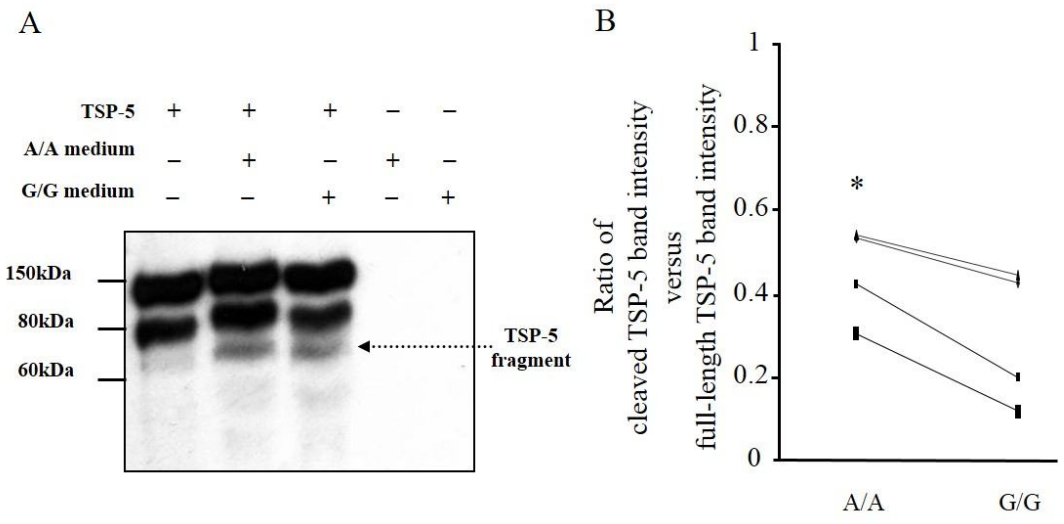

Figure 3.22 *In vitro* TSP-5 digestion assay. **A**: A representative image of Western blot analysis of products from *in vitro* TSP-5 cleavage assays. Recombinant TSP-5 (2µg) was incubated, with or without 5µl concentrated media conditioned by VSMCs of the A/A or G/G genotype, in a digestion buffer at 37°C for 8 hours. The digests, along with undigested TSP-5, were subjected to Western blot analysis using an anti-TSP-5 antibody. **B**: Data shown in graph are ratio of cleaved TSP-5 band intensity versus full-length TSP-5 band intensity (mean ± SEM) (n=4 for each genotype). Student's t-test was used to analyse the data, *p<0.05 comparing A/A (second column) with G/G (third column) genotype group.

3.1.11 SNP rs3825807 affects ADAMTS-7 activation

To further assess the functional effects of the non-synonymous SNP rs3825807 that results in a Ser-to-Pro substitution in the ADAMTS-7 pro-domain, we transfected HEK293 cells with a plasmid to produce a recombinant protein consisting of the ADAMTS-7 signal peptide, pro-domain (of either ADAMTS-7-214Ser or ADAMTS-7-214Pro) and metalloproteinase domain followed by a c-Myc epitope tag. These two plasmids are identical except rs3825807 site. In a previous study, HEK293 cells were transfected with a similar plasmid and then Western blot analyses was carried out using conditioned media, surface washes (with 0.5M NaCl), and lysates of the transfected cells (Somerville et al. 2004). The authors showed that the recombinant protein underwent pro-domain cleavage, leading to an initially processed form (P1), an intermediate form (Pint) and a fully processed form (M) (as schematically illustrated in Figure 3.23A). The recombinant protein has been shown to retain its proteolytic ability to process one of its substrate, A2M (Somerville et al. 2004).

In our study, Western blot analyses of conditioned media of transfected cells using an anti-cMyc antibody showed three bands with sizes corresponding to the P1, Pint and M forms. The relative intensities of Pint and M bands (relative to P1 band) were ~1.7 and ~4 fold higher, respectively, when comparing conditioned media from *ADAMTS7*$_{Pro\text{-}Cat}$*-214Ser* transfected cells with that of *ADAMTS7*$_{Pro\text{-}Cat}$*-214Pro* transfected cells, indicating more processed ADAMTS-7 was released into the cell media in *ADAMTS7*$_{Pro\text{-}Cat}$*-214Ser* transfected HEK293 cells than that of *ADAMTS7*$_{Pro\text{-}Cat}$*-214Pro* transfected HEK293 cells.

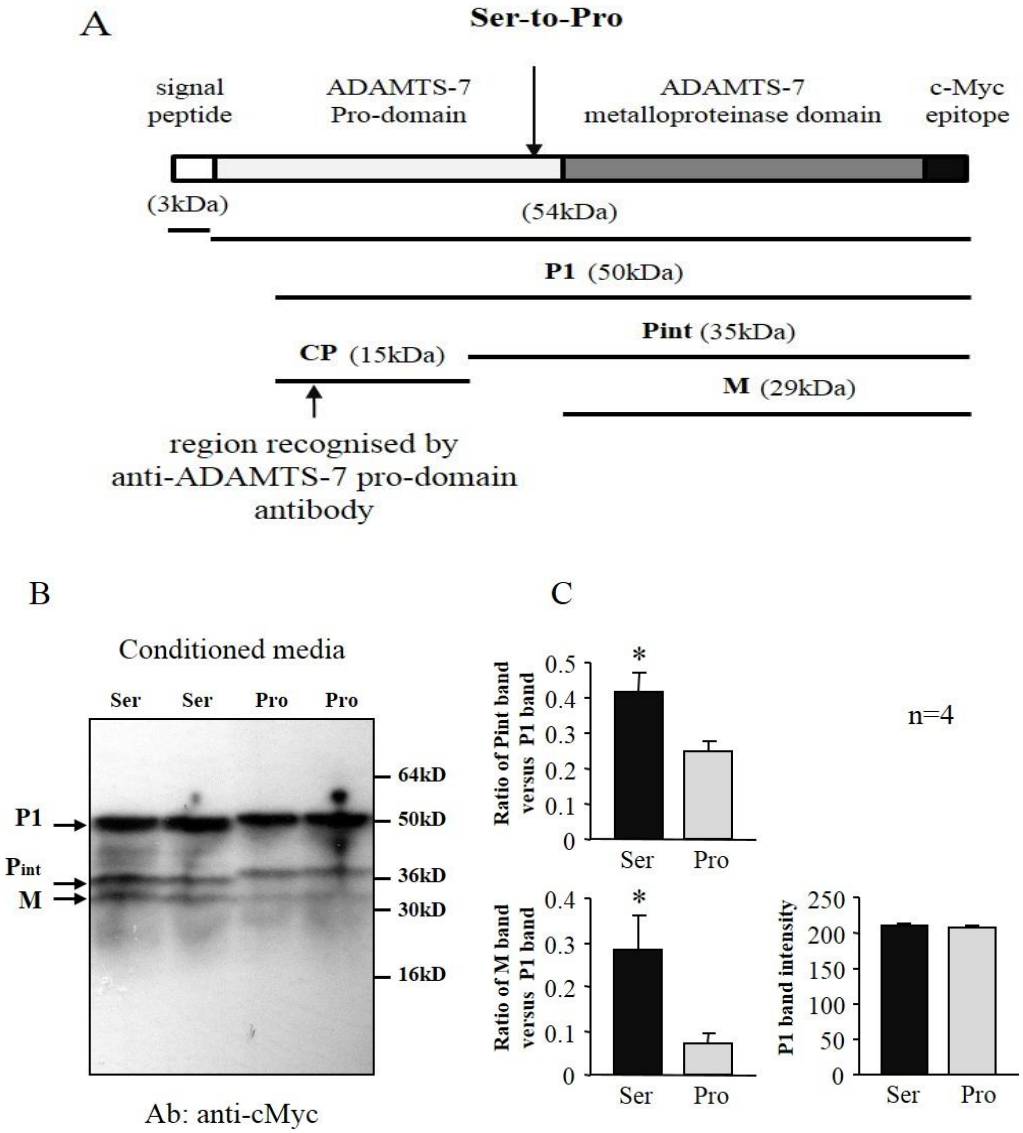

Figures 3.23 SNP rs3825807 has an effect on ADAMTS-7 activation. Cultured HEK293 cells were transfected with a plasmid to produce a recombinant protein containing the ADAMTS-7 pro-domain and metalloproteinase domain followed by a c-Myc epitope tag, with either serine (Ser) or proline (Pro) at residue 214 in the ADAMTS-7 pro-domain. **A**: A schematic diagram for the produced recombinant protein. P1, Pint and M indicate the previously reported initially processed form, intermediately processing form, and fully processed form, respectively; CP indicates a cleaved ADAMTS-7 pro-domain fragment. **B**: A representative image of the conditioned media of the Western blot analysis using an anti-cMyc antibody. Equal amounts of protein (20µg) for each allele was loaded. **C:** Data shown in column chart are presentations of values (mean ± SEM) (n=4 for each allele). Statistical analysis was performed using Student's t-test, *p<0.05 comparing ADAMTS-$7_{Pro\text{-}Cat}$ -214Ser and ADAMTS-$7_{Pro\text{-}Cat}$ -214Pro.

In Western blot analyses of conditioned media of transfected cells using an anti-ADAMTS-7 pro-domain antibody, a cleaved pro-domain band was detected. The relative intensity of cleaved pro-domain band of ADAMTS-7 (relative to P1 band) was ~2 fold higher (Figure 3.24), when comparing conditioned media from *ADAMTS7*$_{Pro\text{-}Cat}$*-214Ser* transfected cells with that of *ADAMTS7*$_{Pro\text{-}Cat}$*-214Pro* transfected cells, indicating more ADAMTS-7 was activated in *ADAMTS7*$_{Pro\text{-}Cat}$*-214Ser* transfected HEK293 cells than that of *ADAMTS7*$_{Pro\text{-}Cat}$*-214Pro* transfected HEK293 cells. However, the cleaved pro-domain band of ADAMTS-7 detected in conditioned media of transfected cells was very weak (Figure 3.24A).

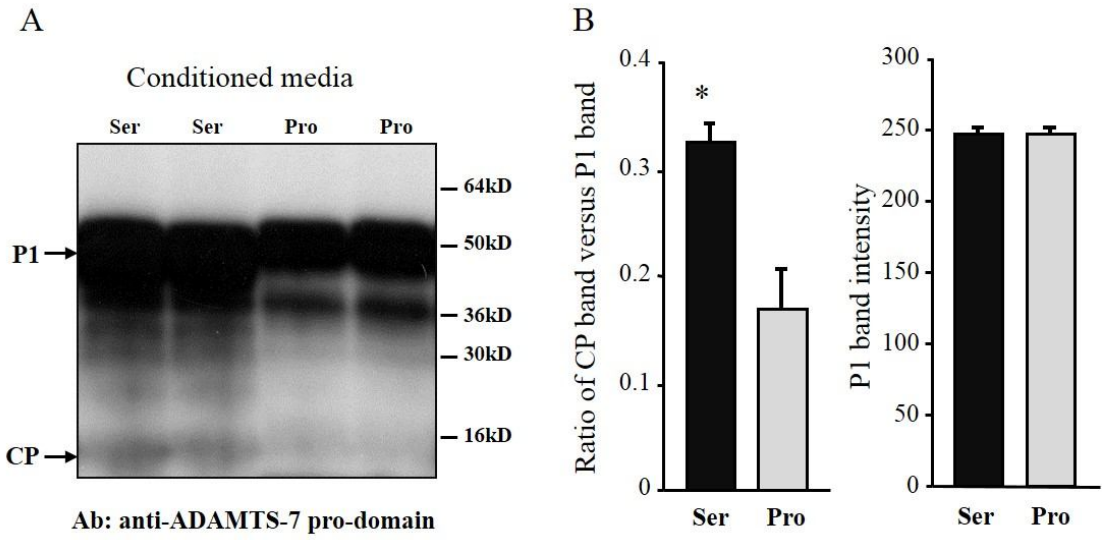

Figures 3.24 SNP rs3825807 has an effect on ADAMTS-7 pro-domain processing. Cultured HEK293 cells were transfected with either *ADAMTS7*$_{Pro\text{-}Cat}$*-214Ser* or *ADAMTS7*$_{Pro\text{-}Cat}$*-214Pro* plasmids, and conditioned media were subjected to Western blot analyses using an anti-ADAMTS-7 pro-domain antibody. Equal amounts of protein (20µg) for each allele was loaded. **A**: A representative image of the Western blot using an anti-ADAMTS-7 pro-domain antibody. **B**: Data shown in column chart are presentations of values (mean ± SEM). (n=4 for each allele). Statistical analysis was performed using Student's t-test, *p<0.05 comparing ADAMTS-7$_{Pro\text{-}Cat}$-214Ser and ADAMTS-7$_{Pro\text{-}Cat}$-214Pro.

These results support the hypothesis that the Ser-to-Pro substitution resulting from SNP rs3825807 affects ADAMTS-7 pro-domain processing. Interestingly, the Pint and P1 forms of ADAMTS-7$_{Pro\text{-}Cat}$-214Pro had a reduced electrophoretic mobility, compared with the Pint and P1 forms of ADAMTS-7$_{Pro\text{-}Cat}$ -214Ser (Figures 3.23B), which is in line with reports in the literature that proline-rich proteins tend to migrate more slowly in SDS-PAGE, presumably due to conformational peculiarities that persist even under reducing conditions (Williamson 1994). Presumably, the conformational change of ADAMTS-7$_{Pro\text{-}Cat}$ -214Pro affects the binding of furin and leads to reduced activation, but to know whether or not this is the case will require further studies.

In order to address whether the cleaved pro-domain of ADAMTS-7 attached to cell surface, cell surface washes (with 0.5M NaCl) of HEK293 cells either transfected with *ADAMTS7*$_{Pro\text{-}Cat}$*-214Ser* or *ADAMTS7*$_{Pro\text{-}Cat}$*-214Pro* plasmids were subjected to Western blot. Western blotting using an antibody against the ADAMTS-7 pro-domain detected a cleaved pro-domain fragment in cell surface washes of the transfected cells, which was much stronger compared with the pro-domain signal in the conditioned media (Figure 3.24A), suggesting binding of the cleaved pro-domain fragment to the cell surface (Figure 3.25A). Noticeably, the intensity of this band was also ~2 fold higher in cell surface washes, similar as in conditioned media, when comparing media conditioned by HEK293 cells transfected with *ADAMTS7*$_{Pro\text{-}Cat}$*-214Ser* plasmid and media conditioned by HEK293 cells transfected with *ADAMTS7*$_{Pro\text{-}Cat}$*-214Pro* plasmid (Figures 3.25B), supporting the SNP rs3825807 affects ADAMTS-7 pro-domain cleavage.

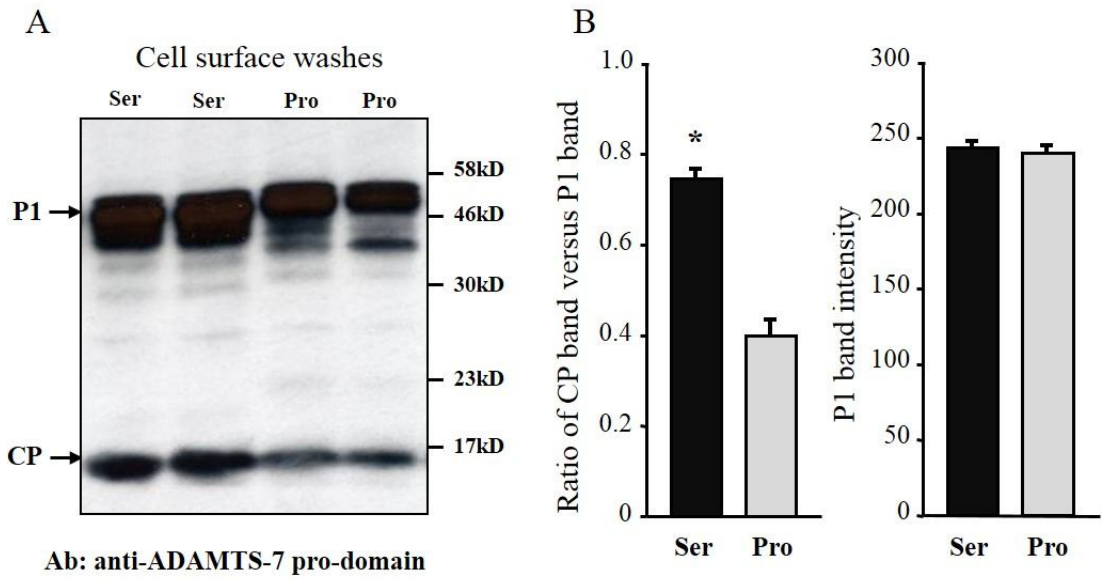

Figures 3.25 SNP rs3825807 affects amount of cleaved ADAMTS-7 pro-domain in the cell surface washes. Cultured HEK293 cells were transfected with either *ADAMTS7*$_{Pro\text{-}Cat}$*-214Ser* or *ADAMTS7*$_{Pro\text{-}Cat}$*-214Pro* plasmid. And then cell surface washes (with 0.5M NaCl) were subjected to Western blot analyses with an anti-ADAMTS-7 pro-domain antibody. **A**: Representative images of the Western blot using an anti-ADAMTS-7 pro-domain antibody. The same amount of proteins (20µg) for each allele was loaded. **B**: Data shown in column chart are presentations of values (mean ± SEM) (n=4 for each allele). Statistical analysis was performed using Student's t-test, *p<0.05 comparing ADAMTS-7$_{Pro\text{-}Cat}$-214Ser and ADAMTS-7$_{Pro\text{-}Cat}$-214Pro.

Western blot analyses of cell surface washes using an anti-cMyc antibody showed one major band with size corresponding to the P1 form, with similar intensities for cells transfected with either plasmid. The M form was almost undetectable, indicating the M form does not attach to the cell surface (Figure 3.26).

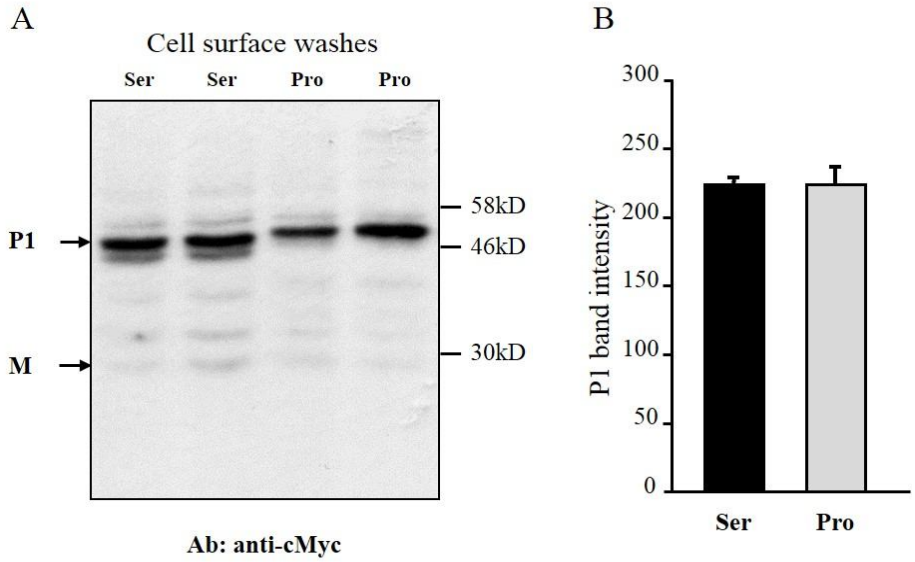

Figure 3.26 Cell surface washes Western blotting with anti-cMyc. Cultured HEK293 cells were transfected with either *ADAMTS7$_{Pro\text{-}Cat}$-214Ser* or *ADAMTS7$_{Pro\text{-}Cat}$-214Pro* plasmids. And then cell surface washes (with 0.5M NaCl) were subjected to Western blot analyses using an anti-cMyc antibody. **A**: A representative image of the Western blot. The same amount of proteins (20µg) for each allele was loaded. **B**: Data shown in column chart are presentations of values (mean ± SEM) (n=4 for each allele).

Western blotting analysis of whole cell lysates of HEK293 cells transfected with either the *ADAMTS7*$_{Pro\text{-}Cat}$*-214Ser* or *ADAMTS7*$_{Pro\text{-}Cat}$*-214Pro* plasmid detected the P1 form by using either an anti-cMyc antibody or an anti-ADAMTS-7 pro-domain antibody. In comparison, the cleaved ADAMTS-7 pro-domain band was much weaker, suggesting pro-domain processing occurs mostly extracellularly (Figure 3.27).

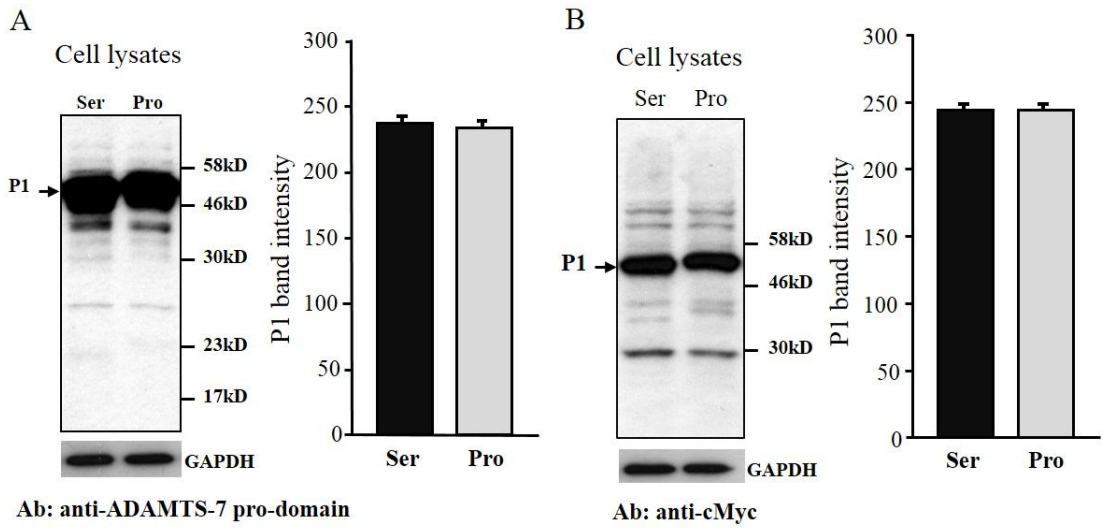

Figure 3.27 SNP rs3825807 has no effect on ADAMTS-7 total protein in cell lysates. Cultured HEK293 cells were transfected with either *ADAMTS7*$_{Pro\text{-}Cat}$*-214Ser* or *ADAMTS7*$_{Pro\text{-}Cat}$*-214Pro* plasmids, and cell lysates were subjected to western blot analyses with either an anti-ADAMTS-7 pro-domain antibody or an anti-cMyc antibody. Equal amounts of protein (40µg) for each allele was loaded. **A**: Representative images of the Western blot analysed with an anti-ADAMTS-7 pro-domain antibody and quantification data. **B**: Representative images of the Western blot analysed with an anti-cMyc antibody and quantification data. Quantification data shown in column chart are P1 band intensity (mean ± standard error of mean) (n=4 for each allele).

3.1.12 Further experiments confirming an effect of SNP rs3825807 on TSP-5 cleavage

To further test the effect of the Ser-to-Pro substitution resulting from SNP rs3825807 on TSP-5 cleavage, TSP-5 cleavage assays were carried out using media conditioned by HEK293 cells transfected with either of the plasmids described above. Recombinant TSP-5 (2μg) was incubated with 1, 2 or 4 μl concentrated media (1μg total proteins/μl) conditioned by HEK293 cells transfected with either *ADAMTS7*$_{Pro\text{-}Cat}$*-214Ser* or *ADAMTS7*$_{Pro\text{-}Cat}$*-214Pro* plasmid, in a digestion buffer at 37°C for 8 hours. The digests, along with undigested TSP-5 and concentrated conditioned media, were subjected to Western blotting analysis with an anti-TSP-5 antibody.

Similar to the TSP-5 *in vitro* digestion assay using VSMC conditioned media, the conditioned media of HEK293 cells transfected with either the *ADAMTS7*$_{Pro\text{-}Cat}$*-214Ser* or *ADAMTS7*$_{Pro\text{-}Cat}$*-214Pro* plasmid digested TSP-5. The digestion of TSP-5 is in the dose-dependent manner, and media conditioned by HEK293 cells transfected with the *ADAMTS7*$_{Pro\text{-}Cat}$*-214Ser* plasmid had two fold higher TSP-5 cleavage activity than media conditioned by *ADAMTS7*$_{Pro\text{-}Cat}$*-214Pro* plasmid transfected cells (Figure 3.28).

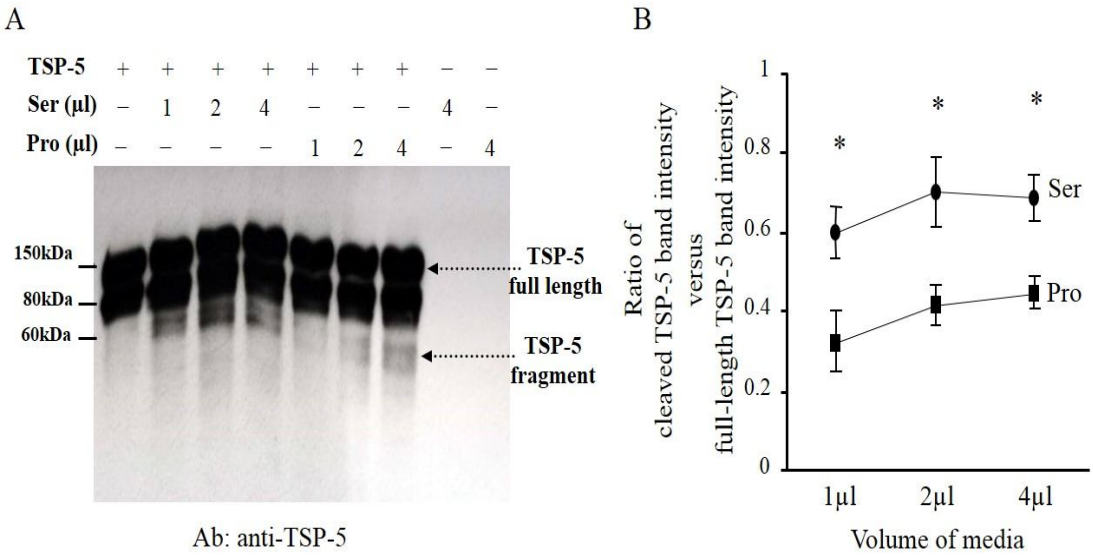

Figure 3.28 Influence of CAD-related SNP rs3825807 on TSP-5 cleavage. Recombinant TSP-5 (2µg) was incubated with 1, 2 or 4 µl concentrated media (1µg total proteins/µl) conditioned by HEK293 cells transfected with either *ADAMTS7*$_{Pro\text{-}Cat}$*-214Ser* or *ADAMTS7*$_{Pro\text{-}Cat}$*-214Pro* plasmid, in a digestion buffer at 37°C for 8 hours. The digests, along with undigested TSP-5 and concentrated conditioned media, were subjected to Western blotting analysis using an anti-TSP-5 antibody. **A**: A representative image of Western blot analysis of products from *in vitro* TSP-5 cleavage assays. **B**: Data shown in graph are ratio of cleaved TSP-5 band intensity versus full-length TSP-5 band intensity (mean ± SEM) (n=3 for each genotype). Statistical analysis was performed using Student's t-test, *p<0.05 comparing ADAMTS-7$_{Pro\text{-}Cat}$-214Ser and ADAMTS-7$_{Pro\text{-}Cat}$-214Pro.

3.1.13 Further experiments confirming an effect of SNP rs3825807 on VSMC migration

To further assess the effect of SNP rs3825807 on VSMC migration, media conditioned by HEK293 cells transfected with either of the plasmids described above were added to VSMC cultures, followed by migration assays. At hour 0 of the assay, A/A genotype VSMCs were treated with serum-free media, HEK293 cell conditioned media containing ADAMTS-7$_{Pro\text{-}Cat}$-214Ser or HEK293 cell conditioned media containing ADAMTS-7$_{Pro\text{-}Cat}$-214Pro. G/G genotype VSMCs were treated in a similar manner. The experiments showed that the migratory ability of G/G genotype VSMCs increased after the addition of HEK293 cell conditioned media containing ADAMTS-7$_{Pro\text{-}Cat}$-214Ser, but did not significantly change after the addition of HEK293 cell conditioned media containing ADAMTS-7$_{Pro\text{-}Cat}$-214Pro, suggesting a migration enhancing effect from ADAMTS-7$_{Pro\text{-}Cat}$-214Ser containing media which presumably had a higher concentration of active ADAMTS-7 (Figure 3.29).

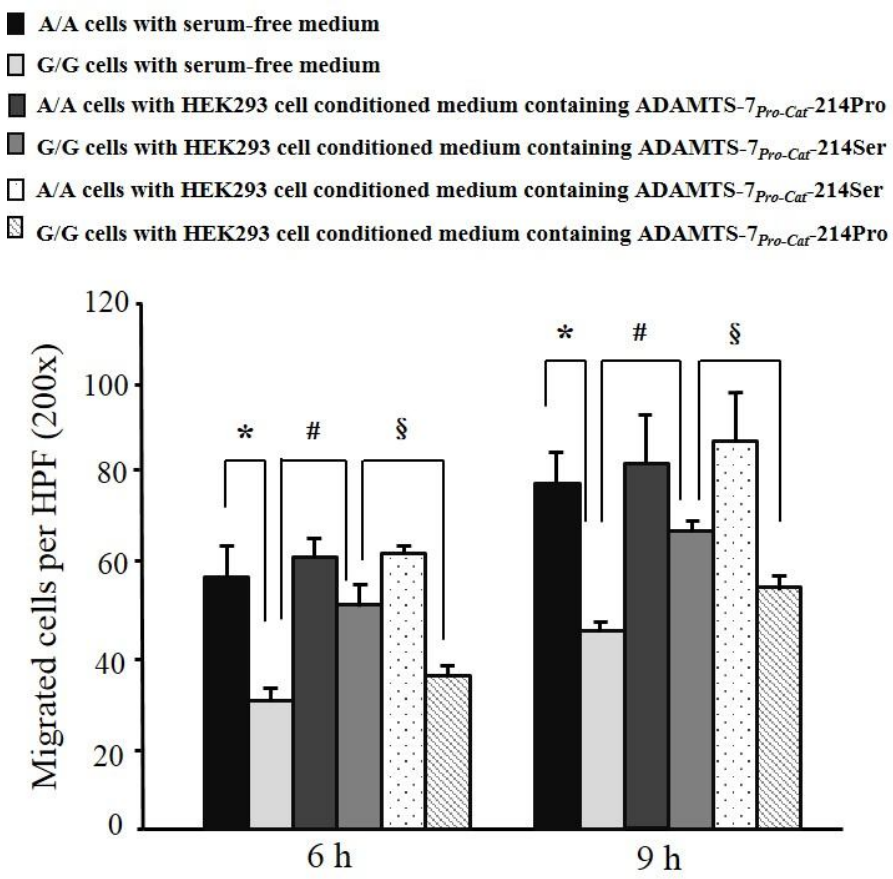

Figure 3.29 Effect of SNP rs3825807 on VSMC migration by trans-well migration assay. Primary cultures of VSMCs of the A/A or G/G genotype were subjected to trans-well migration assays. At the beginning of the assay, A/A or G/G genotype VSMCs were replaced with serum-free media, HEK293 cell conditioned media containing ADAMTS-$7_{Pro\text{-}Cat}$-214Ser or ADAMTS-$7_{Pro\text{-}Cat}$-214Pro. Column chart shows migrated cell number (mean ± SEM) (n=4 for each genotype). Statistical analysis was performed using Student's t-test, *p<0.05 comparing A/A genotype cells with serum-free media and G/G genotype cells with serum-free media; #p<0.05 comparing G/G genotype cells with HEK293 cell conditioned media containing ADAMTS-$7_{Pro\text{-}Cat}$-214Ser versus G/G genotype cells with serum-free media; § p<0.05 comparing G/G genotype cells with HEK293 cell conditioned media containing ADAMTS-$7_{Pro\text{-}Cat}$-214Ser versus G/G genotype cells with HEK293 cell conditioned media containing ADAMTS-$7_{Pro\text{-}Cat}$-214Pro.

3.1.14 Protein modelling – SNP rs3825807 effect on ADAMTS-7 structure

The functional effect of SNP rs3825807 was predicted by using F-SNP (available from Queen's University at http://compbio.cs.queensu.ca/F-SNP/). The prediction demonstrated a deleterious effect of rs3825807 on ADAMTS-7 protein (Figure 3.30), predicting a different secondary structure between ADAMTS-7-214Ser and ADAMTS-7-214Pro (Figure 3.31).

rs3825807 FUNCTIONAL INFORMATION FS score 0.537

Functional Category	Prediction Tool	Prediction Result	Prediction Detail
protein_coding	PolyPhen	benign	rs3825807.html
	SIFT	tolerated	rs3825807.html
	SNPeffect	deleterious	rs3825807_1.html
	LS-SNP	no entry	
	SNPs3D	benign	
	Ensembl-NS	nonsynonymous	rs3825807.html
splicing_regulation	ESEfinder	changed	rs3825807_C.html rs3825807_T.html
	ESRSearch	changed	rs3825807_C.html rs3825807_T.html
	PESX	changed	rs3825807_C.html rs3825807_T.html
	RESCUE_ESE	not changed	rs3825807_C.html rs3825807_T.html
post_translation	OGPET	exist	rs3825807_3_C.html rs3825807_3_T.html
	Sulfinator	not exist	rs3825807_3_C.html rs3825807_3_T.html

Figure 3.30 Functional effect of SNP rs3825807 Prediction.
(From http://compbio.cs.queensu.ca/F-SNP/)

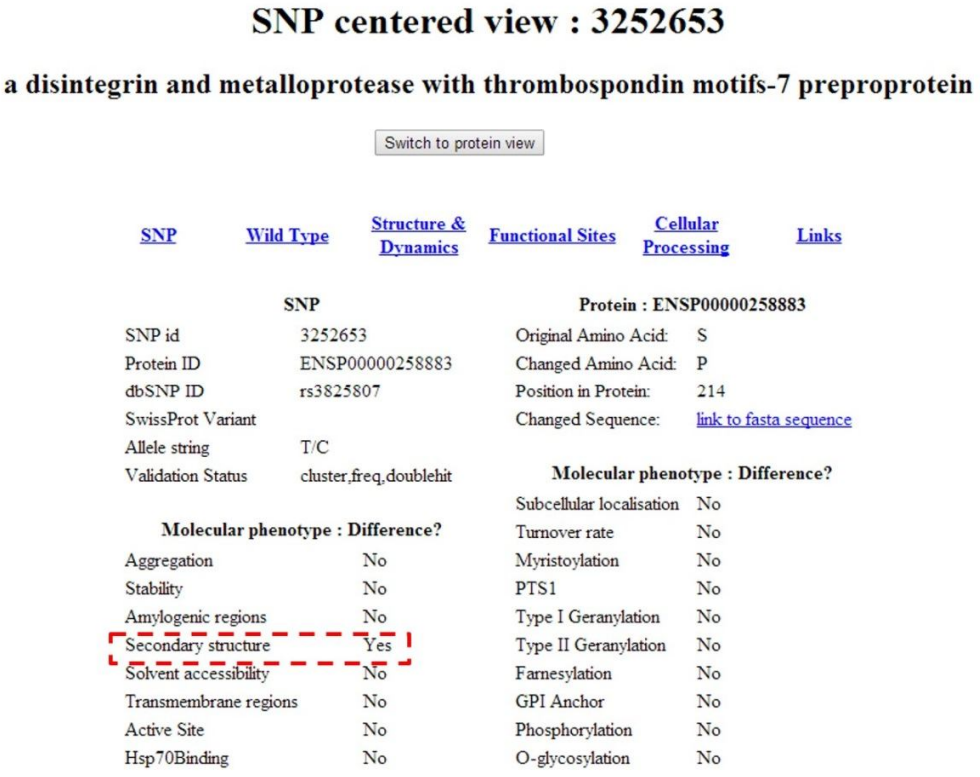

SNP centered view : 3252653

a disintegrin and metalloprotease with thrombospondin motifs-7 preproprotein

Switch to protein view

SNP | Wild Type | Structure & Dynamics | Functional Sites | Cellular Processing | Links

SNP		Protein : ENSP00000258883	
SNP id	3252653	Original Amino Acid:	S
Protein ID	ENSP00000258883	Changed Amino Acid:	P
dbSNP ID	rs3825807	Position in Protein:	214
SwissProt Variant		Changed Sequence:	link to fasta sequence
Allele string	T/C		
Validation Status	cluster,freq,doublehit	**Molecular phenotype : Difference?**	
		Subcellular localisation	No
Molecular phenotype : Difference?		Turnover rate	No
Aggregation	No	Myristoylation	No
Stability	No	PTS1	No
Amylogenic regions	No	Type I Geranylation	No
Secondary structure	Yes	Type II Geranylation	No
Solvent accessibility	No	Farnesylation	No
Transmembrane regions	No	GPI Anchor	No
Active Site	No	Phosphorylation	No
Hsp70Binding	No	O-glycosylation	No

Figure 3.31 SNP rs3825807 is predicted to affect the secondary structure of ADAMTS-7. (From http://compbio.cs.queensu.ca/cgi-bin/compbio/search/view_detail.cgi?id=13&snp_id=3825807&source_no=1&source_name=rs3825807.1.html&category=protein_coding&url=http://snpeffect.vib.be/index.php).

PSIPRED (available from University College London Department of Computer Science Bioinformatics Group at http://bioinf.cs.ucl.ac.uk/psipred/) was further used to predict possible functional effect of non-synonymous SNP rs3825807 on secondary structure of ADAMTS-7. The prediction indicated that the SNP rs3825807 resulted in amino acid substitution Ser-to-Pro would change the helix secondary structure of ADAMTS-7 near this amino acid substitution site (Figure 3.32). This predicted secondary structure change of ADAMTS-7 could potentially affect furin binding to its recognition site next to this amino acid substitution (if this binding happens).

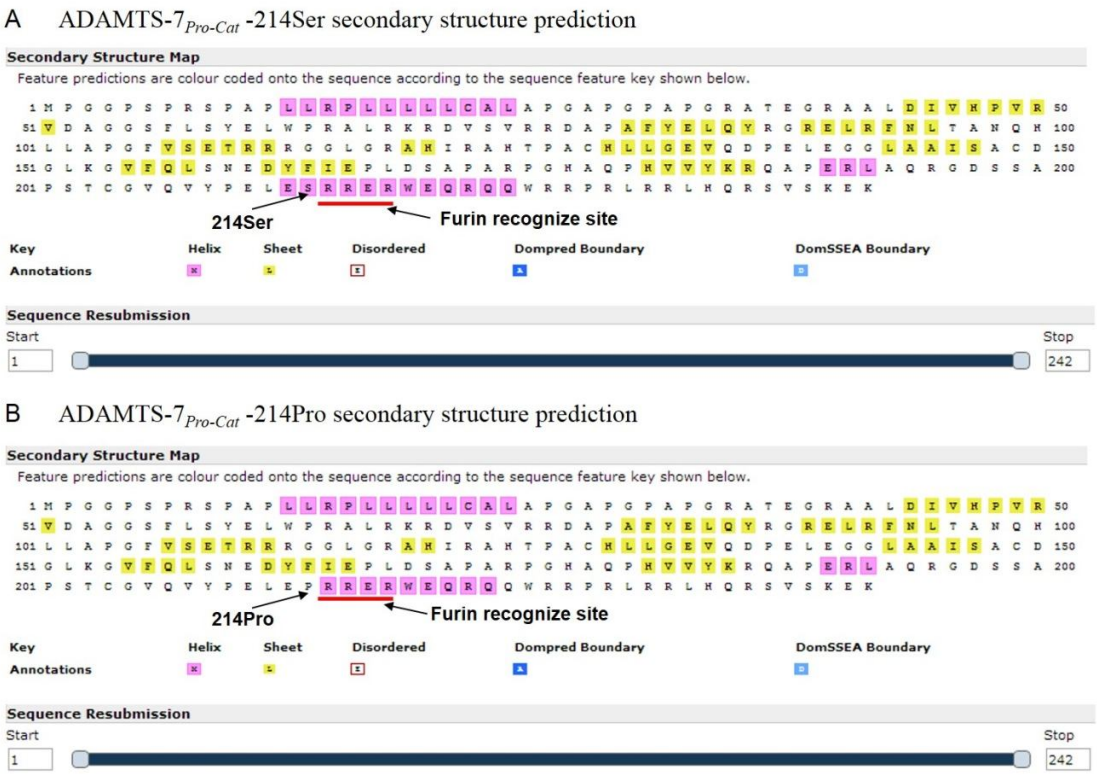

Figure 3.32 ADAMTS-7 secondary structure prediction. Amino acid sequences of ADAMTS-7$_{Pro\text{-}Cat}$ -214Ser or ADAMTS-7$_{Pro\text{-}Cat}$ -214Pro were subjected to secondary structure prediction on PSIPRED. The amino acid substitution Ser-to-Pro was predicted to change the local Helix structure of ADAMTS-7 protein.

Protein-protein interaction is highly regulated by their 3D structure rather than secondary structure, thus we further used QUARK (available from University of Michigan at http://zhanglab.ccmb.med.umich.edu /QUARK/) to predict whether SNP rs3825807 resulted amino acid substitution Ser-to-Pro has an effect on 3D structure of ADAMTS-7. However, the 3D structure prediction results of ADAMTS-7 were highly unreliable (the prediction results of protein's 3D structure is scored from -3 to 3 for its accuracy and reliability, ADAMTS-7 3D structure prediction results had scores close to -3) (Data not shown).

3.2 Discussion

Several GWAS have shown an association between SNPs at the *ADAMTS7* locus and susceptibility to CAD. SNP rs3825807 was the lead SNP associated with CAD in one of these studies (Schunkert et al. 2011) and is in LD with the lead CAD-related SNPs, rs1994016 (Reilly et al. 2011) and rs4380028 (Coronary Artery Disease Genetics 2011, Schunkert et al. 2011), in two other GWAS (r^2>0.8 with rs1994016 and >0.5 with rs4380028, based on data from HapMap and the 1000 Genomes Project). While SNP rs3825807 is located in the coding region and is a non-synonymous SNP, SNP rs1994016 resides in intron 8 of *ADAMTS7* gene whilst SNP rs4380028 is located 7.6 kb upstream of the gene. These GWAS findings suggest that *ADAMTS7* is a candidate gene for CAD. However, GWAS can not inform whether any of these SNPs, or other SNPs in LD with them, have a functional effect on *ADAMTS7* expression or activity. Therefore, functional studies are required to investigate the molecular mechanism underlying the association between these SNPs and CAD, which was the primary aim of this project.

At the outset of this project, apart from the findings from GWAS of an association between *ADAMTS7* gene variants and CAD, there was only one reported study of ADAMTS-7 in vascular disease in which it indicated that ADAMTS-7 promoted neointima formation after mechanical injury of a rat model (Wang et al. 2009). Additionally, the authors showed that ADAMTS-7 facilitated VSMC migration through cleaving the extracellular matrix protein TSP-5, an ADAMTS-7 substrate that hinders VSMC migration and maintains VSMCs in their quiescent state (Riessen et al. 2001, Wang et al. 2009).

Before this project, there was no information in the literature about whether ADAMTS-7 was present in human atheromas. By immunohistochemical analysis, our study showed that ADAMTS-7 was present in human atherosclerotic plaques, and colocalised with VSMCs and ECs. VSMCs that accumulated ADAMTS-7 were mostly located near the intima-media border and the fibrous cap. This finding together with findings of Wang et al in rats described earlier provided the rationale for studying the effects of the CAD-associated ADAMTS-7 SNPs in human VSMCs. In this project, this was carried out with the use of human VSMCs isolated from umbilical arteries since they expressed ADAMTS-7 as shown earlier and because such cells were more accessible (than VSMCs from other arteries) from a relatively large number of individuals required for the study.

Before the functional assays, VSMCs isolated from umbilical cords of different individuals were genotyped for the CAD-associated SNP rs3825807, rs1994016 and rs4380028. The genotyping results showed these three SNPs were in substantial LD (rs3825807 with rs1994016 $r^2 \approx 0.8$, with rs4380028 $r^2>0.6$, and rs4380028 with rs1994016 $r^2>0.6$), which is consistent with data from HapMap and the 1000 Genomes project. As they are in high LD, it is possible that they may represent the same genetic signal.

3.2.1 Effect of SNP rs3825807 on ADAMTS-7 pro-domain cleavage, TSP-5 cleavage, and VSMC migration

One of the key findings of this study was that VSMCs of the A/A genotype had higher migratory ability than G/G genotype cells, and that A/A genotype cell conditioned media had an enhancing effect on migration of G/G genotype cells. The A allele of rs3825807 was found by GWAS to be the CAD risk allele (OR 1.06-1.10) (Schunkert et al. 2011). The findings of our VSMC migration experiments suggest that the higher risk of CAD in individuals carrying the A allele might be in part due to increased VSMC migration which accelerates atherosclerosis progression, providing a possible mechanistic explanation for the association between the *ADAMTS7* SNP and CAD. Similar to rs3825807, the other two CAD-associated SNPs, rs1994016 and rs4380028, exhibited genotypic effects on VSMC migration in our experiments, which could be due to LD between these three SNPs as discussed earlier. The finding from our study that in atherosclerotic plaques, ADAMTS-7 positive VSMCs were predominantly located near the intima-media border is in line with the notion that ADAMTS-7 may play a role in VSMC migration during atherogenesis. In our study, the *ADAMTS7* SNPs showed no effect on VSMC proliferation, senescence and apoptosis, suggesting that the association between these SNPs and CAD is unlikely to be due to a genotypic effect on VSMC proliferation, senescence or apoptosis.

Although a high VSMC content would increase the stability of the atherosclerotic plaque and reduce the risk of plaque rupture to cause such an acute ischemic event as myocardial infarction (MI) and stroke (Libby 1995, Davies 1996), a genetic epidemiological study by Reilly et al. shows that *ADAMTS7* variation is associated with coronary atherosclerosis

but not with risk of MI (Reilly et al. 2011). The findings of our study that the CAD-related *ADAMTS7* genotypes enhance VSMC migration but have no effect on VSMC senescence and apoptosis are in line with that of the genetic epidemiological study by Reilly et al.

In the study of Wang et al mentioned earlier, the authors demonstrated in a rat vascular injury model that overexpression of ADAMTS-7 in VSMCs by an adenovirus infection method enhanced VSMC migration, while suppression of *ADAMTS7* by small interfering RNA (siRNA) retarded VSMC migration, indicating that the level of ADAMTS-7 can have an effect on VSMC migration (Wang et al. 2009). Following the human VSMC migration assays where we found that the CAD-associated *ADAMTS7* SNPs had an effect on VSMC migration, we investigated whether these SNPs had an influence on *ADAMTS7* mRNA or protein levels in VSMCs. Real-time RT-PCR assays showed no association between these SNPs and *ADAMTS7* mRNA level in the VSMC collection. This finding was supported by results of allelic imbalance assays. Thus, the results of these experiments suggest that effect of the *ADAMTS7* SNPs on VSMC migration is unlikely to be due to any of these SNPs having an influence on *ADAMTS7* expression level.

Another possibility was that the CAD-associated *ADAMTS7* SNPs have an effect on ADAMTS-7 enzymatic activity. Therefore, experiments to test this possibility were carried out. Since SNPs rs1994016 and rs4380028 are located in non-coding regions, the experiments were focused on the coding region, non-synonymous SNP which results in a Ser-to-Pro substitution in the ADAMTS-7 pro-domain.

The active or mature form of ADAMTS-7 is a product of pro-domain cleavage by proprotein convertases such as furin. Results of a previous study suggest that the ADAMTS-7 pro-domain is processed sequentially. In that study, after incubation with furin, a recombinant ADAMTS-7 consisting of the pro-domain and metalloprotease domain followed by a His-tag , showed two major bands, 50 kDa and 29 kDa respectively, with several intermediate bands, on PAGE gels detectable by either Coomassie Blue staining or using an anti-cMyc antibody. Edman amino acid sequencing of the 50 kDa and 29 kDa major bands suggest that they were generated by cleavage at two furin cleave sites in the ADAMTS-7 pro-domain (Somerville et al. 2004).

The Ser-to-Pro substitution resulting from SNP rs3825807 is at amino acid residue 214 within the pro-domain of ADAMTS-7 (Figure 3.18). This residue is immediately adjacent to a predicted core recognition site for furin (Somerville et al. 2004). Thus, it is quite possible that this SNP could affect ADAMTS-7 pro-domain cleavage and maturation. This possibility was tested in our study, firstly by analysing conditioned media of VSMCs of different genotypes for SNP rs3825807, and subsequently by analysing conditioned media of HEK293 cells transfected with either a plasmid to produce the ADAMTS-7 Ser214 isoform or a plasmid to produce its Pro214 isoform. The results of assays of the VSMC conditioned media will be discussed immediately below, and the results of the transfected HEK293 experiments will be discussed later.

In Western blot analyses of VSMC conditioned media with the use of an anti-ADAMTS-7 pro-domain antibody, a major band of approximately 34kDa was observed, which is

similar in size to the ADAMTS-9 pro-domain with glycosylation (37kDa) (Koo et al. 2006). The intensity of this band was ~5 fold higher in lanes containing media conditioned by VSMCs of the A/A genotype for SNP rs3825807 than that in lanes containing media conditioned by VSMCs of the G/G genotype. This finding is consistent with the hypothesis that the SNP has an influence on ADAMTS-7 pro-domain cleavage. However, it is a concern that there is no proper loading control for Western blot analyses of VSMC conditioned media.

Little cleaved ADAMTS-7 pro-domain was detected in VSMC lysates in our study, indicating pro-domain processing occurs mainly extracellularly. This is in line with the finding by Somerville et al from their study of ADAMTS-7 produced by transfected HEK293 cells (Somerville et al. 2004). Similarly, pro-domain cleavage of ADAMTS-9 and ADAMTS-5 has been reported to occur at the cell surface (Koo et al. 2006, Longpre et al. 2009). In contrast, the furin processing products of ADAMTS-1 were shown to be present predominantly intracellularly (Longpre and Leduc 2004). Thus, it appears that different mechanisms are involved in the pro-domain processing of different members of the ADAMTS family.

The findings that A/A genotype VSMC conditioned media contained more cleaved ADAMTS-7 pro-domain and had an enhancing effect on cell migration suggest the possibility that SNP rs3825807 affected VSMC migration due to its effect on ADAMTS-7 pro-domain cleavage. It is likely that pro-domain cleavage leads to the release of the active form of ADAMTS-7 which has proteolytic activity to process its substrates. It has

been shown that ADAMTS-7 promotes VSMC migration via cleaving TSP-5 (Wang et al. 2009). Therefore, we further investigated whether there was a difference in the concentration of cleaved TSP-5 in VSMC conditioned media between rs3825807 genotypes. Western blotting analyses of VSMC conditioned media using an anti-TSP-5 antibody detected a band of 70kDa in size, consistent of the ADAMTS-7 digested TSP-5 fragment reported by Wang et al. (Wang et al. 2009). The analyses showed that media conditioned by VSMCs of the A/A genotype for rs3825807 contained approximately ~40% more cleaved TSP-5, compared with the G/G genotype, which is consistent with the postulation mentioned above. This is further supported by data from the TSP-5 *in vitro* digestion assays which showed that VSMC conditioned media were able to cleave TSP-5 and that the media conditioned by VSMCs of the A/A genotype had higher TSP-5 cleavage activity than media conditioned by VSMCs of the G/G genotype. However, there is also the possibility that the difference between the A/A and G/G genotypes in the TSP-5 cleavage is due to an indirect effect of the SNP, for example by an genotype-dependent effect of ADAMTS-7 on activation of other enzymes that can also cleave TSP-5.

Due to the rigidity of proline, the Ser-to-Pro substitution could potentially introduce a conformational change within the protein structure of ADAMTS-7, which might affect the secretion of the protein, the processing of the pro-domain, or its interaction with other molecules on the cell surface. However, there is no evidence to suggest that any of these is the case, as we found similar amounts of full-length ADAMTS-7 and its fragments in lysates of VSMCs of the A/A or G/G genotype, and little ADAMTS-7 pro-domain in cell lysates.

To summarise, the results of the assays of VSMCs suggest that: (1) the CAD-associated SNPs at the *ADAMTS7* locus affect VSMC migration, (2) these SNPs do not affect *ADAMTS7* mRNA and protein levels, (3) the non-synonymous SNP rs3825807 resulting in the Ser-to-Pro substitution might affect ADAMTS-7 pro-domain cleavage, and (4) this might lead to a difference in TSP-5 cleavage. As the three CAD-associated ADAMTS-7 SNPs studied are in LD, the experiments using plasmids for testing the non-synonymous SNP only (and not the other two SNPs) were subsequently carried out, which are further discussed below.

3.2.2 Effect of SNP rs3825807 on ADAMTS-7 pro-domain cleavage, TSP-5 cleavage and cell migration

Effects of the non-synonymous SNP rs3825807 on ADAMTS-7 pro-domain cleavage and TSP-5 cleavage were further tested using HEK293 cells transfected with either a plasmid to produce the Ser214 form of ADAMTS-7 or a plasmid to produce the Pro214 form of this protein. The experiments showed that conditioned media of HEK293 cells transfected with the *ADAMTS7*$_{Pro\text{-}Cat}$*-214Ser* plasmid contained more mature form and cleaved ADAMTS-7 pro-domain, than conditioned media of HEK293 cells transfected with the *ADAMTS7*$_{Pro\text{-}Cat}$*-214Pro* plasmid. This finding supports the notion that the Ser-to-Pro substitution affects ADAMTS-7 pro-domain cleavage and activation. Noticeably, the cleaved pro-domain of ADAMTS-7 was found in conditioned media and more intense in cell surface washes, but not in cell lysate, indicating that the activation of ADAMTS-7 happens at cell surface which is similar to ADAMTS-9 (Koo et al. 2006). This finding also suggests that the cleaved pro-domain could attach back to the cell surface, which is suggested by a previous study (Somerville et al. 2004), although the mechanism has not been elucidated. Interestingly, it appears that VSMCs and HEK293 cells have some different features in ADAMTS-7 pro-domain processing. It appears that in transfected HEK293 cells, multiple cleavage steps lead to the generation of a ~15kDa cleaved pro-domain fragment, whereas in VSMCs, a larger cleaved pro-domain fragment (~34kDa) is detectable in conditioned media. It is also noteworthy that a very small amount of cleaved ADAMTS-7 pro-domain and M form were detected in cell lysate transfected HEK293 cells, suggesting intracellular pro-domain processing of ADAMTS-7 in HEK293 cells is also occurring, although this process is not as efficient as on cell surface.

As a result of the rigidity of proline residue, it is possible that the Ser-to-Pro substitution can alter the conformation of the ADAMTS-7 pro-domain, reducing its accessibility to furin or other proteases and decreasing the efficiency of pro-domain processing. It is interesting that the Pint and P1 fragments of ADAMTS-7-214Pro had slower electrophoretic mobility than those of ADAMTS-7-214Ser (Figures 2.2.23B). Other studies have shown that proline-rich proteins tend to migrate more slowly in SDS-PAGE, presumably due to conformational peculiarities that persist even under reducing conditions (Williamson 1994). It is possible that the Ser-to-Pro substitution has a particularly persistent effect on the conformations of the Pint and P1 fragments.

As discussed earlier, the Ser-to-Pro substitution at residue 214 is immediately adjacent to a predicted core recognition site for furin, the protease primarily responsible for ADAMTS-7 pro-domain processing (Somerville et al. 2004), although it is still unknown as to whether cleavage at this site does occur. Although cleavage at this site could potentially be affected by the Ser-to-Pro substitution at residue 214, it is unlikely to directly account for the reduced mobility of the Pint form of the ADAMTS-7-214Pro, as the cutting site to generate the Pint form is estimated to be >30 residues upstream of position 214, based on the sizes of the Pint bands of both alleles.

Similar to the TSP-5 *in vitro* digestion assay using VSMC conditioned media, the conditioned media of HEK293 cells transfected with either the *ADAMTS7*$_{Pro\text{-}Cat}$*-214Ser* or *ADAMTS7*$_{Pro\text{-}Cat}$*-214Pro* plasmid was able to digest TSP-5 in a dose-dependent manner, and media conditioned by HEK293 cells transfected with the *ADAMTS7*$_{Pro\text{-}Cat}$*-214Ser*

plasmid had two fold higher TSP-5 cleavage activity than media conditioned by *ADAMTS7*$_{Pro\text{-}Cat}$*-214Pro* plasmid transfected cells. Again, similar to the results using VSMC conditioned media, migratory ability of the G/G genotype VSMCs increased after the addition of media conditioned by HEK293 cells transfected with the *ADAMTS7*$_{Pro\text{-}Cat}$*-214Ser* plasmid, whereas media conditioned by HEK293 cells transfected with the *ADAMTS7*$_{Pro\text{-}Cat}$*-214Pro* plasmid had little effect. The results of these two experiments suggest a cell migration promoting and TSP-5 cleavage enhancing effect of conditioned media of HEK293 cells transfected with the *ADAMTS7*$_{Pro\text{-}Cat}$*-214Ser* plasmid, presumably due to a higher concentration of active ADAMTS-7.

These findings indicate that the Ser-to-Pro substitution reduced ADAMTS-7 pro-domain processing, TSP-5 cleavage and VSMC migration. We did not find evidence of between-genotype difference in *ADAMTS7* expression or secretion, or in VSMC proliferation, senescence and apoptosis. Taken together, these results indicate that the Ser-to-Pro substitution resulting from rs3825807 has an effect on ADAMTS-7 maturation, TSP-5 cleavage and VSMC migration and in turn associates with atherosclerosis, providing a mechanistic explanation for the recently reported association between the SNP and CAD susceptibility. The SNP rs3825807 effect on ADAMTS-7 activation is possibly through affecting structure of ADAMTS-7 and binding to proprotein convertase, which is suggested by protein modelling results.

Chapter 4

Functional study of *ADAMTS7* and SNP rs3825807 in endothelial cell migration and *in vitro* angiogenesis

The first part of this project was focused on VSMCs and showed that the CAD-associated SNP rs3825807 had an effect on ADAMTS-7 maturation, TSP-5 cleavage and VSMC migration. As described earlier, immunohistochemical analyses of atherosclerotic plaques showed that ADAMTS-7 was present in VSMCs as well as endothelial cells. Since it would be possible that ADAMTS-7 might play a role in angiogenesis and since neovascularization contributes to atherosclerotic plaque progression, the aim of the second part of this project was to study possible effects of ADAMTS-7 and the non-synonymous SNP rs3825807 in endothelial cell behaviours and angiogenesis. It is worth noting that the immunohistochemical analyses of atherosclerotic plaques showed no significant expression of ADAMTS-7 in macrophages, another important cellular component in atheromas, and therefore, macrophages were not a focus of this project.

4.1 Results

4.1.1 ADAMTS-7 colocalises with ECs in human atherosclerotic plaques

IHC analyses of human atherosclerotic plaques revealed that ADAMTS-7 localised not only to VSMCs as described earlier but also localised to ECs of the neo-vessels within the plaques (Figure 4.1). Adjacent sections showed areas which were positive for the EC marker vWF (Figure 4.1B) as well as ADAMTS-7 (Figure 4.1A). Fluorescent immunostaining for ADAMTS-7 (green) also showed that positive staining in microvessels in human atherosclerotic plaques (Figure 4.1D).

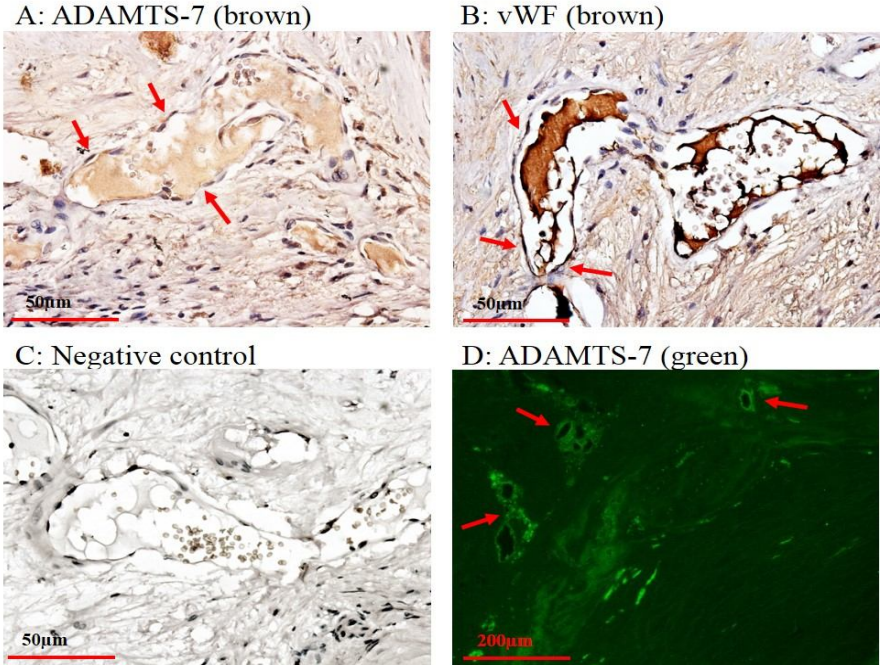

Figure 4.1 ADAMTS-7 colocalises with ECs and associates with neo-vessels in human atherosclerotic plaques. **A & B:** Atherosclerotic carotid artery sections were subjected to single immunostaining of von Willebrand Factor (vWF) or ADAMTS-7 (with a spacer domain antibody). Brown color with DAB indicates vWF or ADAMTS-7 staining. **C:** negative control for ADAMTS-7 and vWF staining (with secondary antibody only). **D**: Atherosclerotic coronary artery sections were subjected to fluorescent immunostaining for ADAMTS-7 (green), followed by fluorescent microscopy examination.

4.1.2 ECs express ADAMTS-7

The finding of colocalisation of ADAMTS-7 with ECs in atherosclerotic plaques prompted us to test whether ECs express ADAMTS-7. Total RNA and whole cell protein extracts of HUVECs were subjected to *ADAMTS7* RT-PCR and Western blotting. RT-PCR showed high levels of *ADAMTS7* mRNA (Figure 4.2A). The Western blotting analyses with either an ADAMTS-7 C-terminus antibody or an ADAMTS-7 pro-domain antibody also demonstrated the presence of ADAMTS-7 protein in ECs (Figure 4.2B&C).

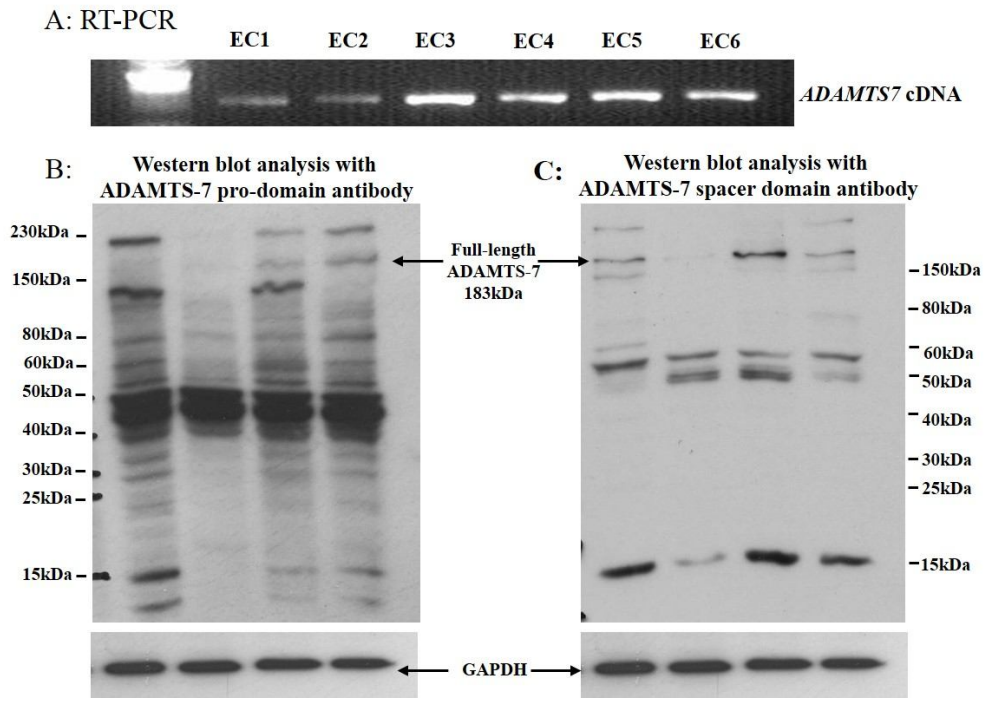

Figure 4.2 ECs express ADAMTS-7. **A:** RT-PCR shows that ECs express *ADAMTS7*. **B&C:** Representative images of Western blot analyses of ADAMTS-7 protein in EC lysates using an ADAMTS-7 spacer domain or pro-domain antibody. Equal amounts of protein (20μg) were loaded in each lane.

4.1.3 SNP rs3825807 genotyping results

A collection of HUVECs from different individuals were used to investigate whether SNP rs3825807 has an effect on EC proliferation, migration and angiogenesis. Therefore, this collection was genotyped for rs3825807. The genotyping results are summarised in Table 4.1.

Table 4.1. Isolated ECs SNP rs3825807 genotyping results

SNP	Genotype	Number	Frequency
rs3825807	A/A	26	58 %
	A/G	13	29 %
	G/G	6	13 %
	Total	45	100 %

4.1.4 SNP rs3825807 has no effect on EC proliferation

Angiogenesis requires ECs to migrate towards the angiogenic stimuli, proliferate and form new vessels. Thus, the proliferation and migration of ECs are critical for neo-vessel formation. Therefore, proliferation assays were carried out to investigate whether SNP rs3825807 affects EC proliferation (Methods described in section 2.5.1.2). During optimization for the assay, 1,000-10,000 cells/well showed linear curves (Figure 4.3A), and 7500 cells/well was used in the subsequent experiments. Subsequent EC proliferation assays were performed on HUVECs from 12 different individuals (n=4 for each genotype).The experiment showed no significant difference in EC proliferation between the three genotypes for SNP rs3825807 (Figure 4.3B).

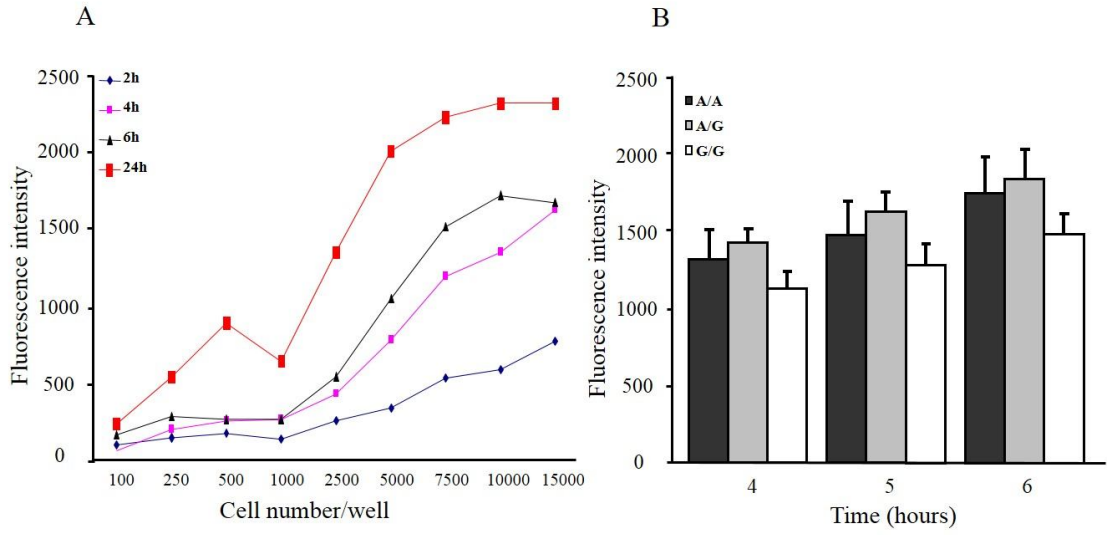

Figure 4.3 SNP rs3825807 has no effect on EC proliferation. Primary cultures of ECs of the A/A, A/G or G/G genotype for rs3825807 were subjected to proliferation assay by using cell proliferation assay kit (Abcam). **A:** Optimization for proliferation assay. **B:** Column chart shows fluorescence signal intensity (mean ± SEM) of ECs of the A/A, A/G or G/G genotype for rs3825807 (n=4 for each genotype). One-way ANOVA (three genotype groups) and Student's t-test (two genotype groups) was used to analyse the difference between genotype groups, $P>0.05$ comparing A/A and G/G genotype group.

4.1.5 SNP rs3825807 has an effect on EC migration

In addition to EC proliferation assays, migration assays were carried out to investigate whether SNP rs3825807 affects EC migration. Similar to the findings from VSMC analyses as described in Chapter 3 where the SNP showed an effect on VSMC migration, the EC experiment showed that the SNP also affected EC migration. A/A genotype ECs showed higher migratory ability, compared with G/G genotype cells (Figure 4.4), similar to our findings for VSMCs. In the VSMC migration experiment, three different conditions (i.e. with serum, serum-free, and serum-free plus PDGF-BB) were used, but the results

were similar in these different conditions. Therefore, only one condition (normal culture media with serum) was used in the EC migration experiment.

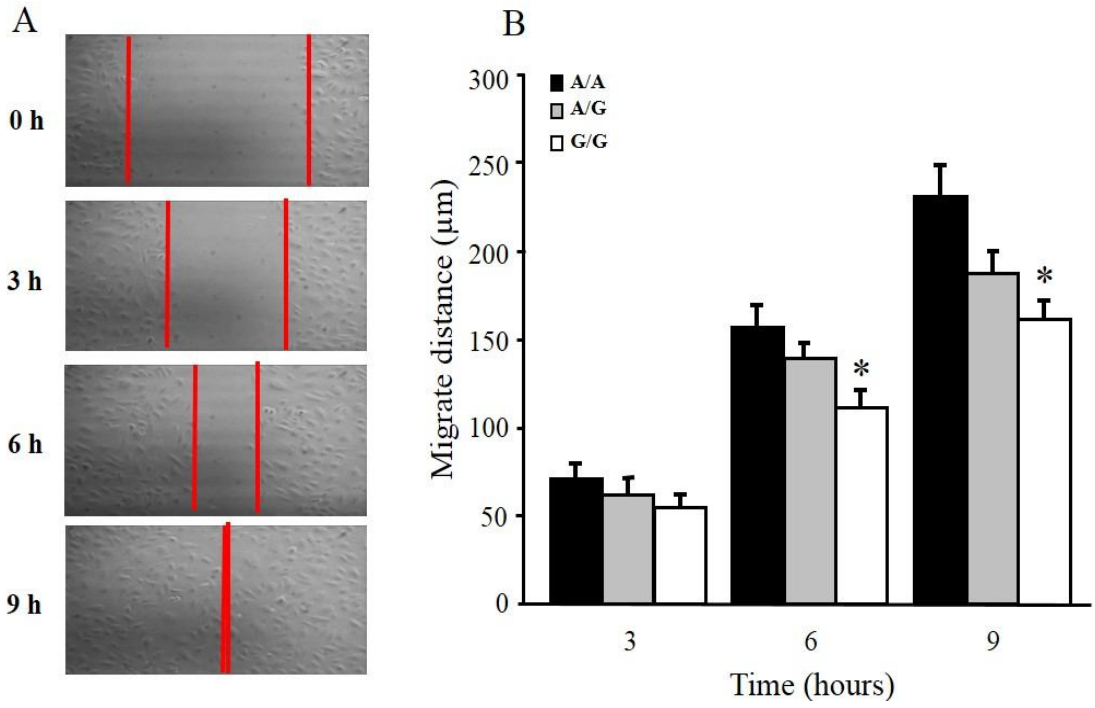

Figure 4.4 SNP rs3825807 has an effect on EC migration. Primary cultures of ECs of the A/A, A/G or G/G genotype for rs3825807 were subjected to the scratch assay. **A:** Representative pictures of migration at different time points. **B:** Column chart shows migration distances (mean ± SEM) of ECs of the A/A, A/G or G/G genotype for rs3825807 (n=4 for each genotype). Student's t-test (two genotype groups) was used to analyse the differences between genotype groups of the SNPs, *p<0.05 comparing A/A and G/G genotype group.

4.1.6 SNP rs3825807 has no effect on *ADAMTS7* mRNA expression in ECs

To investigate whether SNP rs3825807 has an effect on *ADAMTS7* mRNA level in ECs, real-time RT-PCR was carried out with cDNA from ECs from different individuals. The analysis showed that *ADAMTS7* mRNA levels in the ECs did not significantly differ among the three genotypes for rs3825807 (Figure 4.5).

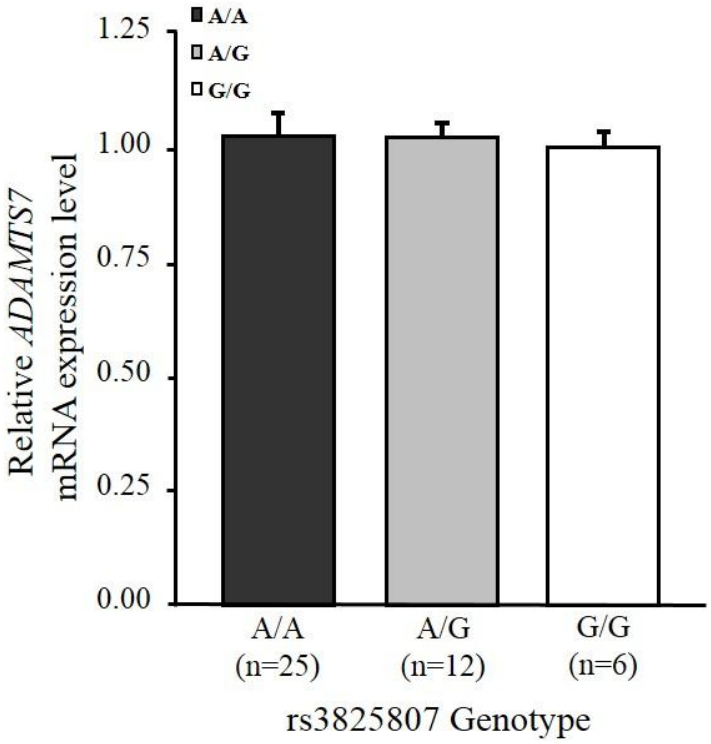

Figure 4.5 SNP rs3825807 has no effect on *ADAMTS7* mRNA expression level in ECs. The ΔΔCt method was used to analyse the data. Data shown are values of mean ± SEM. One-way ANOVA (three genotype groups) and student's t-test (two genotype groups) was used to analyse the difference between genotype groups of the SNP. No significant difference was found between genotype groups.

4.1.7 Augmented *ADAMTS7* expression in ECs increases their migration

Since the assays described above showed that genotypes for SNP rs3825807 had an influence on EC migration, further experiments with *ADAMTS7* overexpression or knockdown in ECs were carried out to investigate whether ADAMTS-7 has an effect on EC migration. A previous study by Wang et.al showed that overexpression of *ADAMTS7* in VSMCs by an adenoviral infection method enhanced VSMC migration, while suppression of *ADAMTS7* by siRNA retarded cell migration (Wang et al. 2009).

In the overexpression experiment, HUVECs that were heterozygous for rs3825807 were transfected with either the *ADAMTS7-214Ser* plasmid or the *ADAMTS7-214Pro* plasmid (Methods described in sections 2.9.2 and 2.10.2). The experiment showed that ECs transfected with the *ADAMTS7-214Ser* plasmid had two fold increased migratory ability compared with the control group, while cells transfected with *ADAMTS7-214Pro* plasmid did not show a significant increase of cell migration (Figure 4.6).

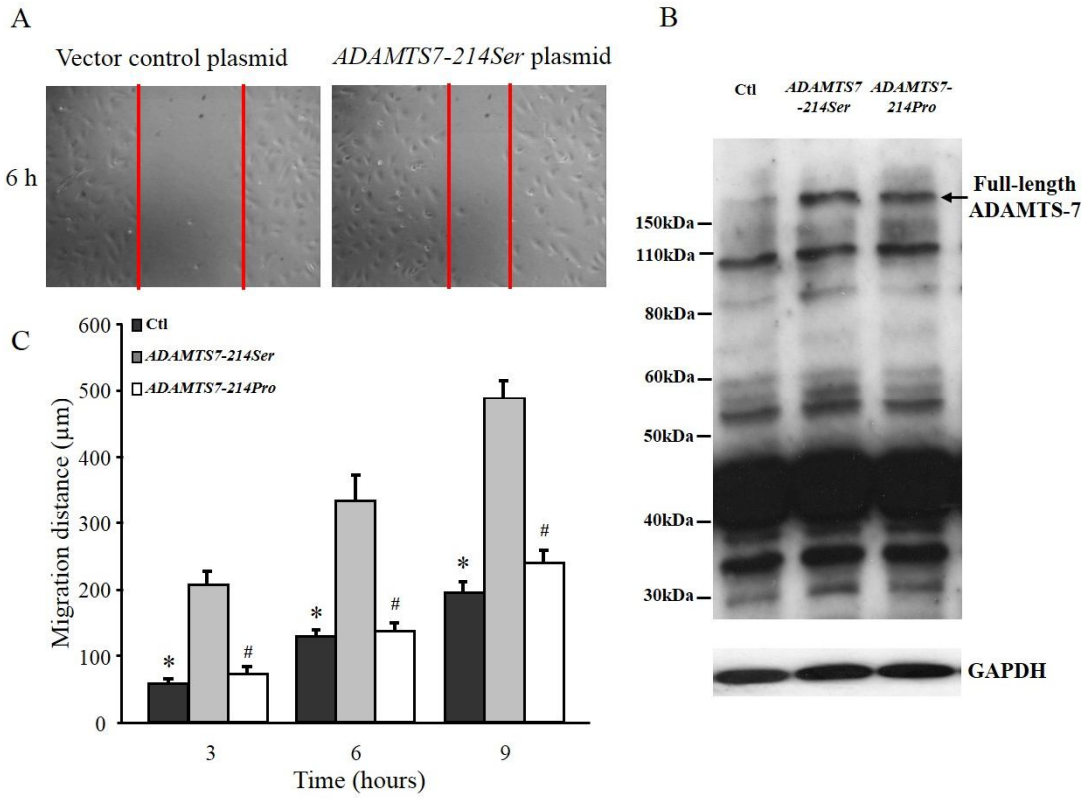

Figure 4.6 Augmented *ADAMTS7* expression accelerates EC migration. ECs were transfected with either *ADAMTS7-214Ser* or *ADAMTS7-214Pro* plasmid, or vector plasmid pcDNA3.1 as control, and then subjected to scratch assay. **A:** Representative pictures of migration assay for ECs transfected with either control plasmid pcDNA3.1 or *ADAMTS7-214Ser* plasmid at 6 hours point. **B:** Over-expression efficiency was tested by Western blot using an anti-ADAMTS-7 pro-domain antibody. **C:** Column chart shows migration distance (mean ± SEM) of ECs transfected with either *ADAMTS7-214Ser* or *ADAMTS7-214Pro* plasmid, or vector control plasmid at different time points (n=3 for each group). Student's t-test (paired samples) to analyse the difference between two groups. * $p<0.05$ comparing control group and *ADAMTS7-214Ser* plasmid transfection group. # $p<0.05$ comparing *ADAMTS7-214Ser* plasmid and *ADAMTS7-214Pro* plasmid transfection group.

4.1.8 *ADAMTS7* knockdown impairs EC migration

In the knockdown experiment, HUVECs were infected with *ADAMTS7* shRNA (Methods described in section 2.12 and 2.13). The experiment showed that *ADAMTS7* knockdown significantly impaired the migratory ability of ECs (Figure 4.7A). The migration of *ADAMTS7* shRNA infected cells decreased by approximately 60%, as compared with non-target control shRNA infected cells (Figure 4.7B), suggesting the important role of ADAMTS-7 in EC migration.

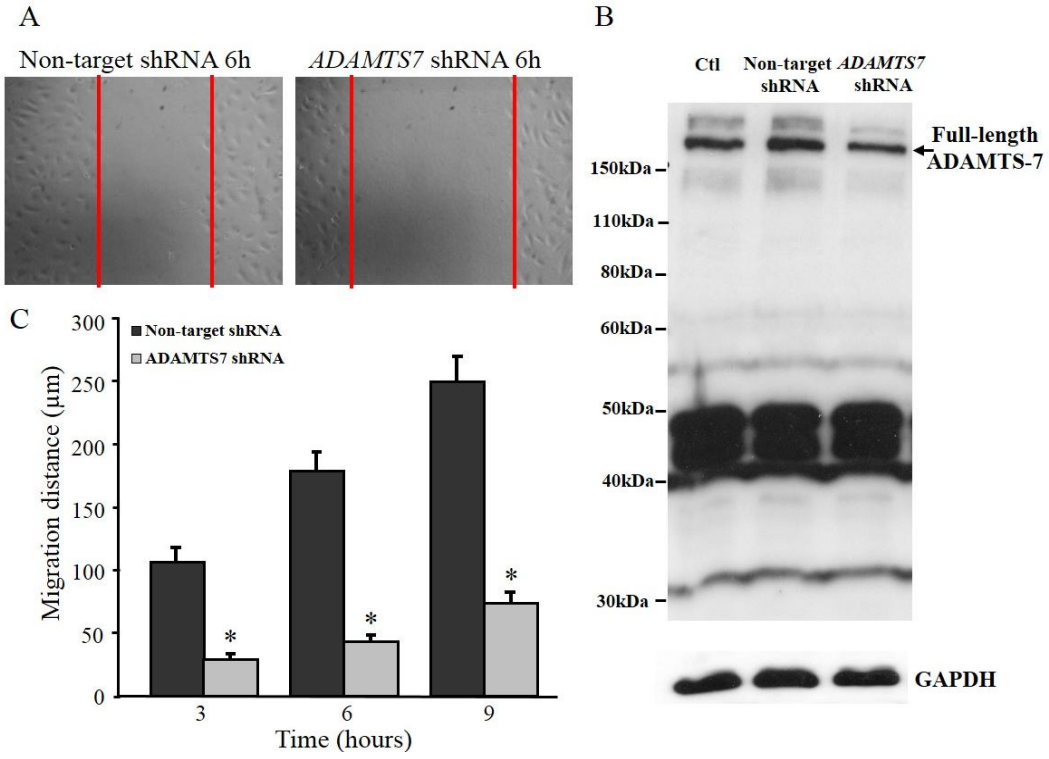

Figure 4.7 *ADAMTS7* knockdown impairs EC migration. ECs were infected with either *ADAMTS7* shRNA or non-target shRNA as control, and then subjected to scratch assay. **A:** Representative pictures of migration assay for ECs infected with either non-target shRNA or *ADAMTS7* shRNA at 6 hours point. **B:** Knock-down efficiency was tested by Western blot. Column chart shows migration distance (mean ± SEM) of ECs infected with either non-target shRNA or *ADAMTS7* shRNA at different time points (n=6 for each group). Student's t-test (paired samples) to analyse the difference between two groups, * $p<0.05$ comparing non-target shRNA control group and *ADAMTS7* shRNA *in*fection group.

4.1.9 Augmented *ADAMTS7* expression in ECs increases capillary-like network formation

Following the EC migration assays, capillary-like network formation assays were carried out with HUVECs transfected with either the *ADAMTS7-214Ser* plasmid or the *ADAMTS7-214Pro* plasmid to investigate whether *ADAMTS7* and SNP rs3825807 have effects on angiogenesis (Methods described in section 2.15).

In the overexpression experiment, ECs transfected with the *ADAMTS7-214Ser* plasmid had significantly increased capillary-like network formation, compared with the control group, while cells transfected with the *ADAMTS7-214Pro* plasmid did not show a significant increase in tube formation. Among the twenty parameters of angiogenesis generated using the angiogenesis analyser in Image J, almost all of them reached statistical significance when comparing the *ADAMTS7-214Ser* group and control group. The most important parameters, such as the number of nodes, the number of junctions and the total branching lengths are presented in Figure 4.8.

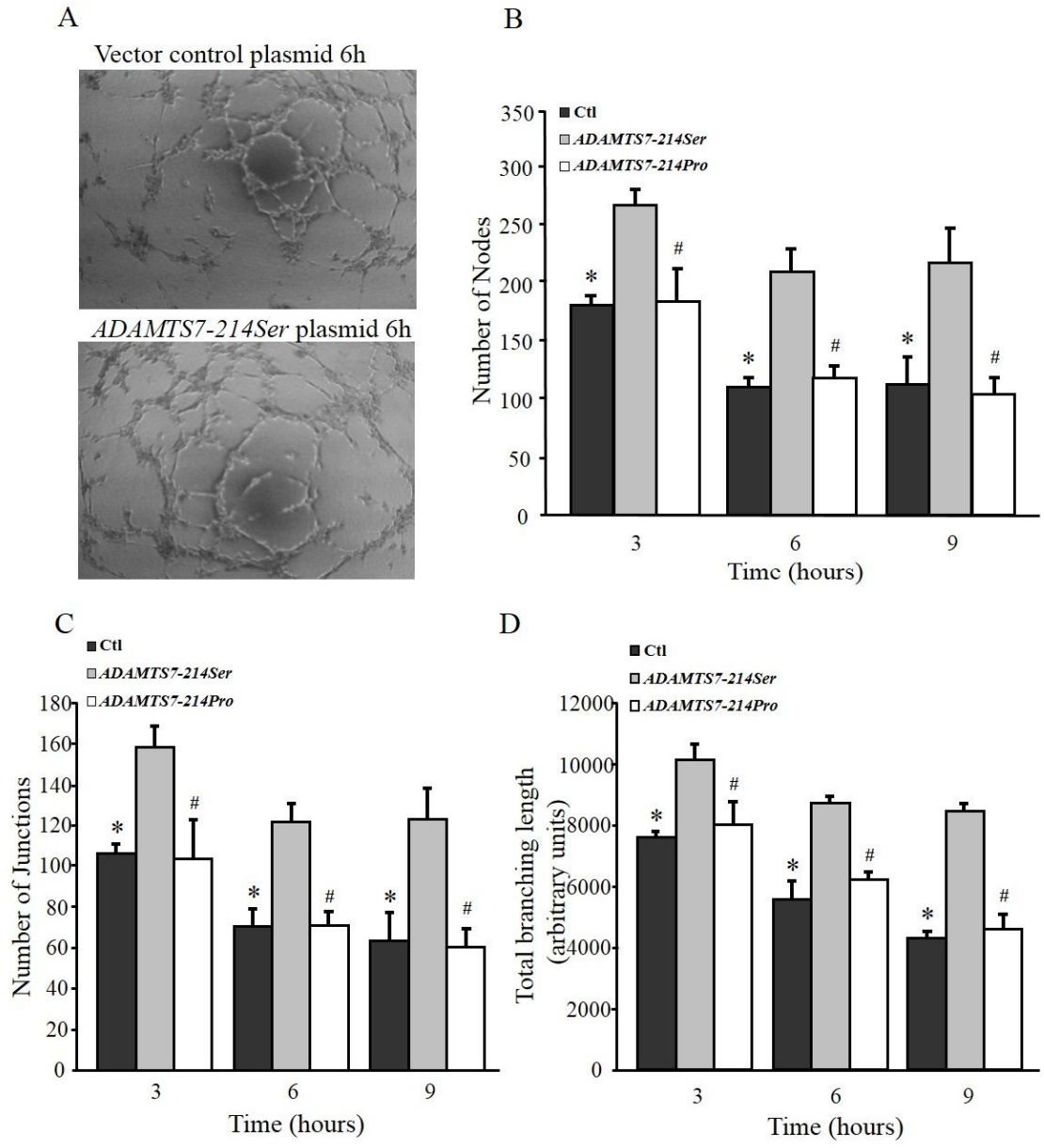

Figure 4.8 Augmented ADAMTS7 expression increases *in vitro* angiogenesis. ECs were transfected with either *ADAMTS7-214Ser* or *ADAMTS7-214Pro* plasmid, or vector control plasmid pcDNA3.1 as control, and then subjected to capillary-like network formation assay. **A:** Representative pictures of capillary-like network formation assay for ECs transfected with either control plasmid pcDNA3.1 or *ADAMTS7-214Ser* plasmid at 6 hours point. **B, C &D:** Column charts show number of nodes, number of junctions and total branching length (mean ± SEM) in capillary-like network formation assay of ECs transfected with either *ADAMTS7-214Ser* or *ADAMTS7-214Pro* plasmid, or vector control plasmid at different time points (n=3 for each group). Student's t-test (paired samples) to analyse the difference between two groups, * $p<0.05$ comparing control group and *ADAMTS7-214Ser* plasmid transfection group; # $p<0.05$ comparing *ADAMTS7-214Ser* plasmid and *ADAMTS7-214Pro* plasmid transfection group.

4.1.10 *ADAMTS7* knockdown in ECs retards capillary-like network formation

Capillary-like network formation assays were carried out with HUVECs infected with *ADAMTS7* shRNA to investigate whether *ADAMTS7* knock-down could affect angiogenesis

In the knockdown experiment, ECs infected with *ADAMTS7* shRNA showed a 40-50% decrease in capillary-like network formation compared with non-target shRNA infected cells, which is concordant with results of the migration assay which showed that *ADAMTS7* knockdown decreased EC migratory ability by approximately 60%. All parameters generated by the angiogenesis analyser showed the similar results, and numbers of nodes, numbers of junctions and total branching lengths are presented in Figure 4.9.

It is noteworthy that all the parameters of capillary-like network formation went down with the growth of time, in concordance with the observed reduction of capillary-like network of ECs. The capillary-like network was almost gone after 24 hours (data not shown). This phenomenon was also found but not obvious in *ADAMTS7* overexpression experiments. Both control group (vector plasmid and non-target shRNA) showed the same trend, so it is possible that our ECs were injured during the treatment (trypsinisation for example) or some toxic component was in transfection and infection solutions.

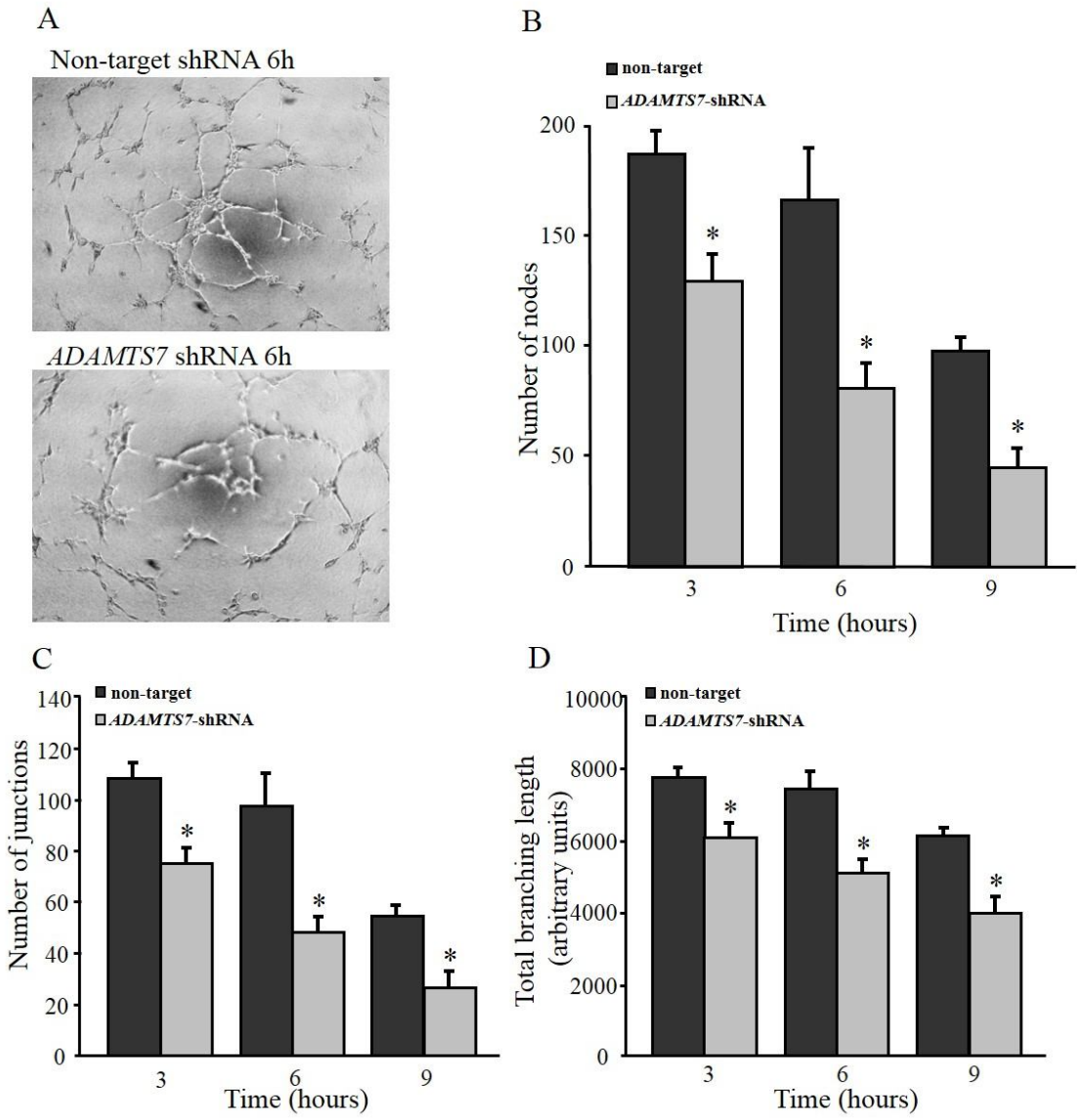

Figure 4.9 *ADAMTS7* knockdown retards *in vitro* angiogenesis. ECs were infected with either *ADAMTS7* shRNA or non-target shRNA as control, and then subjected to capillary-like network formation assay. **A:** Representative pictures of capillary-like network formation assay for ECs infected with either control non-target shRNA or *ADAMTS7* shRNA at 6 hours point. **B, C &D:** Column charts show number of nodes, number of junctions and total branching length (mean ± SEM) in capillary-like network formation assay of ECs infected with either non-target shRNA or *ADAMTS7* shRNA at different time points (n=6 for each group). Student's t-test (paired samples) to analyse the difference between two groups, * $p<0.05$ comparing non-target shRNA control group and *ADAMTS7* shRNA infection group.

4.1.11 SNP rs3825807 affects EC tube formation

Further angiogenesis assays were conducted to investigate whether untranfected ECs from individuals of different genotypes for SNP rs3825807 differ in their ability to form tubes. The assays showed that ECs of the A/A genotype had approximately 20% higher capillary-like network formation ability than G/G genotype cells, and this difference reached significance at the 9 hour time point. Although only 8 parameters showed statistical difference, many other parameters showed a similar trend (p values between 0.05-0.1). Data for the numbers of nodes, the numbers of junctions and the total branching lengths are presented in Figure 4.10. The magnitudes of differences between genotypes in these assays were similar than those in the experiment where cells were transfected with the *ADAMTS7-214Ser* or *ADAMTS7-214pro* plasmid. This is not unexpected since endogenous expression levels of *ADAMTS7* would be lower than the *ADAMTS7* levels in cells transfected with the *ADAMTS7-214Ser* or *ADAMTS7-214pro* plasmid. The SNP rs3825807 effect on angiogenesis was abolished when ECs were transfected with shRNA to knock down *ADAMTS7* (data not shown).

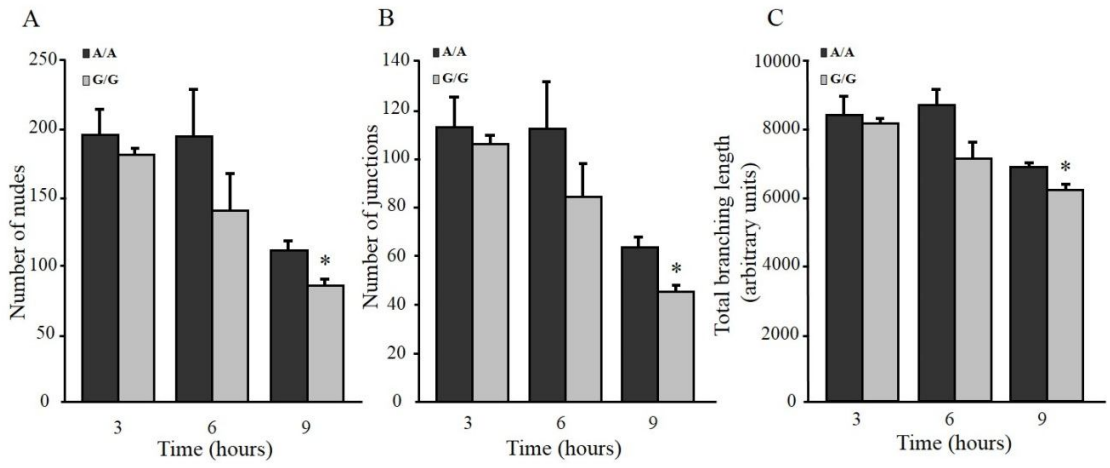

Figure 4.10 SNP rs3825807 has an effect on EC tube formation. Primary cultures of ECs of the A/A, A/G or G/G genotype for rs3825807 were subjected to the capillary-like network formation assay. **A, B &C:** Column chart shows the number of nodes, the number of junctions and the total branching length (mean ± SEM) of ECs of the A/A, A/G or G/G genotype for rs3825807 (n=3 for each genotype). Student's t-test was used to analyse the differences between genotype groups of the SNPs, *p<0.05 comparing A/A and G/G genotype group.

4.1.12 Preliminary data of proteomics analysis

Previous studies described earlier show that ADAMTS-7 promotes VSMC migration by cleaving its substrate TSP-5. Since it has been reported that ECs do not express TSP-5 (Riessen et al. 2001), a proteomics analysis of conditioned media of ECs was carried out to investigate whether there were yet unknown proteolytic targets of ADAMTS-7 that might affect EC migration and angiogenesis. In this experiment, ECs were either transfected with the *ADAMTS7-214Ser* plasmid to augment *ADAMTS7* expression, or infected with shRNA to knock down *ADAMTS7*, or neither. Conditioned media of these cells were then collected and subjected to proteomics analysis carried out by the Central Proteomics Facility of University of Oxford (Methods described in section 2.16).

In this analysis, over 100 different proteins were detected in the conditioned media, and several proteins showed differences in their level (spectral counts) when comparing ECs with augmented *ADAMTS7* expression, ECs with *ADAMTS7* knockdown, and control ECs (Table 4.2). Among them, TSP-1 is of particularly interest. TSP-1 belongs to the TSP family which includes TSP-5, the best studied substrate of ADAMTS-7. More importantly, TSP-1 has been reported to be a strong angiogenesis inhibitor with the ability to inhibit EC migration (Good et al. 1990). A previous study showed that another ADAMTS family member, ADAMTS-1, can cleave TSP-1 (Lee et al. 2006). In our proteomic analysis, the *ADAMTS7* shRNA infected EC conditioned media sample had the highest TSP-1 spectral counts. A possible explanation could be that ADAMTS-7 can degrade TSP-1 and the reduction of ADAMTS-7 in the condition media of ECs infected with the *ADAMTS7* shRNA resulted in less TSP-1 degradation. In contrast, the *ADAMTS7-214Ser* transfected EC conditioned media sample showed that lowest TSP-1 spectral counts, which could possibly result from increased TSP-1 degradation due to a higher concentration of ATAMTS7 in the conditioned media of ECs transfected with the plasmid to over-express ADAMTS7.

Table 4.2 Proteomics preliminary data

				SPECTRAL COUNTS		
Protein	**Description**	**Length (AA)**	**MW (kDa)**	**Control**	**ADAMTS7-214Ser**	**ADAMTS7 shRNA**
TSP-1	Thrombospondin-1	1170	129.50	10.00	3.00	14.00
PAI1	Plasminogen activator inhibitor 1	402	45.00	9.00	3.00	9.00
VIME	Vimentin	466	50.00	3.00	8.00	4.00
COF1	Cofilin-1	166	17.00		2.00	1.00
EF1A1	Elongation factor 1-alpha 1	462	50.00		2.00	1.00
MMP1	Interstitial collagenase	469	54.00	11.00		12.00
PGBM	Heparan sulfate proteoglycan core protein	4391	47.00	5.00		11.00
ANGT	Angiotensinogen	485	53.00	2.00		1.00

4.1.13 TSP-1 Western blotting preliminary results support the proteomics data

To verify the proteomics analysis results for TSP-1, Western blot analyses were performed on conditioned media of ECs either transfected with the *ADAMTS7-214Ser* plasmid to augment *ADAMTS7* expression, or infected with shRNA to knock down *ADAMTS7*, or neither. As shown in Figure 4.11, the Western blot analyses confirmed that conditioned media of cells infected with the *ADAMTS7* shRNA had more undegraded TSP-1 whereas conditioned media of cells transfected with the *ADAMTS7-214Ser* plasmid had less undegraded TSP-1, as compared with conditioned media of control cells. These results are consistent with those of the proteomic analysis. Further experiments would be required to investigate if ADAMTS-7 can indeed degrade TSP-1 and if the effect of ADAMTS-7 on angiogenesis is, to certain extent, mediated by an effect on TSP-1.

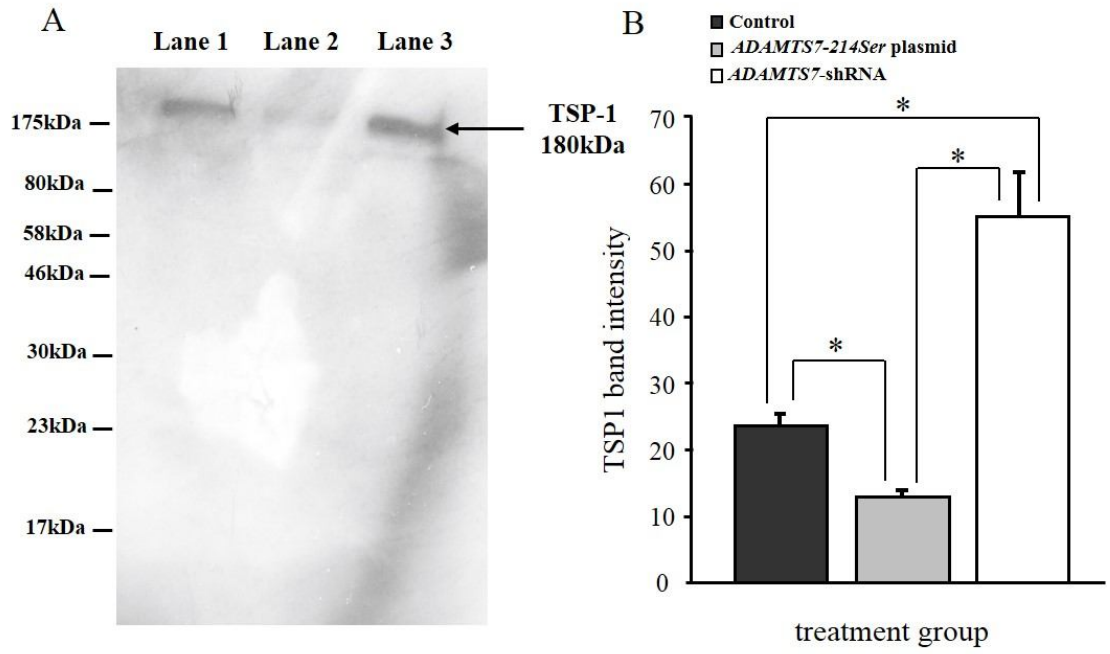

Figure 4.11 Western blot analysis of TSP-1 in EC conditioned media. Conditioned media of ECs either transfected with *ADAMTS7-214Ser* plasmid or infected with *ADAMTS7* shRNA, or ECs without any treatment as control group were subjected to Western blot to detect TSP-1 protein using a specific TSP-1 antibody. **A:** A representative image of Western blot shows weakest TSP-1 band in over-expression group (Lane 2). While strongest TSP-1 band was found in knock-down group (Lane 3). Lane 1 represents the control group. Equal amounts of protein (40 µg) was loaded into each lane. **B:** Data shown in column chart are TSP-1 band intensity (mean ± SEM) (repeated 3 times of Western blotting). Student's t-test was used to analyse the difference between two groups, * $p<0.05$ comparing two groups.

4.2 Discussion

Further to results described in Chapter 2 from the studies of VSMCs, the experiments described in this chapter reveal a role of ADAMTS-7 in angiogenesis with a genotypic/allelic effect of the non-synonymous SNP rs3825807.

4.2.1 Effects of *ADAMTS7* and SNP rs3825807 on EC migration and angiogenesis

An important novel finding of this study is that ADAMTS-7 promotes EC migration and angiogenesis. This finding derived from migration and angiogenesis assays using ECs with either augmented *ADAMTS7* expression or *ADAMTS7* knockdown. The migration assays showed that over-expression of *ADAMTS7* with *ADAMTS7-214Ser* plasmid doubled the migration distance compared with the control group. Similarly, the angiogenesis assays showed ECs transfected with the *ADAMTS7-214Ser* plasmid had increased ability for tube formation.

In contrast to ECs transfected with the *ADAMTS7-214Ser* plasmid, ECs transfected with the *ADAMTS7-214Pro* plasmid did not show a marked increase in their ability to migrate or form tubes. This can not be explained by the possibility of different transfection efficiency, as Western blot analysis showed that full length ADAMTS-7 protein was increased to a comparable degree comparing cells transfected with *ADAMTS7-214Ser* and cells transfected with *ADAMTS7-214Pro*, both having significantly more ADAMTS-7 than cells transfected with the empty vector (Figure 4.6B). One possible explanation

would be that the control cells and *ADAMTS7-214Pro* plasmid transfected cells had similar amounts of active ADAMTS-7. Although the total ADAMTS-7 was markedly increased in the cells transfected with the *ADAMTS7-214Pro* plasmid, the recombinant ADAMTS-7 expressed by this plasmid would be all ADAMTS-7-214Pro which would be resistant to activation (assumed based on data described in Chapter 3), and there was probably little increase in the amount of the active form of ADAMTS-7. The effects of ADAMTS-7 on EC migration and capillary-like network formation presumably derived from active ADAMTS-7.

The results of the experiment using ECs inflected with *ADAMTS7* shRNA supported a role of ADAMTS-7 in EC migration and angiogenesis, as *ADAMTS7* knockdown severely impaired EC migration and tube formation.

A key finding of the experiments described in the Chapter is that the CAD-associated *ADAMTS7* SNP rs3825807 has a genotypic/allelic effect on EC migration and angiogenesis. This genetic effect is likely to be related to the function of ADAMTS-7, as *ADAMTS7* knockdown abolished the effect of SNP rs3825807 on EC capillary-like network formation. The A/A genotype cells showed more capillary-like network formation, although only at 9 hour time point, but this effect was abolished when *ADAMTS7* in ECs was knocked down by shRNA.

Neovascularization arising from angiogenesis plays an important role in atherosclerotic plaque progression. Neovessels in the atherosclerotic plaque provide an additional route for leukocyte migration into the plaque, undermine plaque stability, and are the main

source of intra-plaque haemorrhage (Moulton et al. 2003, Herrmann et al. 2006). Thus, the finding of this study that the CAD-risk allele (A, Ser214) of SNP rs3825807 promotes angiogenesis provides another possible mechanistic explanation for the association between the SNP and CAD.

4.2.2 TSP-1 - a possible substrate of ADAMTS-7?

In the VSMC study, we found that the CAD-associated *ADAMTS7* SNP affected VSMC migration through affecting ADAMTS-7 activation and TSP-5 cleavage. Could it be that the SNP affects EC migration through the same mechanism? This seems unlikely as a previous study showed that ECs do not express TSP-5 (Riessen et al. 2001). It is possible that ADAMTS-7 can degrade as yet unknown substrate proteins which mediate the effect of ADAMTS-7 on EC migration and angiogenesis. The possibility promoted us to use the proteomics analysis to research for the possible substrates of ADAMTS-7.

Among the several proteins showed by the proteomic analysis to differ in their amounts among the different conditions (*ADAMTS7* overexpression, *ADAMTS7* knockdown, and control), TSP-1 is of particular interest. TSP-1 is a matricellular, calcium-binding protein that participates in cellular responses to growth factors, cytokines and injury (Chen et al. 2000). Unlike members of subgroup B of the TSP family, i.e. TSP-3, TSP-4 and TSP-5, which are pentamers, subgroup A members includes trimeric TSP-1 and TSP-2. Each subgroup A member consists of three identical subunits each of which contains multiple domains: N- and C-terminal globular domains, a region of sequence with similarity to

procollagen, and three types of repeated sequence motifs, designated type 1, type 2 and type 3 repeats (Chen et al. 2000). TSP-1 binds to a wide variety of integrin and non-integrin cell surface receptors, such as CD36, CD47 and proteoglycans, and initiates signal transduction. It regulates cell proliferation, migration and apoptosis in a variety of physiological and pathological settings, including wound repair, inflammation, angiogenesis and neoplasia (Chen et al. 2000).

TSP-1 has been shown to be one of the major physiological activators of TGF-β *in vivo*. TGF-β is released from platelet α-granules upon platelet activation along with TSP-1, one of the major components of platelet α-granules. It has been shown that TSP-1 induced TGF-β activity accounts for 60% of the total TGF-β activity released (Murphy-Ullrich et al. 1992, Schultz-Cherry and Murphy-Ullrich 1993, Schultz-Cherry et al. 1994). Since TGF-β affects a wide range of physiological and pathological processes, including regulating cell growth, differentiation, adhesion, motility and death, it comes as no surprise that TSP-1, the major activator of TGF-β, is involved in a variety of physiological and pathological conditions (Chen et al. 2000).

An inhibitory effect of TSP-1 on angiogenesis was revealed in 1990 by Good et al. who showed that a 140-kDa protein that inhibited angiogenesis derived from TSP-1. Subsequent studies showed that two sequences, one in the procollagen homology region and one in the second TSR, of TSP-1 inhibits angiogenesis (Good et al. 1990, Tolsma et al. 1993). Additionally, Dawson et al showed anti-angiogenic activity of the intact TSP-1 molecule which contains the sequence that reportedly binds to CD36 (Dawson et al. 1997).

The interaction of TSP-1 with CD36 plays a significant role in the anti-angiogenic activity of TSP-1 both *in vitro* and *in vivo* (Dawson et al. 1997). CD36 mediates TSP-1 inhibition of EC migration and capillary-like network formation (Dawson et al. 1997). TSP-1 can also activate a P38/MAPK cascade that induces EC apoptosis via binding with CD36 (Guo et al. 1997, Jimenez et al. 2000). Furthermore, it has been reported that TSP-1 inhibits nitric oxide (NO) signaling pathway via CD36, as one of the mechanisms for the anti-angiogenic effect of TSP-1 (Lawler and Lawler 2012). In addition to its inhibition of angiogenesis through binding with its ligand CD36, TSP-1 can also inhibit angiogenesis through its direct binding to VEGF and mediating the uptake and clearance of VEGF from the extracellular space (Gupta et al. 1999, Greenaway et al. 2007, Kaur et al. 2010, Lawler and Lawler 2012).

Another reason makes TSP-1 very interesting and potentially relevant to the findings of our ADAMTS-7 study in angiogenesis is that it has been shown that ADAMTS-1 cleaves TSP-1 (Lee et al. 2006). ADAMTS-1 and ADAMTS-7 belong to the same protease family, while TSP-1 and TSP-5 (a known substrate of ADAMTS-7) belong to the same group of structure proteins with similar structures. The data from the proteomics and Western blot analyses described in this Chapter are consistent with the notion that ADAMTS-7 might be able to cleave TSP-1, although other possibilities can not be precluded, for example, ADAMTS-7 might be able to act on other proteases that in turn cleave TSP-1 or act on molecules that increase TSP-1 expression. To clarify these issues, further experiments will be required.

Chapter 5 Population study

Although the several GWAS mentioned earlier have shown an association between SNPs at the *ADAMTS7* locus and risk of CAD, they did not investigate whether the *ADAMTS7* SNPs influence atherosclerosis progression and severity. Since VSMC migration and angiogenesis are more relevant to atherosclerosis progression than to atherosclerosis initiation, it would be worth noting some results from analyses of relationships between the *ADAMTS7* SNP rs3825807 and atherosclerosis severity scores, which were accomplished by other group members and our collaborators undertaken alongside the functional studies described in Chapters 3 and 4. These results are summarised in the following sections.

5.1 Bruneck study

In a population based prospective study (the Bruneck Study), we observed an inverse association between the *ADAMTS7* rs3825807 G/G genotype and atherosclerosis (Pu et al. 2013). This genotype was associated with lower prevalence of carotid atherosclerosis [odds ratio (95% CI) =0.51 (0.31-0.84) and 0.53 (0.31-0.90) in the data from 1990 and 1995 respectively, after adjustment for covariates], and similarly lower atherosclerosis scores [β (95%CI) =-0.45 (-0.78, -0.11) and -0.50 (-0.86, -0.14) in the same data, after adjustment for covariates] (Table 5.1).

Table 5.1. Association between rs3825807 and carotid atherosclerosis in the Bruneck Study

	Age/sex-adjusted model		**Multivariable model†**	
	OR (95% CI)*	*p*-value	OR (95% CI)*	*p*-value
Presence of atherosclerosis in 1990	0.58 (0.35-0.96)	0.035	0.51 (0.31-0.84)	0.008
Presence of atherosclerosis in 1995	0.51 (0.32-0.82)	0.005	0.53 (0.31-0.90)	0.019
	β (95% CI)*	*p*-value	**β** (95% CI)*	*p*-value
Atherosclerosis score 1990	-0.43 (-0.77, -0.09)	0.013	-0.45 (-0.78, -0.11)	0.010
Atherosclerosis score 1995	-0.53 (-0.89, -0.16)	0.005	-0.50 (-0.86, -0.14)	0.006

* Odds ratios (OR) and regression coefficients (β) were derived from logistic and linear regression analyses respectively, comparing G/G versus A/A and A/G. † Multivariable analyses were performed with adjustment for variables correlated with atherosclerosis parameters in the Bruneck cohort.

5.2 Southampton Atherosclerosis Study

In a study (the Southampton Atherosclerosis Study, SAS) of a large group of patients undergoing coronary angiography, we found that SNP rs3825807 was associated with the extent of >50% stenotic coronary lesions, with G/G genotype patients having significantly lower scores compared with patients of the A/A or A/G genotype, including Gensini score, Sullivan score, Duke index, and modified-Duke score (Figure 5.1).

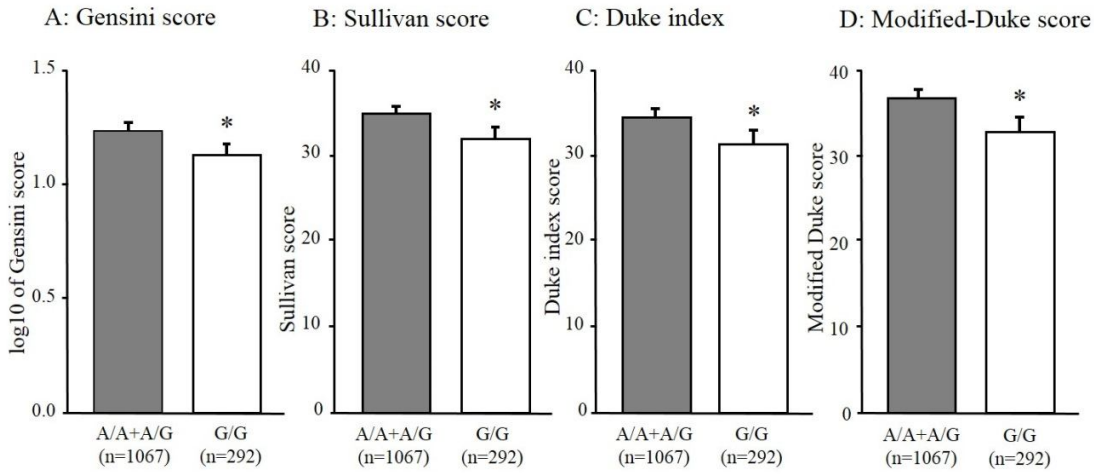

Figure 5.1. SNP rs3825807 associated with angiographic scores in CAD patients. Angiographically verified CAD patients who participated in the Southampton Atherosclerosis Study (SAS) were genotyped for SNP rs3825807. The severity of CAD was compared between the GG genotype patients and the AA and AG genotype patients by multiple angiographic scoring systems. **A:** Gensini angiographic scoring system; **B:** Sullivan scoring system; **C:** Duke index and **D:** modified-Duke score. Student's t-test was used to ascertain differences between the two groups. *p<0.05 comparing A/A + A/G genotypes and G/G genotype.

5.3 ADAMTS-7 proportion in the plaque intima correlates with intima thickness

In addition to the above two studies which showed an association between the ADAMTS-7 SNP rs3825807 and atherosclerosis scores, a relevant finding from a concurrent study of coronary atherosclerotic plaques (n=34) into a relationship between ADAMTS-7 immunostains and plaque intima thickness is also worth noting. This study showed that the percentage of ADAMTS-7 stain positive area in the intima was significantly correlated with the thickness of the intima of the atherosclerotic plaque (Figure 5.2).

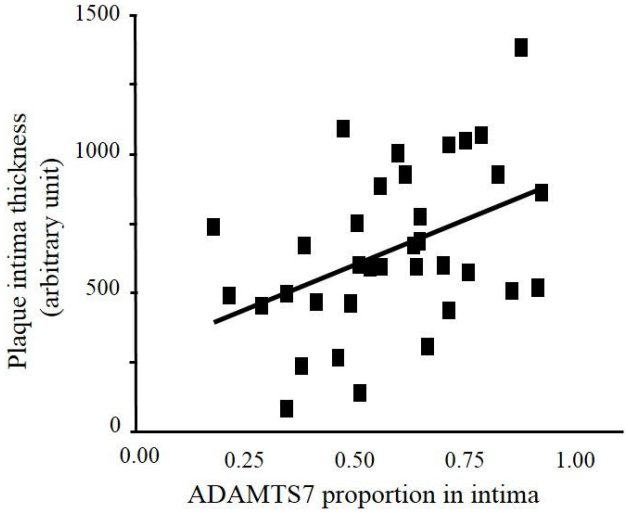

Figure 5.2. ADAMTS-7 proportion in intima correlates with plaque intima thickness in the human coronary atherosclerotic plaques. Atherosclerotic coronary artery sections were subjected to double immunostaining of smooth muscle α-actin (SMA) and ADAMTS-7. The percentage of ADAMTS-7 stain positive area and the intima thickness were analysed by Image Pro Plus. Pearson regression analysis was used to analyse the correlation of the percentage of ADAMTS-7 stain positive area in intima and the plaque intima thickness, $p<0.05$.

In summary, the results of this chapter along with results demonstrated in chapter 3 and 4 indicate that ADAMTS-7 and the non-synonymous SNP rs3825807 have functional effects on VSMC and EC migration and angiogenesis, providing new insights into the biological roles of ADAMTS-7 and a mechanistic explanation for the association between *ADAMTS7* gene SNPs, atherosclerosis severity and susceptibility to CAD.

Chapter 6

General Discussion

6.1 *ADAMTS7* – a potential therapeutic target to CVDs

GWAS, an approach which has only become feasible after the completion of Human Genome Project and subsequent HapMap project, has provided a very powerful method to study the genetic risk factors for polygenic complex diseases, such as CAD, hypertension and type-2 diabetes. Findings from GWAS have helped identify susceptible genes for these diseases. To date, almost 50 genetic loci have been identified to be associated with CAD susceptibility, typically with multiple SNPs at each of these loci associated with susceptibility of CAD (Deloukas et al. 2013). However, for many of these loci, the functional mechanisms leading to the genetic effect remain unknown. Functional characterisation of these genetic variants can aid the understanding of the underlying biological mechanisms and may facilitate the translation of the genetic discoveries to therapeutic development. The findings of our study that the SNP rs3825807 has an effect on ADAMTS-7 pro-domain cleavage, substrate TSP-5 cleavage, VSMC and EC migration, and angiogenesis are pertinent in this context. Many of the genes located in the CAD-associated genomic regions identified by GWAS have not been reported previously to be involved in the pathogenesis of CAD, thus functional studies of these genes will be required to determine whether or not they play a role in relevant pathophysiological processes. Such studies may identify novel pathways or mechanisms, ultimately leading to the discovery of novel therapeutic targets to treat the diseases.

As discussed earlier, three GWAS published in 2011 revealed that SNPs at the *ADAMTS7* gene locus on chromosome 15q25 were associated with CAD (Coronary Artery Disease Genetics 2011, Reilly et al. 2011, Schunkert et al. 2011) including the non-synonymous SNP rs3825807 which results in a Ser-to-Pro substitution in the pro-domain of ADAMTS-7, and SNPs rs1994016 and rs4380028 which respectively reside in intron 8 and 7.6 kb upstream of the *ADAMTS7* gene. However the mechanisms underlying disease association have remained unclear. It remains to be investigated whether any of these SNPs, or other SNPs in LD with them, have a functional effect on *ADAMTS7* expression and/or activity and whether they have an effect on the biological processes related to CAD. So in this study, we sought to investigate these questions.

As described in Chapters 3 and Chapter 4, the results of this study indicate that the non-synonymous SNP rs3825807 has an effect on ADAMTS-7 pro-domain cleavage, TSP-5 cleavage, VSMC and EC migration, and angiogenesis. Therefore, it is plausible that the association between SNPs at the *ADAMTS7* locus and CAD susceptibility is, possibly in part, due to the effect of SNP rs3825807 on VSMC migration and angiogenesis, which in turn contributing to the development and progression of coronary atherosclerosis. Thus, the results of this study provide a plausible mechanistic explanation for the association between SNPs at the *ADAMTS7* locus and CAD susceptibility. Currently there is no evidence that the other CAD-associated SNPs at the *ADAMTS7* locus, specifically rs1994016 and rs4380028, are functional. If they are functionally neutral, their association with CAD can be due to their LD with the functional SNP rs3825807. Genetic variants certainly affect individual's susceptibility to CVD, thus the knowledge of individual's

CVD associated SNPs, especially functionally significant variants, such as SNP rs3825807 identified in this study, might be used to predict disease risk. The more relevant clinical use for such genetic variants is in risk calibration, which is the ability of the genotype to improve the stratification of individuals into risk categories (Humphries, Drenos et al. 2010).

The results of this study provide further evidence of an important role of the ADAMTS-7 protease in VSMC migration, supporting the findings by Wang et al from their study in rats. Perhaps more importantly, our study leads to the novel finding that ADAMTS-7 plays an important role in EC migration and angiogenesis. The finding suggests potentially a previously unknown role of ADAMTS-7 in atherosclerosis, since neovascularization promotes atherosclerotic plaque growth, rupture and haemorrhage. These results suggest that ADAMTS-7 is a potential therapeutic target to treat CVDs.

6.2 Future work

This study provided a mechanistic explanation for the recently reported association between the *ADAMTS7* SNP rs3825807 and CAD susceptibility, with part of this project already published (Pu et al. 2013). However, much more work still needs to be done to further investigate the roles of ADAMTS-7 in the pathogenesis of atherosclerosis. Some of such studies are discussed below.

The studies described in Chapter 4 showed that ADAMTS-7 has an effect on EC migration and *in vitro* angiogenesis. Although the proteomic analysis provided a clue suggesting that TSP-1 is a likely substrate of ADAMTS-7 and might a mediator for the effect of ADAMTS-7 on EC migration and angiogenesis, further experiments need to be done to investigate whether this is the case and to elucidate the molecular mechanism.

To determine whether TSP-1 is a proteolytic substrate of ADAMTS-7, *in vitro* digestion assay can be done by a recombinant TSP-1 with recombinant ADAMTS-7, or conditioned media of ECs transfected with the *ADAMTS7* overexpression plasmid and conditioned media of ECs infected with shRNA to knock down *ADAMTS7*.

To investigate whether ADAMTS-7 affects EC migration and angiogenesis through degradation of TSP-1, one strategy would be knock down/block TSP-1 in ECs and determine if it abolishes the differences in EC migration and angiogenesis between ECs with *ADAMTS7* overexpression and ECs with *ADAMTS7* knockdown.

According to our preliminary proteomic analysis data, several other proteins, apart from TSP-1, differ in their amounts between conditioned media of ECs with *ADAMTS7* overexpression and ECs with *ADAMTS7* knockdown (Table 3.2.3). Further assays can be carried out to investigate whether these proteins are also substrates of ADAMTS-7 and their relationships with ADAMTS-7 functions.

In a broader context, it would be interesting to investigate the role of ADAMTS-7 in other human diseases such as cardiomyopathy and cancer. One study revealed that the deficiency of TSP-5 caused dilated cardiomyopathy (Huang et al. 2013); thus ADAMTS-7 might play a role in this disease. Furthermore, the effect of ADAMTS-7 on EC migration and angiogenesis might be relevant to tumour development and growth, since angiogenesis is a critical process in these processes.

Reference

Aherrahrou, Z., T. Kessler, K. Schmidt, C. de Wit, H. Schunkert and J. Erdmann (2011). "Knockout of the Coronary Artery Disease Risk Gene Adamts-7 Inhibits Neointima Formation and Stenosis of Arteries." Circulation 124(21).

Al-Fakhri, N., J. Wilhelm, M. Hahn, M. Heidt, F. W. Hehrlein, A. M. Endisch, T. Hupp, S. M. Cherian, Y. V. Bobryshev, R. S. Lord and N. Katz (2003). "Increased expression of disintegrin-metalloproteinases ADAM-15 and ADAM-9 following upregulation of integrins alpha5beta1 and alphavbeta3 in atherosclerosis." J Cell Biochem 89(4): 808-823.

Altshuler, D. M., R. A. Gibbs, L. Peltonen, E. Dermitzakis, S. F. Schaffner, F. Yu, P. E. Bonnen, P. I. de Bakker, P. Deloukas, S. B. Gabriel, R. Gwilliam, S. Hunt, M. Inouye, X. Jia, A. Palotie, M. Parkin, P. Whittaker, K. Chang, A. Hawes, L. R. Lewis, Y. Ren, D. Wheeler, D. M. Muzny, C. Barnes, K. Darvishi, M. Hurles, J. M. Korn, K. Kristiansson, C. Lee, S. A. McCarrol, J. Nemesh, A. Keinan, S. B. Montgomery, S. Pollack, A. L. Price, N. Soranzo, C. Gonzaga-Jauregui, V. Anttila, W. Brodeur, M. J. Daly, S. Leslie, G. McVean, L. Moutsianas, H. Nguyen, Q. Zhang, M. J. Ghori, R. McGinnis, W. McLaren, F. Takeuchi, S. R. Grossman, I. Shlyakhter, E. B. Hostetter, P. C. Sabeti, C. A. Adebamowo, M. W. Foster, D. R. Gordon, J. Licinio, M. C. Manca, P. A. Marshall, I. Matsuda, D. Ngare, V. O. Wang, D. Reddy, C. N. Rotimi, C. D. Royal, R. R. Sharp, C. Zeng, L. D. Brooks and J. E. McEwen (2010). "Integrating common and rare genetic variation in diverse human populations." Nature 467(7311): 52-58.

Apte, S. S. (2004). "A disintegrin-like and metalloprotease (reprolysin type) with thrombospondin type 1 motifs: the ADAMTS family." Int J Biochem Cell Biol 36(6): 981-985.

Apte, S. S. (2009). "A disintegrin-like and metalloprotease (reprolysin-type) with thrombospondin type 1 motif (ADAMTS) superfamily: functions and mechanisms." J Biol Chem 284(46): 31493-31497.

Armstrong, L. C. and P. Bornstein (2003). "Thrombospondins 1 and 2 function as inhibitors of angiogenesis." Matrix Biology 22(1): 63-71.

Bacchetti, S. and F. L. Graham (1977). "Transfer of the gene for thymidine kinase to thymidine kinase-deficient human cells by purified herpes simplex viral DNA." Proc Natl Acad Sci U S A 74(4): 1590-1594.

Bai, X. H., D. W. Wang, L. Kong, Y. Zhang, Y. Luan, T. Kobayashi, H. M. Kronenberg, X. P. Yu and C. J. Liu (2009). "ADAMTS-7, a direct target of PTHrP, adversely regulates endochondral bone growth by associating with and inactivating GEP growth factor." Mol Cell Biol 29(15): 4201-4219.

Bergeron, F., R. Leduc and R. Day (2000). "Subtilase-like pro-protein convertases: from molecular specificity to therapeutic applications." J Mol Endocrinol 24(1): 1-22.

Binder, C. J., K. Hartvigsen, M. K. Chang, M. Miller, D. Broide, W. Palinski, L. K. Curtiss, M. Corr and J. L. Witztum (2004). "IL-5 links adaptive and natural immunity specific for epitopes of oxidized LDL and protects from atherosclerosis." J Clin Invest 114(3): 427-437.

Caligiuri, G., M. Rudling, V. Ollivier, M. P. Jacob, J. B. Michel, G. K. Hansson and A. Nicoletti (2003). "Interleukin-10 deficiency increases atherosclerosis, thrombosis, and low-density lipoproteins in apolipoprotein E knockout mice." Mol Med 9(1-2): 10-17.

Cao, Y., Q. Kang, Z. Zhao and A. Zolkiewska (2002). "Intracellular processing of metalloprotease disintegrin ADAM12." J Biol Chem 277(29): 26403-26411.

Chait, A. and T. N. Wight (2000). "Interaction of native and modified low-density lipoproteins with extracellular matrix." Curr Opin Lipidol 11(5): 457-463.

Chang, M. Y., S. Potter-Perigo, C. Tsoi, A. Chait and T. N. Wight (2000). "Oxidized low density lipoproteins regulate synthesis of monkey aortic smooth muscle cell proteoglycans that have enhanced native low density lipoprotein binding properties." J Biol Chem 275(7): 4766-4773.

Chen, H., M. E. Herndon and J. Lawler (2000). "The cell biology of thrombospondin-1." Matrix Biol 19(7): 597-614.

Chen, L., L. Yang, Y. Zha and L. Cui (2011). "Association of serum a disintegrin and metalloproteinase with thrombospodin motif 4 levels with the presence and severity of coronary artery disease." Coron Artery Dis 22(8): 570-576.

Chistiakov, D. A., I. A. Sobenin and A. N. Orekhov (2013). "Vascular extracellular matrix in atherosclerosis." Cardiol Rev 21(6): 270-288.

Coronary Artery Disease Genetics, C. (2011). "A genome-wide association study in Europeans and South Asians identifies five new loci for coronary artery disease." Nat Genet 43(4): 339-344.

Crawford, S. E., V. Stellmach, J. E. Murphy-Ullrich, S. M. F. Ribeiro, J. Lawler, R. O. Hynes, G. P. Boivin and N. Bouck (1998). "Thrombospondin-1 is a major activator of TGF-beta 1 in vivo." Cell 93(7): 1159-1170.

Creemers, E. E., J. P. Cleutjens, J. F. Smits and M. J. Daemen (2001). "Matrix metalloproteinase inhibition after myocardial infarction: a new approach to prevent heart failure?" Circ Res 89(3): 201-210.

Davidson, B., E. Alejandro, V. A. Florenes, J. M. Goderstad, B. Risberg, G. B. Kristensen, C. G. Trope and E. C. Kohn (2004). "Granulin-epithelin precursor is a novel prognostic marker in epithelial ovarian carcinoma." Cancer 100(10): 2139-2147.

Davies, M. J. (1996). "Stability and instability: two faces of coronary atherosclerosis. The Paul Dudley White Lecture 1995." Circulation 94(8): 2013-2020.

Dawn Teare, M. and J. H. Barrett (2005). "Genetic linkage studies." Lancet 366(9490): 1036-1044.

Dawson, D. W., S. F. Pearce, R. Zhong, R. L. Silverstein, W. A. Frazier and N. P. Bouck (1997). "CD36 mediates the In vitro inhibitory effects of thrombospondin-1 on endothelial cells." J Cell Biol 138(3): 707-717.

Deloukas, P., S. Kanoni, C. Willenborg, M. Farrall, T. L. Assimes, J. R. Thompson, E. Ingelsson, D. Saleheen, J. Erdmann, B. A. Goldstein, K. Stirrups, I. R. Konig, J. B. Cazier, A. Johansson, A. S. Hall, J. Y. Lee, C. J. Willer, J. C. Chambers, T. Esko, L. Folkersen, A. Goel, E. Grundberg, A. S. Havulinna, W. K. Ho, J. C. Hopewell, N. Eriksson, M. E. Kleber, K. Kristiansson, P. Lundmark, L. P. Lyytikainen, S. Rafelt, D. Shungin, R. J. Strawbridge, G. Thorleifsson, E. Tikkanen, N. Van Zuydam, B. F. Voight, L. L. Waite, W. Zhang, A. Ziegler, D. Absher, D. Altshuler, A. J. Balmforth, I. Barroso, P. S. Braund, C. Burgdorf, S. Claudi-Boehm, D. Cox, M. Dimitriou, R. Do, A. S. Doney, N. El Mokhtari, P. Eriksson, K. Fischer, P. Fontanillas, A. Franco-Cereceda, B. Gigante, L. Groop, S. Gustafsson, J. Hager, G. Hallmans, B. G. Han, S. E. Hunt, H. M. Kang, T. Illig, T. Kessler, J. W. Knowles, G. Kolovou, J. Kuusisto, C. Langenberg, C. Langford, K. Leander, M. L. Lokki, A. Lundmark, M. I. McCarthy, C. Meisinger, O. Melander, E. Mihailov, S. Maouche, A. D. Morris, M. Muller-Nurasyid, K. Nikus, J. F. Peden, N. W. Rayner, A. Rasheed, S. Rosinger, D. Rubin, M. P. Rumpf, A. Schafer, M. Sivananthan, C. Song, A. F. Stewart, S. T. Tan, G. Thorgeirsson, C. E. van der Schoot, P. J. Wagner, G. A. Wells, P. S. Wild, T. P. Yang, P. Amouyel, D. Arveiler, H. Basart, M. Boehnke, E. Boerwinkle, P. Brambilla, F. Cambien, A. L. Cupples, U. de Faire, A. Dehghan, P. Diemert, S. E. Epstein, A. Evans, M. M. Ferrario, J. Ferrieres, D. Gauguier, A. S. Go, A. H. Goodall, V. Gudnason, S. L. Hazen, H. Holm, C. Iribarren, Y. Jang, M. Kahonen, F. Kee, H. S. Kim, N. Klopp, W. Koenig, W. Kratzer, K. Kuulasmaa, M. Laakso, R. Laaksonen, L. Lind, W. H. Ouwehand, S. Parish, J. E. Park, N. L. Pedersen, A. Peters, T. Quertermous, D. J. Rader, V. Salomaa, E. Schadt, S. H. Shah, J. Sinisalo, K. Stark, K. Stefansson, D. A. Tregouet, J. Virtamo, L. Wallentin, N. Wareham, M. E. Zimmermann, M. S. Nieminen, C. Hengstenberg, M. S. Sandhu, T. Pastinen, A. C. Syvanen, G. K. Hovingh, G. Dedoussis, P. W. Franks, T. Lehtimaki, A. Metspalu, P. A. Zalloua, A. Siegbahn, S. Schreiber, S. Ripatti, S. S. Blankenberg, M. Perola, R. Clarke, B. O. Boehm, C. O'Donnell, M. P. Reilly, W. Marz, R. Collins, S. Kathiresan, A. Hamsten, J. S. Kooner, U. Thorsteinsdottir, J. Danesh, C. N. Palmer, R. Roberts, H. Watkins, H. Schunkert and N. J. Samani (2013). "Large-scale association analysis identifies new risk loci for coronary artery disease." Nat Genet 45(1): 25-33.

Donners, M. M., I. M. Wolfs, S. Olieslagers, Z. Mohammadi-Motahhari, V. Tchaikovski, S. Heeneman, J. D. van Buul, V. Caolo, D. G. Molin, M. J. Post and J. Waltenberger (2010). "A disintegrin and metalloprotease 10 is a novel mediator of vascular endothelial growth factor-induced endothelial cell function in angiogenesis and is associated with atherosclerosis." Arterioscler Thromb Vasc Biol 30(11): 2188-2195.

Donovan, D., N. J. Brown, E. T. Bishop and C. E. Lewis (2001). "Comparison of three in vitro human 'angiogenesis' assays with capillaries formed in vivo." Angiogenesis 4(2): 113-121.

Doran, A. C., N. Meller and C. A. McNamara (2008). "Role of smooth muscle cells in the initiation and early progression of atherosclerosis." Arterioscler Thromb Vasc Biol 28(5): 812-819.

Du, Y., C. Gao, Z. Liu, L. Wang, B. Liu, F. He, T. Zhang, Y. Wang, X. Wang, M. Xu, G. Z. Luo, Y. Zhu, Q. Xu and W. Kong (2012). "Upregulation of a disintegrin and metalloproteinase with thrombospondin motifs-7 by miR-29 repression mediates vascular smooth muscle calcification." Arterioscler Thromb Vasc Biol 32(11): 2580-2588.

Du, Y., Y. Wang, L. Wang, B. Liu, Q. Tian, C. j. Liu, T. Zhang, Q. Xu, Y. Zhu, O. Ake, Y. Qi, C. Tang, W. Kong and X. Wang (2011). "Cartilage Oligomeric Matrix Protein Inhibits Vascular Smooth Muscle Calcification by Interacting With Bone Morphogenetic Protein-2." Circulation Research 108(8): 917-928.

Edelheit, O., A. Hanukoglu and I. Hanukoglu (2009). "Simple and efficient site-directed mutagenesis using two single-primer reactions in parallel to generate mutants for protein structure-function studies." BMC Biotechnol 9: 61.

Edwards, I. J., J. D. Wagner, C. A. Vogl-Willis, K. N. Litwak and W. T. Cefalu (2004). "Arterial heparan sulfate is negatively associated with hyperglycemia and atherosclerosis in diabetic monkeys." Cardiovascular Diabetology 3.

Engelberg, H. (2001). "Endogenous heparin activity deficiency: the 'Missing Link' in atherogenesis?" Atherosclerosis 159(2): 253-260.

Eriksson, E. E., X. Xie, J. Werr, P. Thoren and L. Lindbom (2001). "Importance of primary capture and L-selectin-dependent secondary capture in leukocyte accumulation in inflammation and atherosclerosis in vivo." J Exp Med 194(2): 205-218.

Falk, E. (2006). "Pathogenesis of atherosclerosis." J Am Coll Cardiol 47(8 Suppl): C7-12.

Felgner, P. L., T. R. Gadek, M. Holm, R. Roman, H. W. Chan, M. Wenz, J. P. Northrop, G. M. Ringold and M. Danielsen (1987). "Lipofection: a highly efficient, lipid-mediated DNA-transfection procedure." Proc Natl Acad Sci U S A 84(21): 7413-7417.

Fischer, M., U. Broeckel, S. Holmer, A. Baessler, C. Hengstenberg, B. Mayer, J. Erdmann, G. Klein, G. Riegger, H. J. Jacob and H. Schunkert (2005). "Distinct heritable patterns of angiographic coronary artery disease in families with myocardial infarction." Circulation 111(7): 855-862.

Fischer, M., B. Mayer, A. Baessler, G. Riegger, J. Erdmann, C. Hengstenberg and H. Schunkert (2007). "Familial aggregation of left main coronary artery disease and future risk of coronary events in asymptomatic siblings of affected patients." Eur Heart J 28(20): 2432-2437.

Galis, Z. S. and J. J. Khatri (2002). "Matrix metalloproteinases in vascular remodeling and atherogenesis: the good, the bad, and the ugly." Circ Res 90(3): 251-262.

Galis, Z. S., G. K. Sukhova, M. W. Lark and P. Libby (1994). "Increased expression of matrix metalloproteinases and matrix degrading activity in vulnerable regions of human atherosclerotic plaques." J Clin Invest 94(6): 2493-2503.

Ge, B., S. Gurd, T. Gaudin, C. Dore, P. Lepage, E. Harmsen, T. J. Hudson and T. Pastinen (2005). "Survey of allelic expression using EST mining." Genome Res 15(11): 1584-1591.

Geng, Y. J., L. E. Henderson, E. B. Levesque, M. Muszynski and P. Libby (1997). "Fas is expressed in human atherosclerotic intima and promotes apoptosis of cytokine-primed human vascular smooth muscle cells." Arterioscler Thromb Vasc Biol 17(10): 2200-2208.

Geng, Y. J. and P. Libby (2002). "Progression of atheroma: a struggle between death and procreation." Arterioscler Thromb Vasc Biol 22(9): 1370-1380.

Good, D. J., P. J. Polverini, F. Rastinejad, M. M. Le Beau, R. S. Lemons, W. A. Frazier and N. P. Bouck (1990). "A tumor suppressor-dependent inhibitor of angiogenesis is immunologically and functionally indistinguishable from a fragment of thrombospondin." Proc Natl Acad Sci U S A 87(17): 6624-6628.

Greenaway, J., J. Lawler, R. Moorehead, P. Bornstein, J. Lamarre and J. Petrik (2007). "Thrombospondin-1 inhibits VEGF levels in the ovary directly by binding and internalization via the low density lipoprotein receptor-related protein-1 (LRP-1)." J Cell Physiol 210(3): 807-818.

Gu, L., Y. Okada, S. K. Clinton, C. Gerard, G. K. Sukhova, P. Libby and B. J. Rollins (1998). "Absence of monocyte chemoattractant protein-1 reduces atherosclerosis in low density lipoprotein receptor-deficient mice." Mol Cell 2(2): 275-281.

Guo, F., Y. Lai, Q. Tian, E. A. Lin, L. Kong and C. Liu (2010). "Granulin-epithelin precursor binds directly to ADAMTS-7 and ADAMTS-12 and inhibits their degradation of cartilage oligomeric matrix protein." Arthritis Rheum 62(7): 2023-2036.

Guo, N., H. C. Krutzsch, J. K. Inman and D. D. Roberts (1997). "Thrombospondin 1 and type I repeat peptides of thrombospondin 1 specifically induce apoptosis of endothelial cells." Cancer Res 57(9): 1735-1742.

Gupta, K., P. Gupta, R. Wild, S. Ramakrishnan and R. P. Hebbel (1999). "Binding and displacement of vascular endothelial growth factor (VEGF) by thrombospondin: effect on human microvascular endothelial cell proliferation and angiogenesis." Angiogenesis 3(2): 147-158.

Gupta, S., A. M. Pablo, X. Jiang, N. Wang, A. R. Tall and C. Schindler (1997). "IFN-gamma potentiates atherosclerosis in ApoE knock-out mice." J Clin Invest 99(11): 2752-2761.

Hanby, H. A. and X. L. Zheng (2013). "Biochemistry and physiological functions of ADAMTS7 metalloprotease." Adv Biochem 1(3).

Hansson, G. K. (2001). "Immune mechanisms in atherosclerosis." Arterioscler Thromb Vasc Biol 21(12): 1876-1890.

Hansson, G. K. (2005). "Inflammation, atherosclerosis, and coronary artery disease." N Engl J Med 352(16): 1685-1695.

Hao, H., G. Gabbiani and M. L. Bochaton-Piallat (2003). "Arterial smooth muscle cell heterogeneity: implications for atherosclerosis and restenosis development." Arterioscler Thromb Vasc Biol 23(9): 1510-1520.

Helgadottir, A., S. Gretarsdottir, D. St Clair, A. Manolescu, J. Cheung, G. Thorleifsson, A. Pasdar, S. F. Grant, L. J. Whalley, H. Hakonarson, U. Thorsteinsdottir, A. Kong, J. Gulcher, K. Stefansson and M. J. MacLeod (2005). "Association between the gene encoding 5-lipoxygenase-activating protein and stroke replicated in a Scottish population." Am J Hum Genet 76(3): 505-509.

Helgadottir, A., A. Manolescu, G. Thorleifsson, S. Gretarsdottir, H. Jonsdottir, U. Thorsteinsdottir, N. J. Samani, G. Gudmundsson, S. F. Grant, G. Thorgeirsson, S. Sveinbjornsdottir, E. M. Valdimarsson, S. E. Matthiasson, H. Johannsson, O. Gudmundsdottir, M. E. Gurney, J. Sainz, M. Thorhallsdottir, M. Andresdottir, M. L. Frigge, E. J. Topol, A. Kong, V. Gudnason, H. Hakonarson, J. R. Gulcher and K. Stefansson (2004). "The gene encoding 5-lipoxygenase activating protein confers risk of myocardial infarction and stroke." Nat Genet 36(3): 233-239.

Henney, A. M., P. R. Wakeley, M. J. Davies, K. Foster, R. Hembry, G. Murphy and S. Humphries (1991). "Localization of stromelysin gene expression in atherosclerotic plaques by in situ hybridization." Proc Natl Acad Sci U S A 88(18): 8154-8158.

Herrmann, J., L. O. Lerman, D. Mukhopadhyay, C. Napoli and A. Lerman (2006). "Angiogenesis in atherogenesis." Arterioscler Thromb Vasc Biol 26(9): 1948-1957.

Ho, J. C., Y. C. Ip, S. T. Cheung, Y. T. Lee, K. F. Chan, S. Y. Wong and S. T. Fan (2008). "Granulin-epithelin precursor as a therapeutic target for hepatocellular carcinoma." Hepatology 47(5): 1524-1532.

Holdt, L. M., J. Thiery, J. L. Breslow and D. Teupser (2008). "Increased ADAM17 mRNA expression and activity is associated with atherosclerosis resistance in LDL-receptor deficient mice." Arterioscler Thromb Vasc Biol 28(6): 1097-1103.

Huang, Y., J. Xia, J. Zheng, B. Geng, P. Liu, F. Yu, B. Liu, H. Zhang, M. Xu, P. Ye, Y. Zhu, Q. Xu, X. Wang and W. Kong (2013). "Deficiency of cartilage oligomeric matrix protein causes dilated cardiomyopathy." Basic Res Cardiol 108(5): 374.

Hurskainen, T. L., S. Hirohata, M. F. Seldin and S. S. Apte (1999). "ADAM-TS5, ADAM-TS6, and ADAM-TS7, novel members of a new family of zinc metalloproteases - General features and genomic distribution of the ADAM-TS family." Journal of Biological Chemistry 274(36): 25555-25563.

Hurtcamejo, E., G. Camejo, B. Rosengren, F. Lopez, C. Ahlstrom, G. Fager and G. Bondjers (1992). "Effect of Arterial Proteoglycans and Glycosaminoglycans on Low-Density-Lipoprotein Oxidation and Its Uptake by Human Macrophages and Arterial Smooth-Muscle Cells." Arteriosclerosis and Thrombosis 12(5): 569-583.

Iruela-Arispe, M. L., C. A. Diglio and E. H. Sage (1991). "Modulation of extracellular matrix proteins by endothelial cells undergoing angiogenesis in vitro." Arteriosclerosis and Thrombosis 11(4): 805-815.

Ivey, M. E. and P. J. Little (2008). "Thrombin regulates vascular smooth muscle cell proteoglycan synthesis via PAR-1 and multiple downstream signalling pathways." Thrombosis Research 123(2): 288-297.

Jian, J. L., J. Konopka and C. J. Liu (2013). "Insights into the role of progranulin in immunity, infection, and inflammation." Journal of Leukocyte Biology 93(2): 199-208.

Jimenez, B., O. V. Volpert, S. E. Crawford, M. Febbraio, R. L. Silverstein and N. Bouck (2000). "Signals leading to apoptosis-dependent inhibition of neovascularization by thrombospondin-1." Nat Med 6(1): 41-48.

Jones, G. C. and G. P. Riley (2005). "ADAMTS proteinases: a multi-domain, multi-functional family with roles in extracellular matrix turnover and arthritis." Arthritis Res Ther 7(4): 160-169.

Jonsson-Rylander, A. C., T. Nilsson, R. Fritsche-Danielson, A. Hammarstrom, M. Behrendt, J. O. Andersson, K. Lindgren, A. K. Andersson, P. Wallbrandt, B. Rosengren, P. Brodin, A. Thelin, A. Westin, E. Hurt-Camejo and C. H. Lee-Sogaard (2005). "Role of ADAMTS-1 in atherosclerosis: remodeling of carotid artery, immunohistochemistry, and proteolysis of versican." Arterioscler Thromb Vasc Biol 25(1): 180-185.

Kannel, W. B., T. R. Dawber, A. Kagan, N. Revotskie and J. Stokes, 3rd (1961). "Factors of risk in the development of coronary heart disease--six year follow-up experience. The Framingham Study." Ann Intern Med 55: 33-50.

Kaplan, M. and M. Aviram (2001). "Retention of oxidized LDL by extracellular matrix proteoglycans leads to its uptake by macrophages: an alternative approach to study lipoproteins cellular uptake." Arterioscler Thromb Vasc Biol 21(3): 386-393.

Katsuda, S. and T. Kaji (2003). "Atherosclerosis and extracellular matrix." J Atheroscler Thromb 10(5): 267-274.

Kaur, S., G. Martin-Manso, M. L. Pendrak, S. H. Garfield, J. S. Isenberg and D. D. Roberts (2010). "Thrombospondin-1 inhibits VEGF receptor-2 signaling by disrupting its association with CD47." J Biol Chem 285(50): 38923-38932.

Kawase, R., T. Ohama, A. Matsuyama, T. Matsuwaki, T. Okada, T. Yamashita, M. Yuasa-Kawase, H. Nakaoka, K. Nakatani, M. Inagaki, K. Tsubakio-Yamamoto, D. Masuda, Y. Nakagawa-Toyama, M. Nishida, Y. Ohmoto, M. Nishihara, I. Komuro and S. Yamashita (2013). "Deletion of progranulin exacerbates atherosclerosis in ApoE knockout mice." Cardiovasc Res 100(1): 125-133.

Keys, A., H. L. Taylor, H. Blackburn, J. Brozek, J. T. Anderson and E. Simonson (1963). "Coronary Heart Disease among Minnesota Business and Professional Men Followed Fifteen Years." Circulation 28: 381-395.

Khan, B. V., S. S. Parthasarathy, R. W. Alexander and R. M. Medford (1995). "Modified low density lipoprotein and its constituents augment cytokine-activated vascular cell adhesion molecule-1 gene expression in human vascular endothelial cells." J Clin Invest 95(3): 1262-1270.

Kiechl S. and Willeit J. (1999a) The natural course of atherosclerosis. Part I: incidence and progression. Arterioscler Thromb Vasc Biol *19*, 1484-1490.

Kiechl S. and Willeit J. (1999b) The natural course of atherosclerosis. Part II: vascular remodeling. Bruneck Study Group. Arterioscler Thromb Vasc Biol *19*, 1491-1498.

Koo, B. H., J. M. Longpre, R. P. Somerville, J. P. Alexander, R. Leduc and S. S. Apte (2006). "Cell-surface processing of pro-ADAMTS9 by furin." J Biol Chem 281(18): 12485-12494.

Koo, B. H., J. M. Longpre, R. P. Somerville, J. P. Alexander, R. Leduc and S. S. Apte (2007). "Regulation of ADAMTS9 secretion and enzymatic activity by its propeptide." J Biol Chem 282(22): 16146-16154.

Kullo, I. J. and K. Ding (2007). "Mechanisms of disease: The genetic basis of coronary heart disease." Nat Clin Pract Cardiovasc Med 4(10): 558-569.

Kume, N., M. I. Cybulsky and M. A. Gimbrone, Jr. (1992). "Lysophosphatidylcholine, a component of atherogenic lipoproteins, induces mononuclear leukocyte adhesion molecules in cultured human and rabbit arterial endothelial cells." J Clin Invest 90(3): 1138-1144.

Kuno, K. and K. Matsushima (1998). "ADAMTS-1 protein anchors at the extracellular matrix through the thrombospondin type I motifs and its spacing region." Journal of Biological Chemistry 273(22): 13912-13917.

Kuno, K., Y. Terashima and K. Matsushima (1999). "ADAMTS-1 is an active metalloproteinase associated with the extracellular matrix." J Biol Chem 274(26): 18821-18826.

Lawler, J. (2000). "The functions of thrombospondin-1 and-2." Curr Opin Cell Biol 12(5): 634-640.

Lawler, P. R. and J. Lawler (2012). "Molecular basis for the regulation of angiogenesis by thrombospondin-1 and -2." Cold Spring Harb Perspect Med 2(5): a006627.

Lee, N. V., M. Sato, D. S. Annis, J. A. Loo, L. Wu, D. F. Mosher and M. L. Iruela-Arispe (2006). "ADAMTS-1 mediates the release of antiangiogenic polypeptides from TSP-1 and 2." Embo Journal 25(22): 5270-5283.

Leonard, J. D., F. Lin and M. E. Milla (2005). "Chaperone-like properties of the prodomain of TNFalpha-converting enzyme (TACE) and the functional role of its cysteine switch." Biochem J 387(Pt 3): 797-805.

Levy, G. G., W. C. Nichols, E. C. Lian, T. Foroud, J. N. McClintick, B. M. McGee, A. Y. Yang, D. R. Siemieniak, K. R. Stark, R. Gruppo, R. Sarode, S. B. Shurin, V. Chandrasekaran, S. P. Stabler, H. Sabio, E. E. Bouhassira, J. D. Upshaw, Jr., D. Ginsburg and H. M. Tsai (2001). "Mutations in a member of the ADAMTS gene family cause thrombotic thrombocytopenic purpura." Nature 413(6855): 488-494.

Liang, C. C., A. Y. Park and J. L. Guan (2007). "In vitro scratch assay: a convenient and inexpensive method for analysis of cell migration in vitro." Nat Protoc 2(2): 329-333.

Libby, P. (1995). "Molecular bases of the acute coronary syndromes." Circulation 91(11): 2844-2850.

Libby, P. (2000). "Changing concepts of atherogenesis." J Intern Med 247(3): 349-358.

Libby, P. (2002). "Inflammation in atherosclerosis." Nature 420(6917): 868-874.

Libby, P. (2006). "Inflammation and cardiovascular disease mechanisms." Am J Clin Nutr 83(2): 456S-460S.

Libby, P., P. M. Ridker and G. K. Hansson (2011). "Progress and challenges in translating the biology of atherosclerosis." Nature 473(7347): 317-325.

Libby, P., P. M. Ridker and A. Maseri (2002). "Inflammation and atherosclerosis." Circulation 105(9): 1135-1143.

Little, P. J., L. Tannock, K. L. Olin, A. Chait and T. N. Wight (2002). "Proteoglycans synthesised by arterial smooth muscle cells in the presence of transforming growth factor-beta1 exhibit increased binding to LDLs." Arterioscler Thromb Vasc Biol 22(1): 55-60.

Liu, C. J., W. Kong, K. Ilalov, S. Yu, K. Xu, L. Prazak, M. Fajardo, B. Sehgal and P. E. Di Cesare (2006). "ADAMTS-7: a metalloproteinase that directly binds to and degrades cartilage oligomeric matrix protein." FASEB J 20(7): 988-990.

Longpre, J. M. and R. Leduc (2004). "Identification of prodomain determinants involved in ADAMTS-1 biosynthesis." J Biol Chem 279(32): 33237-33245.

Longpre, J. M., D. R. McCulloch, B. H. Koo, J. P. Alexander, S. S. Apte and R. Leduc (2009). "Characterisation of proADAMTS5 processing by proprotein convertases." Int J Biochem Cell Biol 41(5): 1116-1126.

Luan, Y., L. Kong, D. R. Howell, K. Ilalov, M. Fajardo, X. H. Bai, P. E. Di Cesare, M. B. Goldring, S. B. Abramson and C. J. Liu (2008). "Inhibition of ADAMTS-7 and ADAMTS-12 degradation of cartilage oligomeric matrix protein by alpha-2-macroglobulin." Osteoarthritis Cartilage 16(11): 1413-1420.

Luepker, R. V. (2009). "Careers in Cardiovascular Disease Epidemiology and Prevention." Circulation 120(6): 533-538.

Lusis, A. J. (2000). "Atherosclerosis." Nature 407(6801): 233-241.

Lusis, A. J., R. Mar and P. Pajukanta (2004). "Genetics of atherosclerosis." Annu Rev Genomics Hum Genet 5: 189-218.

Majerus, E. M., X. L. Zheng, E. A. Tuley and J. E. Sadler (2003). "Cleavage of the ADAMTS-13 propeptide is not required for protease activity." Journal of Biological Chemistry 278(47): 46643-46648.

Mallat, Z., S. Besnard, M. Duriez, V. Deleuze, F. Emmanuel, M. F. Bureau, F. Soubrier, B. Esposito, H. Duez, C. Fievet, B. Staels, N. Duverger, D. Scherman and A. Tedgui (1999). "Protective role of interleukin-10 in atherosclerosis." Circ Res 85(8): e17-24.

Marenberg, M. E., N. Risch, L. F. Berkman, B. Floderus and U. de Faire (1994). "Genetic susceptibility to death from coronary heart disease in a study of twins." N Engl J Med 330(15): 1041-1046.

Mayer, G., G. Boileau and M. Bendayan (2003). "Furin interacts with proMT1-MMP and integrin alpha V at specialized domains of renal cell plasma membrane." Journal of Cell Science 116(9): 1763-1773.

Mayer, G., G. Boileau and M. Bendayan (2004). "Sorting of furin in polarized epithelial and endothelial cells: expression beyond the Golgi apparatus." J Histochem Cytochem 52(5): 567-579.

Mitchell, R. S., B. F. Beitzel, A. R. Schroder, P. Shinn, H. Chen, C. C. Berry, J. R. Ecker and F. D. Bushman (2004). "Retroviral DNA integration: ASLV, HIV, and MLV show distinct target site preferences." PLoS Biol 2(8): E234.

Motterle, A., X. Pu, H. Wood, Q. Xiao, S. Gor, F. L. Ng, K. Chan, F. Cross, B. Shohreh, R. N. Poston, A. T. Tucker, M. J. Caulfield and S. Ye (2012). "Functional analyses of coronary artery disease associated variation on chromosome 9p21 in vascular smooth muscle cells." Hum Mol Genet 21(18): 4021-4029.

Moulton, K. S., E. Heller, M. A. Konerding, E. Flynn, W. Palinski and J. Folkman (1999). "Angiogenesis inhibitors endostatin or TNP-470 reduce intimal neovascularization and plaque growth in apolipoprotein E-deficient mice." Circulation 99(13): 1726-1732.

Moulton, K. S., K. Vakili, D. Zurakowski, M. Soliman, C. Butterfield, E. Sylvin, K. M. Lo, S. Gillies, K. Javaherian and J. Folkman (2003). "Inhibition of plaque neovascularization reduces macrophage accumulation and progression of advanced atherosclerosis." Proc Natl Acad Sci U S A 100(8): 4736-4741.

Murphy-Ullrich, J. E., S. Schultz-Cherry and M. Hook (1992). "Transforming growth factor-beta complexes with thrombospondin." Mol Biol Cell 3(2): 181-188.

Murphy, G. and H. Nagase (2008). "Progress in matrix metalloproteinase research." Mol Aspects Med 29(5): 290-308.

Nabel, E. G. (2003). "Cardiovascular disease." N Engl J Med 349(1): 60-72.

Nabel, E. G. and E. Braunwald (2012). "A tale of coronary artery disease and myocardial infarction." N Engl J Med 366(1): 54-63.

Nakashima, Y., T. N. Wight and K. Sueishi (2008). "Early atherosclerosis in humans: role of diffuse intimal thickening and extracellular matrix proteoglycans." Cardiovasc Res 79(1): 14-23.

Nakayama, K. (1997). "Furin: a mammalian subtilisin/Kex2p-like endoprotease involved in processing of a wide variety of precursor proteins." Biochem J 327 (Pt 3): 625-635.

Napoli, C., F. P. D'Armiento, F. P. Mancini, A. Postiglione, J. L. Witztum, G. Palumbo and W. Palinski (1997). "Fatty streak formation occurs in human fetal aortas and is greatly enhanced by maternal hypercholesterolemia. Intimal accumulation of low density lipoprotein and its oxidation precede monocyte recruitment into early atherosclerotic lesions." J Clin Invest 100(11): 2680-2690.

Nasir, K., M. J. Budoff, N. D. Wong, M. Scheuner, D. Herrington, D. K. Arnett, M. Szklo, P. Greenland and R. S. Blumenthal (2007). "Family history of premature coronary heart disease and coronary artery calcification: Multi-Ethnic Study of Atherosclerosis (MESA)." Circulation 116(6): 619-626.

Nasir, K., E. D. Michos, J. A. Rumberger, J. B. Braunstein, W. S. Post, M. J. Budoff and R. S. Blumenthal (2004). "Coronary artery calcification and family history of premature coronary heart disease: sibling history is more strongly associated than parental history." Circulation 110(15): 2150-2156.

Neumann, E., M. Schaeferridder, Y. Wang and P. H. Hofschneider (1982). "Gene-Transfer into Mouse Lyoma Cells by Electroporation in High Electric-Fields." Embo Journal 1(7): 841-845.

Newby, A. C. (2005). "Dual role of matrix metalloproteinases (matrixins) in intimal thickening and atherosclerotic plaque rupture." Physiol Rev 85(1): 1-31.

Orr, A. W., M. Y. Lee, J. A. Lemmon, A. Yurdagul, Jr., M. F. Gomez, P. D. Bortz and B. R. Wamhoff (2009). "Molecular mechanisms of collagen isotype-specific modulation of smooth muscle cell phenotype." Arterioscler Thromb Vasc Biol 29(2): 225-231.

Ottani, V., M. Raspanti and A. Ruggeri (2001). "Collagen structure and functional implications." Micron 32(3): 251-260.

Owens, G. K. (1995). "Regulation of differentiation of vascular smooth muscle cells." Physiol Rev 75(3): 487-517.

Owens, G. K., M. S. Kumar and B. R. Wamhoff (2004). "Molecular regulation of vascular smooth muscle cell differentiation in development and disease." Physiol Rev 84(3): 767-801.

Panka, D. J. and J. W. Mier (2003). "Canstatin inhibits Akt activation and induces Fas-dependent apoptosis in endothelial cells." J Biol Chem 278(39): 37632-37636.

Patel, M. K., J. S. Lymn, G. F. Clunn and A. D. Hughes (1997). "Thrombospondin-1 is a potent mitogen and chemoattractant for human vascular smooth muscle cells." Arteriosclerosis Thrombosis and Vascular Biology 17(10): 2107-2114.

Patel, R. S. and S. Ye (2011). "Genetic determinants of coronary heart disease: new discoveries and insights from genome-wide association studies." Heart 97(18): 1463-1473.

Patel, R. S. and S. Ye (2013). "ADAMTS7: a promising new therapeutic target in coronary heart disease." Expert Opinion on Therapeutic Targets 17(8): 863-867.

Paulissen, G., N. Rocks, M. M. Gueders, C. Crahay, F. Quesada-Calvo, S. Bekaert, J. Hacha, M. El Hour, J. M. Foidart, A. Noel and D. D. Cataldo (2009). "Role of ADAM and ADAMTS metalloproteinases in airway diseases." Respir Res 10: 127.

Pei, D. and S. J. Weiss (1995). "Furin-dependent intracellular activation of the human stromelysin-3 zymogen." Nature 375(6528): 244-247.

Petrovan, R. J., C. D. Kaplan, R. A. Reisfeld and L. K. Curtiss (2007). "DNA vaccination against VEGF receptor 2 reduces atherosclerosis in LDL receptor-deficient mice." Arterioscler Thromb Vasc Biol 27(5): 1095-1100.

Pinderski, L. J., M. P. Fischbein, G. Subbanagounder, M. C. Fishbein, N. Kubo, H. Cheroutre, L. K. Curtiss, J. A. Berliner and W. A. Boisvert (2002). "Overexpression of interleukin-10 by activated T lymphocytes inhibits atherosclerosis in LDL receptor-deficient Mice by altering lymphocyte and macrophage phenotypes." Circ Res 90(10): 1064-1071.

Plenz, G. A., M. C. Deng, H. Robenek and W. Volker (2003). "Vascular collagens: spotlight on the role of type VIII collagen in atherogenesis." Atherosclerosis 166(1): 1-11.

Porter, S., I. M. Clark, L. Kevorkian and D. R. Edwards (2005). "The ADAMTS metalloproteinases." Biochem J 386(Pt 1): 15-27.

Pu, X., Q. Xiao, S. Kiechl, K. Chan, F. L. Ng, S. Gor, R. N. Poston, C. Fang, A. Patel, E. C. Senver, S. Shaw-Hawkins, J. Willeit, C. Liu, J. Zhu, A. T. Tucker, Q. Xu, M. J. Caulfield and S. Ye (2013). "ADAMTS7 cleavage and vascular smooth muscle cell migration is affected by a coronary-artery-disease-associated variant." Am J Hum Genet 92(3): 366-374.

Rehman, A. A., H. Ahsan and F. H. Khan (2013). "alpha-2-Macroglobulin: a physiological guardian." J Cell Physiol 228(8): 1665-1675.

Reilly, M. P., M. Li, J. He, J. F. Ferguson, I. M. Stylianou, N. N. Mehta, M. S. Burnett, J. M. Devaney, C. W. Knouff, J. R. Thompson, B. D. Horne, A. F. Stewart, T. L. Assimes, P. S. Wild, H. Allayee, P. L. Nitschke, R. S. Patel, N. Martinelli, D. Girelli, A. A. Quyyumi, J. L. Anderson, J. Erdmann, A. S. Hall, H. Schunkert, T. Quertermous, S. Blankenberg, S. L. Hazen, R. Roberts, S. Kathiresan, N. J. Samani, S. E. Epstein and D. J. Rader (2011). "Identification of ADAMTS7 as a novel locus for coronary atherosclerosis and association of ABO with myocardial infarction in the presence of coronary atherosclerosis: two genome-wide association studies." Lancet 377(9763): 383-392.

Rekhter, M. D. (1999). "Collagen synthesis in atherosclerosis: too much and not enough." Cardiovasc Res 41(2): 376-384.

Riessen, R., M. Fenchel, H. Chen, D. I. Axel, K. R. Karsch and J. Lawler (2001). "Cartilage oligomeric matrix protein (thrombospondin-5) is expressed by human vascular smooth muscle cells." Arterioscler Thromb Vasc Biol 21(1): 47-54.

Roberts, R., G. A. Wells, A. F. Stewart, S. Dandona and L. Chen (2010). "The genome-wide association study--a new era for common polygenic disorders." J Cardiovasc Transl Res 3(3): 173-182.

Ross, R. (1993). "The pathogenesis of atherosclerosis: a perspective for the 1990s." Nature 362(6423): 801-809.

Ross, R. (1999). "Atherosclerosis--an inflammatory disease." N Engl J Med 340(2): 115-126.

Ross, R. and J. A. Glomset (1976a). "The pathogenesis of atherosclerosis (first of two parts)." N Engl J Med 295(7): 369-377.

Ross, R. and J. A. Glomset (1976b). "The pathogenesis of atherosclerosis (second of two parts)." N Engl J Med 295(8): 420-425.

Rzucidlo, E. M., K. A. Martin and R. J. Powell (2007). "Regulation of vascular smooth muscle cell differentiation." J Vasc Surg 45 Suppl A: A25-32.

Schunkert, H., I. R. Konig, S. Kathiresan, M. P. Reilly, T. L. Assimes, H. Holm, M. Preuss, A. F. Stewart, M. Barbalic, C. Gieger, D. Absher, Z. Aherrahrou, H. Allayee, D. Altshuler, S. S. Anand, K. Andersen, J. L. Anderson, D. Ardissino, S. G. Ball, A. J. Balmforth, T. A. Barnes, D. M. Becker, L. C. Becker, K. Berger, J. C. Bis, S. M. Boekholdt, E. Boerwinkle, P. S. Braund, M. J. Brown, M. S. Burnett, I. Buysschaert, J. F. Carlquist, L. Chen, S. Cichon, V. Codd, R. W. Davies, G. Dedoussis, A. Dehghan, S. Demissie, J. M. Devaney, P. Diemert, R. Do, A. Doering, S. Eifert, N. E. Mokhtari, S. G. Ellis, R. Elosua, J. C. Engert, S. E. Epstein, U. de Faire, M. Fischer, A. R. Folsom, J. Freyer, B. Gigante, D. Girelli, S. Gretarsdottir, V. Gudnason, J. R. Gulcher, E. Halperin, N. Hammond, S. L. Hazen, A. Hofman, B. D. Horne, T. Illig, C. Iribarren, G. T. Jones, J. W. Jukema, M. A. Kaiser, L. M. Kaplan, J. J. Kastelein, K. T. Khaw, J. W. Knowles, G. Kolovou, A. Kong, R. Laaksonen, D. Lambrechts, K. Leander, G. Lettre, M. Li, W. Lieb, C. Loley, A. J. Lotery, P. M. Mannucci, S. Maouche, N. Martinelli, P. P. McKeown, C. Meisinger, T. Meitinger, O. Melander, P. A. Merlini, V. Mooser, T. Morgan, T. W. Muhleisen, J. B. Muhlestein, T. Munzel, K. Musunuru, J. Nahrstaedt, C. P. Nelson, M. M. Nothen, O. Olivieri, R. S. Patel, C. C. Patterson, A. Peters, F. Peyvandi, L. Qu, A. A. Quyyumi, D. J. Rader, L. S. Rallidis, C. Rice, F. R. Rosendaal, D. Rubin, V. Salomaa, M. L. Sampietro, M. S. Sandhu, E. Schadt, A. Schafer, A. Schillert, S. Schreiber, J. Schrezenmeir, S. M. Schwartz, D. S. Siscovick, M. Sivananthan, S. Sivapalaratnam, A. Smith, T. B. Smith, J. D. Snoep, N. Soranzo, J. A. Spertus, K. Stark, K. Stirrups, M. Stoll, W. H. Tang, S. Tennstedt, G. Thorgeirsson, G. Thorleifsson, M. Tomaszewski, A. G. Uitterlinden, A. M. van Rij, B. F. Voight, N. J. Wareham, G. A. Wells, H. E. Wichmann, P. S. Wild, C. Willenborg, J. C. Witteman, B. J. Wright, S. Ye, T. Zeller, A. Ziegler, F. Cambien, A. H. Goodall, L. A. Cupples, T. Quertermous, W. Marz, C. Hengstenberg, S. Blankenberg, W. H. Ouwehand, A. S. Hall, P. Deloukas, J. R. Thompson, K. Stefansson, R. Roberts, U. Thorsteinsdottir, C. J. O'Donnell, R. McPherson, J. Erdmann and N. J. Samani (2011). "Large-scale association analysis identifies 13 new susceptibility loci for coronary artery disease." Nat Genet 43(4): 333-338.

Schultz-Cherry, S. and J. E. Murphy-Ullrich (1993). "Thrombospondin causes activation of latent transforming growth factor-beta secreted by endothelial cells by a novel mechanism." J Cell Biol 122(4): 923-932.

Samani, N. J., P. Burton, M. Mangino, S. G. Ball, A. J. Balmforth, J. Barrett, T. Bishop and A. Hall (2005). "A genomewide linkage study of 1,933 families affected by premature coronary artery disease: The British Heart Foundation (BHF) Family Heart Study." Am J Hum Genet 77(6): 1011-1020.

Schultz-Cherry, S., S. Ribeiro, L. Gentry and J. E. Murphy-Ullrich (1994). "Thrombospondin binds and activates the small and large forms of latent transforming growth factor-beta in a chemically defined system." J Biol Chem 269(43): 26775-26782.

Schwartz, S. M. (1997). "Perspectives series: cell adhesion in vascular biology. Smooth muscle migration in atherosclerosis and restenosis." J Clin Invest 99(12): 2814-2816.

Shi, W., M. E. Haberland, M. L. Jien, D. M. Shih and A. J. Lusis (2000). "Endothelial responses to oxidized lipoproteins determine genetic susceptibility to atherosclerosis in mice." Circulation 102(1): 75-81.

Skjot-Arkil, H., N. Barascuk, T. Register and M. A. Karsdal (2010). "Macrophage-mediated proteolytic remodeling of the extracellular matrix in atherosclerosis results in neoepitopes: a potential new class of biochemical markers." Assay Drug Dev Technol 8(5): 542-552.

Soejima, K., N. Mimura, M. Hirashima, H. Maeda, T. Hamamoto, T. Nakagaki and C. Nozaki (2001). "A novel human metalloprotease synthesised in the liver and secreted into the blood: possibly, the von Willebrand factor-cleaving protease?" J Biochem 130(4): 475-480.

Somerville, R. P., K. A. Jungers and S. S. Apte (2004). "Discovery and characterisation of a novel, widely expressed metalloprotease, ADAMTS-10, and its proteolytic activation." J Biol Chem 279(49): 51208-51217.

Somerville, R. P., J. M. Longpre, E. D. Apel, R. M. Lewis, L. W. Wang, J. R. Sanes, R. Leduc and S. S. Apte (2004). "ADAMTS7B, the full-length product of the ADAMTS7 gene, is a chondroitin sulfate proteoglycan containing a mucin domain." J Biol Chem 279(34): 35159-35175.

Somerville, R. P. T., J. M. Longpre, K. A. Jungers, J. M. Engle, M. Ross, S. Evanko, T. N. Wight, R. Leduc and S. S. Apte (2003). "Characterisation of ADAMTS-9 and ADAMTS-20 as a distinct ADAMTS subfamily related to Caenorhabditis elegans GON-1." Journal of Biological Chemistry 278(11): 9503-9513.

Sorensen, T. I., G. G. Nielsen, P. K. Andersen and T. W. Teasdale (1988). "Genetic and environmental influences on premature death in adult adoptees." N Engl J Med 318(12): 727-732.

Soutar, A. K. and R. P. Naoumova (2007). "Mechanisms of disease: genetic causes of familial hypercholesterolemia." Nat Clin Pract Cardiovasc Med 4(4): 214-225.

Stary, H. C., A. B. Chandler, R. E. Dinsmore, V. Fuster, S. Glagov, W. Insull, M. E. Rosenfeld, C. J. Schwartz, W. D. Wagner and R. W. Wissler (1995). "A Definition of Advanced Types of Atherosclerotic Lesions and a Histological Classification of Atherosclerosis - a Report from the Committee on Vascular-Lesions of the Council on Arteriosclerosis, American-Heart-Association." Circulation 92(5): 1355-1374.

Staton, C. A., S. M. Stribbling, S. Tazzyman, R. Hughes, N. J. Brown and C. E. Lewis (2004). "Current methods for assaying angiogenesis in vitro and in vivo." International Journal of Experimental Pathology 85(5): 233-248.

Stylianou, I. M., R. C. Bauer, M. P. Reilly and D. J. Rader (2012). "Genetic basis of atherosclerosis: insights from mice and humans." Circ Res 110(2): 337-355.

Tabas, I., K. J. Williams and J. Boren (2007). "Subendothelial lipoprotein retention as the initiating process in atherosclerosis - Update and therapeutic implications." Circulation 116(16): 1832-1844.

Tang, W., Y. Lu, Q. Y. Tian, Y. Zhang, F. J. Guo, G. Y. Liu, N. M. Syed, Y. Lai, E. A. Lin, L. Kong, J. Su, F. Yin, A. H. Ding, A. Zanin-Zhorov, M. L. Dustin, J. Tao, J. Craft, Z. Yin, J. Q. Feng, S. B. Abramson, X. P. Yu and C. J. Liu (2011). "The growth factor progranulin binds to TNF receptors and is therapeutic against inflammatory arthritis in mice." Science 332(6028): 478-484.

Thomas, G. (2002). "Furin at the cutting edge: From protein traffic to embryogenesis and disease." Nature Reviews Molecular Cell Biology 3(10): 753-766.

Tolsma, S. S., O. V. Volpert, D. J. Good, W. A. Frazier, P. J. Polverini and N. Bouck (1993). "Peptides derived from two separate domains of the matrix protein thrombospondin-1 have anti-angiogenic activity." J Cell Biol 122(2): 497-511.

Tran-Lundmark, K., P. K. Tran, G. Paulsson-Berne, V. Friden, R. Soininen, K. Tryggvason, T. N. Wight, M. G. Kinsella, J. Boren and U. Hedin (2008). "Heparan sulfate in perlecan promotes mouse atherosclerosis - Roles in lipid permeability, lipid retention, and smooth muscle cell proliferation." Circulation Research 103(1): 43-52.

Tran, P. K., H. E. Agardh, K. Tran-Lundmark, J. Ekstrand, J. Roy, B. Henderson, A. Gabrielsen, G. K. Hansson, J. Swedenborg, G. Paulsson-Berne and U. Hedin (2007). "Reduced perlecan expression and accumulation in human carotid atherosclerotic lesions." Atherosclerosis 190(2): 264-270.

Tregouet, D. A., I. R. Konig, J. Erdmann, A. Munteanu, P. S. Braund, A. S. Hall, A. Grosshennig, P. Linsel-Nitschke, C. Perret, M. DeSuremain, T. Meitinger, B. J. Wright, M. Preuss, A. J. Balmforth, S. G. Ball, C. Meisinger, C. Germain, A. Evans, D. Arveiler, G. Luc, J. B. Ruidavets, C. Morrison, P. van der Harst, S. Schreiber, K. Neureuther, A. Schafer, P. Bugert, N. E. El Mokhtari, J. Schrezenmeir, K. Stark, D. Rubin, H. E. Wichmann, C. Hengstenberg, W. Ouwehand, A. Ziegler, L. Tiret, J. R. Thompson, F. Cambien, H. Schunkert and N. J. Samani (2009). "Genome-wide haplotype association study identifies the SLC22A3-LPAL2-LPA gene cluster as a risk locus for coronary artery disease." Nat Genet 41(3): 283-285.

Uchida, H. A., F. Kristo, D. L. Rateri, H. Lu, R. Charnigo, L. A. Cassis and A. Daugherty (2010). "Total lymphocyte deficiency attenuates AngII-induced atherosclerosis in males but not abdominal aortic aneurysms in apoE deficient mice." Atherosclerosis 211(2): 399-403.

Ulrich-Merzenich, G., C. Metzner, R. R. Bhonde, G. Malsch, B. Schiermeyer and H. Vetter (2002). "Simultaneous isolation of endothelial and smooth muscle cells from human umbilical artery or vein and their growth response to low-density lipoproteins." In Vitro Cell Dev Biol Anim 38(5): 265-272.

Vazquez, F., G. Hastings, M. A. Ortega, T. F. Lane, S. Oikemus, M. Lombardo and M. L. Iruela-Arispe (1999). "METH-1, a human ortholog of ADAMTS-1, and METH-2 are members of a new family of proteins with angio-inhibitory activity." J Biol Chem 274(33): 23349-23357.

Vidricaire, G., J. B. Denault and R. Leduc (1993). "Characterisation of a secreted form of human furin endoprotease." Biochem Biophys Res Commun 195(2): 1011-1018.

Virmani, R., F. D. Kolodgie, A. P. Burke, A. Farb and S. M. Schwartz (2000). "Lessons from sudden coronary death: a comprehensive morphological classification scheme for atherosclerotic lesions." Arterioscler Thromb Vasc Biol 20(5): 1262-1275.

Virmani, R., F. D. Kolodgie, A. P. Burke, A. V. Finn, H. K. Gold, T. N. Tulenko, S. P. Wrenn and J. Narula (2005). "Atherosclerotic plaque progression and vulnerability to rupture: angiogenesis as a source of intraplaque hemorrhage." Arterioscler Thromb Vasc Biol 25(10): 2054-2061.

Wagsater, D., H. Bjork, C. Zhu, J. Bjorkegren, G. Valen, A. Hamsten and P. Eriksson (2008). "ADAMTS-4 and -8 are inflammatory regulated enzymes expressed in macrophage-rich areas of human atherosclerotic plaques." Atherosclerosis 196(2): 514-522.

Wang, H. and S. C. Elbein (2007). "Detection of allelic imbalance in gene expression using pyrosequencing." Methods Mol Biol 373: 157-176.

Wang, L., X. Wang and W. Kong (2010). "ADAMTS-7, a novel proteolytic culprit in vascular remodeling." Sheng Li Xue Bao 62(4): 285-294.

Wang, L., J. Zheng, X. Bai, B. Liu, C. J. Liu, Q. Xu, Y. Zhu, N. Wang, W. Kong and X. Wang (2009). "ADAMTS-7 mediates vascular smooth muscle cell migration and neointima formation in balloon-injured rat arteries." Circ Res 104(5): 688-698.

Wang, L., J. Zheng, Y. Du, Y. Huang, J. Li, B. Liu, C. j. Liu, Y. Zhu, Y. Gao, Q. Xu, W. Kong and X. Wang (2009). "Cartilage Oligomeric Matrix Protein Maintains the Contractile Phenotype of Vascular Smooth Muscle Cells by Interacting With α7β1 Integrin." Circulation Research 106(3): 514-525.

Wang, P., M. Tortorella, K. England, A. M. Malfait, G. Thomas, E. C. Arner and D. Pei (2004). "Proprotein convertase furin interacts with and cleaves pro-ADAMTS4 (Aggrecanase-1) in the trans-Golgi network." J Biol Chem 279(15): 15434-15440.

Wang, T. J., B. H. Nam, R. B. D'Agostino, P. A. Wolf, D. M. Lloyd-Jones, C. A. MacRae, P. W. Wilson, J. F. Polak and C. J. O'Donnell (2003). "Carotid intima-media thickness is associated with premature parental coronary heart disease: the Framingham Heart Study." Circulation 108(5): 572-576.

Whitman, S. C., P. Ravisankar and A. Daugherty (2002). "IFN-gamma deficiency exerts gender-specific effects on atherogenesis in apolipoprotein E-/- mice." J Interferon Cytokine Res 22(6): 661-670.

Wight, T. N. (2005). "The ADAMTS proteases, extracellular matrix, and vascular disease: waking the sleeping giant(s)!" Arterioscler Thromb Vasc Biol 25(1): 12-14.

Willeit J., Kiechl S., Oberhollenzer F., Rungger G., Egger G., Bonora E., Mitterer M., and Muggeo M. (2000) Distinct risk profiles of early and advanced atherosclerosis: prospective results from the Bruneck Study. Arterioscler Thromb Vasc Biol *20*, 529-537.

Williams, K. J. (2001). "Arterial wall chondroitin sulfate proteoglycans: diverse molecules with distinct roles in lipoprotein retention and atherogenesis." Curr Opin Lipidol 12(5): 477-487.

Williams, K. J. and I. Tabas (1995). "The response-to-retention hypothesis of early atherogenesis." Arterioscler Thromb Vasc Biol 15(5): 551-561.

Williams, R. R., S. C. Hunt, G. Heiss, M. A. Province, J. T. Bensen, M. Higgins, R. M. Chamberlain, J. Ware and P. N. Hopkins (2001). "Usefulness of cardiovascular family history data for population-based preventive medicine and medical research (the Health Family Tree Study and the NHLBI Family Heart Study)." Am J Cardiol 87(2): 129-135.

Williamson, M. P. (1994). "The structure and function of proline-rich regions in proteins." Biochem J 297 (Pt 2): 249-260.

Winkelmann, B. R., J. Hager, W. E. Kraus, P. Merlini, B. Keavney, P. J. Grant, J. B. Muhlestein and C. B. Granger (2000). "Genetics of coronary heart disease: current knowledge and research principles." Am Heart J 140(4): S11-26.

Xu, K., Y. Zhang, K. Ilalov, C. S. Carlson, J. Q. Feng, P. E. Di Cesare and C. j. Liu (2007). "Cartilage Oligomeric Matrix Protein Associates with Granulin-Epithelin Precursor (GEP) and Potentiates GEP-stimulated Chondrocyte Proliferation." Journal of Biological Chemistry 282(15): 11347-11355.

Yana, I. and S. J. Weiss (2000). "Regulation of membrane type-1 matrix metalloproteinase activation by proprotein convertases." Mol Biol Cell 11(7): 2387-2401.

Ye S, Dunleavey L, Bannister W, Day LB, Tapper W, Collins AR, Day IN, Simpson I (2003). "Independent effects of the -219 G>T and epsilon2/epsilon3/epsilon4 polymorphisms in the apolipoprotein E gene on coronary artery disease: The Southampton Atherosclerosis Study." Eur J Hum Genet. Jun;11(6):437-43..

Zeller, T., S. Blankenberg and P. Diemert (2012). "Genomewide association studies in cardiovascular disease--an update 2011." Clin Chem 58(1): 92-103.

Zha, Y., Y. Chen, F. Xu, T. Li, C. Zhao and L. Cui (2010). "ADAMTS4 level in patients with stable coronary artery disease and acute coronary syndromes." Biomed Pharmacother 64(3): 160-164.

Zheng, X., E. M. Majerus and J. E. Sadler (2002). "ADAMTS-13 and TTP." Curr Opin Hematol 9(5): 389-394.

Zhou, A., G. Webb, X. Zhu and D. F. Steiner (1999). "Proteolytic processing in the secretory pathway." J Biol Chem 274(30): 20745-20748.

Appendix I Reagents details

Table 2.1.1 Smooth Muscle Cell Growth Media 2 supplements

Supplements	Final concentration
Fetal Calf Serum	5%
Recombinant human Epidermal Growth Factor	0.5 ng/ml
Recombinant human Basic Fibroblast Growth Factor	2 ng/ml
Recombinant human Insulin	5 µg/ml

Table 2.1.2 Final growth factors supplements concentration for HUVEC

Supplements	Final concentration
Thymidine	2.5 µg/ml
Heparin	10 units/ml
Endothelial cell growth supplement	4.5 µg/ml
Beta-Endothelial Cell Growth Factor human	2.5 µg/ml

Table 2.2.1 List of antibodies used in ICC

Antibody	Catalog No.	Titration
Goat anti-human DDR2 polyclonal antibody	sc-7555	1:100
Mouse anti-human CD144 monoclonal antibody	sc-9989	1:100
Rabbit anti-goat IgG antibody	P0449	1:200
Mouse anti-human SMA monoclonal antibody	C6198	1:200
Rabbit anti-mouse IgG antibody	F0261	1:200
Rabbit anti-human ADAMTS-7 spacer domain polyclonal antibody	ab28557	1:100
Goat anti-rabbit IgG antibody	sc-2012	1:100

Table 2.3.1 List of antibodies used in IHC

Antibody	**Catalog No.**	**Titration**
Mouse anti-human SMA monoclonal antibody	C6198	1:200
Alkaline phosphatase conjugated mouse anti-human SMA antibody	C6198	1:100
Rabbit anti-human ADAMTS-7 spacer domain polyclonal antibody	ab28557	1:100
ADAMTS-7 spacer domain antibody blocking peptide	ab41240	1:100
Rat anti-human TSP-5 antibody	MABT36	1:20
Rabbit anti-human vWF antibody	ab9378	1:50
Biotinylated swine anti-rabbit IgG antibody	E-0431	1:200
Alkaline phosphatase conjugated anti-mouse IgG antibody	A-3562	1:200
Biotin-conjugated goat anti-rabbit IgG antibody	E-0432	1:200
Rabbit anti-rat HRP antibody	P0450	1:100
Goat anti-rabbit IgG antibody	sc-2012	1:100

Table 2.4.1 Primers used for KASPar genotyping

SNP	Primer	Sequence
rs3825807	Allele A-FAM	5'-GAAGGTGACCAAGTTCATGCTCCCAACGCTCCCGTCGAGA-3'
	Allele G-HEX	5'-GAAGGTCGGAGTCAACGGATTCCAACGCTCCCGTCGAGG-3'
	Common reverse	5'-CTCCAGTGTACCCAGAGCTGGA-3'
rs1994016	Allele T-FAM	5'-GAAGGTGACCAAGTTCATGCTGAAAGCTCTCCCGCTCCTTTACT-3'
	Allele C-HEX	5'-GAAGGTCGGAGTCAACGGATTAAAGCTCTCCCGCTCCTTTACC-3'
	Common reverse	5'-GTTCTTGGTAGAGGAAGCCTGAGAA-3'
rs4380028	Allele C-FAM	5'-GAAGGTGACCAAGTTCATGCTGGCATGGAAAGGTTAAGTAACTTGC-3'
	Allele T-HEX	5'-GAAGGTCGGAGTCAACGGATTGGGCATGGAAAGGTTAAGTAACTTGT-3'
	Common reverse	5'-ACACTTCCAAATGTGGGACGTTGG-3'

Table 2.4.2 Primers, PCR reagents and condition for restricted enzymes genotyping

Primer	Sequence
Forward Primer	5'-GGAAGTGACACGG GGAGATA-3'
Reverse Primer	5'-CCATGTTCATGATGGTCAGC-3'

PCR reaction system	
Reagent	Volume(µl)
ddH2O	14.86
10x PCR buffer	2.5
MgCl2 (50mM)	1
dNTP (2mM)	2.5
Primer F (10pM)	1
Primer R (10pM)	1
Taq Polymerase(5U/ul)	0.14
DNA (5ng/ul)	2

PCR reaction steps			
Step	Temperature	Time	Cycle
Pre-denature	95℃	5 min	1
Denature	95℃	30 s	
Annealing	55℃	30 s	35
Extension	72℃	30 s	
Final extension	72℃	10 min	1

Table 2.7.1 RT-PCR reaction reagents and conditions

RT-PCR reaction system	
Reagent	Volume(µl)
ddH2O	4.5
5x PCR buffer	5
MgCl2 (25mM)	3
dNTP (25mM)	1
Reverse Transcriptase	1
RNase inhibitor	0.5
RNA and random primers mixture	10

RT-PCR reaction steps		
Step	Temperature	Time
Annealing	25℃	5 minutes
Synthesis	42℃	90 minutes
Inactive Reverse Transcriptase	70℃	15 minutes

Table 2.7.2 Probes, reagents and conditions used in qRT-PCR

Probe	Manufactory	Catalog Number
ADAMTS7 probe	Applied Biosystems	Hs00276223_ml
β-actin probe	Applied Biosystems	Hs03023943_g1

qRT-PCR reaction system	
Reagent	Volume(μl)
ddH2O	2.5
2x Master mix	5
20x Primers and Probe mix	0.5
cDNA (5ng/ul)	2

qRT-PCR reaction steps			
Step	Temperature	Time	Cycle
Holding step	50℃	2 min	1
Activation of enzyme	95℃	10 min	1
Denature	95℃	15 sec	40
Annealing/extension	60℃	1 min	

Table 2.8.1 Primers sequence, PCR reagents and condition for Allelic Imbalance Assay

Primer	Sequence
gDNA Forward Primer	5'-GGAAGTGACACGG GGAGATA-3'
cDNA Forward Primer	5'- TACTTCATTGAGCCCCTGGA -3'
gDNA/cDNA Reverse Primer	5'- CCATGTTCATGATGGTCAGC -3'
Sequencing primer	5'- CCATGTTCATGATGGTCAGC -3'

PCR reaction system	
Reagent	Volume (μl)
ddH2O	14.86
10x PCR buffer	2.5
MgCl2 (50mM)	1
dNTP (2mM)	2.5
Primer F (10pM)	1
Primer R (10pM)	1
Taq Polymerase(5U/ul)	0.14
gDNA/cDNA (5ng/ul)	2

PCR reaction steps			
Step	Temperature	Time	Cycle
Pre-denature	95℃	5 min	1
Denature	95℃	30 s	35
Annealing	55℃	30 s	
Extension	72℃	30 s	
Final extension	72℃	10 min	1

Table 2.9.1 Primers, reagents and PCR for *ADAMTS7*$_{Pro\text{-}Cat}$ pCMV5 Plasmids cloning

Primer	Sequence	enzyme
Outside Forward Primer	5'-GGAAGTGACACGG GGAGATA-3'	
Outside Reverse Primer	5'- TACTTCATTGAGCCCCTGGA -3'	
Inside Forward Primer	5'-CAGGTCGGTACCATGCCCGGCGGCCCCAGTC-3'	KpnI
Inside Reverse primer	5'-TGGCACAAGCTTGAAGTCGATAATGTCCTTGGCAG-3'	Hind III

PCR reaction system	
Reagent	Volume(μl)
ddH2O	14.87
10x PCR buffer	2.5
MgSO4 (50mM)	1
dNTP (2mM)	2.5
Primer F (10pM)	1
Primer R (10pM)	1
pfu high fidelity Taq Polymerase(5U/ul)	0.13
cDNA (5ng/ul)	2

PCR reaction steps			
Step	Temperature	Time	Cycle
Pre-denature	95℃	5 min	1
Denature	95℃	30 s	
Annealing	55℃	30 s	40
Extension	68℃	30 s	
Final extension	68℃	10 min	1

Table 2.9.2 Primers sequence, PCR reagents and condition for Site-directed mutagenesis

Primer	Sequence
Forward Primer	5'-CAGAGCTGGAGCCTCGACGGGAG-3'
Reverse Primer	5'-CTCCCGTCGAGGCTCCAGCTCTG -3'

Site-direct mutagenesis PCR reaction system	
Reagent	Volume(μl)
ddH20	38.64
10x reaction buffer	5
Quick solution	1.5
dNTP mix(provided by kit)	1
Primer forward(125ng,100ng/ul)	1.25
Primer reverse(125ng,100ng/ul)	1.25
Quickchange lighting enzyme	1
Plasmid(100ng,280.3ng/ul)	0.36

PCR reaction steps			
Step	Temperature	Time	Cycle
Pre-denature	95℃	2 min	1
Denature	95℃	20 sec	35
Annealing	55℃	30 sec	
Extension	65℃	4 min	
Final extension	65℃	10 min	1

Table 2.9.3 Primers, reagents and condition for PCR identification of *ADAMTS7* plasmid

ADAMTS7 cDNA Forward Primer	5'- TACTTCATTGAGCCCCTGGA -3'
ADAMTS7 cDNA Reverse Primer	5'- CCATGTTCATGATGGTCAGC -3'

PCR reaction system	
Reagent	Volume(μl)
ddH2O	11.86
10x PCR buffer	2.5
MgCl2 (50mM)	1
dNTP (2mM)	2.5
Primer F (10pM)	1
Primer R (10pM)	1
Taq Polymerase(5U/ul)	0.14
Template DNA	5

PCR reaction steps			
Step	Temperature	Time	Cycle
Pre-denature	95℃	5 min	1
Denature	95℃	30 s	
Annealing	55℃	30 s	35
Extension	72℃	30 s	
Final extension	72℃	10 min	1

Table 2.9.4 Primers sequence for *ADAMTS7*$_{Pro\text{-}Cat}$ plasmid sequencing

ADAMTS7$_{Pro\text{-}Cat}$ primer F1	CCACAGCTCCTGTACGACGCC
ADAMTS7$_{Pro\text{-}Cat}$ primer R1	GTTGCACGTCCTGGTGCGGG
ADAMTS7$_{Pro\text{-}Cat}$ primer R2	CCCGCACCAGGACGTGCAAC

Table 2.9.5 Primers for *ADAMTS7* full length plasmid sequencing

ADAMTS7 primer F1	ATGCAAAGCTTGGTTCCTGCCATGCCCGGCGGCCCCAGTCCCCG
ADAMTS7 primer R1	ATGCAGAATTCGCGGCGGGCAACCCGCTGAT
ADAMTS7 primer F2	GATCACGCACCATGCAGAC
ADAMTS7 primer R2	CTAGAGCTCAGGGGCAGGTC
ADAMTS7 primer F3	GCTGTGACTTCGAGATTGAC
ADAMTS7 primer R3	CATGGTGCCTGGCTTGGGTGATG
ADAMTS7 primer F4	CAACGAGGCTGACTTCATC
ADAMTS7 primer R4	CACCACAGCGGTCCTCCATAG
ADAMTS7 primer F5	GAACCCAGGACCCAAGGGTC
ADAMTS7 primer R5	CACTTGCAGAAGCTCTTCAG

Table 2.11.1 TSP-5 cleavage assay digestion buffer recipe, pH7.5

Tris-HCl	50 mM
NaCl	100 mM
$CaCl_2$	5 mM
$ZnCl_2$	2 mM
Brij-35	0.05%,

Table 2.14.1 Protease inhibitor cocktail recipe

PMSF (phenylmethylsulfonyl fluoride)	1 mM
Leupeptin	2 µM
Pepstatin	1.5 µM
Aprotinin	0.15 µM

Table 2.14.2 Protein lysis buffer recipe

Tris-HCl pH 7.5	50 mM
NaCl	150 mM
EDTA pH 8.0	1 mM
Triton X-100	0.5 %
Protease inhibitor cocktail	1 x

Table 2.14.3 5x protein loading buffer recipe

Tris pH 6.8	312.5 mM
Glycerol	50 %
SDS	10 %
2-ME	5%
Bromophenol blue	0.5%

Table 2.14.4 SDS-PAGE stacking gel recipe

6% stacking gel, final volume 5ml	
ddH_2O	2.6 ml
30% acrylamide	1 ml
Tris 0.5 M pH6.8	1.25 ml
10% SDS	50 µl
10% Ammonium persulphate (APS)	50 µl
TEMED	5 µl

Table 2.14.5 SDS-PAGE separating gel recipe

10% separating gel, final volume 8ml	
ddH_2O	3.2 ml
30% acrylamide	2.67 ml
Tris 1.5 M pH8.8	2 ml
10% SDS	80 µl
10% Ammonium persulphate (APS)	80 µl
TEMED	8 µl

Table 2.14.6 Running buffer recipe

Tris	25mM
Glycine	0.192M
SDS	0.1%

Table 2.14.7 Transfer buffer recipe

Tris	25mM
Glycine	0.192M
Methanol	20%

Table 2.14.8 1x TBST recipe, pH7.6

Tris	50 mM
NaCl	150 mM
Tween 20	0.5 %

Table 2.14.9 List of antibodies used in WB

Antibody	**Catalog No.**	**Titration**
Rabbit anti-human ADAMTS-7 pro-domain antibody	Ab45044	1:1000
Rabbit anti-human ADAMTS-7 spacer domain antibody	ab28557	1:1000
Rat anti-human TSP-5 antibody	MABT36	1:500
Mouse anti-cMyc antibody	M4439	1:3000
Mouse anti-human TSP-1 monoclonal antibody	MAB3074	1:200
Goat anti-rabbit IgG conjugated with HRP antibody	7074	1:2000
Rabbit anti-rat HRP antibody	P0450	1:1000
Anti-mouse IgG conjugated with HRP antibody	7076	1:3000

Table 3.1.1 Detailed information of VSMC genotype for *ADAMTS7* variants

Sample ID	rs 3825807 Genotype	rs 1994016 Genotype	rs4380028 Genotype
HuSMC003		CC	CC
HuSMC004	AG	TC	TT
HuSMC009	AA	CC	CC
HuSMC010	AG	TC	TC
HuSMC011	AA	CC	CC
HuSMC012	AA	CC	TC
HuSMC015	AA	CC	TC
HuSMC016	AG	CC	TC
HuSMC017	AG	TC	TT
HuSMC023	AG	TC	CC
HuSMC026	GG	TC	TT
HuSMC028	AA	CC	CC
HuSMC030	AA	CC	CC
HuSMC031	AG	TC	TC
HuSMC033	AA	CC	CC
HuSMC034	AA	CC	TC
HuSMC035	AG	TC	
HuSMC036	GG	TT	TT
HuSMC040	AA	CC	CC
HuSMC044	AA	CC	CC
HuSMC045		CC	CC
HuSMC046	AG	TC	
HuSMC048	AA	CC	CC
HuSMC049	AG	CC	CC
HuSMC051	AA	TC	CC
HuSMC052	AG	CC	CC
HuSMC054	AA	CC	TC
HuSMC055	AA	CC	CC
HuSMC058	AA	CC	CC
HuSMC059	AA	CC	CC
HuSMC060	AA	CC	CC
HuSMC065	AA	CC	TC
HuSMC066	AA	CC	
HuSMC067	AA	CC	CC
HuSMC069	AA	CC	CC
HuSMC070	AA	CC	CC
HuSMC072	AG	TC	TC
HuSMC074	AA	CC	
HuSMC075	GG	TT	
HuSMC077	GG	TC	TT
HuSMC078	AA		CC
HuSMC079	AA	CC	CC
HuSMC080	AG	TC	TC
HuSMC081	AG	CC	CC
HuSMC083	GG	CC	CC

HuSMC085		CC	TC
HuSMC087	AA	CC	CC
HuSMC088	AA	CC	CC
HuSMC089	AA	CC	CC
HuSMC090		CC	CC
HuSMC091	GG	TC	TC
HuSMC092	AA	CC	CC
HuSMC093	AA	CC	CC
HuSMC094		CC	CC
HuSMC095	AA	CC	CC
HuSMC096	AA	TC	CC
HuSMC097	AA	TC	TC
HuSMC098	AA		TC
HuSMC099	GG	TC	CC
HuSMC100		CC	TT
HuSMC102		CC	TT
HuSMC103		TC	TT
HuSMC104	AA	CC	CC
HuSMC106	AG		CC
HuSMC109	AG		TC
HuSMC110	AG	TC	TC
HuSMC112	AA	CC	CC
HuSMC113	AA	TC	TT
HuSMC114	AA	TC	TC
HuSMC116		CC	TT
HuSMC118		CC	CC
HuSMC119		CC	CC
HuSMC121		TC	CC
HuSMC122		TC	TC
HuSMC124	AA	TC	CC
HuSMC125		CC	
HuSMC129	GG	TC	TT
HuSMC134			TC
HuSMC135	AA	TC	CC
HuSMC138	AG	TC	TT
HuSMC139	AA	CC	CC
HuSMC140		CC	CC
HuSMC144	AA	CC	CC
HuSMC145		TC	TC
HuSMC147	AG	TC	TC
HuSMC149	AG	CC	TC
HuSMC151	AA	TC	CC
HuSMC153	AA	CC	CC
HuSMC154	AG	CC	CC
HuSMC156		TC	CC
HuSMC159	AA	CC	
HuSMC161		CC	CC
HuSMC162	AA		CC

HuSMC163		TT	TC
HuSMC164		TC	CC
HuSMC167	AG	TC	TC
HuSMC168	AA	TC	TC
HuSMC176	AG	TC	CC
HuSMC177	AG	TC	TC
HuSMC178	AA	CC	CC
HuSMC179	AA	CC	CC
HuSMC180	AG	TC	TT
HuSMC181	AA	CC	TC
HuSMC182	GG	TC	TC
HuSMC183	GG	TC	TT
HuSMC184	AA	CC	CC
HuSMC185	AG	TC	TC
HuSMC188	AA	TC	CC
HuSMC189	GG	TC	TT
HuSMC190	AG	TC	TC
HuSMC191	AG	TC	TC
HuSMC193	AG	TC	TC
HuSMC194	AG	TC	TC
HuSMC195	AA	CC	CC
HuSMC196	AA	CC	
HuSMC197	GG	TC	CC
HuSMC198	AA	CC	TC
HuSMC199	AA	CC	TC
HuSMC200	AG	TC	TC
HuSMC201	AA	CC	
HuSMC203	AA	CC	CC
HuSMC204	AG	TC	TC
HuSMC205	AA	CC	TC
HuSMC206	AA	CC	TC
HuSMC207	AA	CC	TT
HuSMC209	AG	TC	TC
HuSMC210	AA	CC	CC
HuSMC211	AG	TC	CC
HuSMC212	AG	TC	TC
HuSMC213	AA	CC	CC
HuSMC214	AG	TC	TT
HuSMC216	AA	CC	CC
HuSMC217	AA	CC	CC

Appendix II: Publications

Full papers

1. **Xiangyuan Pu**, Qingzhong Xiao, Stefan Kiechl, Kenneth Chan, Fu Liang Ng, Shivani Gor, Robin N. Poston, Changcun Fang, Ashish Patel, Ece C. Senver, Sue Shaw-Hawkins, Johann Willeit, Chuanju Liu, Jianhua Zhu, Arthur T. Tucker, Qingbo Xu, Mark J. Caulfield, Shu Ye. ADAMTS7 cleavage and vascular smooth muscle cell migration is affected by a coronary artery disease associated variant. Am J Hum Genet 7; 92(3):366-74; 2013.

   Full paper is attached at the end.

2. Anna Motterle*, **Xiangyuan Pu***, Harriet Wood, Qingzhong Xiao, Shivani Gor, Fu Liang Ng, Kenneth Chan, Frank Cross, Beski Shohreh, Robin N. Poston, Arthur T. Tucker, Mark J. Caulfield, Shu Ye. Functional analyses of coronary artery disease associated variation on chromosome 9p21 in vascular smooth muscle cells. Hum Mol Genet 21(18): 4021-4029; 2012. *** Equal contributors**

   Full paper is attached at the end.

3. Qingzhong Xiao, Feng Zhang, Luyang Lin, Changcun Fang, Guanmei Wen, Tsung-Neng Tsai, **Xiangyuan Pu**, David Sims, Zhongyi Zhang, Xiaoke Yin, Binia Thomaszewski, Boris Schmidt, Manuel Mayr, Ken Suzuki, Qingbo Xu, Shu Ye. A Functional Role of Matrix Metalloproteinase-8 in Stem/Progenitor Cell Migration and Their Recruitment into Atherosclerotic Lesions. Circ Res 112(1):35-47; 2013.

4. Yuan Huang, Luyang Lin, Xiaotian Yu, Guanmei Wen, **Xiangyuan Pu**, Hanqing Zhao, Changcun Fang, Jianhua Zhu, Qingbo Xu, Shu Ye, Li Zhang and Qingzhong Xiao. Functional Involvements of Heterogeneous Nuclear Ribonucleoprotein A1 in Smooth Muscle Differentiation from Stem Cells *in vitro* and *in vivo*. Stem Cells 31(5):906-17; 2013.

5. Zhenling Luo, Guanmei Wen, Gang Wang, **Xiangyuan Pu**, Shu Ye, Qingbo Xu, Wen Wang, Qingzhong Xiao. MicroRNA-200C and -150 play an important role in endothelial cell differentiation and vasculogenesis by targeting transcription repressor ZEB1. Stem Cells 31(9):1749-62; 2013.

Conference oral presentation and posters

1. British Cardiology Society annual meeting (2013) young investigation session oral presentation. Xiangyuan Pu, Qingzhong Xiao, Stefan Kiechl, Kenneth Chan, Fu Liang Ng, Shivani Gor, Robin N. Poston, Changcun Fang, Ashish Patel, Ece C. Senver, Sue Shaw-Hawkins, Johann Willeit, Chuanju Liu, Jianhua Zhu, Arthur T. Tucker, Qingbo Xu, Mark J. Caulfield, Shu Ye. ADAMTS7 cleavage and vascular smooth muscle cell migration is affected by a coronary artery disease associated variant. Heart 2013; 99:A5-A6 doi:10.1136/heartjnl-2013-304019.270

2. William Harvey Day 2013 poster.

Please cite this article in press as: Pu et al., ADAMTS7 Cleavage and Vascular Smooth Muscle Cell Migration Is Affected by a Coronary-Artery-Disease-Associated Variant, The American Journal of Human Genetics (2013), http://dx.doi.org/10.1016/j.ajhg.2013.01.012

ARTICLE

ADAMTS7 Cleavage and Vascular Smooth Muscle Cell Migration Is Affected by a Coronary-Artery-Disease-Associated Variant

Xiangyuan Pu,[1,2,6] Qingzhong Xiao,[1,6] Stefan Kiechl,[3] Kenneth Chan,[1] Fu Liang Ng,[1] Shivani Gor,[1] Robin N. Poston,[1] Changcun Fang,[1] Ashish Patel,[1] Ece C. Senver,[1] Sue Shaw-Hawkins,[1] Johann Willeit,[3] Chuanju Liu,[4] Jianhua Zhu,[2] Arthur T. Tucker,[1] Qingbo Xu,[5] Mark J. Caulfield,[1] and Shu Ye[1,*]

Recent genome-wide association studies have revealed an association between variation at the *ADAMTS7* locus and susceptibility to coronary artery disease (CAD). Furthermore, in a population-based study cohort, we observed an inverse association between atherosclerosis prevalence and rs3825807, a nonsynonymous SNP (A to G) leading to a Ser-to-Pro substitution in the prodomain of the protease ADAMTS7. In light of these data, we sought a mechanistic explanation for this association. We found that ADAMTS7 accumulated in smooth muscle cells in coronary and carotid atherosclerotic plaques. Vascular smooth muscle cells (VSMCs) of the G/G genotype for rs3825807 had reduced migratory ability, and conditioned media of VSMCs of the G/G genotype contained less of the cleaved form of thrombospondin-5, an ADAMTS7 substrate that had been shown to be produced by VSMCs and inhibit VSMC migration. Furthermore, we found that there was a reduction in the amount of cleaved ADAMTS7 prodomain in media conditioned by VSMCs of the G/G genotype and that the Ser-to-Pro substitution affected ADAMTS7 prodomain cleavage. The results of our study indicate that rs3825807 has an effect on ADAMTS7 maturation, thrombospondin-5 cleavage, and VSMC migration, with the variant associated with protection from atherosclerosis and CAD rendering a reduction in ADAMTS7 function.

Introduction

Recently three genome-wide association studies (GWASs) have revealed that coronary artery disease (CAD) is associated with single nucleotide polymorphisms (SNPs) at the *ADAMTS7* (a disintegrin and metalloprotease with thrombospondin motif, 7 [MIM 605009]) locus on chromosome 15q25.[1–3] The lead CAD-associated SNP in one of these studies was rs3825807,[1] an adenine (A) to guanine (G) polymorphism, resulting in a serine (Ser)-to-proline (Pro) substitution in the prodomain of ADAMTS7. The lead SNPs in the other two studies were rs1994016[2] and rs4380028[3] respectively, the former residing in intron 8 of *ADAMTS7* and the latter at 7.6 kb upstream of the gene. It has remained unclear as to whether any of these SNPs, or other SNPs in linkage disequilibrium (LD) with them, has a functional effect on ADAMTS7 expression and/or activity and has any effect on the biological processes related to CAD.

ADAMTS7 belongs to the metalloproteinase family. Newly synthesized ADAMTS7 contains a signal peptide, a prodomain, a metalloproteinase domain, a disintegrin-like domain, and a thrombospondin type-1 motif.[4] The prodomain is cleaved off during ADAMTS7 maturation and activation.[4] Activated ADAMTS7 has proteolytic activity, and its best characterized substrate is thrombospondin-5 (TSP5, also known as cartilage oligomeric matrix protein, COMP),[5] an extracellular protein present in such tissues as vascular walls and cartilages.[5,6]

A recent study in rats demonstrated that ADAMTS7 facilitated vascular smooth muscle cell (VSMC) migration by degrading the extracellular matrix protein TSP5 and thereby promoted neointima formation following vascular mechanical injury.[6] Furthermore, in vitro studies have shown that VSMCs produce TSP5[7] and that TSP5 inhibits VSMC migration.[6] Because VSMC migration is an important process in atherogenesis, it is likely that ADAMTS7 can also play a role in the development of atherosclerosis, the pathology underlying the vast majority of CAD.

In this study, we found that ADAMTS7 was present in human atherosclerotic plaques and that variation at the *ADAMTS7* locus was associated with atherosclerosis in a population-based, longitudinal study. To seek a mechanistic explanation for this association, we further undertook a series of in vitro experiments. Results of these experiments indicate that the CAD-associated *ADAMTS7* genotype has an effect on ADAMTS7 maturation, TSP5 cleavage, and VSMC migration.

Subjects and Methods

The procedures followed were in accordance with the ethical standards of the responsible committees on human experimentation, and appropriate informed consent was obtained.

[1]William Harvey Research Institute, Queen Mary University of London, London EC1M 6BQ, UK; [2]First Affiliated Hospital, School of Medicine, Zhejiang University, Hangzhou 310003, China; [3]Department of Neurology, Innsbruck Medical University, 6020 Innsbruck, Austria; [4]Musculoskeletal Research Center, New York University School of Medicine, New York, NY 10003, USA; [5]Department of Cardiology, King's College London, London SE5 9NU, UK
[6]These authors contributed equally to this work
*Correspondence: s.ye@qmul.ac.uk
http://dx.doi.org/10.1016/j.ajhg.2013.01.012.

Please cite this article in press as: Pu et al., ADAMTS7 Cleavage and Vascular Smooth Muscle Cell Migration Is Affected by a Coronary-Artery-Disease-Associated Variant, The American Journal of Human Genetics (2013), http://dx.doi.org/10.1016/j.ajhg.2013.01.012

Bruneck Study Cohort

Subjects of this study were residents of the Bruneck area in Italy, who participated in the Bruneck Study, details of which have been described previously.[8–10] DNA samples for genotyping were available for 787 subjects. Ultrasound scanning of the right and left internal carotid and common carotid arteries was performed in 1990 and 1995 by the same experienced sonographer.[8–10] Atherosclerotic lesions were defined according to two ultrasound criteria: (1) wall surface (protrusion or roughness of the arterial boundary) and (2) wall texture (echogenicity). The atherosclerosis score, indicative of atherosclerosis severity, was calculated by summing all diameters at 8 well-defined segments of the common and internal carotid arteries. Incident atherosclerosis was defined by the occurrence of atherosclerotic lesions in segments previously free of atherosclerosis or enlargement of nonstenotic lesions by a relative increase in the plaque diameter exceeding twice the measurement error of the method. Intima-media thickness was assessed in plaque-free sections of the common carotid arteries.

Immunohistochemical Analysis

Formaldehyde-fixed paraffin-embedded sections of atherosclerotic coronary arteries or atherosclerotic carotid arteries were deparaffinized, rehydrated, and incubated with sodium citrate for antigen retrieval. The sections were subjected to color or fluorescence immunostaining with an anti-human smooth muscle α-actin (SMA) antibody (Dako, M-0635, or Sigma, A5691 or C6198) and an anti-human ADAMTS7 antibody (Abcam, ab28557). Immunostaining for TSP5 and CD68 respectively in atherosclerotic coronary artery sections was also performed.

Isolation, Culture, and Immunocytochemical Analyses of Primary VSMCs

VSMCs were isolated from umbilical cord arteries. Cultured VSMCs were subjected to immunocytochemical examinations of the VSMC marker SMA, the endothelial cell marker von Willebrand factor (vWF), and the fibroblast marker discoidin domain receptor-2 (DDR2), and verified to be SMA-positive but vWF- and DDR2-negative (data not shown). Cells were also verified for the presence of ADAMTS7 by immunocytochemistry.

Determination of Genotype

Genomic DNA extracted from blood samples of the Bruneck Study subjects, atherosclerotic coronary arteries, and VSMCs was genotyped for rs3825807 with the use of the KASPar (KBiosciences Competitive Allele-Specific PCR SNP genotyping system) method. Accuracy of the genotyping results was verified by sequencing of a random selection of the samples.

Scratch Assay and Cell Migration Assay

Scratch assays were carried out using a previously described method.[11] Migration assays were performed with the use of transwells (8 μm pore size; Greiner Bio-One Inc.), following a standard protocol.

Plasmid and Transfection

We utilized a previously constructed plasmid to generate a protein consisting of the ADAMTS7 signal peptide, prodomain (with ADAMTS7-214Ser) and metalloproteinase domain followed by a c-Myc epitope,[12] and carried out site-directed mutagenesis (PCR forward and reverse primers: 5′-CAGAGCTGGAGCCTCG ACGGGAG-3′ and 5′-CTCCCGTCGAGGCTCCAGCTCTG −3′) to generate a new plasmid for ADAMTS7-214Pro. Cultured HEK293 cells were transfected with the ADAMTS7-214Ser or ADAMTS7-214Pro plasmid.

Immunoblot Analyses

Cell lysates, conditioned media, and cell surface washes (with 0.5 M $NaCl^4$) from VSMCs or transfected HEK293 cells were obtained and subjected to standard immunoblot analysis with an anti-TSP5 antibody (Millipore, MABT36), or an anti-ADAMTS7 prodomain antibody (Abcam, ab45044), or an anti-cMyc antibody (Sigma-Aldrich, M4439).

In Vitro TSP5 Cleavage Assay

Recombinant TSP5 (Abcam, ab104358) was incubated with concentrated media conditioned by VSMCs of the A/A or G/G genotype, or by HEK293 cells transfected with either of the ADAMTS7 plasmids described above, in a digestion buffer[5] at 37°C for 8 hr. The digests, along with undigested TSP5 and concentrated conditioned media were subjected to immunoblot analysis with an anti-TSP5 antibody (Millipore, MABT36).

Real-Time RT-PCR

Quantitative RT-PCR analysis of *ADAMTS7* was carried out in primary VSMCs from different individuals, as described in the legend of Figure S5 available online.

Allelic Expression Imbalance Analysis

Allelic expression imbalance analysis was performed on VSMCs that were heterozygous for rs3825807, as described in the legend of Figure S6.

Statistical Analysis

In the Bruneck Study, associations of rs3825807 with carotid atherosclerosis were tested by logistic and linear regression analyses. Base models were adjusted for age and sex. Multivariable models were adjusted for variables correlated with atherosclerosis parameters in the Bruneck cohort, including presence or absence of hypertension, smoking status, diabetes mellitus, level of alcohol consumption, levels of high density lipoprotein and low density lipoprotein, ferritin, fibrinogen, anithrombin III, the factor V Leiden mutation, body mass index, waist-to-hip ratio, and loge-transformed concentrations of urinary albumin, high-sensitivity C-reactive protein and lipoprotein(a). Variables with a skewed distribution were normalized by logarithmic transformation. Differences between genotypes in the percentage of ADAMTS7 stain area in atherosclerotic plaque area, the percentage of SMA stain area in plaque area, VSMC migration distance in the migration assays, and band intensity in immunoblot analyses were tested by t tests. ANOVA tests were performed to ascertain differences between genotypes in cell proliferation, senescence, and apoptosis. Real-time RT-PCR results were analyzed by the ΔΔCT method. Allelic expression imbalance analysis results were analyzed by Mann-Whitney test. All p values were two-sided.

Results

Association of Variation in ADAMTS7 with Atherosclerosis

In the Bruneck Study, we observed an inverse association between the *ADAMTS7* rs3825807 G/G genotype

Please cite this article in press as: Pu et al., ADAMTS7 Cleavage and Vascular Smooth Muscle Cell Migration Is Affected by a Coronary-Artery-Disease-Associated Variant, The American Journal of Human Genetics (2013), http://dx.doi.org/10.1016/j.ajhg.2013.01.012

Table 1. Association between *ADAMTS7* rs3825807 and Carotid Atherosclerosis in the Bruneck Study

	Age/Sex-Adjusted Model		Multivariable Model[b]	
	OR (95% CI)[a]	p value	OR (95% CI)[a]	p value
Presence of atherosclerosis in 1990	0.58 (0.35–0.96)	0.035	0.51 (0.31–0.84)	0.008
Presence of atherosclerosis in 1995	0.51 (0.32–0.82)	0.005	0.53 (0.31–0.90)	0.019
Incident atherosclerosis in 1990–1995	0.69 (0.43–1.10)	0.121	0.67 (0.40–1.09)	0.108
	β (95% CI)[a]	p value	β (95% CI)[a]	p value
Atherosclerosis score in 1990	−0.43 (−0.77, −0.09)	0.013	−0.45 (−0.78, −0.11)	0.010
Atherosclerosis score in 1995	−0.53 (−0.89, −0.16)	0.005	−0.50 (−0.86, −0.14)	0.006
Carotid intima-media thickness in 1995	−0.02 (−0.06–0.02)	0.427	−0.02 (−0.06–0.02)	0.401

[a]Odds ratios (OR) and regression coefficients (β) were derived from logistic and linear regression analyses respectively, comparing the G/G genotype versus the A/A and A/G genotypes.
[b]Multivariable analyses were performed with adjustment for variables correlated with atherosclerosis parameters in the Bruneck cohort, as described in Subjects and Methods.

and atherosclerosis. This genotype was associated with lower prevalence of carotid atherosclerosis (odds ratio [95% CI] = 0.51 [0.31–0.84] and 0.53 [0.31–0.90] in the data from 1990 and 1995 respectively, after adjustment for covariates, Table 1) and similarly lower atherosclerosis scores (β [95% CI] = −0.45 [−0.78, −0.11] and −0.50 [−0.86, −0.14] in the same data, after adjustment for covariates, Table 1). No association was detected for incident atherosclerosis or carotid intima-media thickness (Table 1).

ADAMTS7 in Human Atherosclerotic Plaques

A recent study in rats demonstrated that ADAMTS7 facilitated VSMC migration and thereby promoted neointima formation following vascular mechanical injury.[6] In this study, we investigated whether ADAMTS7 is present in and around VSMCs in human atherosclerotic plaques. Double immunostaining for ADAMTS7 and the VSMC marker SMA showed that ADAMTS7 colocalized with a proportion of VSMCs in atherosclerotic plaques of coronary and carotid arteries (Figures 1A–1C). We observed that in the atherosclerotic plaque, VSMCs that accumulated ADAMTS7 were mostly located near the intima-media border and the fibrous cap (Figures 1A and 1B). ADAMTS7 stains were detected both within cells (highlighted by black arrowheads) and in the extracellular spaces (highlighted by green arrowheads) (Figures 1A). In an analysis of coronary atherosclerotic plaques from 44 individuals, no significant association was detected between ADAMTS7 abundance and rs3825807 genotype (Figure S2). There was a trend toward a lower percentage of SMA stain area in atherosclerotic plaque area, in individuals of the G/G genotype (Figure S2). Immunostaining

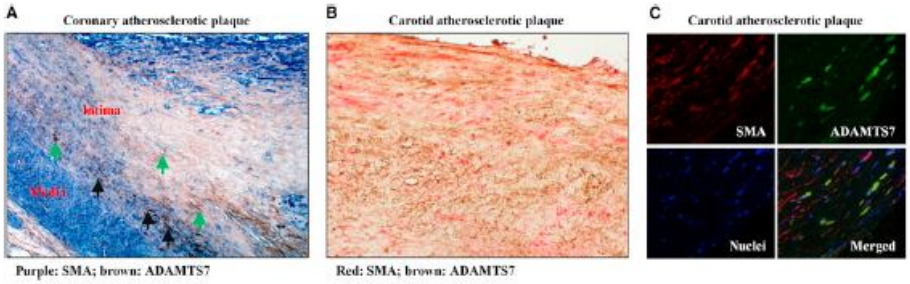

Figure 1. ADAMTS7 Colocalizes with Smooth Muscle Cells in Human Atherosclerotic Plaques
(A) Atherosclerotic coronary artery sections were subjected to double immunostaining of smooth muscle α-actin (SMA) and ADAMTS7. Purple color (NBT/BCIP) indicates SMA staining, and dark brown color with DAB indicates ADAMTS7 staining. Black arrow indicates cell positive for both SMA and ADAMTS7. Green arrow indicates extracellular ADAMTS7 staining. Negative controls are shown in Figure S1.
(B) Atherosclerotic carotid artery sections were subjected to double immunostaining of SMA with Fast red and ADAMTS7 with DAB (brown color). Negative controls are shown in Figure S1.
(C) Atherosclerotic carotid artery sections were subjected to double fluorescent immunostaining for SMA (red) and ADAMTS7 (green) and DAPI fluorescent staining for nuclei (blue), followed by confocal microscopy examination. Upper left panel shows SMA staining; upper right panel shows ADAMTS7 staining; lower left panel shows nuclear staining; lower right panel shows merged image from SMA, ADAMTS7, and nuclear staining.

Please cite this article in press as: Pu et al., ADAMTS7 Cleavage and Vascular Smooth Muscle Cell Migration Is Affected by a Coronary-Artery-Disease-Associated Variant, The American Journal of Human Genetics (2013), http://dx.doi.org/10.1016/j.ajhg.2013.01.012

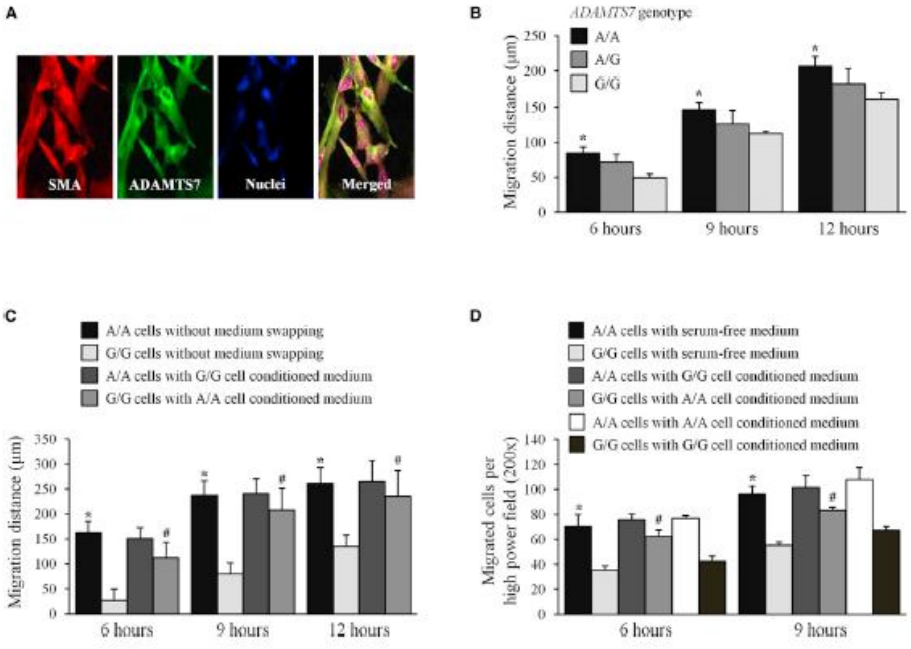

Figure 2. Effect of *ADAMTS7* Genotype on VSMC Migration

(A) Primary cultures of VSMCs were subjected to double fluorescent immunostaining for the smooth muscle α-actin (SMA, red) and ADAMTS7 (green) and nucleus staining with propidium iodide (blue). Representative images are shown.

(B) Primary cultures of VSMCs of the A/A, A/G, or G/G genotype for rs3825807 were subjected to scratch assay by a commonly used method.[33] Column chart shows migration distances (mean ± SEM) of VSMCs of the A/A, A/G, or G/G genotype for rs3825807 (n = 5 different donor cell preparations for each genotype). *$p < 0.05$ comparing A/A and G/G genotype group.

(C and D) Primary cultures of VSMCs of the A/A or G/G genotype were subjected to scratch (C) and migration (D) assays, without or with medium swapping at the outset of the assay (i.e., at hour 0 of the assay, the culture medium of G/G genotype cells was replaced by A/A genotype cell conditioned medium, and vice versa). Column chart shows migration distances or migrated cell numbers (mean ± SEM) (n = 3 different donor cell preparations for each genotype). *$p < 0.05$ comparing A/A genotype cells without medium swapping and G/G genotype cells without medium swapping; #$p < 0.05$ comparing G/G genotype cells with A/A genotype cell conditioned medium versus G/G genotype cells without medium swapping.

showed that TSP5 was also present in human atherosclerotic coronary arteries (Figure S3).

Influence of ADAMTS7 Genotype on VSMC Migration

To investigate whether the atherosclerosis-associated *ADAMTS7* genotype had an influence on VSMC migration, we verified that ADAMTS7 is present in cultured primary VSMCs (Figure 2A) and performed migration assays on primary VSMCs from individuals of different genotypes for rs3825807. The assays showed that VSMCs of the G/G genotype had reduced migratory ability, compared with VSMCs of the A/A genotype (Figures 2B–2D). Replacing the culture media of G/G genotype VSMCs with A/A genotype VSMC conditioned media at the beginning of the migration assay increased the migratory ability of G/G genotype VSMCs (Figures 2C and 2D, the fourth column compared with the second column at 6 hr and at 9 hr respectively), suggesting a migration enhancing effect from A/A genotype VSMC conditioned media, presumably due to a higher concentration of active ADAMTS7.

To ascertain whether *ADAMTS7* genotype had an effect on VSMC proliferation and/or apoptosis, we performed proliferation, senescence, and apoptosis assays on primary VSMCs. We detected no difference between the genotypes in proliferation, senescence, or apoptosis (Figure S4).

Influence of ADAMTS7 Genotype on TSP5 Cleavage

It has been shown that VSMCs produce the extracellular matrix protein TSP5, which VSMCs adhere to[7] and that ADAMTS7 promotes VSMC migration via degrading TSP5.[6] Following the finding that *ADAMTS7* genotype influenced VSMC migration, we investigated whether there

Please cite this article in press as: Pu et al., ADAMTS7 Cleavage and Vascular Smooth Muscle Cell Migration Is Affected by a Coronary-Artery-Disease-Associated Variant, The American Journal of Human Genetics (2013), http://dx.doi.org/10.1016/j.ajhg.2013.01.012

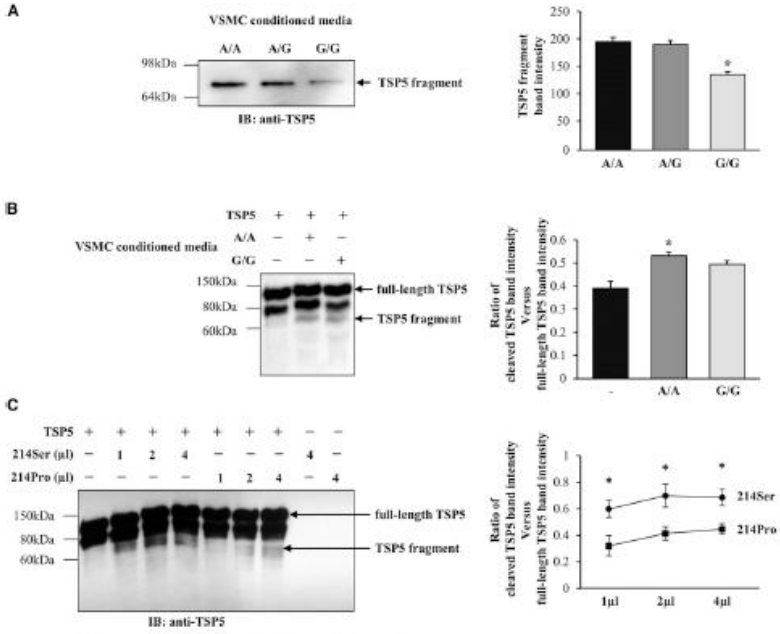

Figure 3. Effect of *ADAMTS7* Genotype on Thrombospondin-5 Cleavage

(A) A representative image of immunoblot (IB) analysis of cleaved TSP5 in media conditioned by VSMCs of the A/A, A/G, or G/G genotype for rs3825807. The same amount (20 μg) of proteins for each genotype was loaded. Data shown in column chart are mean (±SEM) values of cleaved TSP5 band intensity in immunoblots (n = 5 different donor cell preparations for each genotype). *$p < 0.05$ comparing A/A and G/G genotypes.

(B) A representative image and quantifications of immunoblot analysis of products from in vitro TSP5 cleavage assays. Recombinant TSP5 (2 μg) was incubated with or without 5 μl concentrated media conditioned by VSMCs of the A/A or G/G genotype, in a digestion buffer at 37°C for 8 hr. The digests, along with undigested TSP5, were subjected to immunoblot analysis with an anti-TSP5 antibody. Data shown in graph are mean (±SEM) values (n = 4 for each genotype). *$p < 0.05$ comparing A/A (second column) and – (first column) or comparing A/A with G/G (third column).

(C) A representative image and quantifications of immunoblot analysis of products from in vitro TSP5 cleavage assays. Recombinant TSP5 (2 μg) was incubated with 1, 2, or 4 μl concentrated media (1 μg total proteins/μl) conditioned by HEK293 cells transfected with a plasmid to produce the ADAMTS7 prodomain-metalloproteinase-domain of either ADAMTS7-214Ser or ADAMTS7-214Pro, in a digestion buffer at 37°C for 8 hr. The digests, along with undigested TSP5 and concentrated conditioned media, were subjected to immunoblot analysis with an anti-TSP5 antibody. Data shown in graph are mean (±SEM) values (n = 3 for each genotype). *$p < 0.05$ comparing ADAMTS7-214Ser and ADAMTS7-214Pro.

was a difference in the concentration of cleaved TSP5 in VSMC conditioned media between *ADAMTS7* genotypes. We found that media conditioned by VSMCs of the G/G genotype for rs3825807 contained approximately ~30% less cleaved TSP5, compared with the A/A genotype (Figure 3A).

Additionally, we carried out in vitro assays of TSP5 cleavage with media conditioned by VSMCs of the A/A or G/G genotype (Figure 3B) or media conditioned by HEK293 cells transfected with a plasmid to produce either ADAMTS7-214Ser or ADAMTS7-214Pro (Figure 3B). The assays showed that the conditioned media were able to cleave TSP5 and that media conditioned by VSMCs of the G/G genotype had lower TSP5 cleavage activity than media conditioned by VSMCs of the G/G genotype (Figure 3B). Similarly, media conditioned by HEK293 cells transfected with the ADAMTS7-214Pro-plasmid had lower TSP5 cleavage activity than media conditioned by ADAMTS7-214Ser-plasmid transfected cells (Figure 3C).

Effect of rs3825807 on ADAMTS7 Prodomain Processing

The Ser-to-Pro substitution resulting from rs3825807 occurs at amino acid residue 214 in the prodomain of the ADAMTS7 protein. Because proline is rigid, the substitution could potentially introduce a conformational change

Please cite this article in press as: Pu et al., ADAMTS7 Cleavage and Vascular Smooth Muscle Cell Migration Is Affected by a Coronary-Artery-Disease-Associated Variant, The American Journal of Human Genetics (2013), http://dx.doi.org/10.1016/j.ajhg.2013.01.012

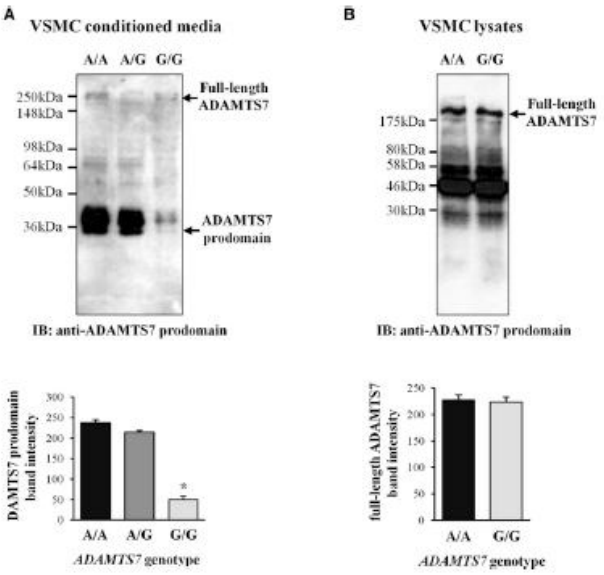

Figure 4. Effect of *ADAMTS7* Genotype on the Amount of Cleaved ADAMTS7 Prodomain in VSMC Conditioned Media
(A) A representative image of immunoblot (IB) analysis of cleaved ADAMTS7 prodomain in media conditioned by VSMCs of the A/A, A/G, or G/G genotype for rs3825807. The same amount (20 μg) of proteins for each genotype was loaded. Data shown in column chart are mean (±SEM) values of cleaved ADAMTS7 prodomain band intensity in immunoblots (n = 5 different donor cell preparations for each genotype). *$p < 0.05$ comparing A/A and G/G genotypes.
(B) A representative image of immunoblot analysis of cleaved ADAMTS7 prodomain in lysates of VSMCs of the A/A or G/G genotype for rs3825807. The same amount (20 μg) of proteins for each genotype was loaded. Data shown in column chart are mean (±SEM) values of full-length ADAMTS7 band intensity in immunoblots (n = 3 different donor cell preparations for each genotype).

that might affect the secretion of the protein or the cleavage of the prodomain or its interaction with other molecules on the cell surface. Immunoblot analyses showed that VSMC conditioned media contained cleaved ADAMTS7 prodomain (Figure 4A), which was undetectable in cell surface washes (data not shown). Importantly, the analyses showed that the amount of the cleaved ADAMTS7 prodomain in media conditioned by VSMCs of the G/G genotype was ~5-fold lower than in media conditioned by VSMCs of the A/A genotype (Figure 4A), whereas cell lysates of the two genotypes had similar amounts of full-length ADAMTS7 and ADAMTS7 fragments (Figure 4B). As reported by other researchers,[4] the full-length ADAMTS7 band was ~250 kDa in size (Figure 4B), which is larger than the predicted molecular weight (185 kDa) calculated based on the amino acid sequence, probably due to posttranslational modifications such as glycosylation.[4] The ADAMTS7 prodomain band was ~34 kDa in size (Figure 4A), which is similar to the reported size (~37 kDa) of the ADAMTS9 [MIM 605421] prodomain with glycosylation.[13]

To further assess effects of the Ser-to-Pro substitution, we transfected cultured HEK293 cells with a plasmid to produce a recombinant protein consisting of the ADAMTS7 single peptide, prodomain (of either ADAMTS7-214Ser or ADAMTS7-214Pro), and metalloproteinase domain followed by a c-Myc epitope tag, and then carried out immunoblot analyses on conditioned media, surface washes (with 0.5M NaCl), and lysates of the transfected cells. Previous studies by other researchers of HEK293 cells transfected with a similar plasmid showed that the recombinant protein underwent prodomain cleavage, leading to an initially processed form (P1), an intermediate form (Pint) and a fully processed form (M)[4] (as schematically illustrated in Figure 5A). In our study, immunoblot analyses of conditioned media with an anti-cMyc antibody showed three bands with sizes corresponding to the P1, Pint, and M forms, with the relative intensities of the Pint and M bands (versus the P1 band) being ~1.7- and ~4-fold lower, respectively, when comparing media conditioned by cells transfected to produce ADAMTS7-214Pro with media conditioned by cells transfected to produce ADAMTS7-214Ser (Figure 5B). Interestingly, the Pint and P1 forms of ADAMTS7-214Pro had a reduced electrophoretic mobility, compared with the Pint and P1 forms of ADAMTS7-214Ser (Figures 5B), which is in line with reports in the literature that proline-rich proteins tend to migrate more slowly in SDS-PAGE, presumably due to conformational peculiarities that persist even under reducing conditions.[14,15] In cell surface washes and lysates, immunoblotting with the anti-cMyc antibody showed only one major band corresponding to the P1 form, with similar intensities for cells transfected with either plasmid (Figures 5E and 5F).

Immunoblotting with an antibody against the ADAMTS7 prodomain detected a cleaved prodomain fragment (indicated by CP in Figures 5A, 5C, and 5D) in conditioned media (Figure 5C) and cell surface washes (Figure 5D), but not in cell lysates (Figure 5G), of the transfected cells, indicating binding of the cleaved prodomain fragment to the cell surface. Noticeably, the intensity of

Please cite this article in press as: Pu et al., ADAMTS7 Cleavage and Vascular Smooth Muscle Cell Migration Is Affected by a Coronary-Artery-Disease-Associated Variant, The American Journal of Human Genetics (2013), http://dx.doi.org/10.1016/j.ajhg.2013.01.012

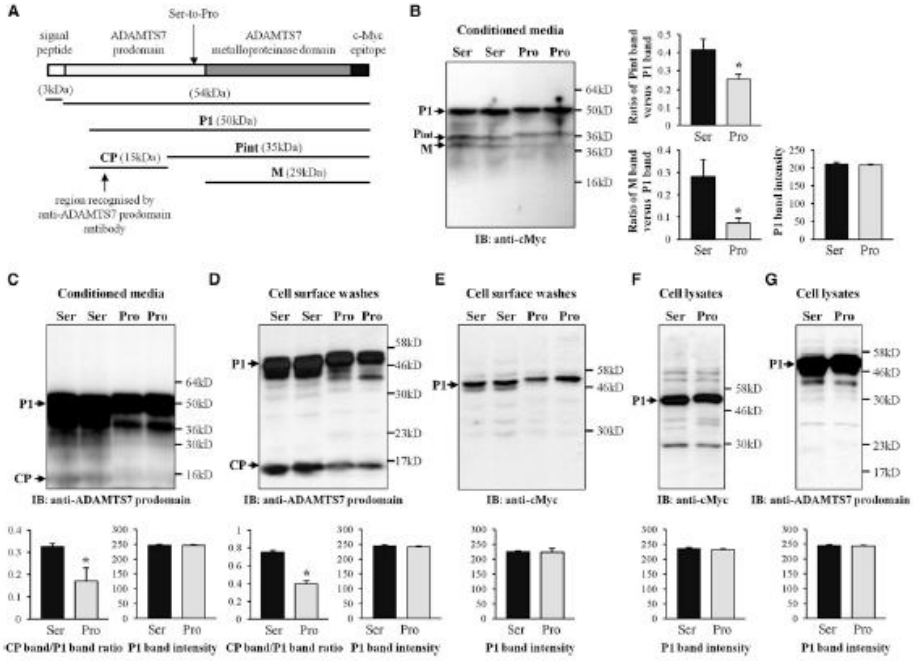

Figure 5. Effect of *ADAMTS7* Genotype on ADAMTS7 Prodomain Processing

Cultured HEK293 cells were transfected with a plasmid to produce a recombinant protein containing the ADAMTS7 prodomain and metalloproteinase domain followed by a c-Myc epitope tag, with either serine (Ser) or proline (Pro) at residue 214 in the ADAMTS7 prodomain. Conditioned media, cell surface washes (with 0.5M NaCl), and cell lysates were subjected to immunoblot analyses with an anti-cMyc antibody or an anti-ADAMTS7 prodomain antibody. The same amount (40 μg) of proteins for each allele was loaded.
(A) A schematic diagram for the produced recombinant protein. P1, Pint, and M indicate the previously reported initially processed form, intermediately processing form, and fully processed form, respectively;[4] CP indicates a cleaved ADAMTS7 prodomain fragment.
(B to G) Representative images of the immunoblot (IB) analyses and column chart presentations of mean (±SEM) values (n = 4 for each allele). *$p < 0.05$ comparing ADAMTS7-214Ser and ADAMTS7-214Pro.

this band was ~2-fold lower in conditioned media and cell surface washes, when comparing cells transfected to produce ADAMTS7-214Pro with cells transfected to produce ADAMTS7-214Ser (Figures 5C and 5D).

No Association between rs3825807 and ADAMTS7 Expression in VSMCs

To investigate whether *ADAMTS7* genotype had an influence on *ADAMTS7* expression in VSMCs, we performed a real-time RT-PCR analysis and an allelic expression imbalance analysis. In the real-time RT-PCR analysis, we detected no association between *ADAMTS7* expression level and rs3825807 genotype (Figure S5), consistent with the results of immunoblot analysis that showed that cell lysates of the A/A and G/G genotypes had similar amounts of the ADAMTS7 protein (Figure 4B). In agreement, an allelic expression imbalance analysis showed no difference in *ADAMTS7* expression level between the A and G alleles in VSMCs that were heterozygous for rs3825807 (Figure S6).

Discussion

In this study, we found an association between *ADAMTS7* variation and atherosclerosis in the Bruneck cohort, with the rs3825807 G/G genotype associating with lower atherosclerosis prevalence and severity (score), which is in line with the finding from a recent GWAS that the G allele is associated to lower susceptibility to CAD.[1] In in vitro assays, we found that VSMCs of the G/G genotype had reduced migratory ability and their conditioned media contained less-cleaved product of the ADAMTS7 substrate TSP5 and less-cleaved ADAMTS7 prodomain. Site-directed in vitro mutagenesis assay indicated that the Ser-to-Pro substitution reduces ADAMTS7 prodomain processing.

Please cite this article in press as: Pu et al., ADAMTS7 Cleavage and Vascular Smooth Muscle Cell Migration Is Affected by a Coronary-Artery-Disease-Associated Variant, The American Journal of Human Genetics (2013), http://dx.doi.org/10.1016/j.ajhg.2013.01.012

We did not find evidence of between-genotype difference in ADAMTS7 accumulation or secretion, or in VSMC proliferation, senescence, or apoptosis. Taken together, these results indicate that the Ser-to-Pro substitution resulting from rs3825807 has an effect on ADAMTS7 maturation, TSP5 cleavage, and VSMC migration and is associated with atherosclerosis, providing a mechanistic explanation for the recently reported association between the SNP and CAD susceptibility.[1]

The effect of the Ser-to-Pro substitution on prodomain processing may be due to reduced accessibility to processing proteases such as furin, as a result of a conformational change induced by the rigidity of proline. The possibility of a conformational change is supported by our observation that the processed forms (Pint and M) of ADAMTS7-214Pro had reduced electrophoretic mobility. Although a conformational change might potentially also affect the secretion of the protein, the results of our study indicate that this would not be the case.

Rs3825807 was the lead SNP associated with CAD in one of the recently reported GWASs[1] and is in LD with the lead CAD-related SNPs, rs1994016 and rs4380028, in two other recent GWASs[2,3] ($r^2 > 0.8$ with rs1994016 and > 0.4 with rs4380028, based on data from HapMap and the 1000 Genomes Project). It is unknown whether rs1994016 and/or rs4380028 have a direct functional effect or act as proxy markers for functional SNPs (e.g., SNP rs3825807) due to LD. Rs1994016 resides in intron 8 of *ADAMTS7*, whereas rs4380028 is located 7.6 kb upstream of the gene. Considering their physical locations in relation to *ADAMTS7*, they might have an influence on *ADAMTS7* expression, although currently there is no reported evidence.

VSMC migration is an important process in the pathogenesis of atherosclerosis.[16] Indeed, VSMCs are one of the major constituents of atherosclerotic lesions.[17] During atherogenesis, VSMCs migrate from the arterial media into the intima where the VSMCs proliferate and produce extracellular proteins,[18] another major constitute of atherosclerotic plaques.[17] The finding from our study that in atherosclerotic plaques, VSMCs that accumulate ADAMTS7 are predominantly located near the intima-media border is in line with the notion that ADAMTS7 plays a role in VSMC migration during atherogenesis.

Although a high VSMC content would increase the stability of the atherosclerotic plaque and reduce the risk of plaque rupture to cause such an acute ischemic event as myocardial infarction (MI),[19,20] a genetic epidemiological study by Reilly et al. shows that *ADAMTS7* variation is associated with coronary atherosclerosis but not with risk of MI.[2] The finding of our study that the CAD-related *ADAMTS7* genotype enhances VSMC migration is in line with that of the genetic epidemiological study by Reilly et al.[2]

Apart from the finding of an association between *ADAMTS7* variation and CAD in genetic epidemiological studies,[1–3] to our knowledge, there has been only one reported study of ADAMTS7 in vascular disease. Results of this latter study indicate that ADAMTS7 plays a role in vascular neointima formation after mechanical injury in a rat model, by inducing VSMC migration resulting from degradation of the extracellular matrix protein TSP5.[6] A previous study shows that VSMCs produce TSP5, to which VSMCs adhere.[7] Therefore, we focused our study on VSMCs. However, it seems warranted in future studies to investigate whether CAD-related *ADAMTS7* variation also affects other cell types such as macrophages and endothelial cells. Our preliminary data, however, did not show an apparent difference in the abundance of CD68 positive cells in atherosclerotic plaques from individuals of rs3825807 A/A or G/G genotype (Figure S7).

Recently over 40 genomic loci have been identified by GWAS to be associated with genetic susceptibility to CAD. However, for many of these loci, the functional mechanisms leading to the genetic effect remain unknown. Functional characterization of these genetic variants can aid the understanding of the underlying biological mechanisms and may facilitate the translation of the genetic discoveries to therapeutic development. The findings of our present study on *ADAMTS7* are pertinent in this context.

Supplemental Data

Supplemental data include seven figures can be found with this article online at http://www.cell.com/AJHG/.

Acknowledgments

We thank the British Heart Foundation and the William Harvey Research Foundation for support. X.P. and C.F. are recipients of scholarships from the Chinese Scholarship Council. Q.X. is the recipient of a British Heart Foundation Intermediate Basic Science Research Fellowship (FS/09/044/28007). The work forms part of the research themes contributing to the translational research portfolio of Barts Cardiovascular Biomedical Research Unit, which is supported and funded by the National Institute for Health Research.

Received: September 27, 2012
Revised: October 31, 2012
Accepted: January 28, 2013
Published: February 14, 2013

Web Resources

The URL for data presented herein is as follows:

Online Mendelian Inheritance in Man (OMIM), http://www.omim.org/

References

1. Schunkert, H., König, I.R., Kathiresan, S., Reilly, M.P., Assimes, T.L., Holm, H., Preuss, M., Stewart, A.F., Barbalic, M., Gieger, C., et al.; Cardiogenics; CARDIoGRAM Consortium. (2011). Large-scale association analysis identifies 13

new susceptibility loci for coronary artery disease. Nat. Genet. *43*, 333–338.

2. Reilly, M.P., Li, M., He, J., Ferguson, J.F., Stylianou, I.M., Mehta, N.N., Burnett, M.S., Devaney, J.M., Knouff, C.W., Thompson, J.R., et al.; Myocardial Infarction Genetics Consortium; Wellcome Trust Case Control Consortium. (2011). Identification of ADAMTS7 as a novel locus for coronary atherosclerosis and association of ABO with myocardial infarction in the presence of coronary atherosclerosis: two genome-wide association studies. Lancet *377*, 383–392.
3. Coronary Artery Disease (C4D) Genetics Consortium. (2011). A genome-wide association study in Europeans and South Asians identifies five new loci for coronary artery disease. Nat. Genet. *43*, 339–344.
4. Somerville, R.P., Longpré, J.M., Apel, E.D., Lewis, R.M., Wang, L.W., Sanes, J.R., Leduc, R., and Apte, S.S. (2004). ADAMTS7B, the full-length product of the ADAMTS7 gene, is a chondroitin sulfate proteoglycan containing a mucin domain. J. Biol. Chem. *279*, 35159–35175.
5. Liu, C.J., Kong, W., Ilalov, K., Yu, S., Xu, K., Prazak, L., Fajardo, M., Sehgal, B., and Di Cesare, P.E. (2006). ADAMTS-7: a metalloproteinase that directly binds to and degrades cartilage oligomeric matrix protein. FASEB J. *20*, 988–990.
6. Wang, L., Zheng, J., Bai, X., Liu, B., Liu, C.J., Xu, Q., Zhu, Y., Wang, N., Kong, W., and Wang, X. (2009). ADAMTS-7 mediates vascular smooth muscle cell migration and neointima formation in balloon-injured rat arteries. Circ. Res. *104*, 688–698.
7. Riessen, R., Fenchel, M., Chen, H., Axel, D.I., Karsch, K.R., and Lawler, J. (2001). Cartilage oligomeric matrix protein (thrombospondin-5) is expressed by human vascular smooth muscle cells. Arterioscler. Thromb. Vasc. Biol. *21*, 47–54.
8. Kiechl, S., and Willeit, J. (1999). The natural course of atherosclerosis. Part I: incidence and progression. Arterioscler. Thromb. Vasc. Biol. *19*, 1484–1490.
9. Kiechl, S., and Willeit, J.; Bruneck Study Group. (1999). The natural course of atherosclerosis. Part II: vascular remodeling. Arterioscler. Thromb. Vasc. Biol. *19*, 1491–1498.
10. Willeit, J., Kiechl, S., Oberhollenzer, F., Rungger, G., Egger, G., Bonora, E., Mitterer, M., and Muggeo, M. (2000). Distinct risk profiles of early and advanced atherosclerosis: prospective results from the Bruneck Study. Arterioscler. Thromb. Vasc. Biol. *20*, 529–537.
11. Liang, C.C., Park, A.Y., and Guan, J.L. (2007). In vitro scratch assay: a convenient and inexpensive method for analysis of cell migration in vitro. Nat. Protoc. *2*, 329–333.
12. Bai, X.H., Wang, D.W., Kong, L., Zhang, Y., Luan, Y., Kobayashi, T., Kronenberg, H.M., Yu, X.P., and Liu, C.J. (2009). ADAMTS-7, a direct target of PTHrP, adversely regulates endochondral bone growth by associating with and inactivating GEP growth factor. Mol. Cell. Biol. *29*, 4201–4219.
13. Koo, B.H., Longpré, J.M., Somerville, R.P., Alexander, J.P., Leduc, R., and Apte, S.S. (2006). Cell-surface processing of pro-ADAMTS9 by furin. J. Biol. Chem. *281*, 12485–12494.
14. Hung, C.Y., Yu, J.J., Seshan, K.R., Reichard, U., and Cole, G.T. (2002). A parasitic phase-specific adhesin of Coccidioides immitis contributes to the virulence of this respiratory Fungal pathogen. Infect. Immun. *70*, 3443–3456.
15. Williamson, M.P. (1994). The structure and function of proline-rich regions in proteins. Biochem. J. *297*, 249–260.
16. Schwartz, S.M. (1997). Perspectives series: cell adhesion in vascular biology. Smooth muscle migration in atherosclerosis and restenosis. J. Clin. Invest. *99*, 2814–2816.
17. Stary, H.C., Chandler, A.B., Dinsmore, R.E., Fuster, V., Glagov, S., Insull, W., Jr., Rosenfeld, M.E., Schwartz, C.J., Wagner, W.D., and Wissler, R.W. (1995). A definition of advanced types of atherosclerotic lesions and a histological classification of atherosclerosis. A report from the Committee on Vascular Lesions of the Council on Arteriosclerosis, American Heart Association. Circulation *92*, 1355–1374.
18. Ross, R. (1993). The pathogenesis of atherosclerosis: a perspective for the 1990s. Nature *362*, 801–809.
19. Davies, M.J. (1996). Stability and instability: two faces of coronary atherosclerosis. The Paul Dudley White Lecture 1995. Circulation *94*, 2013–2020.
20. Libby, P. (1995). Molecular bases of the acute coronary syndromes. Circulation *91*, 2844–2850.

Human Molecular Genetics, 2012, Vol. 21, No. 18 **4021–4029**
doi:10.1093/hmg/dds224
Advance Access published on June 15, 2012

Functional analyses of coronary artery disease associated variation on chromosome 9p21 in vascular smooth muscle cells

Anna Motterle[1,†], Xiangyuan Pu[1,†], Harriet Wood[1], Qingzhong Xiao[1], Shivani Gor[1], Fu Liang Ng[1], Kenneth Chan[1], Frank Cross[2], Beski Shohreh[2], Robin N. Poston[1], Arthur T. Tucker[1,2], Mark J. Caulfield[1] and Shu Ye[1,*]

[1]Barts and The London School of Medicine and Dentistry, William Harvey Research Institute, Queen Mary University of London, London, UK and [2]Barts and The London NHS Trust, London, UK

Received May 20, 2012; Revised May 20, 2012; Accepted June 5, 2012

Variation on chromosome 9p21 is associated with risk of coronary artery disease (CAD). This genomic region contains the *CDKN2A* and *CDKN2B* genes which encode the cell cycle regulators $p16^{INK4a}$, $p14^{ARF}$ and $p15^{INK4b}$ and the *ANRIL* gene which encodes a non-coding RNA. Vascular smooth muscle cell (VSMC) proliferation plays an important role in the pathogenesis of atherosclerosis which causes CAD. We ascertained whether 9p21 genotype had an influence on *CDKN2A/CDKN2B/ANRIL* expression levels in VSMCs, VSMC proliferation and VSMC content in atherosclerotic plaques. Immunohistochemical examination showed that VSMCs in atherosclerotic lesions expressed $p16^{INK4a}$, $p14^{ARF}$ and $p15^{INK4b}$. Analyses of primary cultures of VSMCs showed that the 9p21 risk genotype was associated with reduced expression of $p16^{INK4a}$, $p15^{INK4b}$ and *ANRIL* ($P = 1.2 \times 10^{-5}$, 1.4×10^{-2} and 3.1×10^{-9}) and with increased VSMC proliferation ($P = 1.6 \times 10^{-2}$). Immunohistochemical analyses of atherosclerotic plaques revealed an association of the risk genotype with reduced $p15^{INK4b}$ levels in VSMCs ($P = 3.7 \times 10^{-2}$) and higher VSMC content ($P = 5.6 \times 10^{-4}$) in plaques. The results of this study indicate that the 9p21 variation has an impact on *CDKN2A* and *CDKN2B* expression in VSMCs and influences VMSC proliferation, which likely represents an important mechanism for the association between this genetic locus and susceptibility to CAD.

INTRODUCTION

Genome-wide association studies have revealed a strong association between DNA sequence variation on chromosome 9p21 and the risk of coronary artery disease (CAD) (1–4). This has been confirmed in many independent studies (5–8). Additionally, this genetic locus has been shown to be associated with abdominal aortic aneurysm (9), intracranial aneurysm (9–11), carotid atherosclerosis (12), ischaemic stroke (13) and peripheral vascular disease (14). On the other hand, there is no association between this locus and classic CAD-related intermediate traits such as hyperlipidaemia and hypertension (5,6,12,15). The mechanism by which variation at this locus influences the risk of CAD is currently unclear.

The 9p21 locus contains multiple CAD-associated single-nucleotide polymorphisms (SNPs) in strong linkage disequilibrium, spanning a genomic region of over 50 kb (1–5). This genomic interval does not contain any protein-coding sequences; however, near this interval reside the cyclin-dependent kinase 2A (*CDKN2A*) and 2B (*CDKN2B*) genes (1–5) which encode the cell proliferation regulators $p16^{INK4a}$ (by exons 1α, 2 and 3 of the *CDKN2A* gene), $p14^{ARF}$ (by exons 1β and 2 of the *CDKN2A* gene) and $p15^{INK4b}$ (by the *CDKN2B* gene) (16). In addition, this genomic interval contains a gene for a non-coding RNA

*To whom correspondence should be addressed at: William Harvey Research Institute, Barts and The London School of Medicine and Dentistry, Queen Mary University of London, John Vane Science Building, Charterhouse Square, London EC1M 6BQ, UK. Tel: +44 2078823425; Fax: +44 2078823408; Email: s.ye@qmul.ac.uk
†The authors wish it to be known that, in their opinion, the first two authors should be regarded as joint First Authors.

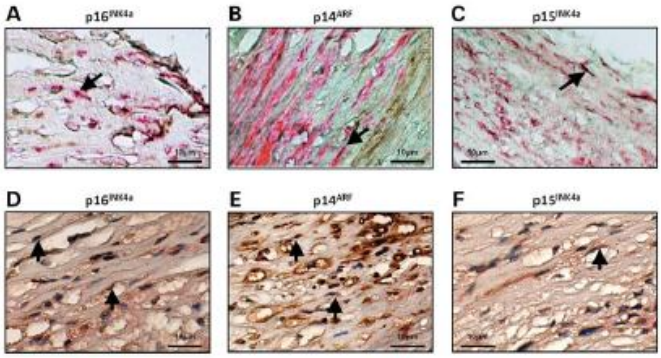

Figure 1. Smooth muscle cells in atherosclerotic lesions express $p16^{INK4a}$, $p14^{ARF}$ and $p15^{INK4b}$. Sections of formaldehyde-fixed paraffin-embedded tissue blocks of atherosclerotic plaques were subjected to double immunostaining of SMA together with $p16^{INK4a}$ (**A** and **D**), $p14^{ARF}$ (**C** and **E**) or $p15^{INK4b}$ (**E** and **F**). In (A–C), Fast red staining indicates expression of the VSMC marker SMA, and dark brown colour (DAB) indicates expression of $p16^{INK4a}$ (A), $p14^{ARF}$ (**B**) or $p15^{INK4b}$ (C). Arrows indicate cell co-expressing SMA with $p16^{INK4a}$ (A), $p14^{ARF}$ (B) or $p15^{INK4b}$ (C). No nuclear counterstaining was used in (A–C). In (D–F), brown staining with DAB indicates expression of the VSMC marker SMA, blue colour (haematoxylin) indicates nuclei and Fast red staining indicates expression of $p16^{INK4a}$ (D), $p14^{ARF}$ (E) or $p15^{INK4b}$ (F). Arrows indicate expression of $p16^{INK4a}$ (D), $p14^{ARF}$ (E) or $p15^{INK4b}$ (F), in the nuclei of smooth muscle cells. The haematoxylin nuclear counterstain has partially obscured Fast red nuclear staining of $p16^{INK4a}$, $p14^{ARF}$ and $p15^{INK4b}$, in (D–F). × 200 magnification.

known as *ANRIL* (*a*ntisense *n*on-coding *R*NA in the *I*NK4 *l*ocus) (1–5) which may have a role in the regulation of *CDKN2A* and *CDKN2B* expression (17,18).

Recently, it has been demonstrated that targeted deletion of the orthologous interval in mice resulted in a significant reduction in cardiac expression of *CDKN2A* and *CDKN2B* (19), indicating that this genomic interval harbours regulatory elements that modulate the expression of these genes. In addition, the study showed that primary cultures of vascular smooth muscle cells (VSMCs) from mice with the deletion of the orthologous interval exhibited excessive proliferation, presumably due to altered *CDKN2A* and *CDKN2B* expression (19). Since VSMCs play important roles in atherosclerosis (20), these findings point to a possible mechanism for the association of the 9p21 locus with susceptibility to CAD in humans, such that the CAD-associated variant at this locus might modulate *CDKN2A* and *CDKN2B* expression in VSMCs, thereby affecting VSMC proliferation and consequently the development and progression of atherosclerosis.

In the present study, we investigated whether there was a relationship between the 9p21 locus SNP rs1333049 which had been repeatedly associated with risk of CAD (1,6,7), and expression levels of *CDKN2A, CDKN2B* and *ANRIL* in primary cultures of VSMCs, and if the SNP was also associated with $p16^{INK4a}$ and $p15^{INK4b}$ expression levels in VSMCs in atherosclerotic plaques and with VSMC content in the plaques.

RESULTS

VSMCs in atherosclerotic lesions express $p16^{INK4a}$, $p14^{ARF}$ and $p15^{INK4b}$

We performed immunohistochemical examinations to investigate $p16^{INK4a}$, $p14^{ARF}$ and $p15^{INK4b}$ expression in VSMCs in atherosclerotic plaques. Double immunostaining of the VSMC marker smooth muscle α-actin (SMA) together with $p16^{INK4a}$, $p14^{ARF}$ or $p15^{INK4b}$ showed that VSMCs in the atherosclerotic lesions expressed $p16^{INK4a}$, $p14^{ARF}$ and $p15^{INK4b}$ (Fig. 1A–F). Similarly, we found that VSMCs in abdominal aortic aneurysmal lesions also expressed $p16^{INK4a}$, $p14^{ARF}$ and $p15^{INK4b}$ (Supplementary Material, Fig. S1).

Relationship between 9p21 variation and expression levels of $p16^{INK4a}$ and $p15^{INK4b}$ in cultured VSMCs

We isolated arterial VSMCs from umbilical cords ($n = 69$) and studied primary cultures of these VSMCs to ascertain a relationship between SNP rs1333049 and expression levels of *CDKN2A* and *CDKN2B*. We observed an association between the SNP and mRNA levels of both $p16^{INK4a}$ and $p15^{INK4b}$, with cells of the C/C genotype having lowest levels ($P = 1.2 \times 10^{-5}$ for $p16^{INK4a}$, Fig. 2A; and $P = 1.4 \times 10^{-2}$ for $p15^{INK4b}$, Fig. 2C). On the other hand, $p14^{ARF}$ expression levels did not show an association with the SNP rs1333049 genotype ($P = 7.3 \times 10^{-1}$; Fig. 2B).

Having found that SNP rs1333049 was associated with $p16^{INK4a}$ and $p15^{INK4b}$ mRNA levels in VSMCs, we examined whether there were differences in the protein levels of $p16^{INK4a}$ and $p15^{INK4b}$ according to genotypes. We found that the levels of $p15^{INK4b}$ protein were lower in cells of the C/C genotype ($P = 2.7 \times 10^{-2}$; Fig. 2D and F) and there was a similar trend for $p16^{INK4a}$ ($P = 8.9 \times 10^{-2}$; Fig. 2D and E).

Relationships of ANRIL with 9p21 variation, $p16^{INK4a}$, $p14^{ARF}$ and $p15^{INK4b}$ in cultured VSMCs

Previous studies in blood cells showed an association between variation at the 9p21 locus and expression levels of the non-

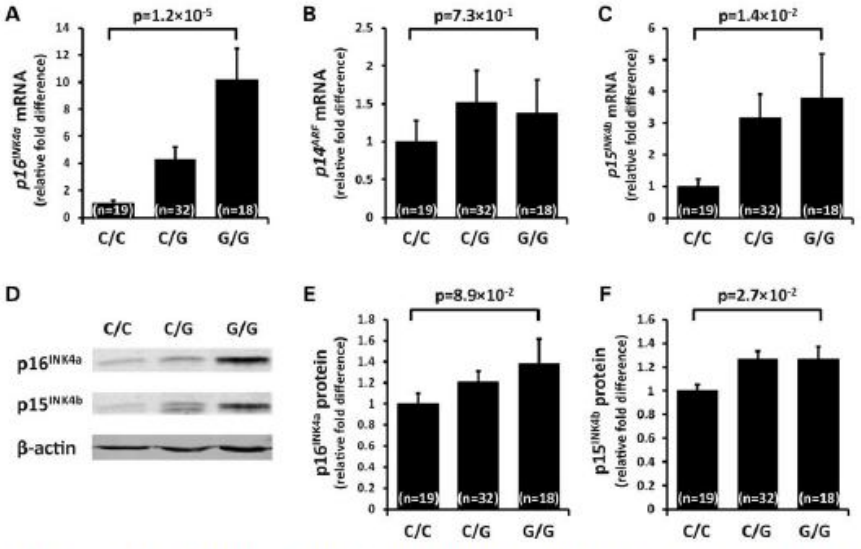

Figure 2. Relationship of 9p21 variation with $p16^{INK4a}$ and $p15^{INK4b}$ expression levels in cultured VSMCs. Primary cultures of VSMCs from different individuals ($n = 69$) were genotyped for SNP rs1333049 and subjected to quantitative reverse transcriptase–polymerase chain reaction and western blot analyses. (**A–C**) Relative fold differences in $p16^{INK4a}$, $p14^{ARF}$ and $p15^{INK4b}$ mRNA levels in VSMCs of the G/C or G/G genotype for SNP rs1333049 compared with mRNA levels of the corresponding genes in VSMCs of the C/C genotype. (**D**) Representative images acquired from western blot analyses of $p16^{INK4a}$ and $p15^{INK4b}$ and the gel load reference protein β-actin. (**E** and **F**) Relative fold differences in $p16^{INK4a}$ and $p15^{INK4b}$ protein levels in VSMCs of the G/C or G/G genotype compared with levels of the corresponding proteins in VSMCs of the C/C genotype. Data shown in (A–C, E and F) are mean ± standard deviation of mean.

coding RNA *ANRIL* (17,21–23). There is evidence indicating that *ANRIL* plays a role in the transcriptional regulation of *CDKN2A* and *CDKN2B* (18,24), and studies in blood cells and vascular tissues have shown that *CDKN2A* and *CDKN2B* expression levels are correlated with *ANRIL* levels (17,22,23,25). Therefore, we investigated whether there was an association between the SNP rs1333049 genotype and *ANRIL* expression in VSMCs and ascertained relationships of *ANRIL* with $p16^{INK4a}$, $p14^{ARF}$ and $p15^{INK4b}$ in these cells. We detected an association between the SNP and *ANRIL* expression, with cells of the C/C genotype having lowest levels ($P = 3.1 \times 10^{-9}$; Fig. 3A). In addition, we observed correlations between *ANRIL* and $p16^{INK4a}$, $p14^{ARF}$ and $p15^{INK4b}$ expression levels ($r = 0.744$, 0.348 and 0.352, respectively; Fig. 3B–D).

Association between 9p21 variation and VSMC proliferation in culture

Since $p16^{INK4a}$ and $p15^{INK4b}$ are negative regulators of cell cycle and proliferation (16,26,27), we investigated whether the levels of the cell proliferation marker *PCNA* (proliferating cell nuclear antigen) were associated with $p16^{INK4a}$ and $p15^{INK4b}$ levels and with the SNP rs1333049 genotype, in VSMCs. We observed an inverse relationship of *PCNA* with $p16^{INK4a}$ ($r = -0.355$; Fig. 4A) and a similar trend with $p15^{INK4b}$ ($r = -0.235$; Fig. 4B). Importantly, we found that *PCNA* levels were significantly associated with the SNP rs1333049 genotype, being highest in VSMCs of the C/C genotype ($P = 2.3 \times 10^{-2}$; Fig. 4C).

Further to the above analyses, we examined whether the 9p21 variant was associated with VSMC proliferation. We performed proliferation assays in another collection of VSMCs from umbilical cords ($n = 73$). This experiment showed an association between SNP rs1333049 and VSMC proliferation, with cells of the C/C genotype having highest values ($P = 1.6 \times 10^{-2}$; Fig. 5).

Relationship between 9p21 variation and expression levels of $p16^{INK4a}$ and $p15^{INK4b}$ in VSMCs in atherosclerotic plaques

Further to the above experiments, we investigated whether the 9p21 variation was associated with levels of $p16^{INK4a}$ and $p15^{INK4b}$ in VSMCs in atherosclerotic plaques. We performed double immunostaining of SMA together with either $p16^{INK4a}$ or $p15^{INK4b}$, in coronary atherosclerotic plaques from different individuals ($n = 41$), and determined the percentage of $p16^{INK4a}$ stain area in VSMC stain area and the percentage of $p15^{INK4b}$ stain area in VSMC stain area, in each plaque.

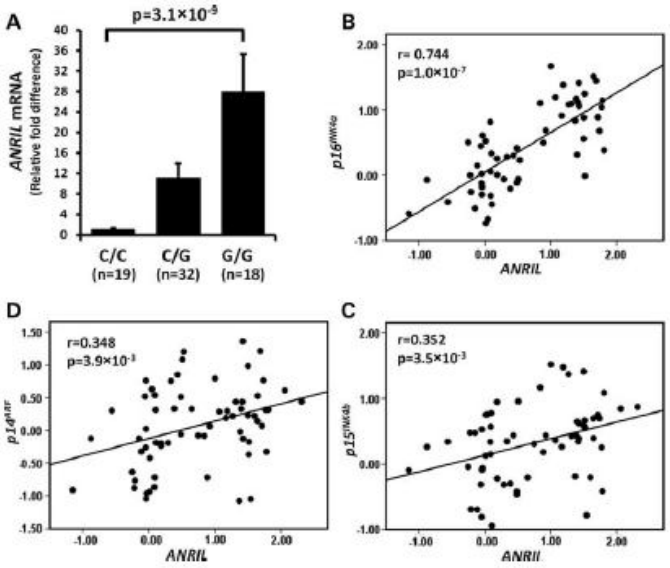

Figure 3. Relationships of *ANRIL* with 9p21 variation, $p16^{INK4a}$, $p14^{ARF}$ and $p15^{INK4b}$ in cultured VSMCs. Primary cultures of VSMCs from different individuals ($n = 69$) were genotyped for SNP rs1333049 and subjected to quantitative reverse transcriptase–polymerase chain reaction analysis of *ANRIL*, $p16^{INK4a}$, $p14^{ARF}$ and $p15^{INK4b}$. (**A**) Relative fold differences in the *ANRIL* level in VSMCs of the G/G or G/C genotype for SNP rs1333049 compared with the *ANRIL* level in VSMCs of the C/C genotype. Data shown are mean ± standard deviation of mean. (**B**–**D**) Pair-wise correlation of *ANRIL* with $p16^{INK4a}$, $p14^{ARF}$ and $p15^{INK4b}$, respectively.

The analysis showed that the percentages of $p15^{INK4b}$ stain areas were lower in individuals carrying the C allele of SNP rs1333049 ($P = 3.7 \times 10^{-2}$; Fig. 6B) and there was a similar trend for $p16^{INK4a}$ ($P = 6.5 \times 10^{-2}$; Fig. 6A).

Association between 9p21 variation and VSMC content in atherosclerotic plaques

Further to the above analysis, we investigated whether there was a relationship of the 9p21 variation with the abundance of proliferating VSMCs and with VSMC content in atherosclerotic plaques. We performed double immunostaining of SMA and the cell proliferation marker Ki67 in coronary atherosclerotic plaques from different individuals ($n = 52$). We found an association between SNP rs1333049 and VSMC content, with atherosclerotic plaques of the C/C genotype having the highest VSMC content ($P = 5.6 \times 10^{-4}$; Fig. 7). Additionally, we observed that plaques of the C/C genotype had a non-significant trend towards higher percentages of Ki67-positive SMCs (Supplementary Material, Fig. S2).

DISCUSSION

Following the finding from genome-wide association studies and many replication studies that variation at the 9p21 locus is a major genetic determinant for CAD (1–8), there have been considerable efforts aimed at elucidating the underlying mechanisms. Further to findings from previous studies by other groups (17–19,21–23,25,28), our present study has provided several lines of new information. Our study shows that in primary cultures of VSMCs, there is an association of 9p21 genotype with *CDKN2A*, *CDKN2B* and *ANRIL* expression levels and with the rate of proliferation. Furthermore, our study reveals a relationship of 9p21 genotype with $p15^{INK4b}$ levels in VSMCs in atherosclerotic plaques and with VSMC content in the plaques. These findings provide new insight into the mechanism underlying the association between variation at the 9p21 locus and risk of CAD.

$p16^{INK4a}$ and $p15^{INK4b}$ encoded by *CDKN2A* and *CDKN2B*, respectively, are known to play important roles in regulating the cell cycle in many cell types (16). They inhibit cell proliferation by suppressing dissociation of the transcription factor E2F from retinoblastoma protein and consequently suppressing E2F-mediated expression of cell proliferation genes (16). Findings from animal models indicate that these cell cycle regulators repress VSMC proliferation in the blood vessel wall (29–31), although it is still unclear whether they exert similar effects in the human vasculature.

Previous studies in human peripheral blood T-lymphocytes (21), peripheral blood mononuclear cells (22) and whole

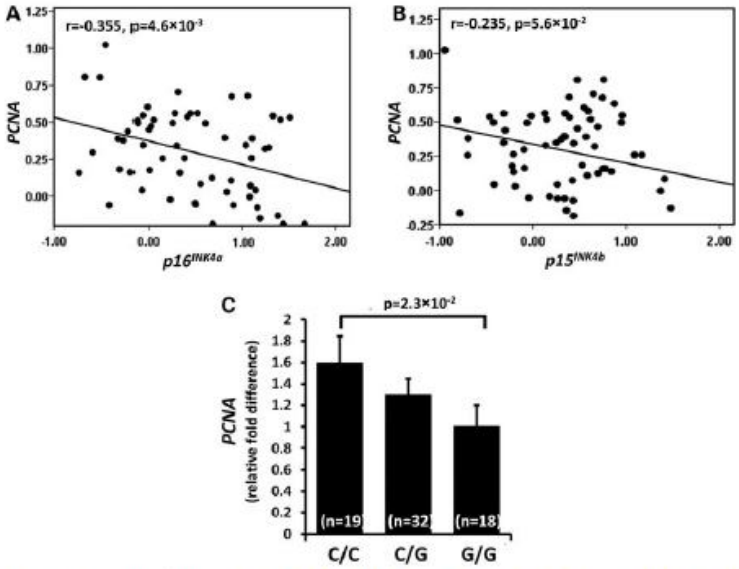

Figure 4. Relationships of $p16^{INK4a}$, $p15^{INK4b}$ and 9p21 variation with the cell proliferation marker *PCNA* in cultured VSMCs. Primary cultures of VSMCs from different individuals ($n = 69$) were genotyped for SNP rs1333049 and subjected to quantitative reverse transcriptase–polymerase chain reaction analysis of *PCNA*, $p16^{INK4a}$ and $p15^{INK4b}$. (**A** and **B**) Correlation of *PCNA* with $p16^{INK4a}$ and $p15^{INK4b}$, respectively. (**C**) Relative fold differences in the *PCNA* mRNA level in VSMCs of the G/C or G/G genotype for SNP rs1333049 compared with the *PCNA* level in VSMCs of the C/C genotype. Data shown are mean ± standard deviation of mean.

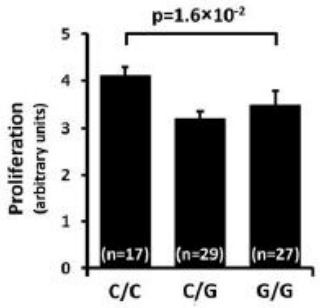

Figure 5. Association between 9p21 variation and VSMC proliferation in culture. Primary cultures of VSMCs from different individuals ($n = 73$) were genotyped for SNP rs1333049 and subjected to cell proliferation assay by the BrdU labelling and detection method. The amount of BrdU incorporated into cellular DNA was detected using the enzyme-linked immunosorbent assay with the use of a 5-Bromo-2′-deoxy-uridine Labeling and Detection Kit (Roche). Presented in the graph are relative fold differences in absorbance of samples from VSMCs of the G/C or G/G genotype for SNP rs1333049 compared with the absorbance of samples from VSMCs of the C/C genotype. Data shown are mean ± standard deviation of mean.

peripheral blood cells (17,22,23) showed a relationship of CAD-associated SNPs at the 9p21 locus with expression levels of *CDKN2A*, *CDKN2B* and/or *ANRIL*. In another study of peripheral blood mononuclear cells, however, *CDKN2A* and *ANRIL* were undetectable and *CDKN2B* expression level was found not to be associated with the CAD-related SNPs at the 9p21 locus but associated with a number of other SNPs in this genomic region (32). Our study differed from these previously studies, in that we examined VSMCs rather than blood cells. We found that in VSMCs, *CDKN2A*, *CDKN2B* and *ANRIL* expression levels were associated with a genotype for SNP rs1333049. Specifically, we found that $p16^{INK4a}$, $p15^{INK4b}$ and *ANRIL* expression levels were lowest in VSMCs from homozygotes of the C allele which has been shown to be associated with increased risk of CAD in many studies (1,6,7). In contrast, $p14^{ARF}$ expression levels did not show an association with this SNP. This is not surprising since, although the risk genotype which reduces $p16^{INK4a}$ and $p15^{INK4b}$ expression may also reduce $p14^{ARF}$ expression, decreased $p16^{INK4a}$ expression will increase the activity of the transcription factor E2F which in turn can up-regulate $p14^{ARF}$ expression (27) and therefore offset the decrease in the $p14^{ARF}$ expression level.

There is evidence indicating that *ANRIL* plays a role in the transcriptional regulation of *CDKN2A* and *CDKN2B*, probably

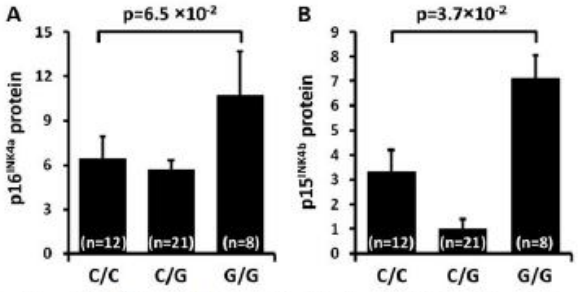

Figure 6. Relationship of 9p21 variation with $p16^{INK4a}$ and $p15^{INK4b}$ protein levels in atherosclerotic plaques. Atherosclerotic coronary arteries from different individuals ($n = 41$) were genotyped for SNP rs1333049 and subjected to double immunostaining of SMA together with $p16^{INK4a}$ or $p15^{INK4b}$. Immunostaining images were analysed using Image-Pro software. Shown in the graphs are percentages of $p16^{INK4a}$ stain area in VSMC stain area (**A**) and percentage of $p15^{INK4b}$ stain area in VSMC stain area (**B**) in plaques of the C/C, C/G and G/G genotypes for SNP rs1333049. Data shown are mean ± standard deviation of mean.

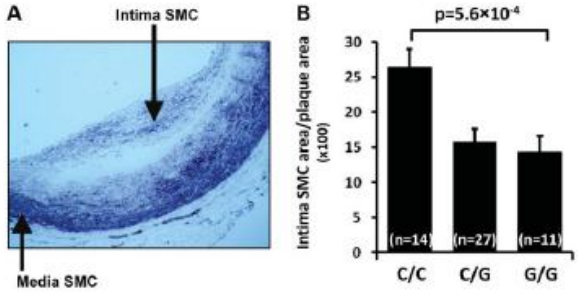

Figure 7. Association of 9p21 variation with smooth muscle cell content in atherosclerotic plaques. Atherosclerotic coronary arteries from different individuals ($n = 52$) were genotyped for SNP rs1333049 and subjected to immunostaining of SMA. Immunostaining images were analysed using Image-Pro software. (**A**) A representative image of immunostaining, purple colour indicates SMA stains, ×40 magnification. (**B**) Percentages of SMA stain area over total plaque area in plaques of the C/C, C/G and G/G genotypes for SNP rs1333049. Data shown are mean ± standard deviation of mean.

via its interaction with chromatin-associated factors that modulate chromatin methylation (18,24). Several different transcript variants of *ANRIL* have been reported (17,18,22,25). Previous studies have shown that expression levels of the long transcript of *ANRIL* were decreased and the short variants increased, in individuals homozygous for the 9p21 high-risk allele compared with those carrying two copies of the low-risk allele (17,21). In the present study, we examined the long transcript of *ANRIL* and, in agreement with the previous studies (17,21), found that its expression levels in VSMCs were lowest in homozygotes of the SNP rs1333049 C allele. Furthermore, similar to previous studies (17,22,23,25), we observed a correlation between the *ANRIL* long transcript and $p16^{INK4a}$ and $p15^{INK4b}$ expression levels. These findings are consistent with the hypothesis which has been proposed recently (17) that the 9p21 risk allele reduces expression of the *ANRIL* long transcript but increases expression of the short transcripts and that the short transcripts down-regulate *CDKN2A* and *CDKN2B* expression.

Importantly, further to the finding that the SNP rs1333049 genotype was associated with $p16^{INK4a}$, $p15^{INK4b}$ and *ANRIL* expression levels in VSMCs, we have discovered that it was also associated with the expression level of the cell proliferation marker *PCNA* and with the rate of VSMC proliferation, both being highest in VSMCs of the C/C genotype, indicating that the CAD risk allele (C allele) increases VSMC proliferation. Although this finding in cultured cells may not necessarily reflect the situation in vascular tissues *in vivo*, our study in coronary atherosclerotic plaques from different individuals shows that the risk allele (C allele) is associated with lower $p15^{INK4b}$ expression in VSMCs and higher VSMC content in plaques. Thus, it is likely that the association between the 9p21 risk allele and increased risk of CAD is partly due to increased VSMC proliferation, since VSMC proliferation plays an important role in the pathogenesis of atherosclerosis (20).

VSMCs and extracellular matrix proteins secreted by VSMCs constitute the main bulk of many atherosclerotic

plaques (33,34). Accumulation of VSMCs and matrix proteins is a major factor for plaque growth (20). However, plaques that contain a thick fibrous cap consisting largely of VSMCs and matrix proteins are less likely to rupture to cause thrombosis and acute ischaemic events such as myocardial infarction (35). Genetic epidemiological studies have shown that the 9p21 risk allele is associated with atherosclerotic lesion development/progression and susceptibility to CAD (1,3,5–8,12), but does not confer an increased risk of myocardial infarction in patients with coronary atherosclerosis (6,36). The finding of our study that the 9p21 variation is associated with VSMC proliferation is in concordance with these genetic epidemiological findings.

In addition to CAD, other vascular diseases that have been shown to be associated with the 9p21 locus include abdominal aortic aneurysm (9), intracranial aneurysm (9–11), carotid atherosclerosis (12), ischaemic stroke (13) and peripheral vascular disease (14). It is interesting that the 9p21 locus is associated with both atherosclerosis and aneurysms. In this study, in addition to confirming that VSMCs in the atherosclerotic lesions express $p16^{INK4a}$, $p14^{ARF}$ and $p15^{INK4b}$ as recently reported (28), we found that VSMCs in abdominal aortic aneurysmal lesions also express these cell cycle regulators. This information may be useful for future studies aimed to investigate the mechanism underlying the association of the 9p21 locus with aneurysms.

In summary, our study shows that the 9p21 variant is associated with *CDKN2A*, *CDKN2B* and *ANRIL* expression levels in VSMC primary cultures and $p15^{INK4b}$ levels in VSMCs in atherosclerotic plaques, and with VSMC proliferation as well as VSMC content in plaques. These findings provide new insight into the mechanism underlying the well-established association between the 9p21 locus and risk of CAD.

MATERIALS AND METHODS

Immunohistochemical analysis

Sections of formaldehyde-fixed paraffin-embedded blocks of atherosclerotic arteries or aneurysmal arteries were subjected to double immunostaining for the VSMC marker SMA together with either $p16^{INK4a}$, $p14^{ARF}$ or $p15^{INK4b}$. In brief, the sections were deparaffined with xylene and rehydrated with ethanol, and then incubated with 0.01 M sodium citrate to retrieve antigens, followed by incubation with an avidin and biotin blocking solution (Avidin Biotin Blocking systems, VectorLab), then a peroxidase blocking solution (3% H_2O_2), and subsequently 10% goat serum (Dako). Thereafter, the sections were incubated with a primary antibody, which was either a rabbit anti-human $p16^{INK4a}$ polyclonal antibody (Proteintech, 10883-1-AP), or a rabbit anti-human $p14^{ARF}$ polyclonal antibody (Abcam, ab3642), or a rabbit anti-human $p15^{INK4b}$ polyclonal antibody (Abcam, ab53034). The sections were then incubated with a biotin-conjugated goat anti-rabbit secondary antibody (Dako, E0432), followed by an incubation with avidin-conjugated horseradish peroxidase and then with 3,3′-diaminodbenzidine (DAB). The sections were then incubated with a mouse anti-human SMA antibody conjugated with alkaline phosphatase (Sigma, A5691) and then with Fast Red (Sigma). In a second immunostaining procedure, the sections were prepared and incubated with the antibodies for $p16^{INK4a}$, $p14^{ARF}$ and $p15^{INK4b}$ as above, then with an anti-rabbit antibody conjugated with alkaline phosphatase (Sigma, A3687) and then with Fast Red. The sections were then incubated with a mouse anti-human SMA antibody (Sigma, A5228), followed by incubation with a biotin-conjugated goat anti-mouse secondary antibody (Sigma, B7264). The sections were then incubated with avidin-conjugated horseradish peroxidase and then with DAB. Subsequently, the sections were counterstained with haematoxylin.

Sections of formaldehyde-fixed paraffin-embedded blocks of atherosclerotic arteries were also subjected to double immunostaining for the VSMC marker SMA together with the cell proliferation marker Ki67. The sections were deparaffinized and re-hydrated in xylene and ethanol, respectively, and then transferred into 0.1 M citrate buffer for antigen retrieval, followed by incubation with 10% goat serum. The sections were then incubated overnight with primary antibodies which were a mouse anti-human SMA antibody (Dako, M-0635) and a rabbit anti-human Ki67 (Abcam, ab66155). After washing in phosphate-buffered saline, the sections were incubated with a biotinylated swine anti-rabbit Ig secondary antibody (Dako, E-0431) for 30 min and then with an anti-mouse Ig alkaline phosphatase-conjugated secondary antibody (Sigma, A-3562) for 30 min. After washing, the sections were incubated with avidin-conjugated horseradish peroxidase for 30 min and then with DAB for 5 min. This was followed by incubation with nitro-blue tetrazolium/5-bromo-4-chloro-3′-indolyphosphate (NBT/BCIP). A methyl green counterstaining was then used before dehydrating and mounting the slides.

Slides were examined using an OLYMPUS BX61 microscope and images taken using a BX-PMTVC camera. Image analysis was done using ImagePro Software (Media Cybernetics) and blind to genotyping data. The study was approved by a National Research Ethics Service committee. The study fully complied with Good Clinical Practice guidelines and Tissue Act regulations.

Isolation, culture and immunocytochemical analyses of primary VSMCs

Arteries in umbilical cords were dissected out and the adventitia removed. They were then cut open, divided into small segments and placed onto gelatin-coated tissue culture flasks with the arterial media surface facing the tissue culture surface of the flasks. The flasks were incubated at 37°C for ~1.5 h to facilitate attachment of the arterial segments to the gelatin-coated tissue culture surface of the flasks. The arterial segments were then cultured in Dulbecco's modified Eagle's medium supplemented with 20% fetal bovine serum, 2% L-glutamine and penicillin/streptomycin at 37°C with 5% CO_2 and 95% humidity. Once reaching ~90% confluence, the VSMCs were harvested by trypsinization. The cells were then cultured in Smooth Muscle Cell Growth Medium (PromoCell) containing fetal calf serum (5%), epidermal growth factor (0.5 ng/ml), basic fibroblast growth factor (2 ng/ml) and insulin (5 μg/ml). Immunocytochemical analyses and

real-time reverse transcriptase polymerase chain reactions described below were carried out using cells at passage 2.

Immunocytochemical analyses were carried out for the VSMC marker SMA, the endothelial cell marker von Willebrand factor and the fibroblast marker discoidin domain receptor-2. In brief, cells were fixed with an acetone and methanol mixture, and then incubated with or without a mouse anti-human SMA monoclonal antibody (Sigma, A5228), or a mouse anti-human von Willebrand factor monoclonal antibody (DAKO, M0616), or a goat anti-human discoidin domain receptor-2 (DDR2) polyclonal antibody (Santa Cruz Biotechnology, sc-7555). The cells were then washed and incubated with either a goat anti-mouse antibody conjugated with FITC (Sigma, F4018) or a rabbit anti-goat conjugated with FITC (Abcam, ab6737). Subsequently, the cell nuclei were stained with 4,6-diamidino-2-phenylindole (DAPI). The cells were visualized using a fluorescence microscope with a digital imaging system. The immunocytochemical analyses showed that the cells expressed the VSMC marker SMA but neither the endothelial cell marker von Willebrand factor nor the fibroblast marker discoidin domain receptor-2 (Supplementary Material, Fig. S3).

Determination of genotypes

Genomic DNA was extracted from cultured VSMCs or sections of formaldehyde-fixed paraffin-embedded blocks of atherosclerotic arteries using the Wizard SV Genomic DNA Purification System (Promega). Genotypes for 9p21 SNP rs1333049 were determined by TaqMan SNP genotyping assay (from Applied Biosystems, C_1754666_10).

Real-time reverse transcriptase–polymerase chain reaction

Expression levels of $p16^{INK4a}$, $p14^{ARF}$, $p15^{INK4b}$, *ANRIL* and *PCNA* in primary VSMC cultures were quantified by reverse transcriptase–polymerase chain reaction. Total RNA samples were prepared from primary cultures of VSMCs, with the use of the SV Total RNA Isolation System (Promega). RNA was reverse transcribed into cDNA using random primers (Promega) and M-MLV reverse transcriptase (Promega). The resultant cDNA was subjected to real-time polymerase chain reactions for $p16^{INK4a}$, $p14^{ARF}$, $p15^{INK4b}$, *ANRIL*, *PCNA* and *β-actin*, respectively. The probes used were $p16^{INK4a}$ (forward primer GAGCAGCATGGAGCCTTC, reverse primer CGTAACTATTCGGTGCGTTG and FAM-labelled probe CTGGCTGG, LightCycler), $p14^{ARF}$ (forward primer CTACTGAGGAGCCAGCGTCT, reverse primer CTGCCCATCATCATGACCT and FAM-labelled probe CAGCAGCC, LightCycler), $p15^{INK4b}$ (Applied Biosystems, Hs00793225_m1), *ANRIL* (forward primer ATTTGGGAAT GAGGAGCACAGT, reverse primer TGCCATGTGAGAGA AGCCAAT and FAM-labelled probe TAAGTCACTGGTCT GAGTTC, Applied Biosystems), *PCNA* (Applied Biosystems, Hs00427214_g1) and *β-actin* (Applied Biosystems, Hs03023943_g1). Delta C_t values for $p16^{INK4a}$, $p14^{ARF}$, $p15^{INK4b}$, *ANRIL* and *PCNA*, respectively, were calculated in relation to the reference gene *β-actin*.

Cell proliferation assay

VSMCs were seeded in duplicate in 96 well-plates (5000 cells per well) and cultured overnight. In the following day, medium was changed and cells were cultured for further 12 h in fresh medium in the presence of 10 μM 5-bromo-2′-deoxyuridine (BrdU), followed by BrdU detection assay with the use of 5-Bromo-2′-deoxy-uridine Labeling and Detection Kit III (Roche, 11444611001).

Statistical analyses

Variables not in normal distribution were normalized by logarithmic transformation. Analyses of variance (ANOVA) tests were performed to ascertain differences between genotypes in $p16^{INK4a}$, $p14^{ARF}$, $p15^{INK4b}$, *ANRIL* and *PCNA* expression levels, cell proliferation, percentage of $p16^{INK4a}$ stain area over SMA stain area in atherosclerotic plaques, percentage of $p15^{INK4b}$ stain area over SMA stain area in plaques, number of Ki67-positive VSMCs over SMA stain area in plaques and percentage of SMA stain area over total plaque area in plaques. Pair-wise correlations between variables were tested by Pearson's correlation analyses.

SUPPLEMENTARY MATERIAL

Supplementary Material is available at *HMG* online.

Conflict of Interest statement. None declared.

FUNDING

We thank support from the British Heart Foundation (FS/07/021 and FS/11/28/28758). Q.X. is the recipient of a British Heart Foundation Intermediate Basic Science Research Fellowship (FS/09/044/28007). This work forms part of the research themes contributing to the translational research portfolio of Barts and the London Cardiovascular Biomedical Research Unit which is supported and funded by the National Institute of Health Research.

REFERENCES

1. Samani, N.J., Erdmann, J., Hall, A.S., Hengstenberg, C., Mangino, M., Mayer, B., Dixon, R.J., Meitinger, T., Braund, P., Wichmann, H.E. *et al.* (2007) Genomewide association analysis of coronary artery disease. *N. Engl J. Med.*, **357**, 443–453.
2. Helgadottir, A., Thorleifsson, G., Manolescu, A., Gretarsdottir, S., Blondal, T., Jonasdottir, A., Jonasdottir, A., Sigurdsson, A., Baker, A., Palsson, A. *et al.* (2007) A common variant on chromosome 9p21 affects the risk of myocardial infarction. *Science*, **316**, 1491–1493.
3. McPherson, R., Pertsemlidis, A., Kavaslar, N., Stewart, A., Roberts, R., Cox, D.R., Hinds, D.A., Pennacchio, L.A., Tybjaerg-Hansen, A., Folsom, A.R. *et al.* (2007) A common allele on chromosome 9 associated with coronary heart disease. *Science*, **316**, 1488–1491.
4. Kathiresan, S., Voight, B.F., Purcell, S., Musunuru, K., Ardissino, D., Mannucci, P.M., Anand, S., Engert, J.C., Samani, N.J., Schunkert, H. *et al.* (2009) Genome-wide association of early-onset myocardial infarction with single nucleotide polymorphisms and copy number variants. *Nat. Genet.*, **41**, 334–341.
5. Broadbent, H.M., Peden, J.F., Lorkowski, S., Goel, A., Ongen, H., Green, F., Clarke, R., Collins, R., Franzosi, M.G., Tognoni, G. *et al.* (2008) Susceptibility to coronary artery disease and diabetes is encoded by

distinct, tightly linked SNPs in the ANRIL locus on chromosome 9p. *Hum. Mol. Genet.*, **17**, 806–814.
6. Schunkert, H., Gotz, A., Braund, P., McGinnis, R., Tregouet, D.A., Mangino, M., Linsel-Nitschke, P., Cambien, F., Hengstenberg, C., Stark, K. *et al.* (2008) Repeated replication and a prospective meta-analysis of the association between chromosome 9p21.3 and coronary artery disease. *Circulation*, **117**, 1675–1684.
7. Dandona, S., Stewart, A.F., Chen, L., Williams, K., So, D., O'Brien, E., Glover, C., Lemay, M., Assogba, O., Vo, L. *et al.* (2010) Gene dosage of the common variant 9p21 predicts severity of coronary artery disease. *J. Am. Coll. Cardiol.*, **56**, 479–486.
8. Patel, R.S., Su, S., Neeland, I.J., Ahuja, A., Veledar, E., Zhao, J., Helgadottir, A., Holm, H., Gulcher, J.R., Stefansson, K. *et al.* (2010) The chromosome 9p21 risk locus is associated with angiographic severity and progression of coronary artery disease. *Eur. Heart J.*, **31**, 3017–3023.
9. Helgadottir, A., Thorleifsson, G., Magnusson, K.P., Gretarsdottir, S., Steinthorsdottir, V., Manolescu, A., Jones, G.T., Rinkel, G.J., Blankensteijn, J.D., Ronkainen, A. *et al.* (2008) The same sequence variant on 9p21 associates with myocardial infarction, abdominal aortic aneurysm and intracranial aneurysm. *Nat. Genet.*, **40**, 217–224.
10. Bilguvar, K., Yasuno, K., Niemela, M., Ruigrok, Y.M., von Und Zu, F.M., van Duijn, C.M., van den Berg, L.H., Mane, S., Mason, C.E., Choi, M. *et al.* (2008) Susceptibility loci for intracranial aneurysm in European and Japanese populations. *Nat. Genet.*, **40**, 1472–1477.
11. Yasuno, K., Bilguvar, K., Bijlenga, P., Low, S.K., Krischek, B., Auburger, G., Simon, M., Krex, D., Arlier, Z., Nayak, N. *et al.* (2010) Genome-wide association study of intracranial aneurysm identifies three new risk loci. *Nat. Genet.*, **42**, 420–425.
12. Ye, S., Willeit, J., Kronenberg, F., Xu, Q. and Kiechl, S. (2008) Association of genetic variation on chromosome 9p21 with susceptibility and progression of atherosclerosis: a population-based, prospective study. *J. Am. Coll. Cardiol.*, **52**, 378–384.
13. Anderson, C.D., Biffi, A., Rost, N.S., Cortellini, L., Furie, K.L. and Rosand, J. (2010) Chromosome 9p21 in ischemic stroke: population structure and meta-analysis. *Stroke*, **41**, 1123–1131.
14. Cluett, C., McDermott, M.M., Guralnik, J., Ferrucci, L., Bandinelli, S., Miljkovic, I., Zmuda, J.M., Li, R., Tranah, G., Harris, T. *et al.* (2009) The 9p21 myocardial infarction risk allele increases risk of peripheral artery disease in older people. *Circ. Cardiovasc. Genet.*, **2**, 347–353.
15. Angelakopoulou, A., Shah, T., Sofat, R., Shah, S., Berry, D.J., Cooper, J., Palmen, J., Tzoulaki, I., Wong, A., Jefferis, B.J. *et al.* (2012) Comparative analysis of genome-wide association studies signals for lipids, diabetes, and coronary heart disease: Cardiovascular Biomarker Genetics Collaboration. *Eur. Heart J.*, **33**, 393–407.
16. Gil, J. and Peters, G. (2006) Regulation of the INK4b-ARF-INK4a tumour suppressor locus: all for one or one for all. *Nat. Rev. Mol. Cell Biol.*, **7**, 667–677.
17. Jarinova, O., Stewart, A.F., Roberts, R., Wells, G., Lau, P., Naing, T., Buerki, C., McLean, B.W., Cook, R.C., Parker, J.S. and McPherson, R. (2009) Functional analysis of the chromosome 9p21.3 coronary artery disease risk locus. *Arterioscler. Thromb. Vasc. Biol.*, **29**, 1671–1677.
18. Burd, C.E., Jeck, W.R., Liu, Y., Sanoff, H.K., Wang, Z. and Sharpless, N.E. (2010) Expression of linear and novel circular forms of an INK4/ARF-associated non-coding RNA correlates with atherosclerosis risk. *PLoS Genet.*, **6**, e1001233.
19. Visel, A., Zhu, Y., May, D., Afzal, V., Gong, E., Attanasio, C., Blow, M.J., Cohen, J.C., Rubin, E.M. and Pennacchio, L.A. (2010) Targeted deletion of the 9p21 non-coding coronary artery disease risk interval in mice. *Nature*, **464**, 409–412.
20. Ross, R. (1993) The pathogenesis of atherosclerosis: a perspective for the 1990s. *Nature*, **362**, 801–809.
21. Liu, Y., Sanoff, H.K., Cho, H., Burd, C.E., Torrice, C., Mohlke, K.L., Ibrahim, J.G., Thomas, N.E. and Sharpless, N.E. (2009) INK4/ARF transcript expression is associated with chromosome 9p21 variants linked to atherosclerosis. *PLoS ONE.*, **4**, e5027.
22. Holdt, L.M., Beutner, F., Scholz, M., Gielen, S., Gabel, G., Bergert, H., Schuler, G., Thiery, J. and Teupser, D. (2010) ANRIL expression is associated with atherosclerosis risk at chromosome 9p21. *Arterioscler. Thromb. Vasc. Biol.*, **30**, 620–627.
23. Cunnington, M.S., Santibanez, K.M., Mayosi, B.M., Burn, J. and Keavney, B. (2010) Chromosome 9p21 SNPs Associated with Multiple Disease Phenotypes Correlate with ANRIL Expression. *PLoS Genet.*, **6**, e1000899.
24. Yap, K.L., Li, S., Munoz-Cabello, A.M., Raguz, S., Zeng, L., Mujtaba, S., Gil, J., Walsh, M.J. and Zhou, M.M. (2010) Molecular interplay of the noncoding RNA ANRIL and methylated histone H3 lysine 27 by polycomb CBX7 in transcriptional silencing of INK4a. *Mol. Cell*, **38**, 662–674.
25. Folkersen, L., Kyriakou, T., Goel, A., Peden, J., Malarstig, A., Paulsson-Berne, G., Hamsten, A., Hugh, W., Franco-Cereceda, A., Gabrielsen, A. and Eriksson, P. (2009) Relationship between CAD risk genotype in the chromosome 9p21 locus and gene expression. Identification of eight new ANRIL splice variants. *PLoS ONE.*, **4**, e7677.
26. Iaquinta, P.J. and Lees, J.A. (2007) Life and death decisions by the E2F transcription factors. *Curr. Opin. Cell Biol.*, **19**, 649–657.
27. Polager, S. and Ginsberg, D. (2009) p53 and E2f: partners in life and death. *Nat. Rev. Cancer*, **9**, 738–748.
28. Holdt, L.M., Sass, K., Gabel, G., Bergert, H., Thiery, J. and Teupser, D. (2011) Expression of Chr9p21 genes CDKN2B (p15(INK4b)), CDKN2A (p16(INK4a), p14(ARF)) and MTAP in human atherosclerotic plaque. *Atherosclerosis*, **214**, 264–270.
29. Gizard, F., Amant, C., Barbier, O., Bellosta, S., Robillard, R., Percevault, F., Sevestre, H., Krimpenfort, P., Corsini, A., Rochette, J. *et al.* (2005) PPAR alpha inhibits vascular smooth muscle cell proliferation underlying intimal hyperplasia by inducing the tumor suppressor p16INK4a. *J. Clin. Invest.*, **115**, 3228–3238.
30. Gizard, F., Nomiyama, T., Zhao, Y., Findeisen, H.M., Heywood, E.B., Jones, K.L., Staels, B. and Bruemmer, D. (2008) The PPARalpha/p16INK4a pathway inhibits vascular smooth muscle cell proliferation by repressing cell cycle-dependent telomerase activation. *Circ. Res.*, **103**, 1155–1163.
31. Segev, A., Nili, N., Qiang, B., Osherov, A.B., Giordano, F.J., Jaffe, R., Gauldie, J., Sparkes, J.D., Fraser, A.R., Ladouceur-Wodzak, M. *et al.* (2011) Inhibition of intimal hyperplasia after stenting by over-expression of p15: a member of the INK4 family of cyclin-dependent kinase inhibitors. *J. Mol. Cell. Cardiol.*, **50**, 417–425.
32. Zeller, T., Wild, P., Szymczak, S., Rotival, M., Schillert, A., Castagne, R., Maouche, S., Germain, M., Lackner, K., Rossmann, H. *et al.* (2010) Genetics and beyond—the transcriptome of human monocytes and disease susceptibility. *PLoS ONE.*, **5**, e10693.
33. Stary, H.C., Chandler, A.B., Glagov, S., Guyton, J.R., Insull, W. Jr, Rosenfeld, M.E., Schaffer, S.A., Schwartz, C.J., Wagner, W.D. and Wissler, R.W. (1994) A definition of initial, fatty streak, and intermediate lesions of atherosclerosis. A report from the Committee on Vascular Lesions of the Council on Arteriosclerosis, American Heart Association. *Circulation*, **89**, 2462–2478.
34. Stary, H.C., Chandler, A.B., Dinsmore, R.E., Fuster, V., Glagov, S., Insull, W. Jr, Rosenfeld, M.E., Schwartz, C.J., Wagner, W.D. and Wissler, R.W. (1995) A definition of advanced types of atherosclerotic lesions and a histological classification of atherosclerosis. A report from the Committee on Vascular Lesions of the Council on Arteriosclerosis, American Heart Association. *Circulation*, **92**, 1355–1374.
35. Libby, P. (1995) Molecular bases of the acute coronary syndromes. *Circulation*, **91**, 2844–2850.
36. Reilly, M.P., Li, M., He, J., Ferguson, J.F., Stylianou, I.M., Mehta, N.N., Burnett, M.S., Devaney, J.M., Knouff, C.W., Thompson, J.R. *et al.* (2011) Identification of ADAMTS7 as a novel locus for coronary atherosclerosis and association of ABO with myocardial infarction in the presence of coronary atherosclerosis: two genome-wide association studies. *Lancet*, **377**, 383–392.